

Cardiac microvascular dysfunction in diabetes mellitus: elucidation of molecular determinants and therapeutic targets

Dissertation

for the award of the degree

“Doctor rerum naturalium” (Dr. rer. nat.)

of the Georg-August-Universität Göttingen

within the doctoral program Molecular Medicine
of the University Medical Center Göttingen (UMG)

submitted by

Mostafa Samak

from Cairo, Egypt

Göttingen, 2022

Thesis Committee

Prof. Dr. Rabea Hinkel

(Direct supervisor – Laboratory Animal Science, German Primate Center)

Prof. Dr. Wolfram H. Zimmermann

(Institute of Pharmacology and Toxicology, UMG)

Prof. Dr. Rüdiger Behr

(Platform Degenerative Diseases, German Primate Center)

Members of the examination board

Reviewer: Prof. Dr. Rabea Hinkel

Second reviewer: Prof. Dr. Wolfram H. Zimmermann

Additional reviewer: Prof. Dr. Rüdiger Behr

Further members of the examination board

Prof. Dr. Susanne Lutz

(Institute of Pharmacology and Toxicology, UMG)

Prof. Dr. Katrin Streckfuß-Bömeke

(Translational Stem Cell Research, UMG)

Prof. Dr. Frauke Alves

(Translational Molecular Imaging, UMG)

Date of the oral examination: 06.02.2023

Acknowledgment

Presenting this doctoral thesis is a lifetime moment of elation that would not be complete without acknowledging the wonderful people who made it true.

First and foremost, my eternal gratitude goes to my supervisor Rabea Hinkel for granting me this honorable opportunity and for over four years of constant support with unprecedented leadership and kindness. I was honored to have her as my mentor.

I owe a debt of gratitude to our lab leader Giulia Germena for every bit of success in this project; it would have not been complete without her professional input, incentive tutoring and amicable encouragement.

My deepest thanks go to Andreas Kues, whose help was indispensable in this project, and for being an elder brother and a good friend. Special recognitions go to Diana Kaltenborn for her diligent cooperation and friendly interaction, and to my officemate Lina Klösener for her good company. My appreciation is extended to all other members of the Laboratory Animal Science department for their perfect collegiality.

I was honored to receive encouragement from Wolfram Zimmermann and Rüdiger Behr as thesis advisors, and to be a member of the German Primate Center as host institution.

I feel utterly privileged to have done both my master's and doctoral studies at the exalted University of Göttingen.

No words can express my gratitude and appreciation to my beloved wife Joana Brandes-Samak and my amazing new family, especially Fritz and Marlis Weidemann and Caren Brandes, who showered me with true love and happiness.

For life, I shall be grateful to my mother Maha Kamal, my sister Rana Samak and all members of my family in Egypt for over three decades of love and nurture.

Finally, I dedicate my success in this doctoral study to the beautiful memory of my beloved father Mohamed Samak.

Table of Contents

Summary.....	6
Zusammenfassung.....	7
1. Introduction	9
1.1. Diabetes mellitus (DM)	9
1.1.1. Type 1 diabetes mellitus (T1DM)	10
1.1.2. Type 2 diabetes mellitus (T2DM)	11
1.2. Cardiovascular complications of DM	12
1.2.1. Macrovascular complications of DM	14
1.2.2. Microvascular complications of DM	14
1.2.3. Molecular mechanisms of diabetic micro-vasculopathy	17
1.2.4. Current treatment regimens – why do they fail?	25
1.3. Micro-RNAs as novel molecules in biology and medicine	26
1.3.1. MiRNA biogenesis and function	26
1.3.2. MiRNAs in pathogenesis and potential therapy of DM and CVD	30
1.3.3. MiR-17~92 cluster	34
1.4. Study objectives	39
2. Materials and Methods	40
2.4. Cell culture.....	40
2.5. Transfection	41
2.6. Tube formation	42
2.7. Wound healing.....	42
2.8. Flow chamber assay	42
2.9. Endothelial spheroid assay	43
2.10. Proliferation assay	44
2.11. Western Blot.....	44
2.12. Quantitative PCR	46
2.13. ImageJ analysis	47
2.14. Immunofluorescence	48
2.15. Dual-Luciferase bioluminescence.....	48
2.16. Glucose uptake assays	49
2.17. Statistical analysis.....	50
3. Results.....	51
3.4. Cardiac microvascular endothelial cells (CMEC).....	51

3.4.1.	<i>In vitro</i> modeling of DM: effects of high glucose culture.....	51
3.4.2.	Characterization of type 2 diabetic HCMEC	55
3.4.3.	MiR-92a inhibition rescued the diabetic phenotype in HCMEC	57
3.4.4.	<i>In silico</i> prediction of miR-92a targets.....	62
3.4.5.	<i>ADAM10</i> : a novel miR-92a target dysregulated diabetic hearts	65
3.4.6.	<i>ADAM10</i> in tube formation and migration of CMEC	70
3.4.7.	<i>KLF2</i> and <i>KLF4</i> are miR-92a targets dysregulated in diabetic myocardia and CMEC.....	74
3.4.8.	KLFs 2 and 4 as regulators of CMEC function	77
3.4.9.	Inter-regulation of KLFs	79
3.4.10.	Downstream inflammatory mediators of KLFs	80
3.4.11.	Myocyte enhancer factors 2 (MEF2): novel targets in diabetic hearts ...	81
3.4.12.	Regulation of KLFs by MEF2	86
3.5.	Human umbilical vein endothelial cells (HUVEC)	87
3.5.1.	High glucose culture on HUVEC function and miR-92a levels	87
3.5.2.	Overexpression of miR-92a in HUVEC	89
3.5.3.	Downstream targets of miR-92a in HUVEC	90
4.	Discussion	92
4.4.	Optimized <i>in vitro</i> models and the 3R principle	92
4.5.	Endothelial cell models & endothelial heterogeneity	93
4.6.	High glucose culture to model DM	95
4.7.	Cardiac microvascular dysfunction in DM: the phenotype and the rescue.....	97
4.8.	Why miR-92a is upregulated in DM: glucose-uptake hypothesis.....	98
4.9.	How miR-92a is upregulated in DM.....	99
4.10.	Fishing for targets: rationale of target selection	101
4.11.	<i>ADAM10</i> : a novel player in diabetic microcirculatory dysfunction.....	102
4.12.	KLFs dysregulation model to explain the diabetic vascular inflammation .	103
4.13.	MEF2D as a novel player in diabetic microvascular dysfunction.....	106
4.14.	Translational prospects	108
5.	Conclusion	109
6.	Study publications	110
7.	Literature	111
	Curriculum vitae	145

Summary

Microvascular dysfunction is a pathological hallmark of the diabetic myocardium, and is central to the etiology of diabetes-associated cardiac events. Herein, previous studies highlighted the role of the vasoactive micro-RNA 92a (miR-92a) in small, as well as large animal models. In this study, the effects of miR-92a in primary human cardiac microvascular endothelial cells (HCMEC) and their mouse equivalents (MCMEC) were explored. I characterized endothelial dysfunction and inflammation in HCMEC from diabetic patients and reported their upregulation of miR-92a. Importantly, I could show that inhibition of miR-92a in diabetic HCMEC rescued angiogenesis and ameliorated endothelial bed inflammation. The *in silico* analysis identified four conserved targets downstream of miR-92a with direct relevance to the observed phenotypes. Of novelty, I reported the miR-92a-dependent downregulation of the coronary essential metalloproteinase, ADAM10, in diabetic HCMEC. This was also shown in diabetic porcine ventricular tissue. Accordingly, downregulation of ADAM10 impaired angiogenesis, sprouting and wound healing in HCMEC and MCMEC. Further, a dysregulation of the anti-inflammatory Krüppel-like factors (KLF) 2 and 4 in diabetic HCMEC and diabetic porcine left ventricles was observed. Indeed, ablation of KLF2 in non-diabetic HCMEC elicited the same inflammatory phenotype as their diabetic counterparts. Upstream of KLFs, dysregulation of myocyte enhancer factor 2D (MEF2D) in diabetic HCMEC and porcine ventricular tissue was demonstrated. By virtue of dual luciferase reporter assays, I confirmed direct interaction between miR-92a and all four targets. Importantly, inhibition of miR-92a was also shown to restore their levels in diabetic HCMEC.

Altogether, my results highlight novel molecular mechanisms in the pathogenesis of cardiac microvascular dysfunction in diabetes and strongly qualify miR-92a as a therapeutic target.

Zusammenfassung

Die mikrovaskuläre Dysfunktion ist ein pathologisches Merkmal des diabetischen Myokards und spielt eine zentrale Rolle bei der Ätiologie von Diabetes-assoziierten Herzerkrankungen. Frühere Studien haben die Rolle der vasoaktiven Mikro-RNA 92a (miR-92a) sowohl in kleinen als auch in großen Tiermodellen aufgezeigt. In dieser Studie wurden die Auswirkungen von miR-92a in primären humanen kardialen mikrovaskulären Endothelzellen (HCMEC) und ihren Gegenstücken aus der Maus (MCMEC) untersucht. Ich habe die endotheliale Dysfunktion und Entzündung in HCMEC von Diabetikern charakterisiert und ihre Hochregulierung von miR-92a beschrieben. Außerdem konnte ich zeigen, dass die Hemmung von miR-92a in diabetischen HCMEC die Angiogenese unterstützte und die Entzündung des Endothelbetts verringerte. Die *in silico*-Analyse identifizierte vier konservierte Zielmoleküle, die miR-92a nachgeschaltet sind und einen direkten Bezug zu den beobachteten Phänotypen haben. Neu ist, dass ich die miR-92a-abhängige Herunterregulierung der koronaren essentiellen Metalloproteinase ADAM10 in diabetischen HCMEC nachweisen konnte. Dies konnte auch in diabetischem ventrikulärem Gewebe von Schweinen gezeigt werden. Dementsprechend beeinträchtigte die Herunterregulierung von ADAM10 die Angiogenese, Sprossung und Wundheilung in HCMEC und MCMEC. Darüber hinaus ist eine Dysregulation der entzündungshemmenden Krüppel-like Faktoren (KLF) 2 und 4 in diabetischen HCMEC und diabetischen Schweineventrikeln festgestellt worden. Tatsächlich führte die Ablation von KLF2 in nicht-diabetischen HCMEC zum gleichen Entzündungsphänotyp wie in ihren diabetischen Pendants. Upstream von KLFs wurde eine Fehlregulierung des Myozyten-Enhancer-Faktors 2D (MEF2D) in diabetischen HCMEC und Schweineventrikeln festgestellt. Mit Hilfe von dualen Luziferase-Reporter-Assays bestätigte ich eine direkte Interaktion zwischen miR-92a und allen vier Zielmolekülen. Es hat sich auch

Zusammenfassung

gezeigt, dass die Hemmung von miR-92a die Werte dieser Targets in diabetischen HCMEC wiederherstellt.

Insgesamt zeigen meine Ergebnisse neue molekulare Mechanismen in der Pathogenese der kardialen mikrovaskulären Dysfunktion bei Diabetes mellitus auf und qualifizieren miR-92a nachdrücklich als therapeutisches Ziel.

1. Introduction

1.1. Diabetes mellitus (DM)

From the Greek word *diabetes*, i.e. to siphon or pass, and the Latin word *mel*, for honey or sweet, diabetes mellitus (DM) is a metabolic disorder known from antiquity and describes the inability to handle glucose, leading to a persistent state of hyperglycemia. While our modern understanding identifies hyperglycemia as a hallmark of diabetes, the disease was previously defined by its symptoms. The ancient Egyptian medical papyri, such as those of Kahun (2000 BC) and Ebers (1500 BC) described the symptoms of patients of extreme thirst and polyurination. The sweet urine of patients was first described in ancient Indian medicine in the 5th century. The Chinese, Greco-Roman, and Arab medical practices further described the symptoms of DM over eleven centuries AD. However, it was not until the 19th century that pancreatic DM was described by Oskar Minkowski and Joseph von Mering in Strasbourg. From identification of the role of the pancreas in glucose homeostasis, it was not long until Frederick Banting and John MacLeod discovered insulin as key in this process, for which they earned the Nobel prize in 1923 (reviewed in [1]). In over four millennia of documented human history, DM remains a health affliction of contemporary humans, harvesting the lives of over 3 million people annually, according to the World Health Organization (WHO) [2]. In 2019, an estimate of 463 million adults worldwide had diabetes, a number that was back then expected to rise to 578 million by the year 2030 [3]. Only 2 years later, the International Diabetes Federation (IDF) reported in their 2021 atlas edition on 537 million adults with DM [4]. In Europe, sixty million people aged 25 and older have DM, this sums to over 10% of Europeans of both sexes [2, 5]. As per Robert Koch Institute, the prevalence of DM in Germany had experienced a 10-fold increase since the 1960 [6]. Herein, Germans with DM had twice as much the risk of death compared to non-diabetics. In the United States, almost 1 in 10 people have DM, and 2 of every 10 diabetics don't know they have it. As a consequence of ageing and obesity, the number of Americans diagnosed with DM has doubled in the last two decades [7]. The situation in low- and middle-income countries is not any brighter, if not worsening [8]. In fact, almost 80% of diabetic people live in low- and middle-income countries [9]. While a number of pathological, and in the case of gestational diabetes, temporary conditions lead to hyperglycemia, the term *diabetes* commonly refers to two major types with distinct etiologies.

1.1.1. Type 1 diabetes mellitus (T1DM)

Type 1 DM is a chronic autoimmune disease characterized by progressive destruction of the pancreatic insulin producing beta cells (β -cells) in the islets of Langerhans by cytotoxic T-cells, resulting in insulin deficiency and hyperglycemia [10]. T1DM is a polygenic disease, wherein various susceptibility genes, along with precipitating environmental and/or infectious agents trigger an overt immune reaction to β -cells [11]. As a result, the endocrine pancreas is infiltrated with cytotoxic CD8+ T-cells along with cells of the innate immune system, as well as B-lymphocytes [10-11]. The latter release autoantibodies against β -cell proteins, which are characteristic measures in the blood of T1DM patients [10]. The disease usually presents itself in children or young individuals, hence previously known as juvenile-onset DM. This can be misleading, since T1DM can occur in any age, with 50% of cases occurring in adults, of which half are misdiagnosed as type 2 DM [12-13]. T1DM affects one in every 250 individuals on average, with more male than female bias [14]. The incidence of T1DM has been on the rise, with overall annual increase of 2 – 3%, mostly children under 15 years old, peaking at those < 5 years old [15]. Type 1 diabetic patients are strictly dependent on exogenous insulin with high risk of life-threatening bouts of hypoglycemia, and on the other end, diabetic ketoacidosis [10]. These critical conditions have been associated with neurocognitive complications in type 1 diabetic patients, which are linked to diabetes-induced vascular disease [16-18]. Type 1 diabetics succumb to the notorious long-term complications of DM, including retinopathy, nephropathy and neuropathy, and above all cardiovascular disease (CVD) (discussed below) [19-22]. Despite recent improvements in management, T1DM continues to be associated with increased total mortality. In young adults with T1DM, i.e. <45 years old, total mortality is 5 fold higher than among age-matched non-diabetics [23].

1.1.2. Type 2 diabetes mellitus (T2DM)

The second type of DM accounts for over 90% of all cases of diabetes. T2DM is rather a metabolic syndrome, where a suite of both genetic and lifestyle factors contributes to its etiology [4]. Herein, T2DM ensues mainly as a result of poor diet; one characterized by frequent consumption of food with high glycemic index and trans-fats, which leads to elevated blood insulin levels, as well as triglycerides [24-25]. Combined with a sedentary lifestyle and obesity, insulin-sensitive organs gradually develop a state of insulin resistance, which in turn triggers a feedback response of increased insulin secretion (hyperinsulinemia). Overtime, the pancreatic compensation fails in face of insulin resistance, leading to β -cell dysfunction [26-27]. The triad of increased blood glucose, insulin and free fatty acids is an ominous metabolic state that evoke a number of deleterious cascades, such as glucotoxicity, lipotoxicity, oxidative stress, dyslipidemia and inflammation, that inflict all organ systems [28-29]. These manifest in a wide range of diabetic infamous complications, such as retinopathy, neuropathy, nephropathy and above all, CVD (discussed below) [26]. Importantly, T2DM harbors a genetic component that has recently become appreciated thanks to advancing genome wide association studies (GWAS). Over 500 risk variants and susceptibility genes have been identified in T2DM, and its associated disease conditions [30-32]. The ever growing ageing population highlighted age as another risk factor for T2DM [33]. Nevertheless, the increasing incidence of T2DM among young adults and children portends a dismal public health future. In Germany, the projected number of future T2DM cases is estimated between 10.7 – 12.3 million cases in 2040, with a relative increase of 54% – 77% compared to 6.9 million in 2015 [34]. Worldwide, an estimate of 462 million people have T2DM, which contributed to over a million deaths in 2017 [35]. It is estimated that by the year 2035, 600 million adults will be living with T2DM [36].

1.2. Cardiovascular complications of DM

“Those with cardiovascular disease not identified with diabetes are simply undiagnosed”

The quote belongs to Dr. Joseph R. Kraft (1920 – 2017), also known as the father of the insulin assay or Kraft test. Dr. Kraft dedicated his career to develop a better understanding for the etiology of diabetes-associated complications. His work highlighted the shortcomings in the antiquated fasted oral glucose tolerance tests in identification of diabetics. He pioneered the notion that DM and its induced cardiovascular damage starts years, if not decades, before the first affirmative oral glucose tolerance test. For Kraft, abnormal and/or prolonged hyperinsulinemia was a more sensitive metric, wherein 75% of subjects with normal glucose tolerance tests had abnormal insulin response patterns, i.e. ‘diabetes in-situ’ [37]. From this point onwards, patients had already stepped foot into the vicious cycle of the diabetic metabolic syndrome, and their cardiovascular pathology had already started. Kraft’s prophecy from the 70’s has nowadays become widely accepted by virtue of more recent international studies revealing that the risk of cardiovascular disease (CVD) had progressively increased among ‘normoglycemic’ individuals, much more in those with the slightest deviations in glucose tolerance [38]. In fact, a 1 mmol/L increase in fasting plasma glucose levels was associated with a 17% increase in the risk of future cardiovascular events and even death [39]. In their 2019 guidelines, the European Society of Cardiology (ESC), and the European Association for the Study of Diabetes (EASD) advocated the screening for T2DM in all patients with CVD [40]. Indisputably, DM is the number one risk factor; diabetics are 2 – 4 times more likely to develop CVD, which accounts for 70 – 80% of deaths among them [41-43]. In Germany, based on survey data from the Robert Koch Institute, age- and sex-adjusted odds for CVD was 2.35 times higher in diabetics aged 50 or older [44]. Strikingly, the onset for CVD commences 15 years earlier in diabetics [45]. Not only does this debilitate an individual’s quality of life, but also constitutes a huge economic burden and encumbers every healthcare system. After all, CVD, particularly myocardial ischemia and stroke, remain the top global causes of death [46].

Intuitively, the vascular system is at the forefront with the diabetic state of hyperglycemia and, in T2DM, hyperinsulinemia. The hemovascular interface is where most of the diabetic pathophysiology takes place, and perpetual insults thereof predispose to the most frequent causes of morbidity and mortality in diabetic patients. While a plethora of cellular and molecular pathways contribute to the pathogenesis of CVD in DM (discussed below), a prominent straight forward example is the direct injurious effect of glucose.

Introduction

Elevated blood glucose damages the endothelial lining of vessels by non-enzymatic glycation of proteins, the so called “Maillard reaction”, including structural proteins, e.g. collagen, intracellular proteins, as well as circulating blood hormones and enzymes, leading to the formation of advanced glycation end products (AGE) [47-48]. On one hand, AGE bind to cell surface receptors (RAGE) and elicit maladaptive inflammatory and fibrotic response. On the other hand, AGE promote crosslinking of connective tissue components, such as collagens and laminins, compromising cardiac and vascular tissue compliance and leading to stiffness [49]. Moreover, the state of hyperglycemia/hyperinsulinemia in T2DM has been attributed deleterious alterations in both the endothelium and the myocardium. Herein, cardiomyocytes (CM), the functional units of the heart, undergo a series of metabolic adaptations and functional dysregulations. This includes CM insulin resistance, impaired calcium (Ca^{2+}) handling, mitochondrial dysfunction and elevated stress of the endoplasmic reticulum (ER) [50-51]. This is a drastic cellular condition for CM given the crucial functions of the ER in lipid synthesis, Ca^{2+} handling and protein folding. Diabetic CM hence accumulate an abundance of misfolded proteins and display impaired autophagy, leading to increased cell death [52]. The term “diabetic cardiomyopathy” (DCM), first coined in the 70’s, describes such state of adverse structural remodeling and dysfunction of the diabetic heart, including hypertrophy, stiffness and fibrosis, which are independent of other risk factors, such as coronary artery disease (CAD), hypertension or valvular disease [50, 53-54]. DCM develops silently, and presents itself later in the chronic setting of the disease. Initially, the diabetic myocardium displays diastolic dysfunction and, in later stages, systolic dysfunction, culminating in heart failure [53]. The repertoire of cellular and molecular mechanisms underlying DCM are beyond the scope of the current project. Importantly however, coronary microvascular dysfunction has been shown to be central to the etiology of DCM. To emphasize, diabetic microvascular pathology inculcates most other organ system complications of DM, e.g. retinopathy, nephropathy.

In the following sections I discuss the presentation and pathogenesis of cardiovascular complications in DM, which can be categorized from a clinical perspective as macrovascular and microvascular [55-56].

1.2.1. Macrovascular complications of DM

Arteriosclerosis is a pathological hallmark in DM, and predisposes patients to a number of life threatening complications, such as myocardial ischemia, pulmonary hypertension and stroke [56]. Acute myocardial infarction (MI) and stroke represent the second most causes of death from CVD in diabetics, amounting to 21% [57]. In Germany, almost one third of diabetic patients undergo MI with higher rates of recurrence and in-hospital death, i.e. 11 – 13%, compared to non-diabetics [58]. On the other hand, DM doubles the risk for stroke, especially in women [59]. These substantially elevated risks are direct products of macrovascular pathology manifested in atherosclerosis as a result of chronic inflammation, smooth muscle proliferation and dysfunction of the endothelial lining of arterial walls in diabetes [56]. Herein, the diabetic macrocirculation displays abundant plaques which contribute to vessel narrowing and platelet aggregation leading to thrombosis and obstruction [60]. Moreover, sudden cardiac death (SCD) is the most prevalent cause of death in diabetics, representing 27% of all cardiovascular deaths [57]. Here, coronary artery disease (CAD) of macro- and microvessels, is evidently the main contributor to SCD in diabetics, accounting for 47% of all cases [61].

1.2.2. Microvascular complications of DM

Microvessels are those with an internal diameter less than 200 – 300 μm (excluding pre-arterioles), i.e. from first to fourth order arterioles and venules to capillaries (3 μm). They are the body's main pivot for gas exchange, nutrient delivery, waste export, endocrine signaling and systemic drug distribution [62]. Beside endothelial cells (EC) and their basement membrane (BM), microvessels harbor other types of cells, such as vascular smooth muscles (VSM) (mainly in arterioles), fibroblasts and pericytes. The microvascular endothelium is the inner lining of these vessels and the interface with blood. In a healthy state, it is tightly connected to its perivascular tissue by means of physical, neural and paracrine signaling [63]. Herein, reciprocal relations are established between microvessels and the parenchyma (microvascular units) while simultaneously receiving and responding to systemic signals of all flavors and regulating tissue homeostasis [62].

The human heart has countably more endothelial cells than cardiomyocytes; they are ~3 times as many [64]. Each mm^2 myocardium harbors 3000 to 4000 capillaries [63]. This is not surprising, given the exceedingly high demand on oxygen from cardiomyocytes. At rest, myocardial oxygen extraction is 20 times that of skeletal muscles [65]. Upon increasing myocardial metabolic demand, the coronary circulation has to instantly increase blood flow.

Introduction

The coronary microcirculation is especially vigilant in this regard, quickly adapting arteriolar diameters to increasing demands [62]. Yet diabetic coronary microvessels fail on every aspect of their duty.

Upon examination, diabetic myocardia typify a conspicuous microvascular pathology of capillary and arteriolar rarefaction (Figure 1) [66]. These hearts also display loss of pericytes and increased fibrosis. Such microvascular phenotype correlates with deteriorated myocardial functional parameters, represented by increased wall stiffness, reflecting a state of diastolic dysfunction [66]. Diabetic microvessels fail to regulate their arteriolar diameters, displaying impaired vasodilation and increased vasoconstriction [67]. Studies on animal models reported inward thickening of arterioles and increasing wall-to-lumen ratio [68-69]. Moreover, the diabetic myocardial microvasculature is in a high pro-inflammatory state, characterized by increased vascular leakage and adhesive properties leading to leukocyte and platelet adhesion and infiltration in the vascular intima, as well as accumulation of activated macrophages contributing to plaque formation, vessel narrowing and thrombosis [70-71].

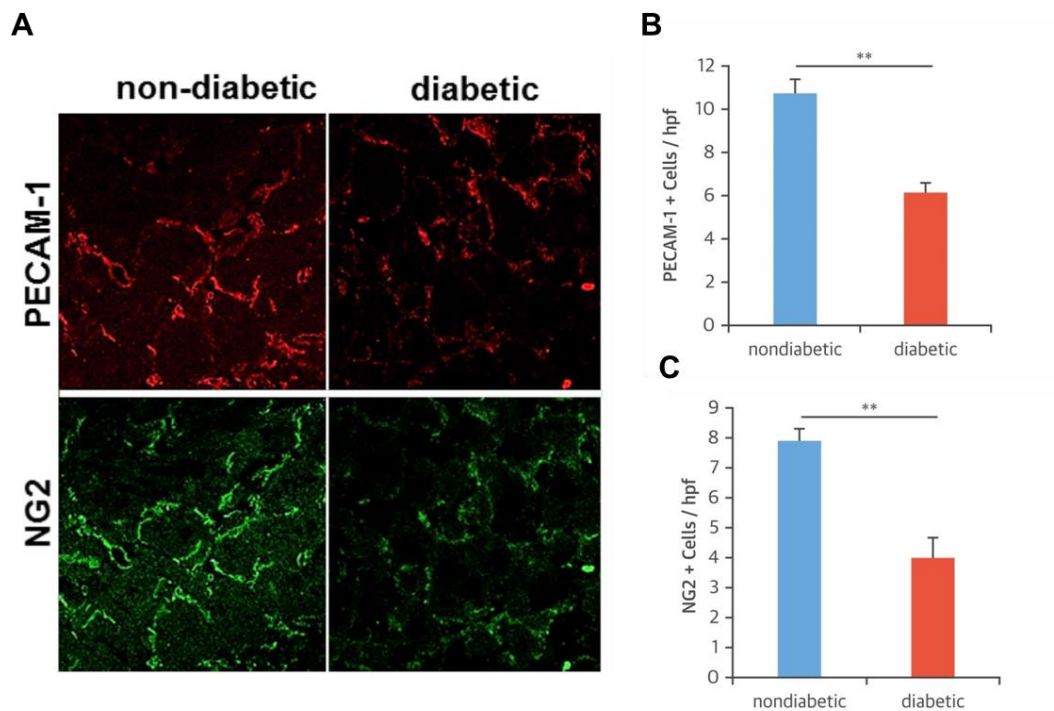


Figure 1. Cardiac microvascular phenotype in DM. (A) Tissue samples of patients with diabetes mellitus (DM) undergoing heart transplantation display capillary rarefaction. (B) Besides a reduced capillary density (platelet endothelial cell adhesion molecule-1 positive [PECAM-1 +]), (C) these patients demonstrated a loss of pericytes (NG2 +). Adapted from Hinkel et al., 2017 [66].

Introduction

These structural anomalies (remodeling) severely reduce coronary flow reserve and jeopardize the diabetic heart. They are also the underlying cause of failure of revascularization procedures, e.g. percutaneous coronary intervention, to correct myocardial ischemia. Here, the “no-reflow” phenomenon is a manifestation of myocardial microvascular pathology [72]. Moreover, microvascular pathology is a common denominator in diabetic patients with heart failure with preserved ejection fraction (HFpEF) and greater left ventricular remodeling [73].

Importantly, more patients with DM die from SCD than any other cardiovascular complication. While the true underlying mechanisms for SCD in diabetes remain poorly understood, they encompass a combination of cardiac ischemia and cardiac autonomic dysfunction. In this regard, coronary microvascular complications are the main culprit, and have been associated with elevated risk for SCD in diabetics [74]. Indeed, coronary microvascular dysfunction renders the diabetic myocardium in a state of silent ischemia, and predisposes to fatal arrhythmias [75]. Herein, diabetics with cardiac microvascular complications displayed longer QT intervals upon electrocardiographic studies [76-77]. Together, these clinical findings strongly implicate cardiac microvascular pathology in SCD among diabetic patients.

The ingrained pathological implications of cardiac microvascular dysfunction in DM and its associated morbidity and mortality framed it as the main focus of the current study.

1.2.3. Molecular mechanisms of diabetic micro-vasculopathy

Endothelial dysfunction – introduction to metabolic derangements

The default state of the endothelium is quiescence, an adaptive state of EC to regulate their metabolism in face of high blood oxygen and shear stress [78]. When activated by physiological cues, EC undergo metabolic rewiring to prepare for growth and migration. Herein, EC rely on glucose, whose uptake occurs directly through glucose transporters (GLUT), mainly GLUT1, in an insulin independent manner [79-80]. Despite being in constant contact with oxygen, glycolysis, rather than oxidative phosphorylation, remains the major pathway, by which EC not only produce energy, but also their main anti-oxidant molecule, glutathione [78, 80]. The latter is a product of the pentose pathway, where a fraction of glucose-6-phosphate is utilized to produce nicotinamide adenine dinucleotide phosphate (NADPH), which mediates regeneration of active glutathione (GSH) from glutathione disulfide (GSSG) [80]. Due to their insulin-independent glucose uptake, EC, especially microvascular, are vulnerable to hyperglycemia and elevated intracellular glucose levels. Herein, excess glucose is shunted to a number of biochemical pathways with rather cytotoxic ramifications [81]. These include the hexosamine, the polyol and the glycation pathways [82].

The hexosamine pathway produces uridine 5'-diphosphate N-acetylglucosamine (UDP-GlcNAc) from the glycolytic intermediate fructose-6-phosphate. UDP-GlcNAc is usually involved in protein glycosylation, a process that gets out of control in diabetic EC and starts impacting important cellular machinery, e.g. nitric oxide (NO) production, and impairs angiogenesis (discussed below) [83-84]. In the polyol pathway, glucose is converted to sorbitol, a precursor for formation of AGE, which wreak havoc on vital biochemical systems, such as those involved in barrier function, NO bioavailability and endothelial redox signaling, among others [85-88]. Upon binding to their receptors (RAGE), they trigger a cascade of oxidative stress and inflammation [89-90]. Finally, the glycation pathway is activated from the abundant glycolytic intermediates being converted to methylglyoxal, a pernicious metabolite impacting both endothelial and myeloid cells leading to increased inflammation, thrombosis and cell death [91].

The aforementioned biochemical derangements represent the basis, upon which DM hampers every aspect of EC functionality. A plethora of downstream cellular and molecular pathways weave an intricate network, which culminates in endothelial dysfunction. These have been the subject of immense scrutiny by myriads of studies. Therefore, I shall introduce the main of such pathways, emphasizing those with particular relevance to the present study.

Nitric oxide bioavailability and endothelial insulin resistance

As previously narrated, the diabetic endothelium loses its pliability in response to sheer stress, and in the heart, fails to adapt to increased myocardial demand. Tracing of this phenomenon leads to nitric oxide (NO), the effector molecule in vascular smooth muscle relaxation. NO is produced in the endothelium from L-arginine by the constitutively activated endothelial nitric oxide synthase (eNOS or NOS3) downstream of laminar shear stress [92]. A number of molecular derangements impact the endothelial NO production machinery and bioavailability in DM. These include reduced eNOS expression and activity. The latter is a function of phosphorylation ratio between two eNOS regulatory sites, Ser¹¹⁷⁷ and Thr⁴⁹⁵ leading to activation or inhibition, respectively. Diabetic eNOS displays an inhibitory shift by increasing N-acetyl glycosylation of Ser¹¹⁷⁷ as a direct result of the hexosamine pathway, as well as hyperglycemia-induced mitochondrial superoxide overproduction [83, 93]. Moreover, the diabetic endothelium fails to balance the production of reactive oxygen species (ROS). This mainly occurs as a results of over activation of the main ROS producing enzymes known as NOX, short for NADPH oxidases. When balanced, NOX activity is crucial for vascular homeostasis. In diabetes, however, NOX is increasingly activated, leading to overproduction of superoxide anion ($O_2^{\cdot-}$), which in turn renders NO inactive by converting it to peroxynitrite ($ONOO^-$) [94]. The latter can by itself further decrease NO bioavailability by inducing eNOS enzymatic uncoupling, a process whereby eNOS produces superoxide anion instead of NO [94]. Of particular importance in this process, is the eNOS cofactor tetrahydrobiopterin (BH_4), of which decreased availability contributes to eNOS uncoupling [95]. BH_4 is readily ablated in the diabetic endothelium as a result of the increasing oxidative environment [96]. Indeed, BH_4 supplementation was reported to enhance NO production and ameliorate endothelial dysfunction in animal models, as well as in patients of T2DM [96-97].

Interestingly, one important stimulus for NO production in the healthy endothelium is insulin [98]. Binding of insulin to its tyrosine kinase receptor (IR) entails a cascade of phosphorylation events that go in two different transduction pathways. The first starts with the IR substrate (IRS-1), of which phosphorylation creates a binding motif for the Src homology 2 (SH2)-domain containing effector kinase, phosphatidylinositol 3-kinase (PI3K). Activation of PI3K in turn triggers another cascade of phosphorylation events with multiple downstream targets including eNOS [99-100]. Herein, eNOS is phosphorylated on Ser¹¹⁷⁷ by virtue of PI3K-mediated activation of Akt [99, 101]. Importantly, this is a very sensitive pathway of insulin action with crucial physiological outcomes; it results in a significant increase in endothelial

NO and local blood flow. Moreover, it accounts for 25 to 40 % of muscle glucose uptake in response to insulin [29]. The second arm of insulin signaling transduction involves the Ras, Raf, and mitogen activated protein (MAP)-kinase/extracellular signal-regulated kinase kinase (MEK) and MAP-kinase (MAPK) signaling axis [102]. This pathway is responsible for the mitogenic effects of insulin, including its role in growth and differentiation. Though this is probably an oversimplification of the pleiotropic actions of insulin, it is important to lay down an understanding for its role in cardiovascular homeostasis. Importantly, the MAPK pathway of insulin is involved in secretion of endothelin-1 (ET-1), a major vasoconstrictor that opposes NO action [103]. Moreover, the mitogenic pathway of insulin promotes expression of pro-inflammatory endothelial adhesion molecules, such as vascular endothelial adhesion molecule 1 (VCAM1) and E-selectin, involved in leukocyte adhesion to the endothelial lining; a critical step in vascular inflammation [102, 104].

In diabetes, particularly T2DM, hyperglycemia and insulin resistance impose a selective obliteration of the PI3K arm of insulin signaling and an overdrive of the mitogenic one. This occurs as a result of cumulative insults of glucotoxicity, lipotoxicity, ROS and AGE, among others (reviewed in [29]). Of note, coronary endothelial IR can exist in a hybrid heterodimer form with the insulin-like growth factor 1 (IGF-1)-receptor (IGF-1R), which is 10-fold more abundant than endothelial IR [105]. At physiological concentrations, i.e. 100–500 pM, insulin selectively activates IR, with downstream activation of the PI3K pathway leading to NO production [106]. At higher insulin levels, the IGF-1R is activated with consequential inhibition of NO production [107].

Loss of endothelial barrier function – the role of PKC

Increased vascular permeability is another hallmark of the diabetic endothelium and among the earliest pathophysiological cues. Herein, the endothelial barrier function is disturbed as a result of diminished cell junction proteins, and elevated integrin expression. Moreover, hyperglycemia induces activation of protein kinase C (PKC) downstream of glucose-induced de novo synthesis of diacylglycerol (DAG), leading to phosphorylation of tight junction occludins and subsequent increase in vascular permeability [108]. Increased PKC activity, especially the beta isoform, has been reported to induce coronary vascular leakage in streptozotocin (STZ)-induced diabetic porcine cardiac microvessels [109]. Glucose-activated PKC β also phosphorylates vascular endothelial cadherin (VE-cadherin), the main component of inter-endothelial adherens junctions (AJs), thereby corrupting vascular barrier function [110].

Angiogenic failure – the role of ADAM10/Notch

Myocardial capillary rarefaction in DM describes a state of reduced density of microvascular networks. This is a direct reflection of the recession, as well as inability of endothelium to infiltrate the myocardial tissue by angiogenesis. Angiogenesis denotes the formation of new blood vessels from pre-existing ones, and it is the most distinguishing aspect of EC [111]. Herein, EC sense their environment and assign themselves different roles that are crucial to grow a vascular network. The so called “tip cells” are at the distal end of the growing sprout; they assume polarized, motile and invasive characters to guide the nascent sprout; while the “stalk” cells trail behind by proliferation, driving the sprout forward [111]. Communication between tip and stalk cells is imperative, as they constantly shuffle roles competing for leading positions, and relies on a number of prudently regulated signaling molecules/pathways [112]. The most important pathway in such regulation is the vascular endothelial growth factor (VEGF) and Notch pathway [113]. Herein, different members of the extracellular VEGF family bind with varying preferences to mainly 3 types of surface transmembrane receptors (VEGFR) on EC. The differential expression of these 3 receptor types dictate selection and/or maintenance of EC identity, tip or stalk [112]. Binding of VEGF to its receptor, VEGFR2 on one cell induces the expression of ligands for the transmembrane Notch receptors present on adjacent cells. Mainly 4 types of Notch (1 to 4) and 4 types of ligands (Delta-like 1, 4 and Jagged 1, 2) constitute the canonical Notch signaling [114]. Binding of Delta-like 4 (DLL4) to its the extracellular domain of the Notch receptor on adjacent cells leads to proteolytic cleavage events, ultimately releasing the intracellular domain of Notch (NICD), which translocates to the nucleus and, together with other cofactors, activates transcription of several target genes. Herein, DLL4-mediated activation of Notch represses tip cell behavior in a neighboring cell, by regulation of VEGFR expression, a process referred to as “lateral inhibition” [112, 115]. Notch activity regulates the expression of VEGFR, as well as its own ligands, e.g. a tip cell would express relatively higher VEGFR2 and VEGFR3, lower VEGFR1, higher DLL4 and low Notch, while a stalk cell would display higher VEGFR1, lower VEGFR2 and VEGFR3, lower DLL4 and higher Notch [112-113]. Such cross talk between Notch and VEGFR is imperative in initiation of sprouting, tube network formation and maintenance.

Activation of the Notch receptor upon binding to its membrane-anchored ligand on neighboring cells starts by endocytosis of the ligand. This in turn leads to pulling of the Notch extracellular domain (NEC) and exposing it to the first proteolytic cleavage event, which is carried out by a membrane anchored metalloproteinase called ADAM10, short for a disintegrin and

metalloproteinase 10 [116]. Notch ectodomain shedding by ADAM10 is a critical step in Notch activation; it prepares it for another inevitable cleavage by presenilin, a γ -secretase complex protease [117]. This releases the NICD, allowing for its transcriptional activity to take place.

The ADAM10/Notch signaling is essential for vascular development; transgenic mice lacking ADAM10 in EC (*A10AEC*) recapitulate the same vascular defects seen in those with endothelial specific Notch1 and systemic Notch4 knockouts (*N1AEC/N4^{-/-}*) [118-119]. Herein, *A10AEC* mice experience a severe coronary vascular phenotype, dedifferentiation of arterial EC, dysregulated VEGFR gene expression as well as deterioration of myocardial function [119]. Besides its indispensable role in cardiovascular development, Notch1 has been found to be cardioprotective in several pathological conditions [120-121]. Several lines of evidence indicate that Notch1 dysregulation is involved in vascular inflammation and atherosclerosis, as well as cardiomyocyte apoptosis upon ischemia/reperfusion injury [121]. Importantly, the aforementioned impairment in glucose metabolism, and the associated deleterious consequences in DM heavily impact the Notch pathway and angiogenesis [80]. However, the role of ADAM10/Notch signaling in diabetic cardiac microvascular dysfunction is unexplored.

Inflammation – the roles of NF- κ B, KLFs and MEF2

The aforementioned metabolic derangements in the diabetic endothelium all feed into a heightened state of oxidative stress. Combined with mitochondrial dysfunction and defective anti-oxidant detoxification machinery, superfluous amounts of ROS accumulate inside the diabetic EC [122]. Together with hyperglycemia, AGE and dyslipidemia, especially in T2DM, these factors elicit a strong inflammatory reaction. Clinical, as well as animal studies revealed that the diabetic circulation is flooded with inflammatory mediators and cytokines [123-125]. These include C-reactive protein, tumor necrosis factor alpha (TNF- α), interleukin 6 (IL6), intercellular adhesion molecule 1 (ICAM1), among others [123-125]. Both intracellular and systemic pro-inflammatory signals converge on activation of inflammatory cascades, most notably through the nuclear factor kappa B (NF- κ B) [126]. NF- κ B describes a family of 5 members sharing a Rel homology domain, which enables their homo- or hetero-dimerization, DNA binding, as well as interaction with other inhibitory proteins, i.e. inhibitors of κ B (I κ B) [127]. Only RelA (p65), c-Rel and RelB possess a transcriptional activation domain. Commonly however, NF- κ B refers to the most abundant heterodimer of p65 with p50; the latter is also referred to as NF- κ B1. This dimer is held inactive in the cytoplasm by association with its inhibitor, I κ B α . Canonical activation of the dimer takes place upon multiple inflammatory, but also viral and bacterial components, e.g. downstream of the Toll-like receptors.

Introduction

Signaling through these stimuli activates kinases of the I κ B (IKK), which in turn phosphorylate I κ B, leading to its degradation, thereby unleashing the heterodimer, allowing for its nuclear translocation [127]. Since its discovery in 1986 by David Baltimore, NF- κ B has become the most characterized family of transcription factor in the biology of inflammation [127-129]. In fact, the majority of transcriptionally regulated genes upon endothelial inflammation harbor NF- κ B binding sites in their promotor regions [130-131]. These include, interleukins, 1beta (IL1), IL6, IL8, and interferon gamma (IFN γ), among others [130]. Whereas expression of these pro-inflammatory molecules is activated by NF- κ B, some can feedback an activation of NF- κ B, such as TNF- α and IL1 [127]. NF- κ B is a potent inducer of endothelial adhesive properties, by regulating the expression of a suite of adhesion molecules, including P-selectin, E-selectin, ICAM1, and VCAM1 [126]. On the myeloid side of inflammation, NF- κ B regulates macrophage differentiation from monocytes by inducing colony stimulating factor (CSF) [132-133]. Moreover, NF- κ B promotes expression of matrix metalloproteinase 9 (MMP9) in macrophages, which enables extracellular matrix degradation, thereby infiltrating vascular walls [134].

The aforementioned molecular events downstream of aberrantly activated NF- κ B by diabetic signals are key steps in the development of vascular inflammation, atherosclerosis and thrombosis in DM [71, 131]. Nevertheless, it is important to emphasize that NF- κ B is essential for development and function of the vascular and immune system. Therefore, in the healthy endothelium, NF- κ B is under surveillance by crucial other factors with great implications in vascular homeostasis.

Evolution of vertebrates relied on key transitions that endowed them with their characteristic vascular endothelium 540 – 510 million years ago [135]. Herein, exaptation of homologs from ancestors into novel developmental and regulatory functions of the vertebrate endothelium was crucial, and is best represented by the so called Krüppel-like factors (KLFs) [136]. German for “cripple”, the name refers to the identified functions of Krüppel protein in *Drosophila* regulating body segmentation, the absence of which resulted in a “crippled” appearance of larva. KLFs describe a family of highly conserved zinc-finger transcription factors with a wide range of tissue distribution and function [137]. Their general structure bears a characteristic 3-finger DNA binding domains towards the carboxylic terminus, a repression domain and an activation domain towards the amine terminus [137]. They regulate gene expression by binding to CACCC elements in GC-rich regions of their target genes [138].

Introduction

At the moment there are 17 KLF members identified in mammals, of which the second member, KLF2 is the best characterized for its crucial roles in hemovascular development and homeostasis. Along with KLF4 and KLF6, the 3 KLFs are particularly enriched in the endothelium, with KLF2 and KLF4 being renowned for their vascular essential properties [139-140].

KLF2 is essential for early mammalian embryonic development; null mice die early due to defects in vasculogenesis and hemorrhage [141]. Laminar flow is the major driver of endothelial KLF2 expression, where it maintains endothelial homeostasis by transcriptional activation of a number of anti-inflammatory and anti-thrombotic effectors [142-145]. Herein, KLF2 is a strong competitor of NF- κ B [146]. In EC and monocytes, KLF2 thwarts the transcriptional activity of the p65/p50 heterodimer by hijacking its transcriptional co-activators p300 and PCAF (short for p300/cyclic adenosine monophosphate response element binding protein (CBP)-associated factor), resulting in a strong abrogation of the aforementioned NF- κ B transcriptional activity [143, 147]. Moreover, association of KLF2 with p300/CBP/PCAF leads to transactivation of a suite of endothelial protective factors. These include the coronary atheroprotective phosphatidic acid phosphatase type 2B (PPAP2B), the anti-thrombotic thrombomodulin (TM) and the barrier protective occludin [148-150]. Importantly, one long appreciated aspect of KLF2 is its ability to strongly drive eNOS expression [143, 151]. More recently, however, it was shown that it also protects against eNOS uncoupling via restoration of EC antioxidant depots of BH₄ and GSH [152]. Finally, KLF2 has been shown to maintain the state of endothelial quiescence by repression of EC main glycolytic enzyme 6-phosphofructo-2-kinase/fructose-2,6-biphosphatase 3 (PFKFB3) downstream of laminar flow, thereby reducing glycolysis [153].

Similar to KLF2, KLF4 attributes vascular protective anti-inflammatory and anti-thrombotic effects by regulating many of the same gene targets in EC [154-157]. This is evident in such a way that the two paralogs are regarded as partially redundant, wherein one makes up for the other [154]. While EC deletion of both *KLFs* is embryonically lethal, preserving a single allele of either one is sufficient for life [154, 158]. However, whereas KLF2 is constitutive in EC, KLF4 is rather adaptive [137]. Importantly, KLF4 activity has been more conspicuously highlighted in myeloid cells, where it regulates macrophage polarization and inflammatory gene expression [159]. Like macrophages, KLF4 was particularly demonstrated to be involved in phenotypic switch of vascular smooth muscle (VSM) cells, a critical phenomenon in atherosclerosis [160-161]. Importantly, KLF4 was also found ablated in VSM in diabetic

Introduction

patients as well as arteries of diabetic animal models [162]. Unsurprisingly, dysregulation of these crucial KLFs has been reported in *in vitro* studies as well as animal models of DM, with concomitant augmentation of NF- κ B signaling [162-165]. However, their role in diabetic human myocardial microcirculatory endothelium is still lacking.

Laminar flow (LF) has long been associated with atheroprotective properties; it maintains endothelial quiescence, suppresses inflammation, as well as smooth muscle intimal migration. As mentioned above, LF is, after all, the main driver of endothelial KLF expression with its associated anti-inflammatory and anti-thrombotic transcriptional activity. One way this is achieved is by myocyte enhancer factors 2 (MEF2), a family of highly conserved transcription factors indispensable for cardiovascular development, morphogenesis and homeostasis [166]. MEF2 are categorized under the MADS-box (short for mini-chromosome maintenance (MCM1) Agamous–Deficiens–Serum response factor) family with conserved A/T rich binding motifs conserved in all eukarya [167]. In mammals, MEF2 comprises 4 members, MEF2A, -B, -C, and -D, with a similar DNA-binding domain and diverse C-terminal transactivation domains [167]. Beside a plethora of target genes, MEF2 are potent inducers of *KLF2* and *KLF4* expression. In fact, the way inflammation and NF- κ B signaling can counter KLFs is via repressing MEF2 at KLF promoters [168]. The tight connection between MEF2 and KLFs is clearly demonstrated in knockout models. Herein, EC-specific deletion of *MEF2* in mice copies the severe vascular phenotypes of those from EC-specific combined *Klf2* and *Klf4* knockouts [169]. Interestingly, like KLF2 and KLF4, MEF2 members exhibit partial redundancies in the endothelium [169]. Whereas the 4 MEF2 are essential for cardiovascular development, in the adult heart, however, MEF2A and MEF2D are the predominant isoforms [170]. Despite their importance, MEF2's role in diabetic vascular dysfunction remains to be elucidated.

1.2.4. Current treatment regimens – why do they fail?

Diabetes has become a lingering malady of the human race. A plethora of therapeutic approaches have been developed, not only to reform the roots of diabetes, but also halt its devastating outcomes. These include a wide range of life style modifications and correction of CV risk factors, e.g. obesity, and indeed insulin therapy for type 1 diabetic patients [171-172]. Moreover, a number of glucose lowering medications, as well as pharmacological and surgical treatment of the failing organ systems have been in use [173]. Unfortunately, the cardiovascular pathology of DM has been ever reluctant. Herein, several pharmacological agents have been trialed to control blood glucose, dyslipidemia, hypertension, arrhythmias, inflammation, and hypercoagulability. These include metformin, statins, renin-angiotensin system blockers, antianginals, beta-blockers, aspirin, among others [174-177]. None of these pharmacological treatments have so far achieved considerable benefits in terms of reducing morbidity and or mortality from CVD in diabetics, especially with regard to coronary microvascular dysfunction [175]. Of gravity, revascularization in diabetic patients with coronary microvascular disease has constantly failed in myocardial reperfusion due to the previously mentioned “no-reflow” phenomenon [72, 178]. Several *in vitro* and pre-clinical studies have conveyed promising results with analogues of the human glucagon-like peptide-1 (GLP-1) as well GLP-1 receptor agonists (GLP-1 RA) (reviewed in [175]). GLP-1 is a glucoregulatory hormone with potent anti-hyperglycemic effects. Nevertheless, several studies have attributed cardioprotective effects, including anti-atherosclerotic, anti-inflammatory and vascular restorative effects [175]. GLP-1 based therapies include liraglutide, semaglutide, albiglutide, exenatide, among others [179-181]. Herein, a number of clinical trials reported benefits in terms of percentage risk reduction of cardiovascular events and mortality in T2DM patients, which entailed recommendations of such GLP-1 RAs by the American Diabetic Association [182-183]. These benefits were rather limited to non-fatal macrovascular events. However, when GLP-1 based therapies were tentatively trialed in diabetics with coronary microvascular disease, they were rather frail (reviewed in [175]).

These, among other examples of therapeutic interventions have so far yielded unconvincing – if not frustrating – results. Hence, there is an incessant need for novel and innovative therapies that are specifically catered to the multifaceted nature of the disease. Herein, our recently advancing knowledge of molecular biology has opened doors for promising therapeutic approaches based on small RNA molecules that have captured increasing glamour over the past three decades, i.e. micro-RNAs.

1.3. Micro-RNAs as novel molecules in biology and medicine

In 1993, Rosalind Lee and colleagues from the Ambros lab in Harvard reported on small transcriptional products of the *lin-4* gene, regulating the proper timing of post-embryonic larval development in *Caenorhabditis elegans* (*C. elegans*) [184]. They found that *lin-4* produced two transcripts of 61- and 22-nucleotide long, wherein the longer one formed a stem-loop structure that acted as a precursor to the smaller one. The smaller *lin-4* displayed sequence complementarity in the 3'-UTR of its target, *lin-14*, messenger RNA (mRNA) leading to its downregulation. The year 2000 brought about the discovery of the second small regulatory RNA in *C. elegans*, *let-7*, which served as a heterochronic switch, essential for coordination of later larval stage developmental timing, which acted in the same manner as *lin-4* [185-186]. The aforementioned functions of *lin-4* and *let-7* earned them the name “small temporal RNAs” (stRNA). Importantly, *let-7* was later found to be conserved in a wide range of metazoans, and was the first stRNA described in human [187-188]. Ever since, these small regulatory RNAs instigated a surge of research studies in all biology, and were re-named as “micro” RNAs (miRNAs) [189]. In one issue of Science in 2001, three articles featured with over a hundred miRNAs identified in several metazoan taxa, some of which showing high level of conservation [190]. Now, we know of 2600 mature miRNAs encoded in the human genome by virtue of the miRBase registry (v. 2), and over 200,000 transcripts of different isoforms (GENCODE v. 29) [191-192]. MiRNAs are small non-coding RNAs of 18 – 24 nucleotide long that are ubiquitous in all phyla of life [193]. In fact, miRNAs have recently been described in viruses, with wide implications in viral virulence [194]. Aside from their pivotal roles in development, miRNAs are now known to regulate a vast range of biological functions.

1.3.1. MiRNA biogenesis and function

The process by which mature miRNAs are generated to mediate negative post-transcriptional regulation involves multiple steps. While most miRNA genes are intragenic, i.e. residing within intronic regions of genes or alternatively the 3'-UTR (untranslated region) of coding genes, some are found within exons [195]. Nevertheless, some miRNAs occupy their own transcriptional units in intergenic regions of the genome. Of these, some have their own promoter (monocistronic), while other miRNAs are found clustered together under the control of a single promoter (polycistronic) [196]. In case of the latter, the cluster is transcribed as one long transcript encoding more than one miRNA [197]. Almost 40% of miRNAs are transcribed from such clusters [198]. Transcription of miRNAs is carried out in the nucleus by RNA Polymerase II, and to a lesser extent, Polymerase III [199]. The transcription product is a

double-stranded RNA with a stem loop, referred to as “primary” miRNA (pri-miRNA). Upon transcription, the nascent pri-miRNA is instantly processed by a co-transcriptionally recruited protein complex called the Microprocessor. The microprocessor is composed of two main subunits, DGCR8 (short for DiGeorge syndrome critical region 8) and an RNase III-like enzyme called Drosha. DGCR8 recognizes the junction between the single- and double-stranded region (SD junction) and the stem of its pri-miRNA substrate, whereas Drosha cleaves it at its stem, a process called “cropping”. Cropping of the nascent pri-miRNA results in a shorter ~ 60 nucleotide-long hairpin structure, referred to as “precursor” miRNA (pre-miRNA) [199-200]. This is the canonical pathway to generate pre-miRNAs. Notwithstanding, studies in *Drosophila* and *C.elegans* revealed another unconventional way for pre-miRNA generation, that passes the Drosha cleavage event [201]. Here, pre-miRNAs are usually a product of mRNA splicing of host genes, where spliced-out introns mimic pre-miRNAs structure, and are therefore called “mirtrons” [202]. Due to such similarity, mirtron-derived pre-miRNAs would then feed into later steps of miRNA maturation. Upon generation, pre-miRNAs are recognized by the exportin 5 protein complex (Exp5 / XPO5), which harbors a Ran guanosine triphosphate protein, and carries the processed pre-miRNA in a U-shape-like pocket [203]. As implied by its name, XPO5 then mediates nuclear export of pre-miRNAs [203]. Once in the cytoplasm, pre-miRNAs are subjected to further processing by an RNase III ribonuclease called Dicer, which cleaves a pre-miRNA on its 3'- and 5'-arms, yielding a miRNA duplex [204]. Dicer exerts its function with cooperating partners, including the HIV-1 TAR RNA binding protein (TRBP), together referred to as RISC-loading complex (RLC). RISC, short for the ‘RNA-induced silencing complex’, is a ribonucleoprotein (RNP) complex, harboring a core argonaute (AGO) effector protein, that brings about the process of RNA interference (RNAi) [205]. RISC accepts different classes of endogenous as well as exogenous small RNAs, e.g. small interfering RNAs (siRNAs) and Piwi-interacting RNAs (piRNAs) [206]. Like miRNAs, siRNAs and piRNAs are negative post-transcriptional regulators of genes [206]. In the RISC, duplex miRNAs are accommodated and further processed by argonaute proteins [207]. Therein, the duplex miRNA is unwound, and based on the thermodynamic stability of either end, one stand is “selected” for RNAi by the ribonucleoprotein complex, i.e. mature miRNA, and the other is degraded, i.e. passenger strand [208]. As a result, the mature miRNA in the effector RISC may be produced from the 5'-arm (5p) or the 3'-arm (3p) [209]. Mature single stranded miRNAs loaded on the RISC are referred to as miRISC. Figure 2 depicts the general steps in miRNA biogenesis and maturation.

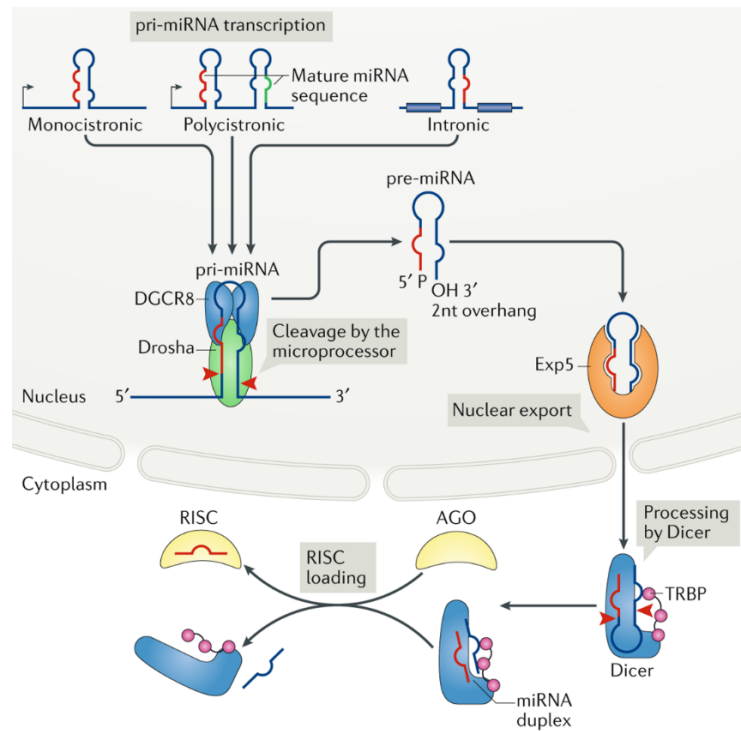


Figure 2. Biogenesis and maturation of miRNAs. Adapted from Treiber et al., 2019 [210].

MiRNAs regulate gene expression at post-transcriptional level by targeting messenger RNAs (mRNAs) on their 3'-UTR by antisense Watson-Crick base pairing, leading to cleavage and degradation of the target mRNA, or alternatively, prohibition of its translation [211-212]. Here, miRNAs serve as guides in the process, where the mature miRNA guide the effector RISC to bring about silencing by either mRNA degradation or translation inhibition, usually depending on the degree of miRNA-mRNA sequence complementarity [213]. When near perfect complementarity is established between miRNA and its target RNA, RISC exerts endonucleolytic cleavage of the target mRNA by virtue of its slicer RNase, Argonaute 2 (AGO2) [213-215]. However, miRNAs more often display imperfect complementarity with their target RNA [216-217]. Studies in *Drosophila* and *C. elegans* revealed that a 6- to 7-nucleotide sequence, usually the positions 2-7 or 2-8 from the 5' end of miRNAs, referred to as “seed” sequence, recognizes its binding motifs in the target 3'-UTR [218-220]. The seed sequence can establish a match with up to 8 nucleotides in the target mRNA 3'-UTR with even higher efficacy [221]. As a result, four types of seed matches can be generated with a hierarchy of targeting efficiency, i.e. 8mer > 7mer-m8 > 7mer-A1 > 6mer; these are referred to as the canonical site types (Figure 3) [220-221]. Such canonical, also known as “standard”, binding to the seed match in the target mRNA is enough for miRNA-RISC (miRISC) complex to exert its silencing effect, mainly by mRNA deadenylation, eventually leading to transcript decay [222].

Canonical site types

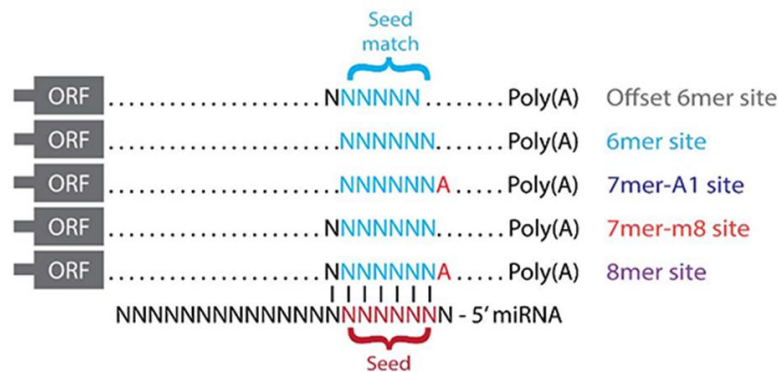


Figure 3. Canonical site types. In increasing order of binding targeting efficiency (weak to strong), the matching of mature miRNA seed to target 3'-UTR is in the following order: Offset 6mer (position 3-8 match), 6mer (position 2-7 match), 7mer-A1 (position 2-7 match + an 'A' match to position 1), 7mer-m8 (position 2-8) and 8mer (position 2-8 + and 'A' match to position 1). Adapted from TargetScan (www.targetscan.org) and Agarwal et al., 2015 [221]. N: nucleotide, ORF: open reading frame, Poly(A): mRNA 3'-Poly adenine tail.

MiRNAs can also non-canonically bind to the open reading frame (ORF) of mRNA, however, as in 6mer and offset 6mer canonical matches, with very low efficacy [221, 223]. In other cases, target RNA pairing with the 3' region of the miRNA can support mismatches in the seed at the 5' end or even totally compensate for the lack of canonical pairing [216-217, 223-224]. Interestingly, non-canonical binding has also been found to include non-Watson-Crick base pairing, e.g. G:U pairs, as well as bulges; this has been referred to as the “expanded” model of miRNA targeting [225]. Binding of a miRNA to its target mRNA does not necessarily lead to transcript cleavage or decay. Less often, yet well-documented, miRNA-mediated silencing of target genes operates via translation inhibition, usually by miRISC-mediated interference with ribosomal translation initiation factors, or ribosomal drop off upon elongation [226-227]. MiRNA-loaded AGO2 has been also shown to thwart the process of translation initiation by binding to the 7-methyl guanosine cap (m⁷G) of mRNA, thereby precluding the recruitment of initiation factors [228]. Regardless of the silencing outcome, mRNA-miRNA interaction leads to reduced expression of the target gene. Bioinformatics, as well as high throughput experimental data revealed that a single miRNA can have hundreds of direct mRNA targets and regulate the expression of up to a thousand genes [216, 221, 229-230]. Moreover, a single mRNA can be controlled by several miRNAs. In fact, it has been shown that most mammalian genes are conserved miRNA targets and almost one third of human genes were predicted miRNA targets [223, 231]. Now we know that miRNAs are involved in intricate gene regulatory networks (GRN) involved in a wide range of biological functions essential for

development, cellular differentiation, metabolism and homeostasis [232-233]. Herein, the action of miRNAs is not limited to direct reduction of gene expression; they are integrated in feedback loops within the global GRN, where they serve by buffering deleterious gene expression variation caused by new mutations [234]. In fact, the expression-buffering hypothesis qualifies miRNAs as an engine for evolution of animal complexity [234-236]. Indeed, dysfunctional miRNA-induced RNA silencing has been linked to multiple genetic diseases [213]. More recently, however, the direct implication of miRNAs in the pathogenesis of several disease has become increasingly appreciated [237-239].

1.3.2. MiRNAs in pathogenesis and potential therapy of DM and CVD

Dysregulation of several miRNAs has been reported in DM as well as CVD. The following are prominent examples of aberrantly expressed miRNAs in the contexts of pancreatic β -cell pathology, insulin resistance and importantly, cardiovascular disease in DM.

The pancreatic islet-specific miR-375 is among the earliest and most studied in the context of β -cell dysfunction. It interferes with the process of glucose-stimulated insulin secretion (GSIS) by inhibiting insulin granule fusion and exocytosis [240]. While essential for pancreatic alpha- and beta-cell turn over, miR-375 has been shown to increase β -cell apoptosis in response to lipid overload [241-242]. Moreover, miR-375 interferes with the phosphatidylinositol 3-kinase (PI3K) signaling pathway downstream of insulin [243]. Interestingly, higher miR-375 levels have been reported in T2DM and obesity mouse models, as well as type 2 diabetic patients [242, 244]. Other miRNAs have also been implicated in the process of GSIS. Here, miR-9 acts by targeting the GSIS-essential transcription factor, *Onecut 2*, whereas miR-96 brings about the same outcome via upregulation of Granuphilin, a negative regulator of insulin exocytosis [245-246]. Another miRNA, MiR-335 was also shown to interfere with the granular priming of insulin vesicles by downregulation of exocytotic proteins. Herein, miR-335 was clinically demonstrated to be negatively correlated with insulin secretion index in prediabetics [247].

The inflammatory insult to the pancreatic β -cell is a hallmark of T1DM; pro-inflammatory cytokines liberated by cytotoxic immune cells promote β -cell death, i.e. insulinitis. Studies in non-obese diabetic mice (NOD), which recapitulate the autoimmune insulinitis of T1DM, as well as human pancreatic islets revealed the role of miRNAs in the aforementioned process. Herein, the research team of Romano Regazzi in Lausanne has shown that pro-inflammatory cytokines induced β -cell expression of three miRNAs, miR-21a, miR-34a and miR-146a [248-249].

Introduction

Importantly, inhibition of miR-34a and miR-146a by specific antagomirs rescued β -cell death in human cells as well as in *db/db* mice models of T2DM [248].

MiRNAs have also been reported in regulation of insulin action in target tissues. In the liver, miR-33a and b target the hepatocyte insulin receptor substrate-2 (*IRS-2*), essential for insulin signaling [250]. Studies on obese mice with metabolic syndrome highlighted the involvement of several miRNAs in the dysregulated hepatic insulin receptor expression and insulin resistance thereof; these include miR-1271, miR-497, miR-424-5p, miR-15b, miR-96, and miR-195 [251-256]. In the adipose tissues, the miR-29 family was reported in adipocyte insulin resistance [257]. MiRNA microarray analysis revealed tens of differentially regulated miRNAs in insulin-resistant adipocytes, of which miR-320 displayed a 50-fold increase. Therein, anti-miR-320 oligo enhanced insulin sensitivity by enhancing downstream PI3K-mediated Akt phosphorylation and GLUT4 trafficking [258]. In skeletal muscles, microarray profiling of the Goto-Kakizaki (GK) rat model of T2DM identified several dysregulated miRNAs, including the cluster of miR-23, miR-24, and miR-27 [259]. Recent studies on knock-out mice models of this cluster displayed glucose intolerance. A finding that was translated in children with T1DM, where expression of this miRNA cluster correlated with other disease-specific immunometabolic derangements [260-261]. Skeletal muscle insulin sensitivity is mediated through IRS-1. In mice models of metabolic syndrome, IRS-1 was found to be a target of miR-29a, which mediated insulin resistance in these models [262]. Interestingly, this was later confirmed in human patients with T2DM, where miR-29a and c were both found to be upregulated in their skeletal muscles, which correlated with their reduced GLUT4 levels and the extent of their insulin resistance [263].

In the diabetic heart, a number of dysregulated miRNAs have been shown to contribute to the development of DCM. Cardiac tissue from STZ-induced diabetic mice were significantly depleted in miR-133a, a miRNA that has been shown to regulate CM glucose uptake via GLUT4 downstream of Krüppel-like 15 (KLF15) [264]. Herein, overexpression of miR-133a in rat neonatal CM prevented high glucose-induced hypertrophy. In contrast, miR-133a has been attributed deleterious effects in the context of diabetes-induced prolongation of QT interval, a phenomenon that has been also recapitulated in diabetic rabbit models. MiR-133a targets the *KCNH2*, also known as $I_K/HERG$ (human ether-à-go-go), encoding the alpha subunit of potassium ion channel, implying a role in diabetic arrhythmias [265]. Further, studies on glucose-induced mitochondrial dysfunction in CM implicated miR-1 as a mediator of CM apoptosis by targeting the anti-apoptotic insulin growth factor-1 (*IGF-1*) [266].

Introduction

Impaired autophagy is another pathological hallmark of the diabetic CM. Overexpression of miR-34a in the diabetic CM from mice models or *in vitro* in response to high glucose culture was reported [267]. The researchers found that inhibition of this miRNA by the flavonoid Dihydromyricetin restored CM autophagy [267]. The congruence between diabetic animal models and human patients of CVD were highlighted by studies from Li et al.; they employed microarray profiling of plasma from patients with heart failure and revealed a number of miRNAs that intersected with small RNA sequencing data from hearts of *db/db* mice [268-269]. These include miR-340-5p, miR-34a-5p, and miR-320 [269]. They found that miR-320, upregulated in CM, was involved in diabetic lipotoxicity and mitochondrial dysfunction. Inhibition of miR-320 was deemed cardioprotective in this model [269]. Other cardiac miRNAs were rather protective against DCM. Herein, miR-21 was found to be significantly depleted in the failing hearts of *db/db* mice, and when restored, its expression attenuated diastolic dysfunction in these mice and protected against diabetic lipotoxicity and hypertrophy of CM *in vitro* [270].

The first insights on miRNA dysregulation in the diabetic cardiovascular component came from on myocardial microvascular endothelial cells (MMVEC). Wang et al. performed a microarray profiling on MMVEC from GK rats, and identified eleven differentially regulated miRNAs: let-7e, miR-129, miR-291-5p, miR-320, miR-327, mir-333, miR-363-5p, miR-370, miR-494, miR-503 and miR-664 [271]. Of these, miR-320 was functionally asserted to impair angiogenesis, proliferation and migration of MMVEC by targeting VEGF-A as well as IGF-1 signaling. Inhibition of this particular miRNA was suggested as a therapeutic intervention for cardiac microvascular dysfunction in DM [271]. Another miRNA, i.e. miR-503, was later emphasized by the group of Costanza Emanuelli in the context of diabetic limb ischemia and EC dysfunction. Here, Caporali et al. reported upregulation of this miRNA in ischemic muscular tissue from diabetic mice and in response to high glucose and AGE-induced injury to human umbilical vein EC (HUVEC), as well as microvascular endothelial cells (HMVEC) [272]. The underlying mechanism, they found, was via direct targeting of the cell cycle regulators *cdc25A* and cyclin E1 (*CCNE1*). While angiogenesis is defective in cardiac microvessels in DM, it is pathologically enhanced in the retina. Overactive VEGF signaling and increased vascular permeability are involved in the pathogenesis of diabetic retinopathy [273]. Herein, miRNA expression profiling from STZ-mice informed on the downregulation of miR-200b. Intraocular injection of miR-200b mimics rescued retinal vascular permeability in those mice, and normalized glucose-induced upregulation of VEGF *in vitro* [274]. The

Introduction

researchers in the cited study verified the findings from the murine diabetic models in human retinal tissue from diabetic patients, where downregulation of miR-200b was observed by *in situ* hybridization.

In the context of vascular inflammation, miRNAs displayed a great diversity. A potent anti-inflammatory miRNA, miR-181b has been shown to operate by inhibiting NF-κB nuclear translocation, hence thwarting the expression of a plethora of responsive genes, including EC adhesion molecules [275]. Moreover, treatment with miR-181b ameliorated vascular inflammation and atherosclerosis in apolipoprotein E-deficient mice (*ApoE*^{-/-}), as well as models of endotoxemia [275-276]. Importantly, patients with sepsis displayed lower levels of miR-181b, and could therefore greatly benefit from such treatment [275]. Studies from the *ApoE* knockout mice highlighted the role of other rather inflammatory miRNAs. Therein, miR-155 was reported in macrophage uptake of oxidized LDL particles and ROS formation [277]. Systemic delivery of miR-155 antagomirs ameliorated atherosclerotic plaque formation in those mice. Patients with coronary heart disease had higher levels of this miRNA in their monocytes, yet another clinically translatable finding [277]. Vascular smooth muscles cells (VSMC) have their share of dysregulated miRNAs in diabetes. A study on *db/db* mice reported elevated levels of miR-125b in VSMC, which promoted inflammation by inhibition of histone H3 lysine-9 methyltransferase (*Suv39h1*), hence thwarting its repressive activity on multiple inflammatory genes leading to their sustained expression [278]. This is a prominent example for the epigenetic alterations imposed on vascular cells by the diabetic environment and the deeply ingrained role for miRNAs thereof.

1.3.3. MiR-17~92 cluster

In 2004, a paper by Ota et al. reported a region of the human genome pertaining to the long arm of chromosome 13, i.e. 13q31-q32, which was amplified in patients of B-cell lymphoma [279]. Designated as ‘Chromosome 13 open reading frame 25’ or *C13orf25*, the novel gene encoded two transcripts, one of which harboring a cluster of mature miRNAs, i.e. miR-17~92. *C13orf25*, also miR-17~92 cluster host gene (*MIR17HG*), stretches over 7 kb and encodes an 800-nucleotide transcript of a polycistronic cluster of six miRNAs: miR-17, miR-18a, miR-19a, miR-20a, miR-19b-1 and miR-92a-1. Earlier reports described the cluster’s oncogenic attributes due to its augmented expression in multiple solid and hematological malignancies; it was hence dubbed an ‘oncomir’ [280]. Indeed, one of the first identified transcriptional activators of the miR-17~92a cluster was the proto-oncogenic transcription factor c-Myc [281]. Notably, two paralogous miRNA families of the miR-17~92 cluster have been identified on human chromosomes 7q22.1 and Xq26.2, namely the miR-106b~25 and the miR-106a~363 clusters, comprising 3 and 6 miRNAs, respectively [282]. A total 15 miRNAs in those three families combined share 4 distinct seed sequence families defined after those of the miR-17~92 members: the miR-17 family, the miR-18 family, the miR-19 family and the miR-92 family (Table 1) [283].

Table 1. Sequence and seed families of the miR-17~92 and their paralogs

miR-17 family	miR-17-5p	CAAAGUGCUUACAGUGCAGGUAGU
	miR-20a 5p	UAAAGUGCUUAUAGUGCAGGUAG
	miR-20b-5p	CAAAGUGCUCAUAGUGCAGGUA
	miR-106a-5p	CAAAGUGCUAACAGUGCAGGUA
	miR-106b-5p	UAAAGUGCUGACAGUGCAGAU
	miR-93-5p	CAAAGUGCUGUUCGUGCAGGUAG
miR-18 family	miR-18a-5p	UAAGGUGCAUCUAGUGCAGAUUA
	miR-18b-5p	UAAGGUGCAUCUAGUGCAGUUA
miR-19 family	miR-19a-3p	UGUGCAAAUCUAUGCAAAACUGA
	miR-19b-1-3p	UGUGCAAAUCCAUGCAAAACUGA
	miR-19b-2-3p	UGUGCAAAUCCAUGCAAAACUGA
miR-92 family	miR-92a-3p	UAUUGCACUUGUCCCGGCCUGU
	miR-92b-3p	UAUUGCACUUGUCCCGGCCUCC
	miR-25-3p	CAUUGCACUUGUCCCGGCCUGA
	miR-363-3p	AAUUGCACUUGUCCCGGCCUGAA

The seed sequences are in red

Introduction

Despite the initial oncogenic view on the cluster, later studies have reported their deletion in breast and ovarian cancers, as well as melanoma [284]. Moreover, it was found that miR-17 alone exhibits anti-tumorigenic effects [285-286]. Ever since, miR-17~92 gained a more context-specific perspective. Unlike its paralogs, recent studies have identified over 30 transcription factors that regulate the expression of the miR-17~92 cluster in different tissues [283]. Further, the cluster members were also found to regulate a number of its own transcription factors, placing them in GRN with multiple feedback loops [283]. Herein, loss-of-function studies highlighted the life and developmentally essential functions of the miR-17~92 cluster. Ventura et al. performed the first study of such kind on the 3 paralogous clusters. Both miR-106b~25 and miR-106a~363 were deemed dispensable, while loss of miR-17~92 resulted in post-natal lethality due to lung, heart and B cell developmental defects [282]. It was not long until several studies ensued examining the biological activity of each member of the family [283]. The full repertoire of miR-17~92 action and/or its individual members is well beyond the scope of the current project [287]. Their cardiovascular roles, however, are of particular interest. Perhaps the most striking of all is their role in cardiovascular development. Upon cardiogenesis, miR-17~92 was found to orchestrate cardiac outflow tract development downstream of the bone morphogenic protein (Bmp) signaling pathway by regulation of *Isll* and *Tbx1* [288]. Herein, miR-17 and miR-20a are highlighted. Moreover, conditional overexpression of miR-19a/b led to lethal arrhythmias and cardiomyopathy by targeting the phosphatase and tensin homolog (*Pten*) and Connexin43 (*Cx43*) [289]. MiR-19b was also found to promote differentiation of CM *in vitro* by regulation of the Wnt/ β -catenin and the glycogen synthase kinase-3 beta (GSK3 β) pathways [290]. Importantly, one of the earliest findings on the miR-17~92 cluster was their crucial role in vascular development and angiogenesis. The team of Yajaira Suárez and William Sessa at Yale School of Medicine was first to report the role of miRNAs in EC biology and angiogenesis by interrogating the role of Dicer in conditional knockout models [291]. It had been already known that global Dicer knockout was embryonically lethal due to severe angiogenic defects [292]. Herein, conditional inactivation of Dicer in EC revealed its role in mediating the proangiogenic effect of VEGF. When examined in HUVEC, the loss of Dicer impacted EC proliferation and led to dysregulation of important signaling molecules, such as the angiopoietin-1 and VEGF receptors tyrosine kinases (i.e. TEK (Tie-2) and KDR (VEGFR2), respectively), eNOS and IL8 [293]. VEGF was found to induce expression of the miR-17~92 cluster, wherein the miR-18a, miR-17-5p, and miR-20a could, in the absence of Dicer, restore EC proliferation. Moreover, they reported the specific targeting of anti-angiogenic thrombospondin 1 (*Tsp1*) by miR-18a.

They then went further by examining the particular role of miR-17~92 cluster in EC by generating inducible vascular EC-specific miR-17~92 knockout mice, where they reported reduced retinal and ear angiogenesis by derepression of *Pten* as a common target shared by all members of the cluster [294]. However, in another study by the same group on the same mouse model, they reported a phenotype of enhanced EC morphogenesis and coronary arterial vessel count. When subjected to limb ischemia, these mice displayed accelerated recovery and arteriogenesis by 3D micro-computed tomography (micro-CT). Herein, they highlighted the role of miR-19 as an inhibitor of arteriogenesis via direct targeting of the canonical WNT signaling downstream Frizzled receptors (FZD) and its co-receptor of the low-density lipoprotein receptor-related protein 5/6 class (LRP5/6) [295]. They also managed to enhance blood flow in aged mice by specific locked-nucleic anti-sense (LNA) to miR-19. It was clear that individual members of the miR-17~92 exhibit context- and tissue-specific functions.

MiR-92a

As the miR-17~92 cluster started to gain momentum in research describing the activity of its individual members in the context of development and tumor angiogenesis, it was not long until the last member on the 3'-end of the polycistronic cluster revealed its potential. The group of Stefanie Dimmeler at the Goethe-University in Frankfurt were first to interrogate the activity of miR-92a in EC, as well as in animal models. In 2009, a leading paper by Angelika Bonauer et al. featured on *Science*, describing the anti-angiogenic properties of miR-92a. Herein, miR-92a overexpression blocked sprouting and tube formation network of HUVEC *in vitro*, and reduced the number of vessels they formed in nude mice when implanted in Matrigel plugs [296]. In zebrafish (*Danio rerio*), overexpression of miR-92a by pre-miR-92a injection in embryos led to severe developmental defects in their inter-segmental vessels (ISV). In mice models of limb or myocardial ischemia, targeted inhibition of miR-92a by intravenous injection of specific anti-sense oligos (antagomirs) led to significant improvements in neovascularization and tissue perfusion of the ischemic limb, as well as cardiac left ventricular systolic and diastolic functions. They went on examining miR-92a downstream targets by Affymetrix mRNA expression profiles of differentially regulated genes upon its overexpression in EC, and identified a number of vasoactive direct, as well as indirect, targets essential for vascular development and homeostasis. These include mRNAs for integrin subunits $\alpha 5$ (*ITGA5*), endothelial nitric oxide synthase (*NOS3*) and the histone deacetylase, sirtuin 1 (*SIRT1*), among others. These pioneering findings propelled a deluge of studies investigating the role of miR-92a and/or the therapeutic potential of its inhibitors in a number of CVD models.

Introduction

A study by Wu et al. was inspired by the miR-92a-mediated regulation of eNOS, a direct downstream target of the flow-sensitive and anti-inflammatory KLF2 [297]. In their study on HUVEC, they confirmed the flow-dependent regulation of miR-92a, where oscillatory / atherogenic flow upregulated miR-92a, which was indeed found to target *KLF2*, and its downstream eNOS and Thrombomodulin (TM). Herein, miR-92a upregulation was deemed an ominous atherogenic miRNA, of which inhibitors promise vascular protective properties.

In 2013, another elegant study featured in *Circulation* with powerful translational implications [298]. Rabea Hinkel and colleagues from Ludwig Maximilian University of Munich demonstrated the cardioprotective effects of miR-92a inhibitors in rather large animal models, i.e. pigs. Herein, local myocardial delivery of locked-nucleic anti-sense to miR-92a (LNA-92a) via heart catheter, either antegrade or retrograde, significantly reduced infarct size and improved all measured parameters of myocardial function in porcine models of ischemia/reperfusion injury. Importantly, LNA-92a enhanced capillary density (Figure 4), and ameliorated inflammation. Moreover, they showed that mice models of global or CM-specific knockout of miR-92a maintained their cardiac functional parameters upon induction of acute myocardial ischemia. Finally, *in vitro* experiments highlighted the anti-inflammatory effects of LNA-92a in HUVEC, as well as its cardiomyocyte protective effects.

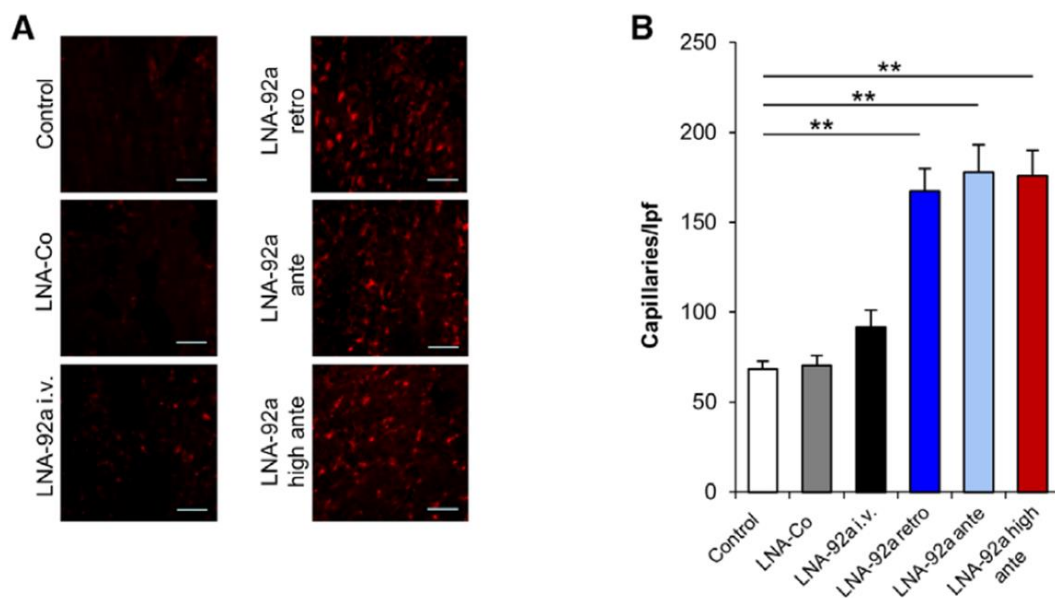


Figure 4. Regional locked nucleic acid modified antisense miR-92a (LNA-92a) application improves vascularization. Capillary density was determined by platelet endothelial cell adhesion molecule-1 staining (red) in the ischemic area at risk. Representative staining is shown in A (scale bar = 50 μm), and quantification in shown in B. Adapted from Hinkel et al., 2013 [298].

Introduction

More on miR-92a's involvement in vascular pathology was addressed in a study by Loyer et al., this time highlighting another vascular enriched KLF, i.e. KLF4, as a miR-92a target [299]. In their study, both *in vitro* and *in vivo* (using LDL receptor knock-out mice *Ldlr*^{-/-}) models of atherosclerosis displayed overexpression of miR-92a, as well as a number of inflammatory markers, including IL6, ICAM1, and monocyte chemotactic protein 1 (MCP1), coupled with reduced KLF2 and KLF4 expression. Moreover, miR-92a regulation was also found to be flow-dependent; it was upregulated in atheroprone vascular regions (aortic arch) compared to more protected ones (descending thoracic aorta). Antagomir inhibition of miR-92a was also found to be protective against atherosclerosis in *Ldlr*^{-/-} mice and oxidized LDL-induced injury in HUVEC. Both KLFs were deemed direct targets of miR-92a, of which downregulation together with another novel target described by the authors, i.e. suppressor of cytokine signaling 5 (SOCS5), exacerbate the observed vascular inflammatory phenotypes

The vascular protective role of miR-92a inhibition was further demonstrated in a study by Daniel et al. from Hannover Medical School as well as the Dimmeler group. In mice models of arterial injury, systemic LNA-92a delivery promoted re-endothelialization and attenuated vascular scar (neointima) formation [300]. Importantly, such protective effect was recapitulated in EC-specific miR-92a knockout mice. The underlying mechanisms were attributed to derepression of the miR-92a targets, *Sirt1*, *Itga5* and the KLFs, *Klf2* and *Klf4*, and their downstream eNOS.

In yet another breaking finding from 2017, Hinkel and colleagues reported upregulated levels of miR-92a in porcine models of DM [66]. Herein, characterization of *INS*^{C94Y} transgenic pigs of permanent neonatal diabetes not only reflected the cardiac pathohistological phenotype of microvascular dysfunction in human diabetic patients, but also functional deterioration of the myocardial function.

Despite the abovementioned findings on miR-92a in CVD models, its role in DM-induced cardiovascular phenotype remains elusive. Does overexpression of miR-92a in diabetic pig myocardia reflect the situation in man? Is miR-92a involved in the diabetic vascular phenotype, particularly its morbid microvascular complications? How does miR-92a behave in cardiac microvessels on a molecular level? Are therapeutic interventions with miR-92a inhibitors translatable in man, particularly in the context of diabetic microvascular dysfunction? These are all questions that provoked the research endeavor presented in this doctoral study.

1.4. Study objectives

In light of the available knowledge on diabetic cardiovascular complications, the pivotal role of miRNAs in their pathogenesis, and the empirical evidence on miR-92a dysregulation from animal models of CVD and DM, the present study is set to the following epistemic goals:

- 1- Characterization of human cardiac microvascular phenotype in DM.
- 2- Does miR-92a play a role in such phenotype?
- 3- Elucidation of the underlying molecular mechanisms.

The methodology combines a set of qualitative and quantitative experiments to characterize aspects of cardiac microvascular endothelial dysfunction in multiple relevant models of DM compared to controls, measure the levels of miR-92a therein, conduct a treatment study based on the findings, and finally identify and verify downstream molecular targets that contribute to the observed phenotype. To this end I designed *in vitro* experiments to address the pathological hallmarks of the diabetic myocardium in human patients, e.g. angiogenic defects and inflammation. I applied molecular biology to quantify miR-92a in the diabetic models. Moreover, I experimented with miR-92a specific inhibitors as well as mimics to establish whether a correlation exists between miR-92a and the diabetic phenotype. Further, I conducted *in silico* analysis to identify relevant and/or novel downstream molecular targets of miR-92a. By means of molecular biology, I identified expression levels of these targets in diabetic models and validated their contribution to the observed phenotype by independent loss-of-function experiments. I described the relation and/or direct interaction between miR-92a and its targets in human as well as two other mammalian species. Finally, I suggest a model by which miR-92a dysregulation ensues as a result of diabetes and/or hyperglycemia.

2. Materials and Methods

2.4. Cell culture

Primary human cardiac microvascular endothelial cells (HCMEC) (PromoCell C-12286) obtained from cardiac ventricles of a 38-year old Caucasian female (Lot no. 446Z001.1), 63-year old non-diabetic (Lot no. 447Z026.3), 63-year old type 2 diabetic (Lot no. 451Z015.1), or 51-year old non-diabetic (PromoCell C-12285 - Lot no. 470Z011.7) Caucasian males were cultured in PromoCell microvascular media (MV) (C-22020) or MV2 (C-22022) media, supplemented with corresponding supplement mixes (C-39225 or C-39226, respectively) and 0.1% penicillin/streptomycin (PS). Cells were used for experiments between passages 2 to 8.

Human umbilical vein endothelial cells (HUVEC) from a single donor (ATCC PCS-100-010TM) or pooled from multiple donors (Lonza CC-2519 Lot: 463156) were cultured in PromoCell endothelial growth media (EGM) (C-22010) or EGM2 (C-22011), supplemented with their corresponding supplement mixes (C-39215 or C-39216, respectively) and 0.1% penicillin/streptomycin (PS). Cells were used for experiments between passages 4 to 8.

MV/MV2 and EGM/EGM2 have a glucose concentration of 5.5 mM, reflecting that of non-diabetic plasma [301]. For high glucose experiments, concentration was raised to 30 mM.

Mouse cardiac microvascular endothelial cells (MCMEC) (Cedarlane CLU510) were cultured according to provider in Dulbecco's Modified Eagle Medium (DMEM) (GibcoTM 11965092) with 10 mM 4-(2-hydroxyethyl)-1-piperazineethanesulfonic acid buffer (HEPES) (PanBiotechTM P05-01100), 1% PS and 5% fetal bovine serum (FBS). Cells are received at passage 40, sub-cultured and used for experiments until passage 46.

THP-1 monocytes (ATCC TIB-202) were maintained in Roswell Park Memorial Institute medium 1640 (RPMI 1640) (Biowest L0498-100), supplemented with 10% FBS, 0.05 mM 2-mercaptoethanol (Roth[®] 4227) and 1% PS. Cells were kept in culture, and passaged indefinitely by dilution in medium to a suspension concentration of 500,000 cells/mL.

All cells were cultured and maintained in polystyrene tissue culture flasks (Sarstedt, Germany), and kept in a humidified incubator at 37° Celsius and 5% CO₂.

Passaging of adherent cells was done at near confluence, i.e. 80 – 90%. Herein, the culture medium was sucked using a sterile glass tip attached to a vacuum pump. Cells were then washed with pre-warmed calcium and magnesium ions-free phosphate buffer saline (PBS)

(Gibco™ 10010023) to remove serum and/or growth factor residues. Cell detachment was achieved by proteolytic digestion of cell adhesion proteins to culture vessel surface, and facilitated by ion chelation. To this end, cells were incubated for 2 – 3 minutes with pre-warmed 0.25% trypsin / Ethylenediaminetetraacetic acid (EDTA) (Gibco™ 25200-072) at 37° C. Upon verification of cell detachment by microscopic examination, trypsinization was then interrupted by addition of serum or serum-containing culture medium. Cells in suspension were collected in sterile Falcon™ polypropylene tubes and centrifuged at 250 RCF for 5 minutes. Cell pellets were re-suspended in fresh medium and a 10 µL sample was diluted in 0.4% trypan blue solution (Gibco™ 15250061), applied to C-Chip Hemocytometer (Neubauer Improved). Live (Trypan-negative) cells were counted under inverted light microscope. Cell count was determined by the following equation:

$$\text{Cells per mL} = \frac{\text{Count in 4 corner squares}}{4} \times \text{dilution factor} \times 10000$$

2.5. Transfection

Cells in culture were transfected at 80% confluence in MV2 (HCMEC); EGM2 (HUVEC) or serum-free DMEM (MCMEC) with Lipofectamine RNAiMAX reagent (Invitrogen 13778150) and small RNA at a final concentration of 10 nM using manufacturer's protocol. Transfection complexes were first prepared by dilution of reconstituted small RNA solutions and Lipofectamine in OptiMEM® (Gibco™ 31985062) according to manufacturer's protocol and culture vessel size. The two dilutions are mixed 1:1 and incubated for 10 minutes at room temperature. Transfection complexes were then added to the cells and incubated for 4 – 6 hours, followed by medium change and incubation for additional 24 hours in complex-free medium before cells were used for assays. For wound healing and flow chamber assays, the cells are collected by trypsinization 4 – 6 hours after transfection and seeded in their respective assay culture vessel and regular culture medium for 24 hours or until a confluent layer is established. The following small RNA (Ambion®) were used in this study: Anti-miR™ hsa-miR-92a-3p (Ant-92a) (AM10916); anti-miR™ Negative Control (Ant-Ctrl) (AM17010); pre-miR™ miRNA precursors hsa-miR-92a (PM10916) and mmu-miR-92a (PM10312) (pre-92a); pre-miR™ miRNA precursor negative controls (pre-Ctrl) (AM17110 / AM17111) or Silencer® siRNAs against human *ADAM10* (ID: s1006) (siADAM10); *KLF2* (ID: s20269) (siKLF2); *KLF4* (ID: s17793) (siKLF4); *MEF2D* (ID: s8656); *MEF2A* (ID: s230700) or mouse *Adam10* (ID: 59937) (siAdam10); *Klf2* (ID: s68830) (siKlf2); *Klf4* (ID: s68837) (siKlf4); or negative controls (4390844 / 4390846) (siCtrl).

2.6. Tube formation

Angiogenesis by tube formation was performed in μ -Slide Angiogenesis (Ibidi 81506) according to manufacturer's protocol (Application Note 19), and the following modifications. 10.5 μ L Matrigel[®] matrix basement membrane (Corning[®] 354234) were pipetted at 0 – 4° C using pre-chilled pipette tips in the slide inner-wells, and allowed to solidify at room temperature. An average of 12,500 – 13,000 endothelial cell suspension/well were seeded on top (outer-well), and incubated in a humidified incubator at 37° C and 5% CO₂. Tube formation was examined after 12 hours of incubation and bright-field 5x-microscopic images were taken by Leica DMI8 (Leica Microsystems, Germany).

2.7. Wound healing

Wound healing assays were performed in a Culture-Insert 2 Well in μ -Dish 35 mm (Ibidi 80206) according to manufacturer's protocol (Application Note 21). Alternatively, the 2-well culture inserts for self-insertion (Ibidi 80209) were used wherever feasible. Cell suspensions of 5×10^5 cells/mL were prepared and 50 – 70 μ L cell suspensions were added per well of the 2-well insert, and cells were incubated for 24 – 36 hours to form monolayers. The inserts were then carefully removed with sterile forceps and the cells were washed with PBS, and fresh medium was added. Phase contrast 5x-microscopic images were taken at time intervals 0, 8 and 24 hours.

To perform wound healing with BioTek Cytation 1[™] multimode reader (Agilent), the Culture-Insert 2 Well for self-insertion was inserted in the middle of a 6-well cell culture plate (TPP[®] 92006), and the procedure was followed as mentioned above. The time-lapse imaging was performed using the device's bright field camera. Using the device's software, a protocol was established, wherein 5x-microscopic images were taken at 5-minute intervals over 6-hours. The image beacons were adjusted manually for every wound.

2.8. Flow chamber assay

HCMEC suspensions were prepared at a 5×10^5 cells/mL, and 40 μ L were added to each channel of μ -Slide VI^{0.4} (Ibidi 80606). Cells were incubated for 24 – 36 hours to form stable monolayers. The flow chamber experiment was adapted with modifications from Stachel et al., 2013 [302]. Briefly, THP-1 monocytes were stained with Vybrant[™] Cell-Labeling Solutions DiI (V-22885) or DiO (V-22886) according to manufacturer's protocol. Cells were washed with PBS and a concentration of 7.5×10^5 cells/mL was prepared in their culture medium.

A perfusion system was established; two 50 mL Original-Perfusor® syringes (Braun) were filled with THP-1 cell suspension or MV2 medium (washing medium), connected with perfusion lines to a 3-way valve and placed each in Perfusor® Space pumps (Braun). A tube adapter set (Ibidi 10831) was connected to the valve and in the flow chamber inlets. A flow of 47.4 mL/hour was established to simulate venous shear stress 1 dyn/cm^2 and flow round was run for each channel as the follows: 2-minute washing medium, 5-minute cell suspension and 2-minute washing medium. The flow slide was then imaged by phase contrast and fluorescent imaging (Leica Microsystems, Germany).

Figure 5 depicts the general setup for methods: 2.3, 2.4 and 2.5 from Ibidi.

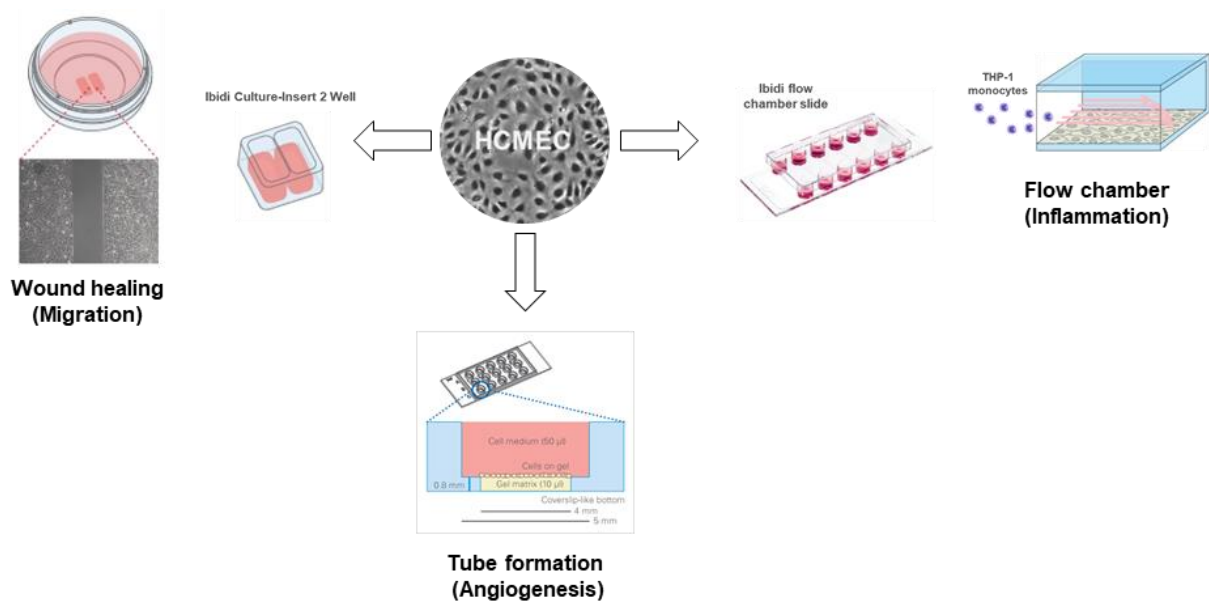


Figure 5. Assay of endothelial cell function (e.g. HCMEC) using Ibidi culture vessels.

2.9. Endothelial spheroid assay

The endothelial spheroid assay is an established method to evaluate sprouting behavior. When EC are cultured in hanging drops, they form spheroids; when these spheroids are embedded in collagen matrices they tend to form sprouts, the count and length of which can be analyzed as read-outs for angiogenic behavior in a 3D environment.

We applied the protocol from Tetzlaff and Fischer, 2018, using MCMEC instead of HUVEC [303]. Briefly, MCMEC were cultured, transfected, trypsinized, collected and counted as previously mentioned in 2.1 and 2.2, and 80000 cells were suspended in 4 mL microvascular media and 1 mL methocel stock solution. Methocel stock solution was prepared by dissolving 3 g of autoclaved methyl cellulose (Sigma-Aldrich M9512, 4000 centipoises) in preheated

serum-free EGM (PromoCell C-22010), and centrifuged to 5000 x g. Using a multi-pipette 25 μ L drops of the cell suspension-methocel were pipetted in Petri dishes and incubated upside down in humidified 37° Celsius and 5% CO₂ incubator for 24 hours. Spheroid formation was examined under inverted cell culture microscope and upon successful formation, spheroids were collected in warm PBS, and centrifuged at 200 x g for 5 minutes. The supernatant is discarded and Spheroids are then re-suspended in 2 mL methocell solution containing 20% FBS. Collagen medium was prepared on ice by mixing 6 mL collagen stock solution* and 0.75 mL 10x M-199 medium (Sigma-Aldrich M0650), then pH was adjusted by μ L-wise addition of sodium hydroxide (NaOH) until color change is observed (yellow to orange) as indicator. Two mL of the collagen medium are added to 2 mL of spheroid suspension and carefully mixed to avoid air bubbles, and 1 mL of the mix is added per well of 24-well plates, and incubated at 37° Celsius and 5% CO₂. An hour later, 100 μ L microvascular medium is added per well; in our hands this was important to induce sprouting. Sprouts were examined after 24 and 48 hours, imaged and analyzed for sprout length and count by Leica DMi8 and built-in software (Leica Microsystems, Germany).

2.10. Proliferation assay

10,000 HCMEC cells were seeded in fibronectin-coated (Sigma-Aldrich F1141) μ -Slide 8 Well chambered coverslip (Ibidi 80806) and incubated overnight. Proliferation assay was performed following the manufacturing instructions of the Click-iT™ Plus EdU Cell Proliferation Kit (Alexa Fluor™ 488) (Invitrogen C10637). Cells were treated with 10 μ M EdU for 24 hours. Medium was sucked and cells were washed with PBS, fixed with cold 4% formaldehyde for 10 minutes, and washed again with PBS. Nuclei were stained by 4', 6-Diamino-2-phenylindole dihydrochloride in Antifade solution (DAPI/Antifade) (Chemicon® S7113) for 10 minutes, washed with PBS, and imaged with fluorescent microscopy (Leica Microsystems, Germany). Proliferating cells were detected by positive EdU staining and the percentage of proliferating cells was calculated on the total cell number by nuclear staining.

2.11. Western Blot

Cells were collected by trypsinization, centrifuged at 250 RCF for 5 minutes and washed with calcium and magnesium ions-free PBS and centrifuged at 250 RCF for 5 minutes. Cells were lysed for 10 minutes on ice in lysis buffer (10 mM Tris/HCl pH 7.5; 150 mM NaCl; 0.5 mM EDTA; 0.5% NP-40) containing cOmplete™ protease inhibitor cocktail (Sigma 11697498001) and PhosphoSTOP™ phosphatases (Roche) (Sigma 04906845 001). Lysates were centrifuged

Materials and Methods

at 8000 RCF and 4° C for 10 minutes. Supernatants were recovered and protein concentration was quantified by Pierce™ Detergent Compatible Bradford Assay Kit (Thermo Scientific™ 23246). Herein, 30 µL samples were diluted in 1 mL Bradford reagent (i.e. added to 970 µL) in single use Nano-photometer cuvettes (Roth Rotilabo® PMMA Semi-micro 1.6 mL XK23), and colorimetric measurements were performed at 595 nm in NanoPhotometer® NP80 (IMPLEN, Germany). Protein concentrations are identified relative to a previously set standard curve with Albumin Standard (Thermo Scientific™ 23209). Samples were diluted to equal concentrations in Laemmli buffer (BioRad 1610747) with 50 µM Dithiothreitol (Roche) and incubated at 95° C for 7 minutes to fully denature proteins according to U. K. Laemmli [304]. Gel electrophoresis of protein samples was performed according to manufacturer's instruction manual (Biorad 1658100) [305-307]. Laemmli-denatured protein samples were run on stacking and resolving Tris-Glycine gels (TGX Stain-Free™ FastCast™ Acrylamide Kit – Biorad 1610180 or 1610182), or precasted Mini-PROTEAN TGX Stain-Free Gels (Biorad 4568083) and in Tris/Glycine/Sodium dodecyl sulfate (SDS) running buffer. Protein transfer to polyvinylidene difluoride (PVDF) membranes was performed in transfer buffer (Biorad 10026938) and Trans-Blot® Turbo™ Transfer System (Biorad 1704150). Membranes were blocked for 1 hour with 3% bovine serum albumin (BSA) (Roth® T844.4) in Tris-buffered saline with 0.3% Tween® 20 detergent (TBST), and incubated overnight with the following primary antibodies in blocking solution at a 1:1000 dilution: mouse monoclonal anti-GAPDH (Cell Signaling 97166); rabbit monoclonal anti-ADAM10 (Abcam ab124695); rabbit monoclonal anti-Cleaved Notch1 (Val1744) (Cell Signaling 4147); rabbit polyclonal anti-KLF2 (Thermofisher PA5-40591); rabbit polyclonal anti-KLF4 (Cell Signaling 4038); mouse monoclonal anti-VCAM1 (Santa Cruz sc-13160) or mouse monoclonal anti-ICAM1 (Santa Cruz sc-8439). Membranes were washed thrice in TBST and once in TBS for 5 minutes on a rocking plate. Membranes were then incubated accordingly in Horseradish-Peroxidase-linked secondary anti-mouse (Cell Signaling 7076S), or anti-rabbit (Cell Signaling 7074S) antibodies in 3% BSA in TBST for 1 hour at room temperature. Membranes were then washed as previously and the signals were developed by treatment with enzymatic chemiluminescence (ECL) reagents (Amersham™ RPN 2232). Chemiluminescent signals were read on the membranes by ChemiDoc™ Imaging System from Biorad and analyzed by Image Lab 6.1 software from Biorad. Adjusted band volumes for target proteins were normalized to those of GAPDH as housekeeping control.

2.12. Quantitative PCR

Cells were collected by trypsinization, centrifuged at 250 RCF for 5 minutes and small and/or large RNA was extracted by NucleoSpin® miRNA kit (Macherey & Nagel, Germany) according to manufacturer's protocol. RNA quality and quantification was performed by spectrophotometry (NanoDrop™ - Thermo Scientific); guidelines regarding wave length absorbance ratio of 260/280 and 260/230 were followed, so that the ratios between wave lengths 230:260:280 = 1:2:1 were accepted. For gene expression analysis, 500 ng RNA were used for cDNA synthesis by Omniscript® Reverse Transcription kit (Qiagen 205113) following manufacturer's protocol. Quantitative PCR was run using TaqMan™ Fast Advanced Master Mix (Applied Biosystems 4444557) and the following TaqMan assays (primers): human beta-actin (*ACTB*) (Hs99999903_m1); *ADAM10* (Hs00153853_m1); *KLF2* (Hs00360439_g1); *KLF4* (Hs00358836_m1); *NOS3* (*eNOS*) (Hs01574659_m1); *MEF2A* (Hs01050409_m1); *MEF2C* (Hs00231149_m1); *MEF2D* (Hs00954735_m1); *SLC2A4* (*GLUT4*) (Hs00168966_m1); *SLC2A1* (*GLUT1*) (Hs00892681_m1); mouse beta-actin (*Actb*) (Mm02619580_g1); *Adam10* (Mm00545742_m1); *Klf2* (Mm00500486_g1); *Klf4* (Mm00516104_m1).

For miRNA quantification, 20 ng RNA were used for the cDNA synthesis using TaqMan™ Advanced miRNA cDNA Synthesis Kit (A28007) and TaqMan™ Advanced miRNA Assay (A25576) and the following assays for both human and mouse: hsa-miR-92a-3p (assay ID 477827_mir) and hsa-miR-26a-5p (assay ID 477995_mir) as endogenous control. Real-Time PCR (RT-PCR) was run using the recommended thermal cycling profiles and StepOnePlus™ software v2.3 (Applied Biosystems) to calculate the comparative C_T (relative quantification).

Myocardial tissue from *INS*^{C94Y} transgenic diabetic pigs and non-diabetic littermates were obtained from the Institute of Molecular Animal Breeding and Biotechnology, Gene Center, LMU Munich [66, 308]. Those pigs harbor an insulin mutation that disrupts a sulfide bond between the A and B chains of the insulin molecule leading to misfolded insulin structure and impaired secretion, as well as pancreatic β-cell apoptosis [308]. Tissue was dissociated in ML buffer from NucleoSpin® miRNA kit (Macherey & Nagel, Germany), and gentleMACS™ Dissociator and M-tubes (Miltenyi Biotec). RNA extraction and gene expression analysis was performed as previously described using the following TaqMan assays (primers): pig beta-actin (*ACTB*) (Ss03376563_uH); *ADAM10* (Ss03373280_m1); *KLF2* (Ss06942161_g1); *KLF4* (Ss03391985_m1) and *MEF2D* (Ss06884968_m1).

2.13. ImageJ analysis

Tube formation was analyzed using Angiogenesis Analyzer software of ImageJ. A tube in my analysis is the structure referred to by the program as “master segment”, and was included in measures if it contributed to a continuous mesh structure (Figure 6). To minimize artifacts, a threshold of 120 pixels was set for the master segment size. Upon running the automatic analysis, network features are detected, analyzed and values are provided by the software. Two parameters were considered as endpoints for tube formation measures: total tube length (μM) and tube count.

Wound healing was analyzed using ImageJ polygon selection to trace and measure the open wound area on native phase contrast images. Wound healing is represented as percentage of open wound at a later time point relative to the initial wound area upon chamber removal (time 0).

Adherent THP-1 to endothelial monolayers in flow chambers were counted by particle number quantification in ImageJ. Briefly, images were split in 3 color components, and depending on the dye (DiI or DiO), the red- or green-colored image was subjected to threshold adjustment. Particle analysis settings were applied and particles were counted.

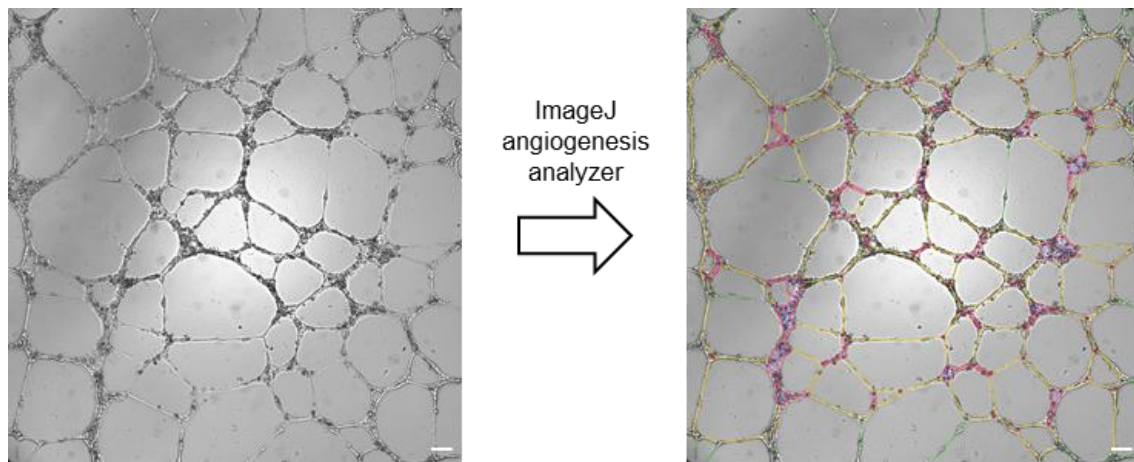


Figure 6. Automatic detection of tube formation network in bright field images by ImageJ angiogenesis analyzer. Elements are color-coded to distinguish master segments (yellow); small segments (double red); branches (green); junctions (blue dots at branch bases) and master junctions (blue dots encircled in red). Scale bars equal 100 μM .

2.14. Immunofluorescence

Myocardial tissue from *INS*^{C94Y} transgenic diabetic pigs and non-diabetic littermates (see 2.9.) were cryo-sectioned to 5 µm-thick sections, mounted on histology slides. Sections were fixed with cold acetone for 10 minutes, washed with PBS and blocked for 1 hour with a blocking solution of 2% bovine serum albumin (BSA) (Sigma A9647) and 0.2% Triton[®]-X (Roth 3051.2) in PBS. Sections were incubated overnight with rabbit monoclonal anti-ADAM10 (Abcam ab124695) and mouse monoclonal anti-CD31 (PECAM1) (Invitrogen MA1-80069) primary antibodies at 1:50 dilutions. Sections were then washed thrice with PBS before incubation with secondary antibodies. Goat anti-rabbit Alexa Fluor[®] 488-coupled (Invitrogen A-11008) and goat anti-mouse Alexa Fluor[®] 594-coupled (Invitrogen A-11005) secondary antibodies were incubated with sections for 2 hours at 1:200 dilutions. Sections were washed thrice with PBS, and 40x magnification images were taken by fluorescence microscopy (Leica Microsystems, Germany). Analysis of fluorescence intensity was performed by the microscope's built-in software.

2.15. Dual-Luciferase bioluminescence

Human embryonic kidney 293 cells (HEK293) (ATCC CRL-3216) were cultured in BRAND[®] bioluminescence-compatible, i.e. white with transparent flat bottom, 96-well plates (cellGrade[™] 781974) at 30,000 cells/well seeding density in antibiotic-free DMEM, supplemented with 5% FCS. At 90-95% confluence, transfection of predicted targets' 3'-UTR in expression vectors (pEZX-MT06 backbone) with reporter Firefly and *Renilla* luciferase reporters (GeneCopoeia[™]) was performed according to manufacturer's protocol using EndoFectin[™] Max Transfection Reagent (EF013). One hundred ng of the following plasmids DNA were transfected / well: mouse *Adam10* (NM_007399.4) (GeneCopoeia[™] MmiT090821-MT06); mouse *Klf2* (NM_008452.2) (GeneCopoeia[™] MmiT088487); mouse *Klf4* (NM_010637.3) (GeneCopoeia[™] MmiT054570); mouse *Itga5* (NM_010577.4) (GeneCopoeia[™] MmiT093043); human *MEF2D* (NM_001271629.2) (GeneCopoeia[™] HmiT130501) and control vector (GeneCopoeia[™] CmiT000001-MT06). After 4 - 6 hours, pre-92a or pre-Ctrl were transfected as previously mentioned (section 2.2) and incubated for another 48 hours. Assay of luciferase activity was performed according to manufacturer's user manual of Luc-Pair[™] Duo-Luciferase Assay Kit 2.0 (LF001). Bioluminescence was read by BioTek Cytation 1[™] multimode reader (Agilent) and the ratio of firefly to *Renilla* (FLuc/RLuc) was calculated. Figure 7 depicts the method's general setup.

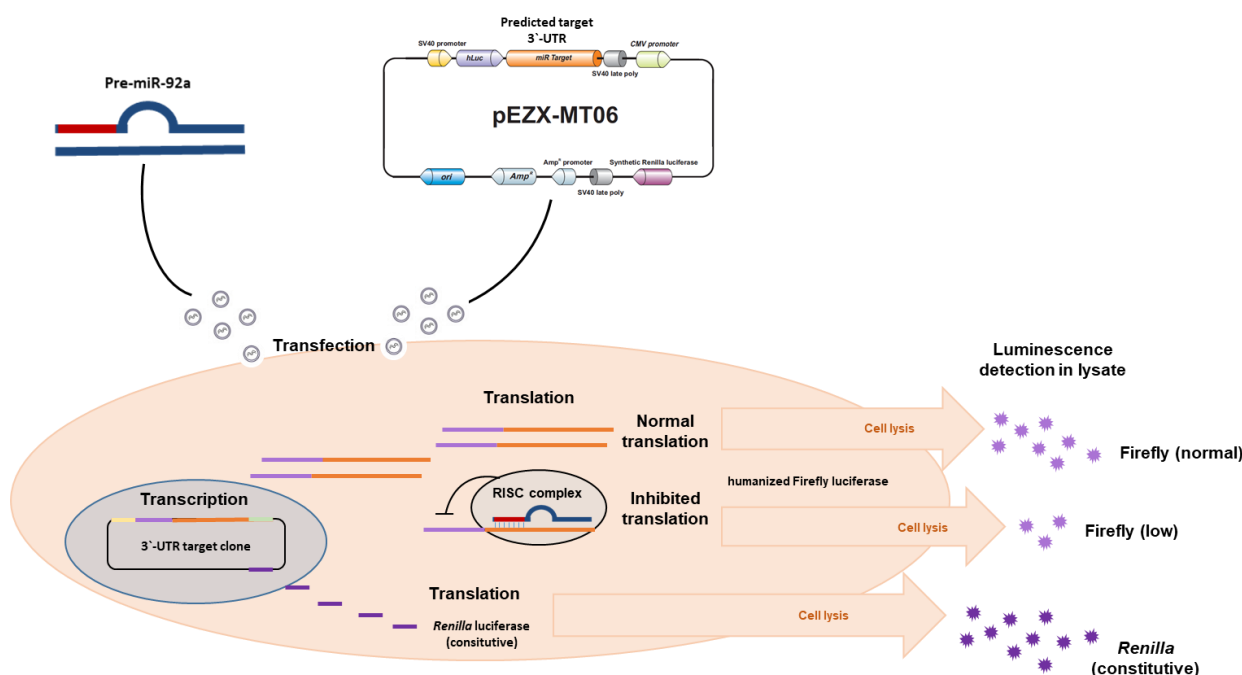


Figure 7. Assay of miR-92a direct interaction with predicted target gene mRNA 3'-UTR by bioluminescence.

2.16. Glucose uptake assays

Glucose uptake in HCMEC was measured by means of bioluminescence using Glucose Uptake-Glo™ (Promega J1342). The assay principle relies on treating the cells with 2-deoxyglucose, which can be transported across the cellular membrane similar to normal glucose. Inside the cell, phosphorylation of 2DG occurs in the same manner as glucose and leads to the formation of 2-deoxyglucose-6-phosphate (2DG6P). Unlike glucose-6-phosphate (G6P), 2DG6P cannot be utilized by cellular enzymes, leading to its accumulation. Cell lysis by kit-provided acid detergent releases 2DG6P and destroys cellular NADPH. 2DG6P can then be detected via exogenously provided G6P dehydrogenase, which oxidizes 2DG6P in the presence of nicotinamide diphosphate ions (NADP⁺) to form 6-phosphodeoxygluconate and NADPH. NADPH is then further utilized by kit-provided reductase enzyme to convert pro-luciferin to luciferin, which is then used by kit-provided recombinant luciferase to generate light. Cells were cultured in BRAND® bioluminescence-compatible 96-well plates (cellGrade™ 781974) at 100,000 cells per well. Transfections were done as previously described, and cells were incubated with the transfection complex for 4 – 6 hours before medium was refreshed and cells were incubated for 24 hours. On the assay day, cells were washed twice with PBS to remove residual glucose in the media and pulsed for 10 minutes with 50 µL/well 1 mM 2DG. Uptake was then stopped and cells were lysed by the kit's Stop Buffer, and the acid is

Materials and Methods

neutralized by the kit's Neutralization Buffer using recommended volumes. Wells were then treated with 100 μ L of equilibrated detection buffer prepared according to manufacturer's protocol (below):

Component	Per Reaction
Luciferase Reagent	100 μ l
NADP+	1 μ l
G6PDH	2.5 μ l
Reductase	0.5 μ l
Reductase Substrate	0.0625 μ l

Luminescence was then read using BioTek Cytation 1[™] multimode reader (Agilent), and values were normalized to their respective controls.

2.17. Statistical analysis

Data were analyzed using GraphPad Prism or Microsoft Excel 2016 software and were presented as mean \pm SEM (error bars). Sample size and experimental replicates were indicated in figure legends. Statistical analysis was performed by Student's t test (two groups) or one-way ANOVA (4 groups). P values, *P < 0.05; **P < 0.01; ***P < 0.001; and ****P < 0.0001 were considered statistically significant, whereas "ns" denotes statistically not significant difference.

3. Results

To characterize EC dysfunction in the diabetic cardiac microcirculation, the impact of miR-92a therein and the underlying molecular mechanisms, I employed three different EC models; HUVEC, HCMEC and MCMEC. They were utilized wherever technically feasible to answer different study questions. Both HCMEC and MCMEC are from cardiac origin. Primary HCMEC were obtained from human cardiac ventricles, and are therefore the most relevant model to address the diabetic cardiac microcirculation, and importantly, the translational potential of miR-92a targeting. MCMEC, being an immortalized mouse cell line, enabled initial pilot studies on conserved downstream targets and more feasible molecular biology assays. HUVEC, on the other hand, provided informative insights to endothelial heterogeneity and shall be presented later in the Results section.

To verify the molecular findings from CMEC of both man and mouse in a third species, ventricular tissue samples from diabetic porcine models, i.e. *INS^{C94Y}* transgenic, were utilized wherever applicable. These shall be contextually presented within the Results chapter 3.4.

3.4. Cardiac microvascular endothelial cells (CMEC)

3.4.1. *In vitro* modeling of DM: effects of high glucose culture

In a simple experimental setting to examine the effect of glucose on endothelial cell function, HCMEC were cultured and passaged in two glucose concentrations in their culture medium, i.e. 5.5 mM (normal) or 30 mM (high). Cells were then subjected to tests of endothelial cell function, i.e. tube formation, wound healing and flow chamber assays.

Analysis of the angiogenic potential revealed a significant reduction in tube formation parameters, such as total tube length and tube count, in HCMEC cultured in high glucose compared to those in normal glucose. The finding applied to both male and female cells with initially notable difference in angiogenic phenotypes. Female HCMEC displayed higher sensitivity to glycemic stress, with 58.4% decrease in total tube length, and 59.27% decrease in total tube count (Figure 8). Male HCMEC, however, were less sensitive to high glucose culture conditions, with 16.57% decrease in total tube length, and 21.28% decrease in tube count (Figure 8).

Results

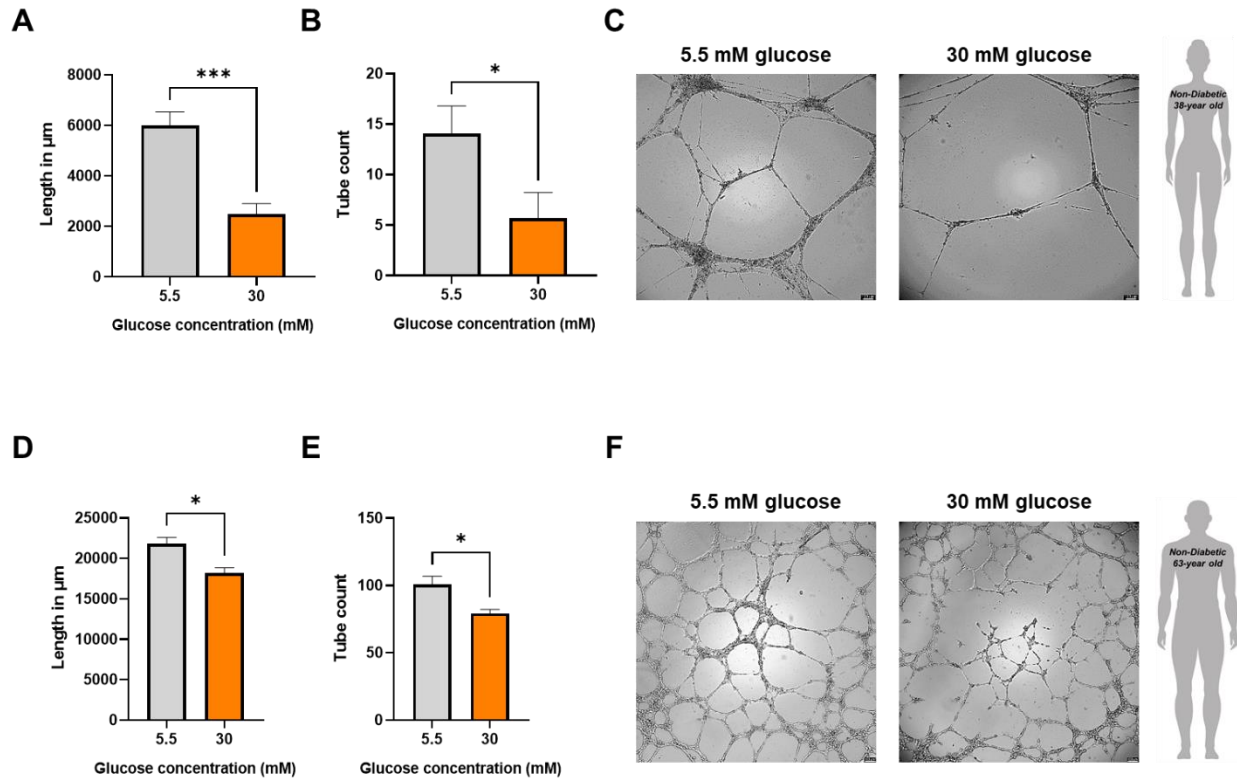


Figure 8. Effect of high glucose culture on HCMEC angiogenesis. (A – C) Analysis of tube formation parameters ($n = 6$), and representative bright field images in female HCMEC under 5.5 or 30 mM glucose. (D – F) Analysis of tube formation parameters ($n = 5$), and representative bright field images in male HCMEC under 5.5 or 30 mM glucose. Scale bars equal 100 μm .

In wound healing assays, female HCMEC showed a trend of reduction in migration under high glucose conditions compared to normal glucose. High glucose wound areas were 28.9% bigger at 8 hours (Figure 9). Statistically, however, the difference was not significant. Despite a relatively slower baseline migration rate in male HCMEC, evident in relatively larger open wound area at 8 hours, they did not show a significant difference in migration upon wound healing when assayed under high glucose conditions (Figure 9).

Results

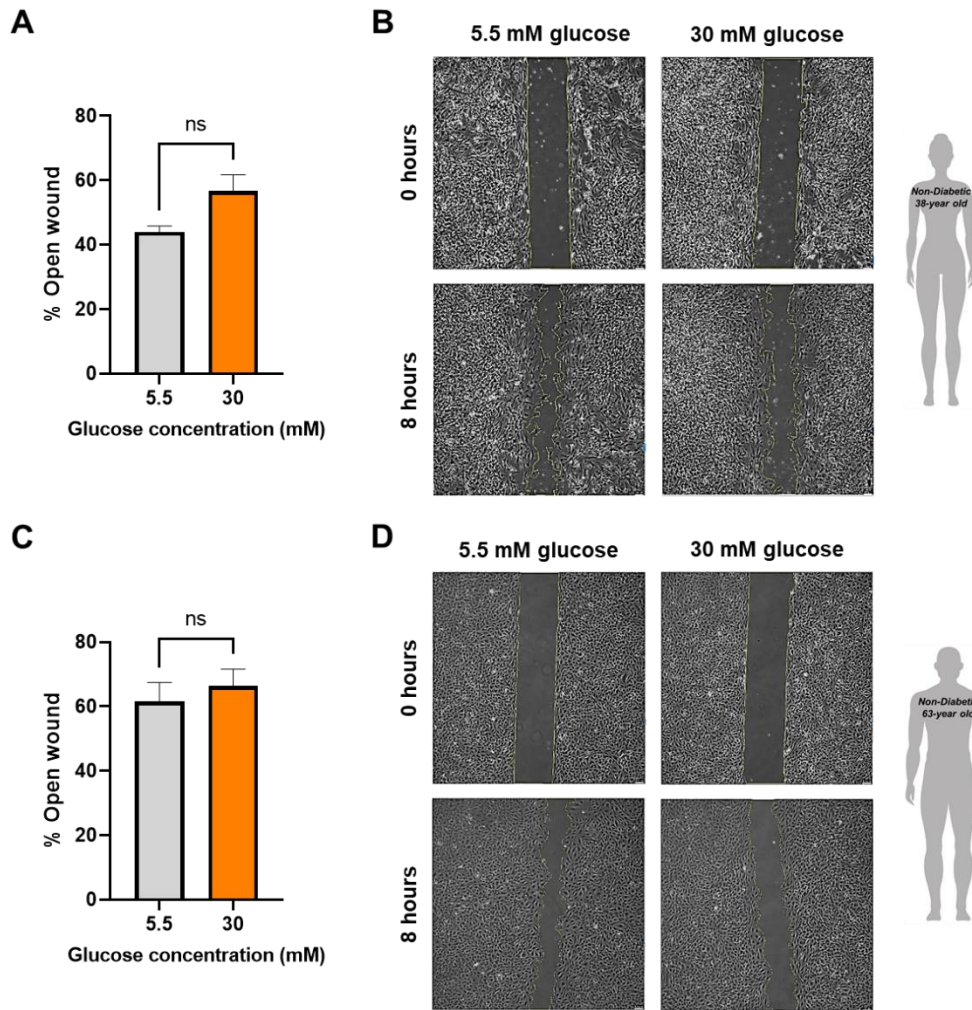


Figure 9. Effect of high glucose culture on HCMEC migration in wound healing experiment. (A, B) Analysis of wound area (yellow trace on images) in percentage in female HCMEC under 5.5 or 30 mM glucose at 0 and 8 hours ($n = 3$), and representative phase contrast images. (C, D) analysis of wound area (yellow trace on images) in percentage in male HCMEC under 5.5 or 30 mM glucose at 0 and 8 hours ($n = 4$), and representative phase contrast images and. Scale bars equal 100 μm .

The inflammatory state of male HCMEC cultured in normal or high glucose was tested in flow chamber assays, where fluorescently labeled THP-1 monocytes were allowed to flow over unstimulated HCMEC monolayers. Analysis showed a significant increase (i.e. ≈ 1.9 fold) in adherent THP-1 cell count to HCMEC monolayers cultured in high glucose compared to those cultured in normal glucose (Figure 10).

Results

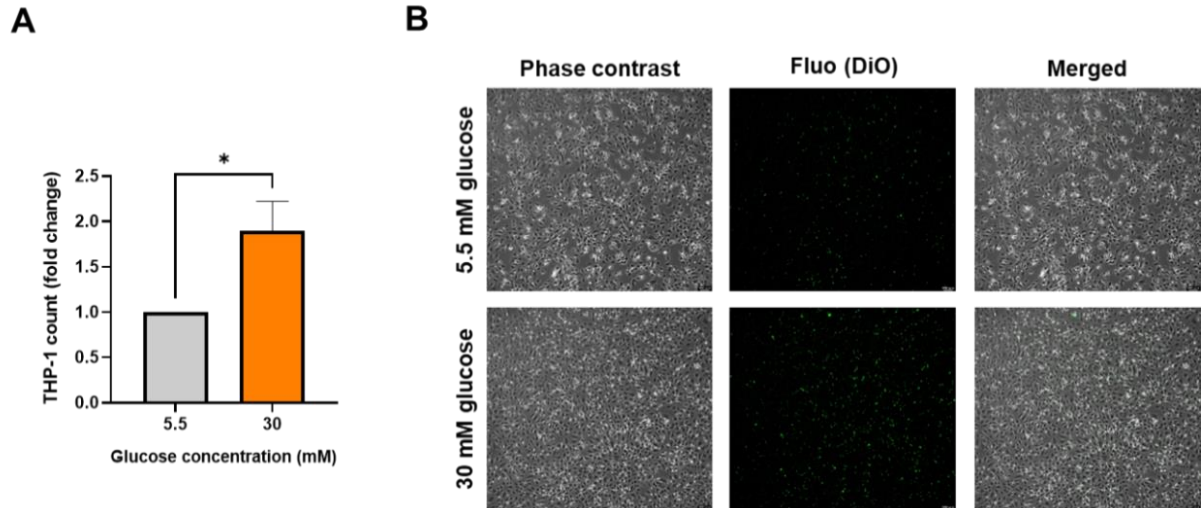


Figure 10. Characterization of the inflammatory phenotype of HCMEC under high glucose culture. (A) Analysis of fold change in adherent THP-1 monocytes count to HCMEC monolayers cultured in 5.5 or 30 mM glucose ($n = 4$). (B) Phase contrast, fluorescence and merged images of HCMEC monolayers cultured in 5.5 or 30 mM glucose; and adherent THP-1 monocytes (green). Scale bars equal 100 μm .

Moreover, quantitative PCR analysis of miR-92a relative expression displayed significant upregulation of ≈ 1.44 - and ≈ 1.77 -fold in both female and male HCMEC upon high glucose culture, respectively (Figure 11).

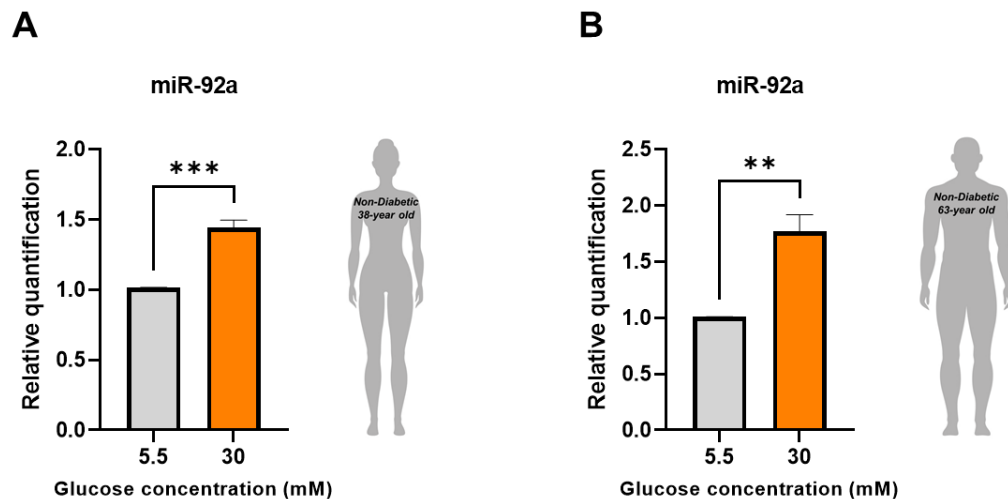


Figure 11. Effect of high glucose culture on miR-92a levels in HCMEC. Quantitative PCR analysis of miR-92a levels in female (A) and male (B) HCMEC cultured in 5.5 or 30 mM glucose ($n = 3$).

3.4.2. Characterization of type 2 diabetic HCMEC

To validate the previous findings in a pathologically relevant model, HCMEC from a type 2 diabetic patient were obtained and compared to those from an age-, sex- and ethnically-matched non-diabetic control donor.

Diabetic HCMEC displayed significantly compromised angiogenic potential in tube formation assays compared to non-diabetic controls. Analysis of tube formation parameters showed \approx 23% reduction in total tube length, and \approx 35% decrease in tube count of diabetic tube network on Matrigel compared to non-diabetic controls (Figure 12).

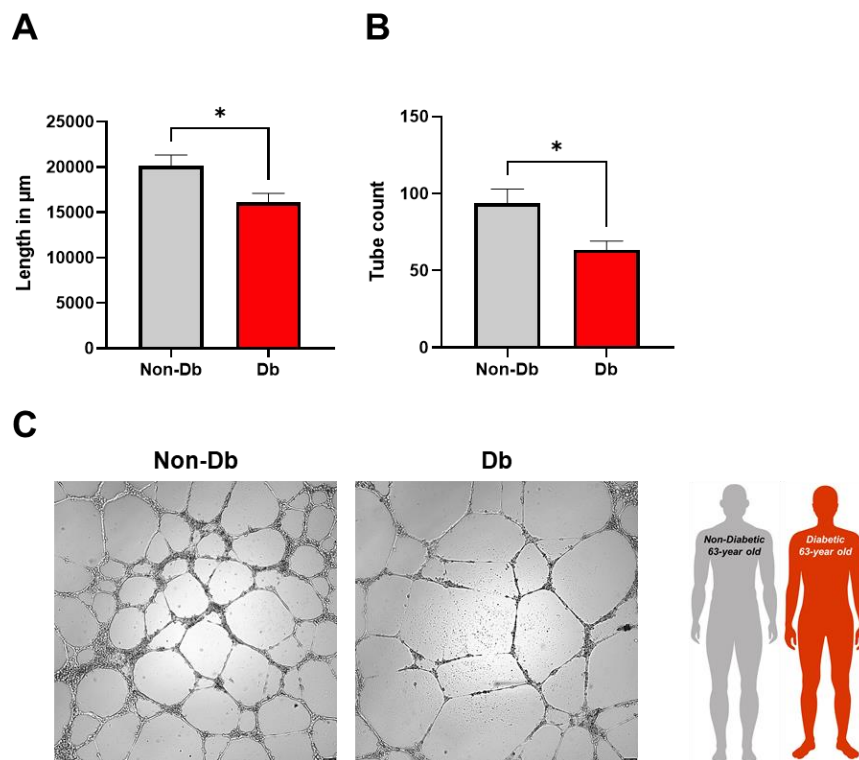


Figure 12. Characterization of the angiogenic phenotype in diabetic HCMEC. (A, B) Analysis of total tube length and tube count in HCMEC from matching non-diabetic or diabetic males ($n = 4$). (C) Representative bright field images of tube formation. Scale bars equal 100 μm .

Furthermore, migration of diabetic HCMEC was significantly reduced when compared to non-diabetic controls. In a wound healing assay, diabetic wound areas were \approx 20.4% larger at 8 hours, and \approx 79% larger at 24 hours than non-diabetic controls (Figure 13).

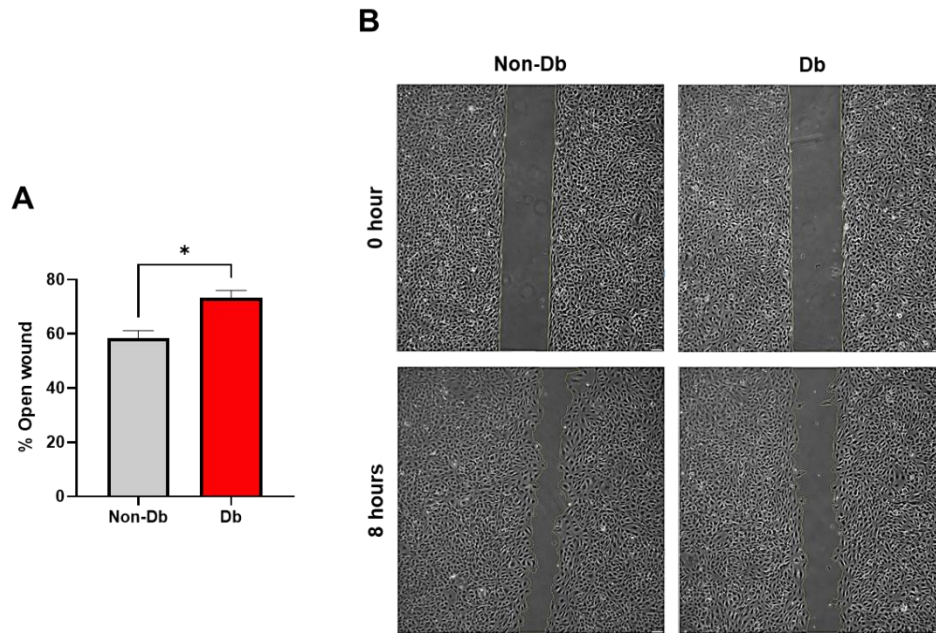


Figure 13. Characterization of migration in diabetic HCMEC. (A) Analysis of wound area (yellow trace on images) in percentage over 8 hours of migration in non-diabetic or diabetic HCMEC from matching donor males ($n = 3$). (B) Representative phase contrast images. Scale bars equal 100 μm .

Moreover, endothelial beds from diabetic HCMEC showed a pronounced inflammatory phenotype in the flow chamber assay, where monocyte retention was ≈ 2 times higher than non-diabetic controls (Figure 14).

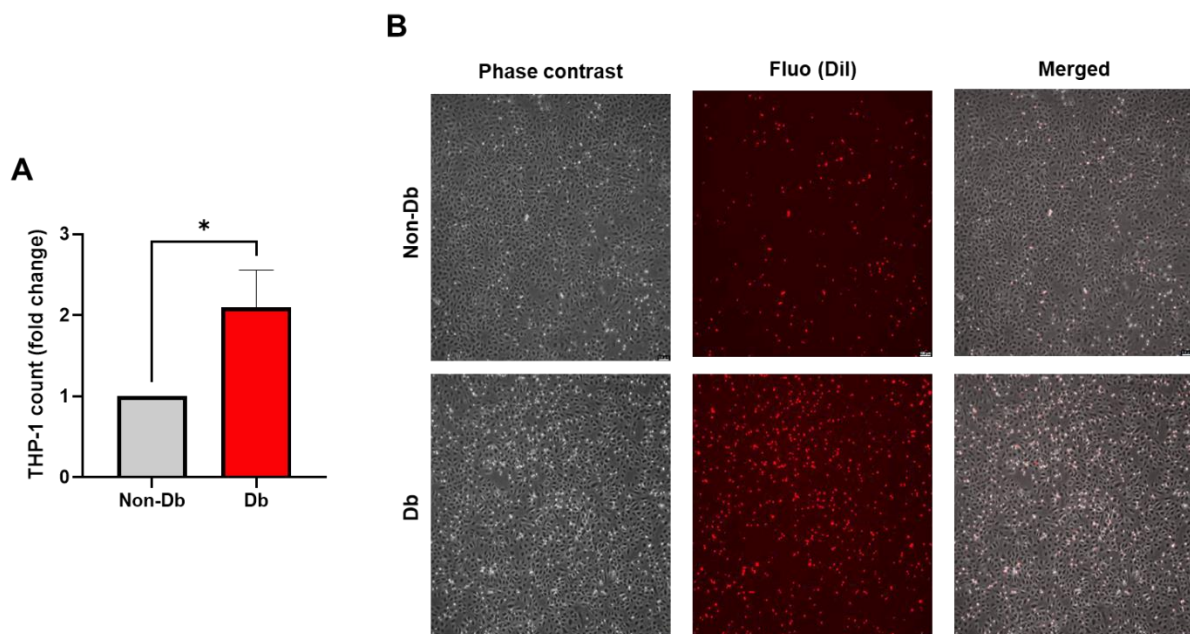


Figure 14. Characterization of the inflammatory phenotype in diabetic HCMEC. (A) Analysis of fold change in adherent THP-1 monocyte count to HCMEC monolayers from matching non-diabetic or diabetic donors ($n = 4$). (B) Representative phase contrast, fluorescence and merged images of HCMEC monolayers and Dil-labeled THP-1 monocytes (red) from matching non-diabetic or diabetic donors. Scale bars equal 100 μm .

Results

Importantly, the aforementioned phenotypes of endothelial cell function correlated with significantly upregulated levels of miR-92a in diabetic HCMEC. Quantitative PCR analysis showed ≈ 1.8 -fold increase in relative expression of miR-92a in diabetic compared to non-diabetic HCMEC (Figure 15).

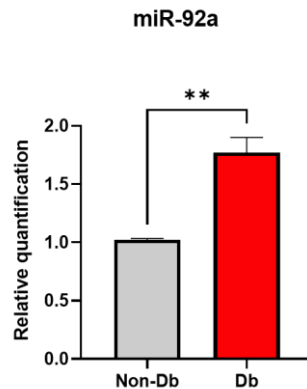


Figure 15. MiR-92a expression in diabetic HCMEC. Quantitative PCR analysis of miR-92a expression levels in non-diabetic or diabetic HCMEC from matching male donors ($n = 4$).

3.4.3. MiR-92a inhibition rescued the diabetic phenotype in HCMEC

To investigate the therapeutic potential of targeting miR-92a in the cardiac microcirculation under diabetic conditions, I transfected non-diabetic HCMEC cultured under normal or high glucose with antisense small RNA (antagomir) to miR-92a (Ant-92a) or non-targeting control (Ant-Ctrl). Likewise, I transfected diabetic HCMEC with Ant-92a or Ant-Ctrl. Upon verification of the transfection efficiency, I performed the aforementioned tests of endothelial cell function, wherever technically possible, given the limitations of primary cell culture.

Transfection efficiency was first evaluated with a fluorophore-labeled small non-targeting RNA (Figure 16). Indeed, Ant-92a transfection led to $\approx 98\%$ decrease in miR-92a expression compared to control as per qPCR relative quantification (Figure 16).

Results

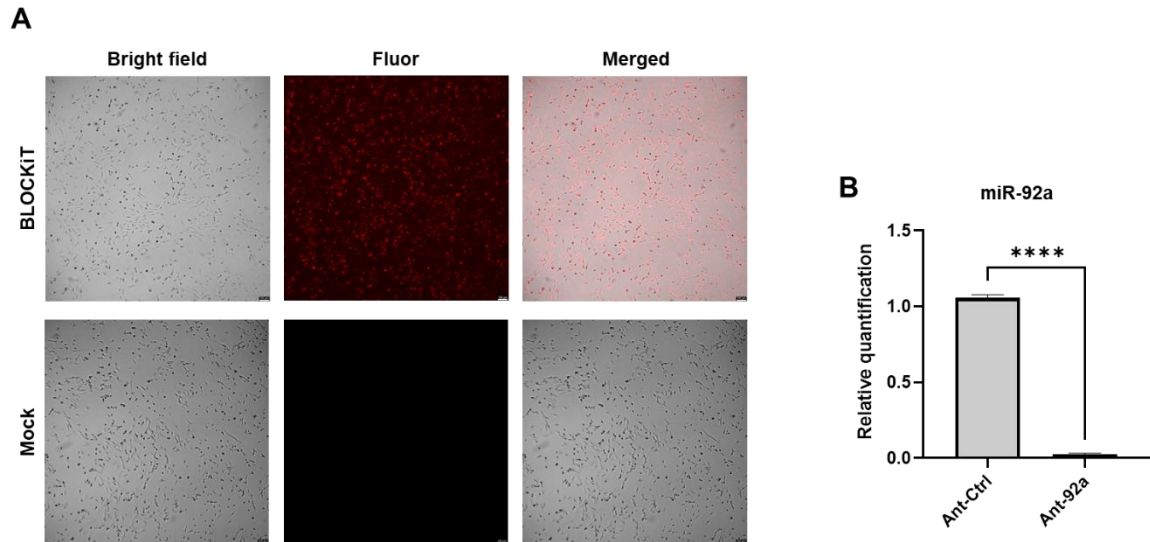


Figure 16. Small RNA transfection efficiency and efficacy in HCMEC. (A) Bright field and fluorescence images of HCMEC upon transfection with BLOCKiT Cy-3-labeled RNA with RNAiMAX Lipofectamine transfection kit. (B) qPCR quantification of miR-92a upon specific antagomir transfection (Ant-92a) compared to control (Ant-Ctrl) ($n = 4$). Scale bars equal 100 μm .

In angiogenesis assay, no difference was found in either tube length or count in male non-diabetic HCMEC when cultured in normal or high glucose upon transfection with Ant-92a compared to control (Ant-Ctrl) (Figure 17).

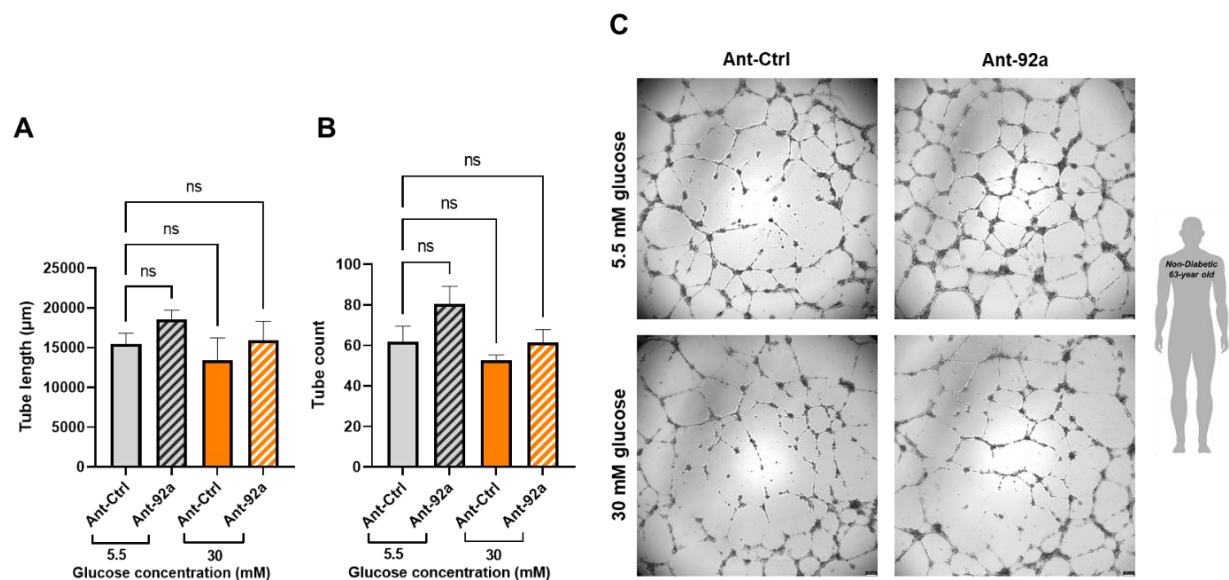


Figure 17. Inhibition of miR-92a on angiogenesis in HCMEC under high glucose culture. (A, B) Analysis of total tube length and tube count in male non-diabetic HCMEC cultured in 5.5 or 30 mM glucose upon transfection with miR-92a inhibitor (Ant-92a) compared to control (Ant-Ctrl) ($n = 4$). (C) Representative bright field images. Scale bars equal 100 μm .

Results

On the other hand, inhibition of miR-92a in type 2 diabetic HCMEC rescued angiogenesis in tube formation assays. Ant-92a transfection led to significant increases in total tube length and tube count in diabetic HCMEC compared to control-transfected cells (Figure 18).

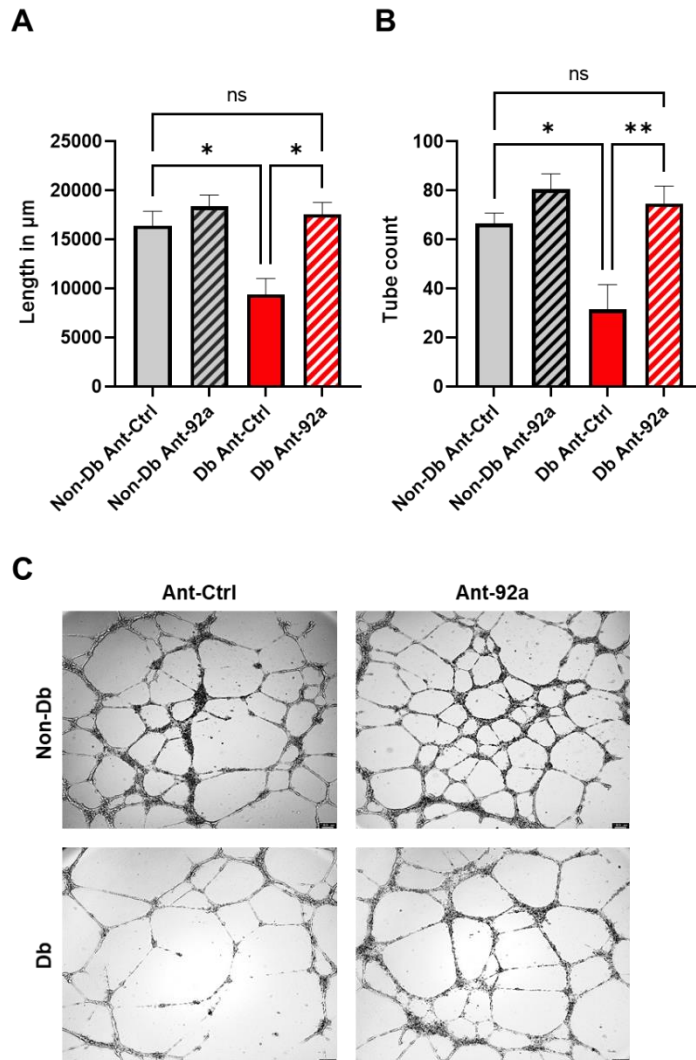


Figure 18. Inhibition of miR-92a rescues angiogenesis in diabetic HCMEC. (A, B) Analysis of total tube length and tube count in non-diabetic or diabetic HCMEC from matching donors upon inhibition of miR-92a by (Ant-92a) compared to controls (Ant-Ctrl) ($n = 4$). (C) Representative bright field images of tube formation network. Scale bars equal 100 μm .

In the wound healing assay, however, miR-92a inhibition did not influence diabetic HCMEC migration (Figure 19). Likewise, in EdU incorporation assays, no difference in cell proliferation was observed in either non-diabetic or diabetic HCMEC upon miR-92a inhibition by antagomir transfection compared to control-transfected cells (Figure 20).

Results

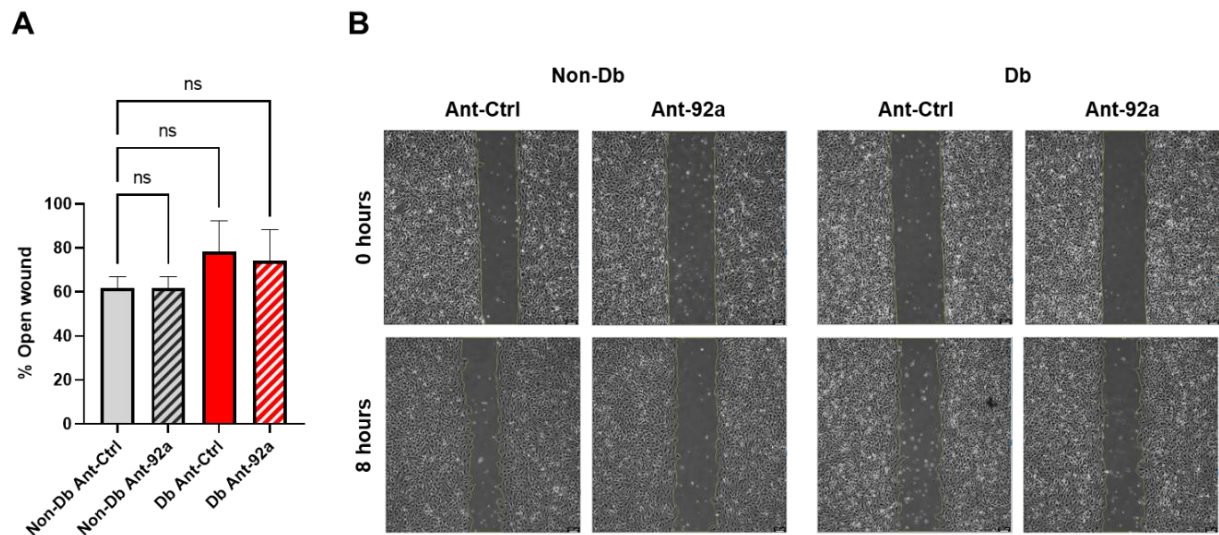


Figure 19. Migration in non-diabetic or diabetic HCMEC upon miR-92a inhibition. (A) Analysis of open wound in percentage over 8 hours of migration in non-diabetic or diabetic HCMEC from matching donors upon miR-92a inhibition (Ant-92a) compared to controls (Ant-Ctrl) ($n = 4$). (B) Representative phase contrast images. Scale bars equal 100 μm .

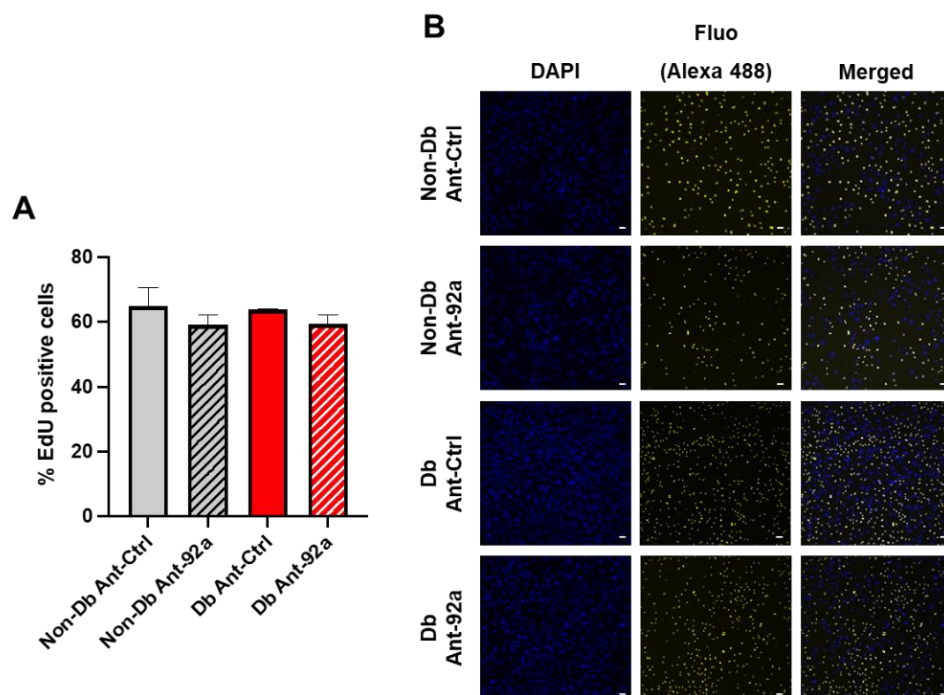


Figure 20. Proliferation assay in non-diabetic or diabetic HCMEC upon miR-92a inhibition. (A) Analysis of EdU-positive cell count (in percentage) of non-diabetic or diabetic HCMEC upon treatment with miR-92a inhibitor (Ant-92a) or control (Ant-Ctrl) ($n = 3$). (A) Representative fluorescence images of nuclei (DAPI) and DNA-incorporated EdU (Alexa 488). Scale bars equal 100 μm .

Results

Importantly, miR-92a inhibition correlated with noticeable amelioration of the inflammatory phenotype in diabetic HCMEC. In the flow chamber assay, there was a marked reduction in adherent THP-1 count to diabetic endothelial beds transfected with Ant-92a compared to controls. Analysis showed that the reduction in adherent THP-1 count upon Ant-92a transfection in diabetic HCMEC rendered their values not statistically different from the non-diabetic HCMEC of either transfection (Figure 21).

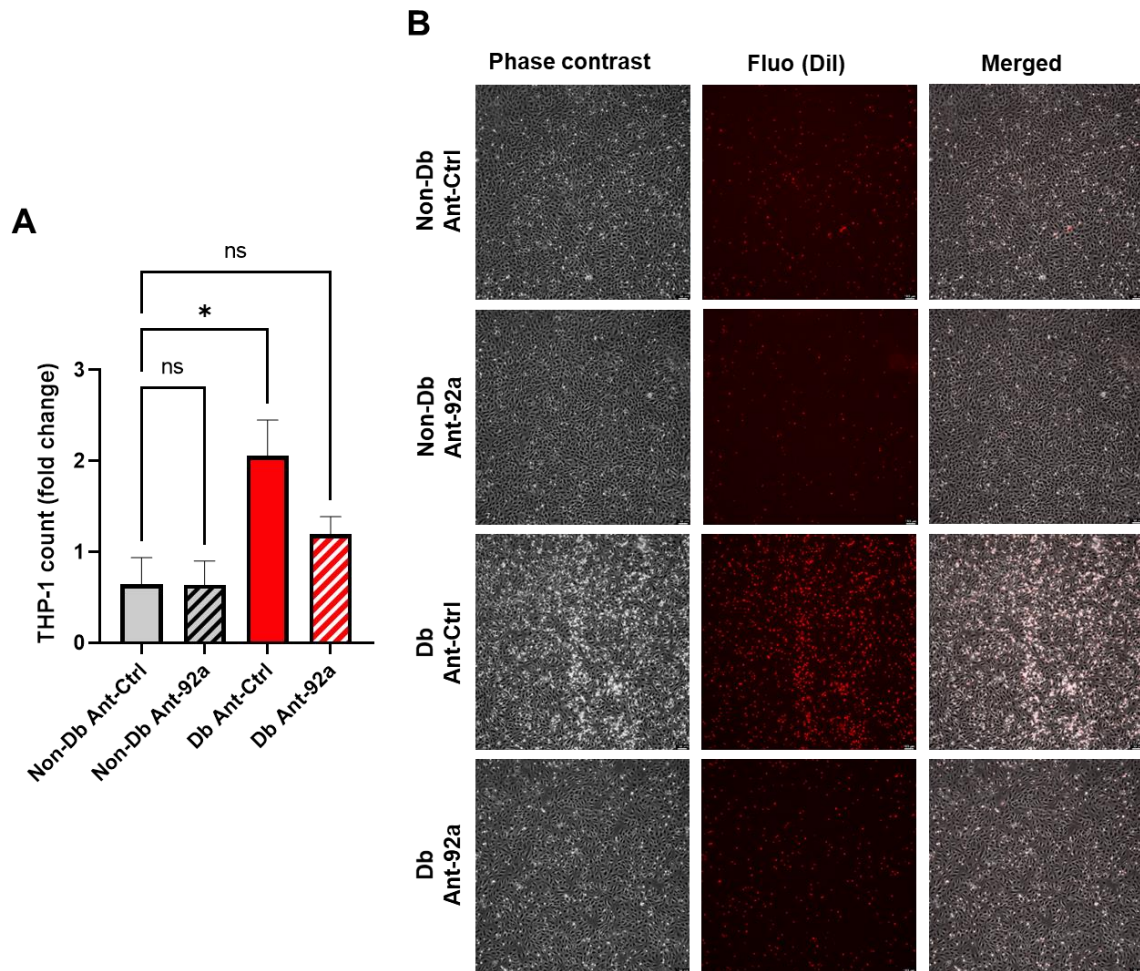


Figure 21. Inhibition of miR-92a rescues the diabetic inflammatory phenotype in HCMEC. (A) Analysis of fold change in adherent THP-1 monocyte count upon flow assay on HCMEC monolayers from matching non-diabetic or diabetic male donors upon inhibition of miR-92a (Ant-92a) compared to controls (Ant-Ctrl) ($n = 4$). (B) Representative phase contrast, fluorescence and merged images of HCMEC monolayers and Dil-labeled THP-1 monocytes (red). Scale bars equal 100 μm .

3.4.4. *In silico* prediction of miR-92a targets

To identify the underlying molecular mechanisms of observed endothelial phenotype in diabetes upon miR-92a overexpression or inhibition, I performed *in silico* analysis of predicted miR-92a gene regulatory networks. To this end, I used TargetScan (version 7.2; targetscan.org – March 2018 update) as a database for canonical miRNA-mRNA targeting [221]. TargetScan adopts a quantitative model that takes into account several features which correlate with target repression to come up with the so called “context++” model. The context++ score is the sum of contribution of 14 site features identified by Agarwal et al., 2015 and attributed a predictive value that adds to a quantitative model of miRNA targeting efficacy. Figure 18A depicts an example search result for the TargetScan-predicted miR-92a target *ADAM10* in human, and a breakdown of the context++ score calculation for the position 490-496. Sites with higher complementarity and stronger binding, e.g. 8mer or 7mer-m8 generally have lower context scores than 6mer sites. However, other factors included in the context++ score calculation explain the varying efficacy of a given site in one 3'-UTR than in another. Figure 18B shows conservation of miR-92a seed sequence matches in orthologs of human and mouse target genes' mRNAs.

In light of available literature data, several miR-92a targets were found to be of particular relevance to the aforementioned EC functions, i.e. *ADAM10*, *KLF2*, *KLF4*, and *MEF2D*. Furthermore, previous Affymetrix chip analysis in HUVEC revealing differentially regulated genes upon miR-92a inhibition has as well guided our selection of some plausible targets.

Table 2 lists my selection of conserved targets in human (*Homo sapiens*), mouse (*Mus musculus*) and pig (*Sus scrofa*) that were further studied *in vitro* within the scope of this doctoral thesis, and their calculated context++ scores for each miR-92a binding site in the corresponding 3'-UTR. TargetScan does not offer the match position or context++ score calculations for the predicted targets in the pig. The former can, however, be identified using the Nucleotide data base from the National Library of Medicine.

Results

A

	Predicted consequential pairing of target region (top) and miRNA (bottom)	Site type	Context++ score	Context++ score percentile	Weighted context++ score	Conserved branch length	PCT	Gencode transcript ID	ENST00000260408.3
Position 490-496 of ADAM10 3' UTR	5' ...ACACUGUACUCUCU--GUGCAAU... 3' ...ACACUGUACUCUCU--GUGCAAU...	7mer-m8	-0.25	94	-0.25	4.632	0.76	miRBase ID	hsa-miR-92a-3p
hsa-miR-92a-3p	3' ...ACACUGUACUCUCU--GUGCAAU... 5' ...ACACUGUACUCUCU--GUGCAAU...	7mer-m8	-0.22	93	-0.22	4.632	0.76	position of site	490-496
Position 490-496 of ADAM10 3' UTR	5' ...ACACUGUACUCUCU--GUGCAAU... 3' ...ACACUGUACUCUCU--GUGCAAU...	7mer-m8	-0.19	92	-0.19	4.632	0.76	site type	-0.224
hsa-miR-92a-3p	3' ...ACACUGUACUCUCU--GUGCAAU... 5' ...ACACUGUACUCUCU--GUGCAAU...	7mer-m8	-0.22	92	-0.22	4.632	0.76	supplementary pairing	-0.011
Position 490-496 of ADAM10 3' UTR	5' ...ACACUGUACUCUCU--GUGCAAU... 3' ...ACACUGUACUCUCU--GUGCAAU...	7mer-m8	-0.20	92	-0.20	4.632	0.76	local AU	-0.149
hsa-miR-92b-3p	3' ...ACACUGUACUCUCU--GUGCAAU... 5' ...ACACUGUACUCUCU--GUGCAAU...	7mer-m8	-0.21	92	-0.21	4.632	0.76	min dist	0.032
Position 490-496 of ADAM10 3' UTR	5' ...ACACUGUACUCUCU--GUGCAAU... 3' ...ACACUGUACUCUCU--GUGCAAU...	7mer-m8	-0.18	90	-0.18	4.633	0.76	sRNA1A	0
hsa-miR-92a-3p	3' ...ACACUGUACUCUCU--GUGCAAU... 5' ...ACACUGUACUCUCU--GUGCAAU...	7mer-m8	-0.17	89	-0.17	4.633	0.76	sRNA1C	0
Position 490-496 of ADAM10 3' UTR	5' ...ACACUGUACUCUCU--GUGCAAU... 3' ...ACACUGUACUCUCU--GUGCAAU...	7mer-m8	-0.21	92	-0.21	4.632	0.76	sRNA1G	0
hsa-miR-92b-3p	3' ...ACACUGUACUCUCU--GUGCAAU... 5' ...ACACUGUACUCUCU--GUGCAAU...	7mer-m8	-0.13	87	-0.13	4.633	0.76	sRNA8A	0
Position 490-496 of ADAM10 3' UTR	5' ...ACACUGUACUCUCU--GUGCAAU... 3' ...ACACUGUACUCUCU--GUGCAAU...	7mer-m8	-0.13	87	-0.13	4.633	0.76	sRNA8C	-0.031
hsa-miR-92a-3p	3' ...ACACUGUACUCUCU--GUGCAAU... 5' ...ACACUGUACUCUCU--GUGCAAU...	7mer-m8	-0.15	87	-0.15	4.633	0.76	sRNA8G	0
Position 490-496 of ADAM10 3' UTR	5' ...ACACUGUACUCUCU--GUGCAAU... 3' ...ACACUGUACUCUCU--GUGCAAU...	7mer-m8	-0.13	87	-0.13	4.633	0.76	sRNA8B	0
hsa-miR-92b-3p	3' ...ACACUGUACUCUCU--GUGCAAU... 5' ...ACACUGUACUCUCU--GUGCAAU...	7mer-m8	-0.13	87	-0.13	4.633	0.76	site8A	0
Position 490-496 of ADAM10 3' UTR	5' ...ACACUGUACUCUCU--GUGCAAU... 3' ...ACACUGUACUCUCU--GUGCAAU...	7mer-m8	-0.13	87	-0.13	4.633	0.76	site8C	0
hsa-miR-92a-3p	3' ...ACACUGUACUCUCU--GUGCAAU... 5' ...ACACUGUACUCUCU--GUGCAAU...	7mer-m8	-0.13	87	-0.13	4.633	0.76	site8G	0
Position 490-496 of ADAM10 3' UTR	5' ...ACACUGUACUCUCU--GUGCAAU... 3' ...ACACUGUACUCUCU--GUGCAAU...	7mer-m8	-0.13	87	-0.13	4.633	0.76	UTR length	0.076
hsa-miR-92a-3p	3' ...ACACUGUACUCUCU--GUGCAAU... 5' ...ACACUGUACUCUCU--GUGCAAU...	7mer-m8	-0.13	87	-0.13	4.633	0.76	SA	-0.024
Position 490-496 of ADAM10 3' UTR	5' ...ACACUGUACUCUCU--GUGCAAU... 3' ...ACACUGUACUCUCU--GUGCAAU...	7mer-m8	-0.13	87	-0.13	4.633	0.76	ORF length	0.061
hsa-miR-92a-3p	3' ...ACACUGUACUCUCU--GUGCAAU... 5' ...ACACUGUACUCUCU--GUGCAAU...	7mer-m8	-0.13	87	-0.13	4.633	0.76	ORF 8mer count	0
Position 490-496 of ADAM10 3' UTR	5' ...ACACUGUACUCUCU--GUGCAAU... 3' ...ACACUGUACUCUCU--GUGCAAU...	7mer-m8	-0.13	87	-0.13	4.633	0.76	offset 6mer count	-0.011
hsa-miR-92a-3p	3' ...ACACUGUACUCUCU--GUGCAAU... 5' ...ACACUGUACUCUCU--GUGCAAU...	7mer-m8	-0.13	87	-0.13	4.633	0.76	TA	0.071
Position 490-496 of ADAM10 3' UTR	5' ...ACACUGUACUCUCU--GUGCAAU... 3' ...ACACUGUACUCUCU--GUGCAAU...	7mer-m8	-0.13	87	-0.13	4.633	0.76	SPS	0.090
hsa-miR-92a-3p	3' ...ACACUGUACUCUCU--GUGCAAU... 5' ...ACACUGUACUCUCU--GUGCAAU...	7mer-m8	-0.13	87	-0.13	4.633	0.76	PCT	-0.101
Position 490-496 of ADAM10 3' UTR	5' ...ACACUGUACUCUCU--GUGCAAU... 3' ...ACACUGUACUCUCU--GUGCAAU...	7mer-m8	-0.13	87	-0.13	4.633	0.76	context++ score	-0.221
hsa-miR-92a-3p	3' ...ACACUGUACUCUCU--GUGCAAU... 5' ...ACACUGUACUCUCU--GUGCAAU...	7mer-m8	-0.13	87	-0.13	4.633	0.76	AIR	1.000
Position 490-496 of ADAM10 3' UTR	5' ...ACACUGUACUCUCU--GUGCAAU... 3' ...ACACUGUACUCUCU--GUGCAAU...	7mer-m8	-0.13	87	-0.13	4.633	0.76	weighted context++ score	-0.221
hsa-miR-92a-3p	3' ...ACACUGUACUCUCU--GUGCAAU... 5' ...ACACUGUACUCUCU--GUGCAAU...	7mer-m8	-0.13	87	-0.13	4.633	0.76		

B

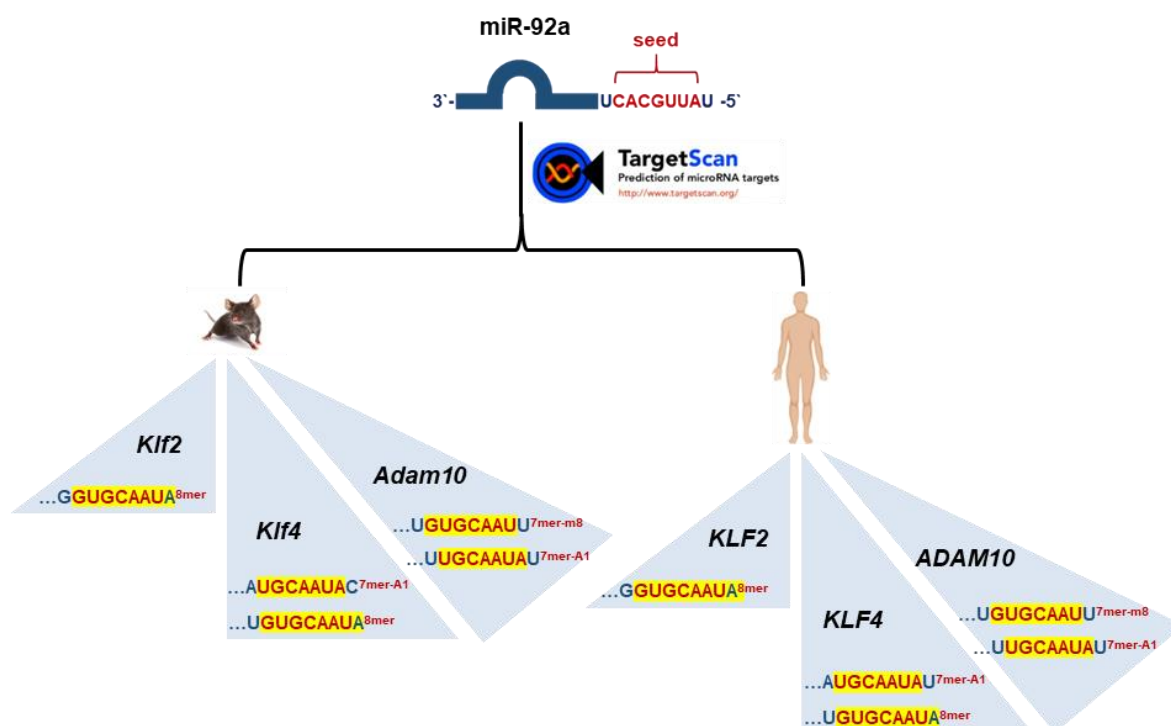


Figure 22. In silico prediction of miR-92a targets by TargetScan. (A) Example search result for the TargetScan-predicted miR-92a target ADAM10 in human, and a breakdown of the context++ score calculation for the position 490-496. (B) Conserved seed sequence matches in human and mouse miR-92a target genes. The sequence highlighted in yellow is target sequence of miR-92a in the corresponding 3'-UTR of mRNAs of represented genes in mouse and human.

Results

Table 2. In silico analysis results of miR-92a predicted downstream targets by TargetScan

Target mRNA	Match position	Site type	Site context score
Hs-ADAM10	490-496	7mer-m8	-0.22
	510-516	7mer-A1	-0.13
Hs-KLF2	242-249	8mer	-0.50
Hs-KLF4	362-368	7mer-A1	-0.06
	674-681	8mer	-0.41
Hs-MEF2D	858-865	8mer	-0.28
	2814-2821	8mer	-0.09
Mm-Adam10	489-495	7mer-m8	-0.22
	509-515	7mer-A1	-0.10
Mm-Klf2	214-221	8mer	-0.57
Mm-Klf4	433-439	7mer-A1	-0.10
	751-758	8mer	-0.36
Mm-Mef2d	1057-1064	8mer	-0.24
Ss-ADAM10	NA	7mer-m8	NA
		7mer-A1	
Ss-KLF2	NA	8mer	NA
Ss-KLF4	NA	8mer	NA
Ss-MEF2D	NA	8mer	NA
		8mer	

NA: not available at TargetScan

3.4.5. *ADAM10*: a novel miR-92a target dysregulated diabetic hearts

The metalloproteinase ADAM10 was selected as an *in silico*-predicted miR-92a target. It has been previously shown to play an important role in regulation of EC tip-stalk behavior and therefore studied in the context of angiogenesis, sprouting and EC migration [118].

Gene expression analysis of *ADAM10* by qPCR showed a significant reduction in diabetic HCMEC compared to non-diabetic controls. Relative quantification of *ADAM10* mRNA recovered from diabetic HCMEC samples revealed a 68% decrease (Figure 23). This was also shown on protein levels, wherein ADAM10 was 33% lower in protein lysates recovered from diabetic HCMEC compared to non-diabetic controls as shown by Western blot analysis (Figure 23).

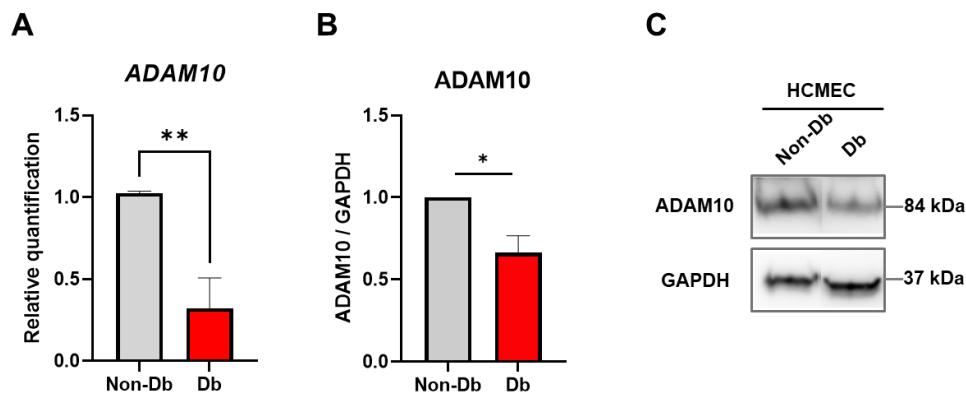


Figure 23. *ADAM10* expression in diabetic HCMEC. (A) Quantitative PCR analysis of *ADAM10* in non-diabetic or diabetic HCMEC ($n = 4$). (B) Western blot analysis of relative quantification of *ADAM10* to GAPDH as housekeeping protein in non-diabetic or diabetic HCMEC ($n = 4$). (C) Representative blot of bands at corresponding molecular mass in kilodalton (kDa).

Results

Interestingly, gene expression analysis of *ADAM10* in the ventricular myocardial tissue from *INS^{C94Y}* transgenic diabetic porcine models shows a spatial differentiation over the long axis, where *ADAM10* is significantly downregulated towards the apex in diabetic porcine ventricle compared to their non-diabetic wild-type littermates (Figure 24).

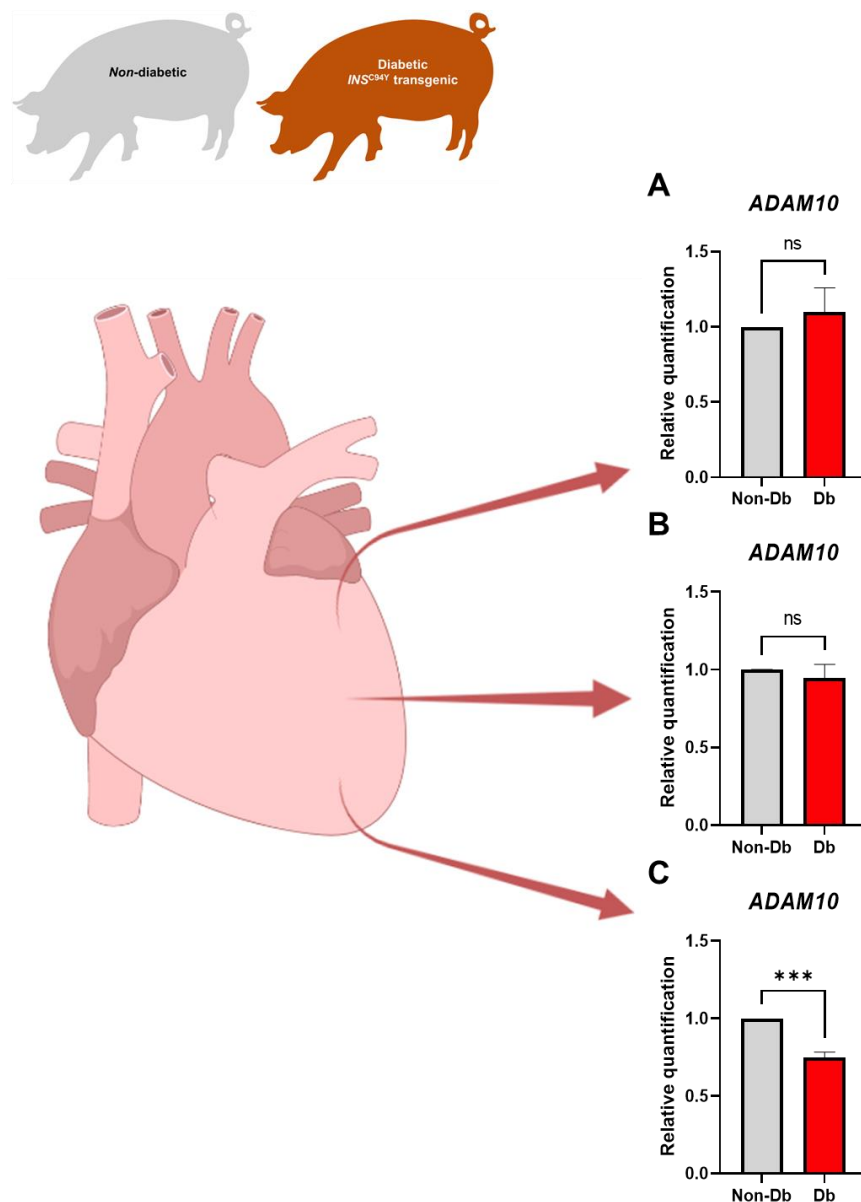


Figure 24. Differential expression of *ADAM10* in the left ventricular tissue of diabetic porcine models. (A – C) qPCR analysis of *ADAM10* gene expression over the long axis of the left ventricle in non-diabetic (Non-Db) vs *INS^{C94Y}* transgenic diabetic (Db) pig tissue from base to apex, respectively ($n = 4$).

Results

Importantly, visualization of ADAM10 in myocardial tissue sections of diabetic pigs showed a marked reduction in immunofluorescence intensity in both micro- and macro-vascular compartments (PECAM1 co-localization) compared to those from non-diabetic littermates (Figure 25).

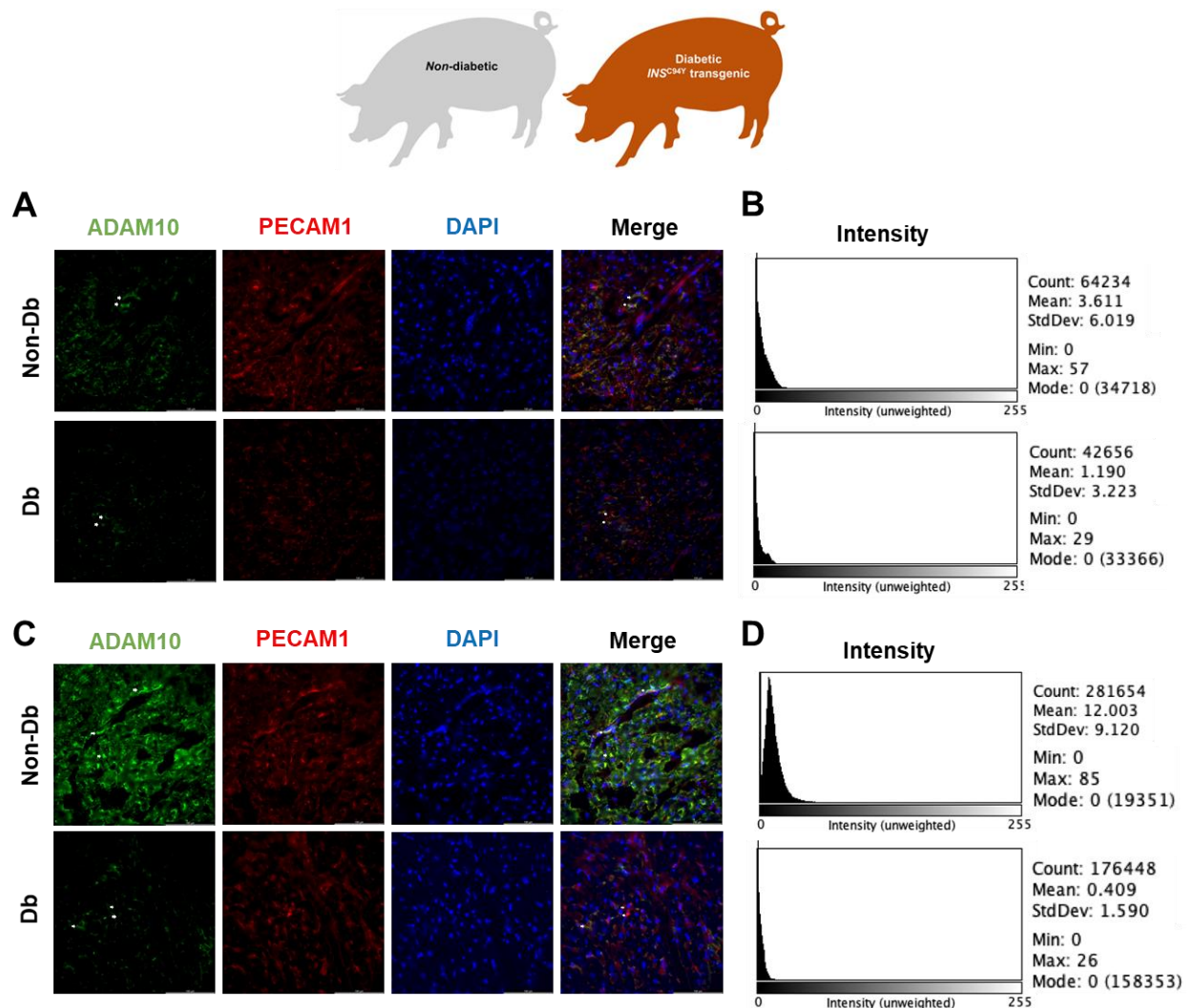


Figure 25. Dysregulation of ADAM10 in the diabetic porcine cardiovascular system. (A) Immunohistochemistry of ADAM10 (green) and PECAM1 (red) in micro- and (C) macrocirculation in non-diabetic (Non-Db) or *INS^{C94Y}* transgenic diabetic (Db) pig heart slices. Co-localization marked in merged images with white arrows. (B, D) Fluorescence intensity measurement of ADAM10 expression of corresponding images. Scale bars = 100 μ m.

Results

To find out whether miR-92a levels correlate with ADAM10 gene expression and protein levels, CMECs were transfected with pre-miRs to miR-92a (pre-92a) or control-miR (pre-Ctrl). Transfection with pre-92a results in ≈ 85 -fold increase in miR-92a levels in CMEC by qPCR analysis (Figure 26).

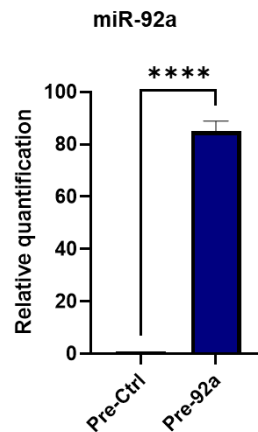


Figure 26. Overexpression of miR-92a by pre-miR transfection. qPCR of miR-92a in non-diabetic HCMEC upon transfection with pre-92a compared to control (pre-Ctrl).

Indeed, overexpression of miR-92a in non-diabetic HCMEC by pre-92a transfection led to significant downregulation of *ADAM10* mRNA by qPCR analysis compared to control-transfected cells (Figure 27). Similarly, on protein levels, overexpression of miR-92a in either non-diabetic HCMEC or MCMEC led to significant ablation of ADAM10 in protein lysates analogous to those from cells transfected with siRNA to *ADAM10* (siADAM10) and compared to control-transfected cell (siCtrl or pre-Ctrl) (Figure 27).

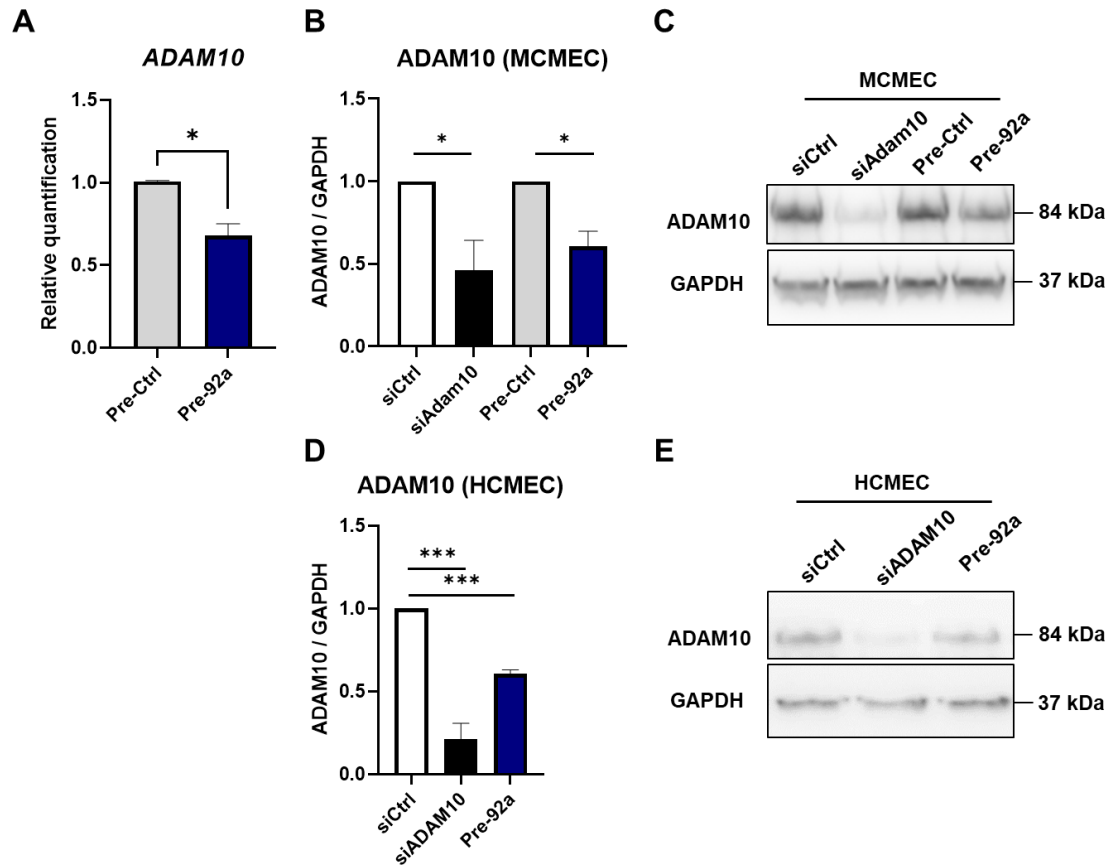


Figure 27. miR-92a overexpression on *ADAM10* gene and protein expression in CMEC. (A) qPCR analysis of *ADAM10* relative expression levels in non-diabetic male HCMEC upon overexpression of miR-92a (pre-92a) or control (pre-Ctrl). (B, C) Western blot analysis of *ADAM10* relative protein levels to GAPDH (housekeeping) in MCMEC upon its knockdown (siAdam10) or miR-92a overexpression (pre-92a) compared to controls (siCtrl or pre-Ctrl) ($n = 3$), and representative blot with corresponding molecular mass in kilodalton (kDa). (D, E) Western blot analysis and representative blot of *ADAM10* relative protein levels to GAPDH (housekeeping) in non-diabetic male HCMEC upon *ADAM10* knock-down (siADAM10), miR-92a overexpression (pre-92a) or control (siCtrl) ($n = 3$).

Importantly, inhibition of miR-92a in diabetic HCMEC by antagomir transfection (Ant-92a) led to statistically significant increase, i.e. 24%, in *ADAM10* levels by qPCR analysis compared to control transfected diabetic HCMEC (Figure 28). These data show a strong correlation between diabetes and/or miR-92a levels and *ADAM10* gene expression and protein levels.

Finally, to find out whether the aforementioned apparent regulation of *ADAM10* by miR-92a is a result of direct interaction, I performed a dual-luciferase reporter assay by co-transfection of pre-92a and a mammalian expression vector of mouse Adam10-3'-UTR downstream of reporter Firefly luciferase, and *Renilla* luciferase as constitutive endogenous control. Indeed, pre-92a transfection led to significant reduction in FLuc/RLuc ratio compared to control transfected cells (pre-Ctrl) (Figure 28), indicating direct interaction.

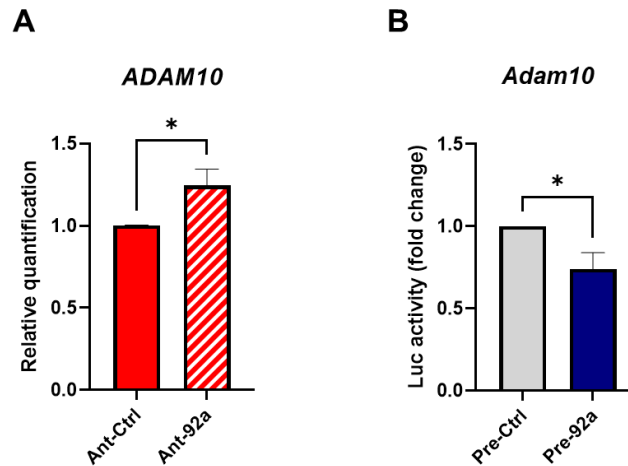


Figure 28. Restoration of ADAM10 expression levels in diabetic HCMEC upon miR-92a inhibition, and proof of direct interaction. (A) qPCR analysis of ADAM10 relative expression levels in Db HCMEC upon miR-92a inhibition (Ant-92a) compared to control (Ant-Ctrl) ($n = 5$). (B) Dual luciferase reporter assay analysis of activity (Firefly / Renilla Luc) in mammalian expression vector of mouse Adam10-3'-UTR downstream of firefly luciferase upon overexpression of miR-92a (pre-92a) in HEK293 cells compared to control (pre-Ctrl) ($n = 4$).

3.4.6. ADAM10 in tube formation and migration of CMEC

To investigate the functional attributes of ADAM10 in CMEC, I knocked-down *Adam10* in MCMEC by siRNA transfection (siAdam10), and cells were subjected to different assays of EC migration and tube formation. Ablation of *Adam10* mRNA in siAdam10-transfected MCMEC cells was verified by qPCR analysis (Figure 29). Figure 27 shows the corresponding ablation of ADAM10 protein in MCMEC upon *Adam10* knock-down.

In angiogenesis assays, knock-down of *Adam10* led to significantly reduced loop counts compared to controls (siCtrl) (Figure 29). In spheroid assays, knock-down of *Adam10* led to significant reduction of sprout lengths, whereas sprout counts showed no significant differences (Figure 29). In congruence with these findings, knock-down of ADAM10 in non-diabetic HCMEC led to minor, yet significant decrease in total tube length in angiogenesis assays, while the decrease in tube count was not statistically significant (Figure 29). These data show a strong correlation between ADAM10 levels and the observed phenotype in CMEC tube formation. Moreover, the observed angiogenesis and sprouting phenotypes indicate a strong involvement of ADAM10 in the regulation of tip-stalk cell behavior in CMEC.

Results

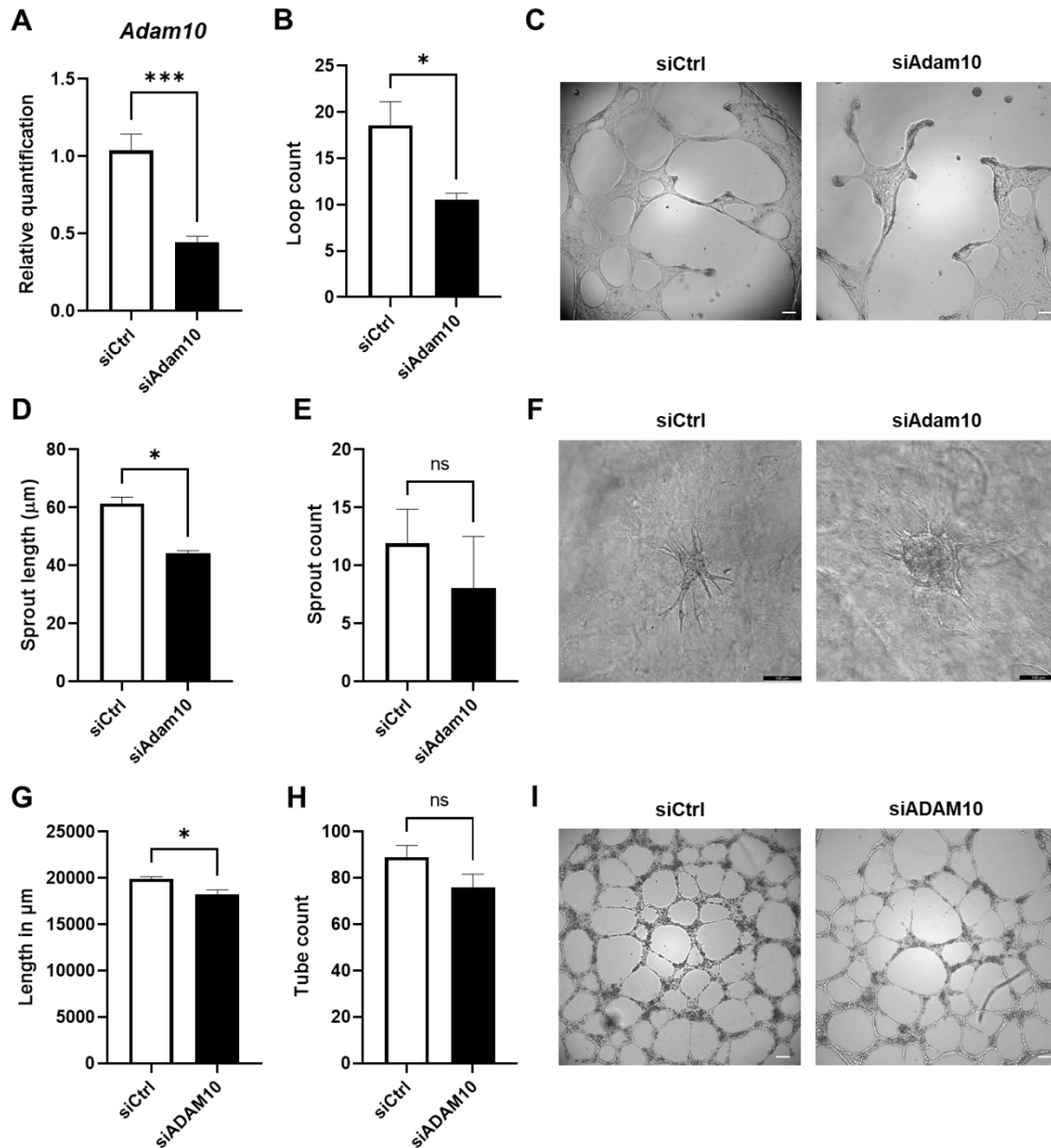


Figure 29. Characterization of ADAM10 role in CMEC angiogenesis. (A) qPCR analysis of *Adam10* expression in MCMEC upon siRNA-mediated knock-down (siAdam10) relative to control (siCtrl) ($n = 4$). (B) Analysis of loop count in MCMEC upon knock-down of *Adam10* vs control ($n = 4$). (C) Representative bright field images of tube formation phenotype. (D, E) Analysis of sprout length (μm), and count in MCMEC spheroids in collagen upon knock-down of *Adam10* vs control. (F) Representative bright field images. (G, H) Analysis of total tube length, and tube count in non-diabetic male HCMEC upon knock-down of ADAM10 (siADAM10) vs control (siCtrl) ($n = 3$). (I) Representative bright field images of tube formation. Scale bars equal $100 \mu\text{m}$.

Results

In wound healing assays, knock-down of *Adam10* led to significant reduction in migration; knock-downs' wound areas were $\approx 29\%$ larger at the 6th hour time point compared to controls (Figure 30). The availability of Cytation 1 multimode reader allowed for further characterization of the migratory ability of MCMEC by time lapse imaging. Wound healing analysis parameters by Cytation 1 are represented in Figure 30. Plotting the percent change in open wound area over time shows significant differences in the slope, as well as the area under curve in Adam10-ablated MCMEC compared to controls, which are in line with earlier readouts from fixed time point.

Analysis of single cell kinetics revealed a more restricted migration pattern in *Adam10* knock-downs compared to controls demonstrated in significantly decreased accumulated distance (Figure 30).

Results

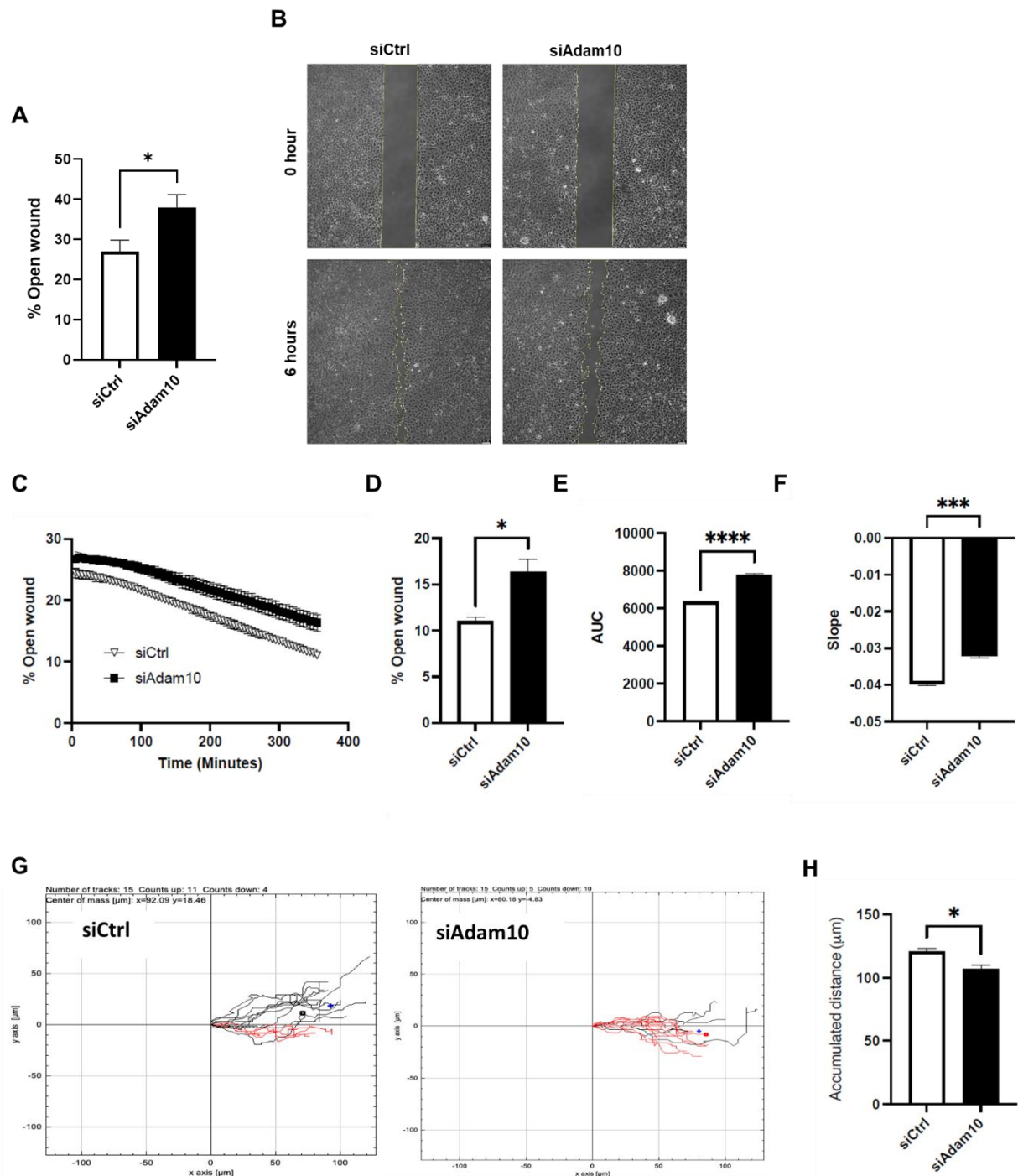


Figure 30. Characterization of ADAM10 role in MCMEC migration. (A) Analysis of relative open wound area in percentage in MCMEC at 6 hour-migration upon knock-down of Adam10 by siRNA (siAdam10) vs control (siCtrl), ($n = 4$). (B) Representative phase contrast images. Scale bars equal 100 μm . (C – F) Analysis of the same experimental conditions repeated with time-lapse imaging (Cytation 1) showing the slope and area under curve (AUC). (G, H) Corresponding single cell kinetics and analysis of accumulated distance ($n = 4$).

3.4.7. *KLF2* and *KLF4* are miR-92a targets dysregulated in diabetic myocardia and CMEC

The Krüppel-like factors 2 and 4 were selected as miR-92a targets that have been validated in previous reports to play pivotal roles in EC biology [154, 297, 299].

Indeed, gene expression analysis by qPCR showed significant reductions in *KLF2* ($\approx 70.9\%$) and *KLF4* ($\approx 78\%$) mRNA levels in diabetic HCMEC compared to matched non-diabetic controls (Figure 31). On protein levels, however, only *KLF2* showed significant reduction in relative expression in diabetic HCMEC compared to the non-diabetic control by Western blot analysis (Figure 31). Notably, the Western blot analysis in Figure 31 correspond to a different non-diabetic donor, i.e. 51-year old Caucasian. Moreover, inhibition of miR-92a in diabetic HCMEC restored *KLF2* gene expression as shown by qPCR analysis, where the increment in relative *KLF2* mRNA in Ant-92a-transfected diabetic HCMEC was statistically significant in comparison to their Ant-Ctrl-transfected counterparts (Figure 31). However, this did not apply to *KLF4*, as inhibition of miR-92a in diabetic HCMEC did not lead to significant changes in its relative expression levels as analyzed by qPCR (Figure 31). Interestingly, overexpression of miR-92a in non-diabetic HCMEC by pre-92a transfection did not alter *KLF2* mRNA levels, whereas *KLF4* mRNA were decreased by $\approx 24\%$ compared to pre-Ctrl-transfected non-diabetic HCMEC (Figure 31).

Results

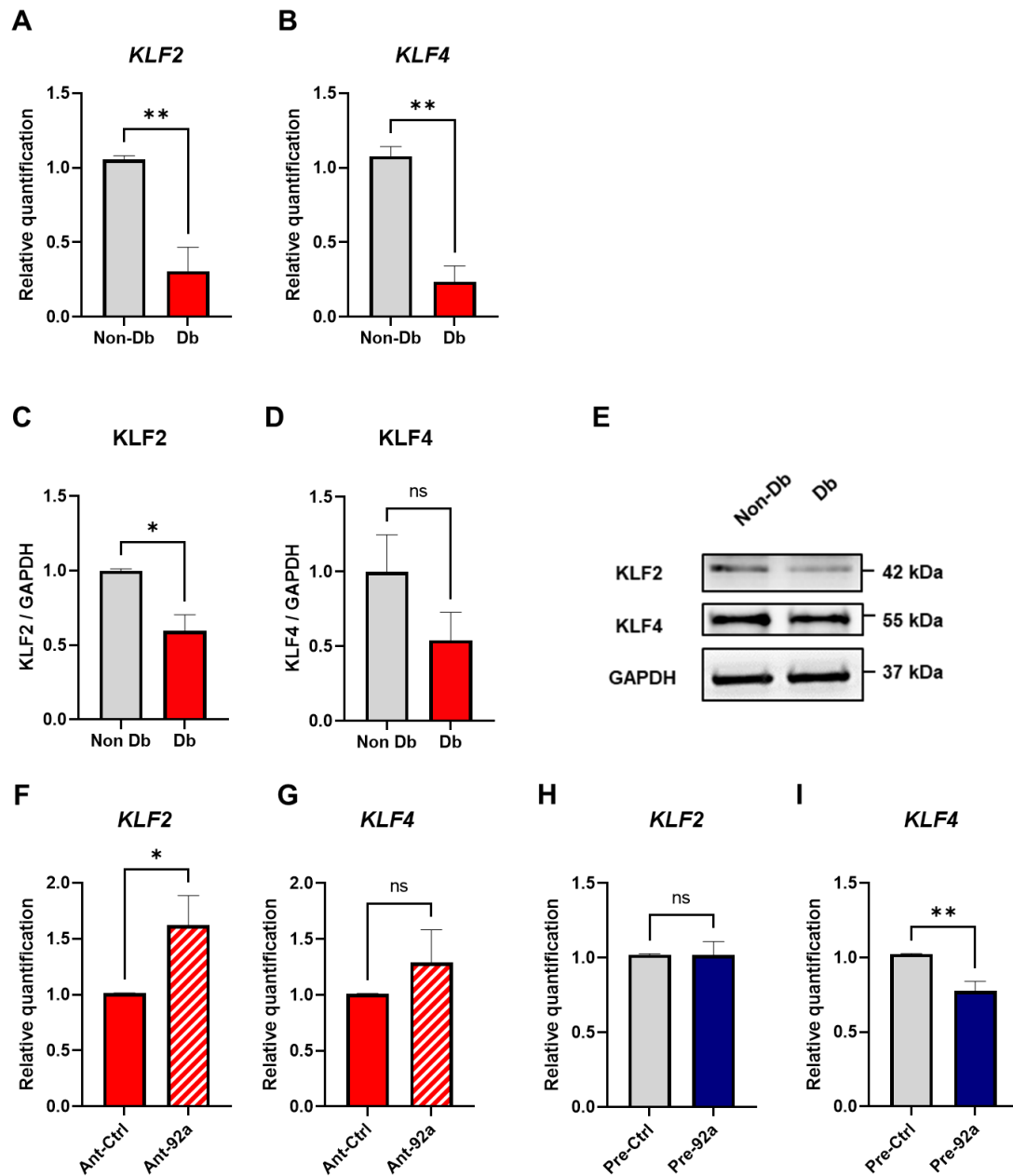


Figure 31. Expression of KLF2 and KLF4 in diabetic HCMEC and in correlation of miR-92a. (A, B) Quantitative PCR, and (C - E) Western blot analyses with representative blot of KLF2 and KLF4 relative gene, and protein expression, respectively, in non-diabetic or diabetic HCMEC ($n = 3$). The Western blot analysis here correspond to a different non-diabetic male donor than the qPCR experiments in the figure. (F, G) Quantitative PCR of KLF2, and KLF4 in diabetic HCMEC upon antagomir-mediated inhibition of miR-92a (Ant-92a) vs control (Ant-Ctrl) ($n = 4$), and (H, I) in non-diabetic HCMEC upon pre-miR-mediated overexpression of miR-92a (pre-92a) vs control (pre-Ctrl) ($n = 4$).

Results

In the *INS^{C94Y}* transgenic diabetic porcine hearts, gene expression analysis of *KLF2* and *KLF4* showed significant downregulation of both genes in the left ventricle over the cardiac long axis from base to apex compared to their wild-type littermates (Figure 32).

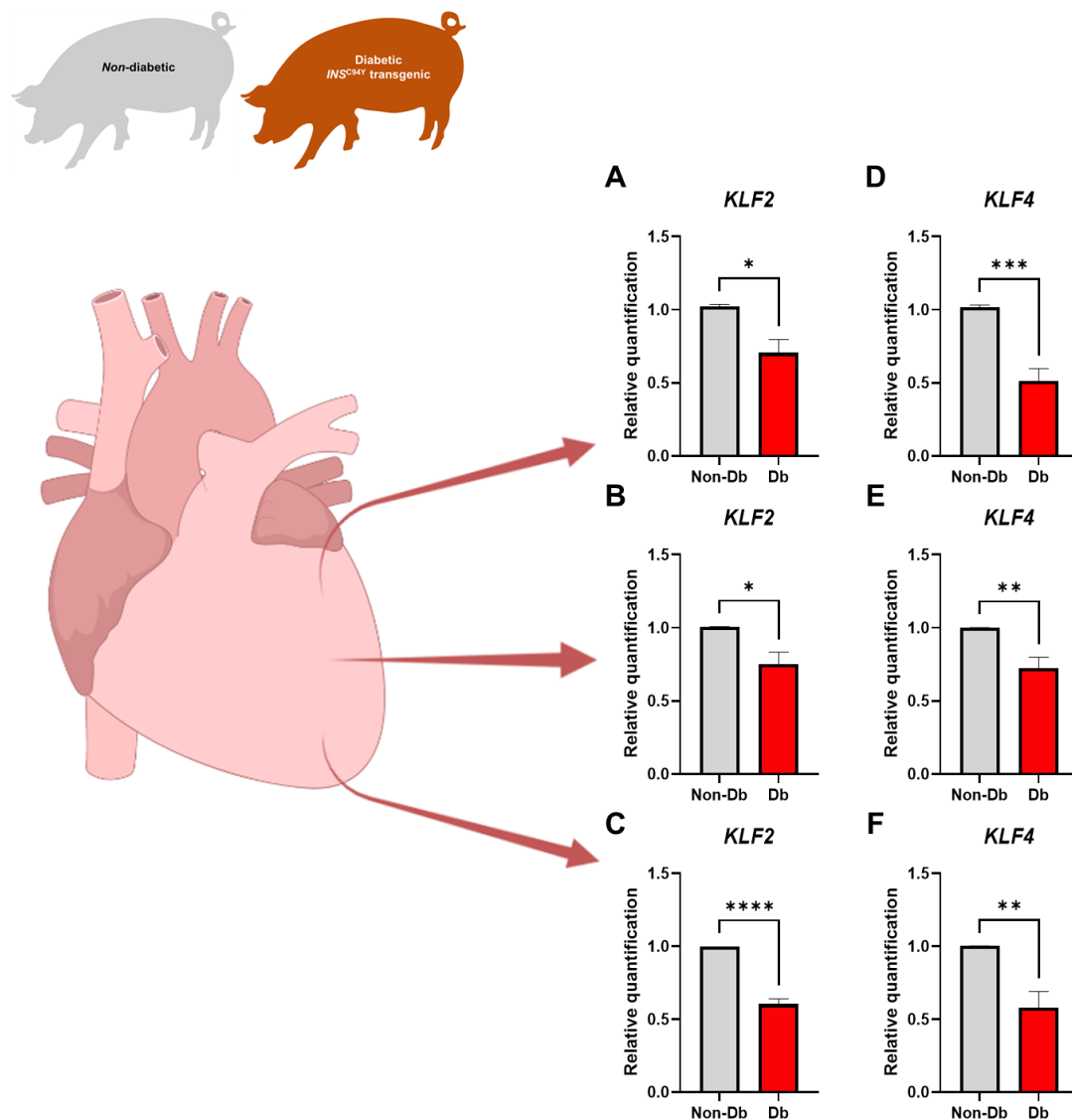


Figure 32. Differential expression of *KLF2* and *KLF4* in the left ventricular tissue of diabetic porcine models. Quantitative PCR analysis of (A – C) *KLF2* and (D – F) *KLF4* over the long axis of the left ventricle in non-diabetic (Non-Db) vs *INS^{C94Y}* transgenic diabetic (Db) pig tissue from base to apex, respectively ($n = 4$).

Results

To verify whether miR-92a can directly target *KLF2* and *KLF4*, I performed dual luciferase assays with the corresponding 3'-UTR target clones as previously described. Due to high degree of conservation, I used mammalian expression vectors bearing mouse *Klf2* and *Klf4* 3'-UTR. I co-transfected the vector with pre-miR-92a (pre-92a) or control pre-miR (pre-Ctrl). Indeed, miR-92a overexpression by pre-92a co-transfection diminished the reporter activity of both *Klf2* and *Klf4* 3'-UTR target clone expression vectors when assayed by bioluminescence, indicating direct interaction (Figure 33).

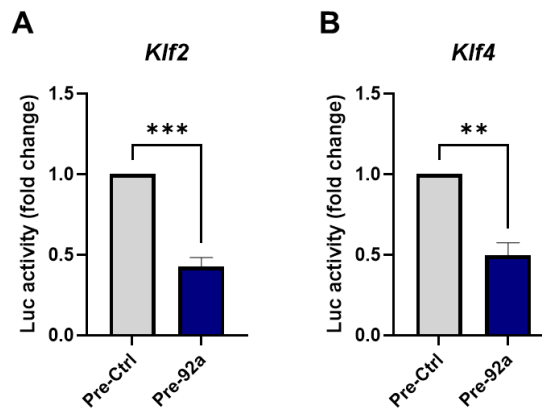


Figure 33 Direct targeting of *Klf2* and *Klf4* by miR-92a. Analysis of dual luciferase reporter activity fold change (Firefly / Renilla Luc) in mammalian expression vectors of mouse *Klf2*- and *Klf4*-3'-UTR upon overexpression of miR-92a (pre-92a) in HEK293 cells compared to controls (pre-Ctrl) ($n = 4$).

3.4.8. KLFs 2 and 4 as regulators of CMEC function

The anti-inflammatory roles of KLFs 2 and 4 has been reported in a number of *in vivo* and *in vitro* studies. To verify this in CMEC, I knocked-down *KLF2* or *KLF4* in non-diabetic HCMEC by siRNA transfection, and performed flow chamber assays with labeled THP-1 monocytes. Evidence of knock-down is shown in Figure 34.

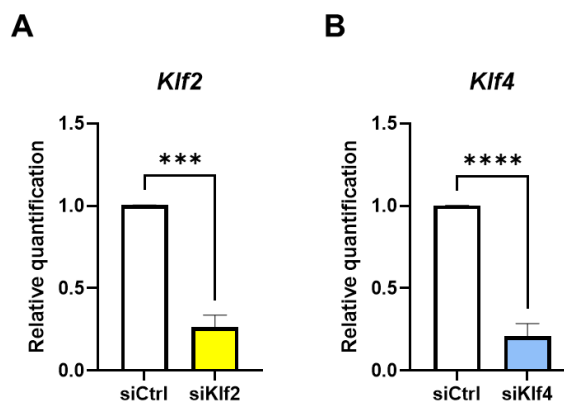


Figure 34. Knock-down of *Klf2* and *Klf4* in MCMEC. qPCR analysis of (A) *Klf2*, and (B) *Klf4* relative quantification in MCMEC upon siRNA knock-down ($n=4$).

Results

Indeed, knockdown of *KLF2* in non-diabetic HCMEC correlated with significant increase in adherent THP-1 monocytes count ($\approx 70\%$) to the endothelial monolayers compared to the control-transfected (Figure 35). Interestingly, analysis show no significant difference in adherent THP-1 to non-diabetic HCMEC monolayers where *KLF4* was downregulated (Figure 35).

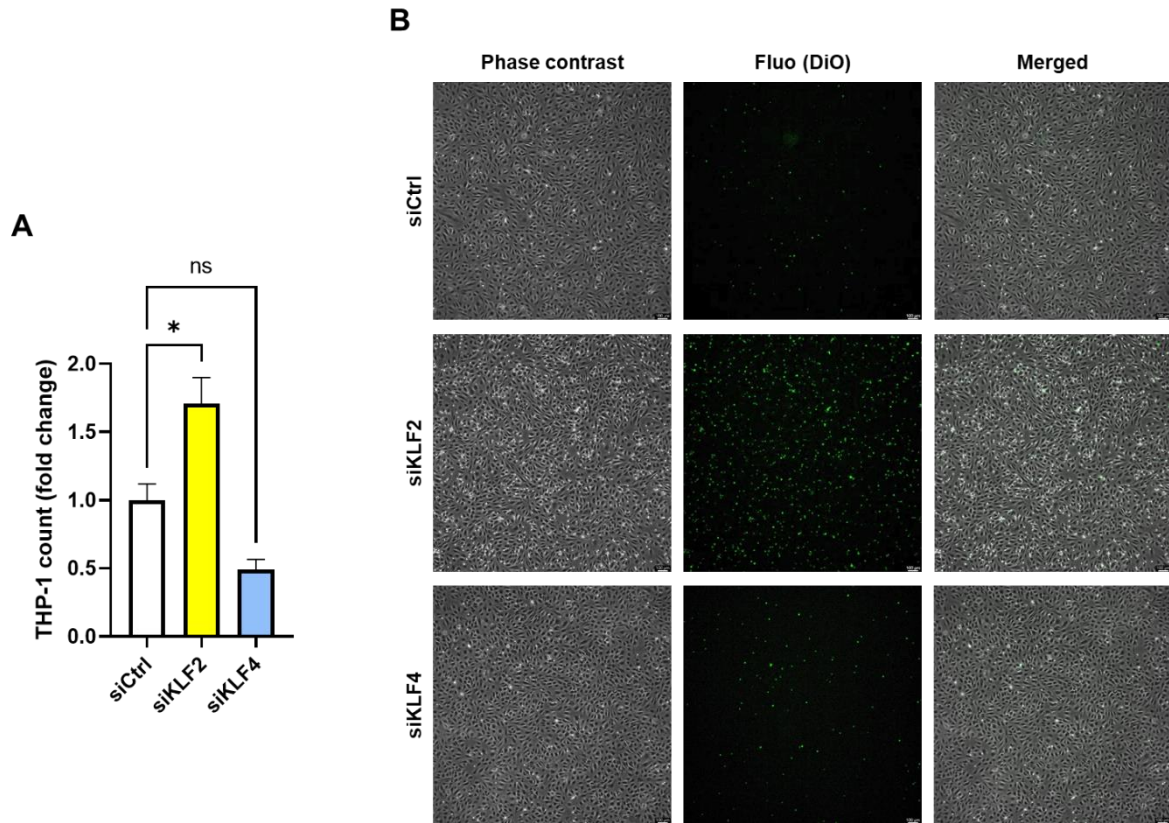


Figure 35. Characterization of the inflammatory phenotype in HCMEC upon *KLF2* or *KLF4* knock-down. (A) Analysis of fold change in adherent THP-1 count in non-diabetic HCMEC monolayers upon knock-down of *KLF2* (siKLF2) or *KLF4* (siKLF4) relative to controls (siCtrl) ($n = 4$). (B) Representative phase contrast, fluorescence and merged images of HCMEC monolayers and DiO-labeled THP-1 (green). Scale bars equal 100 μm .

To investigate the role of our target KLFs in CMEC migration, I performed wound healing assays in MCMEC upon knockdown of *Klf2* or *Klf4* by siRNA transfections. Analysis of open wound area by automated time lapse imaging showed that only the downregulation of *Klf2* brought about significant decrease in cell migration (Figure 36).

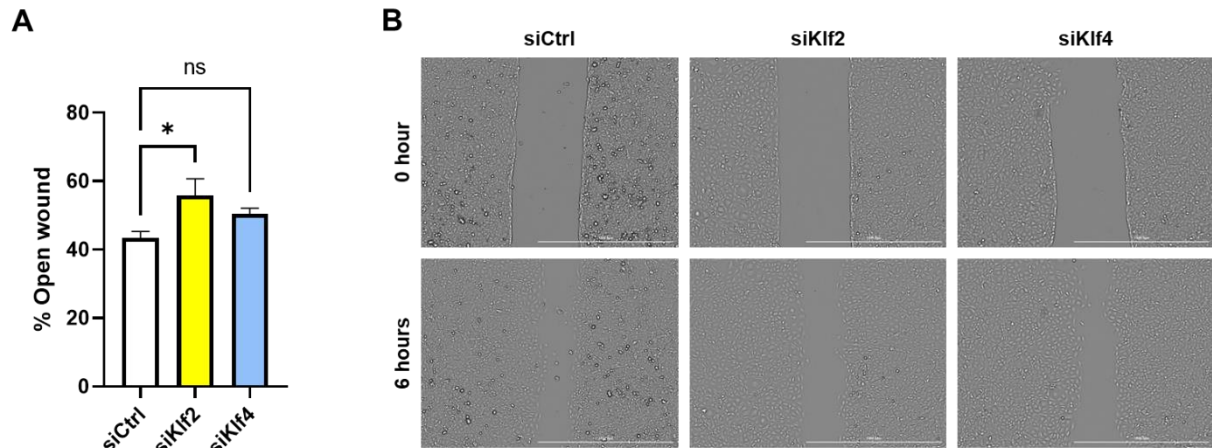


Figure 36. Migration phenotype in MCMEC upon ablation of *Klf2* or *Klf4*. (A) Bright field images by Cytation 1 plate reader of MCMEC migration at 0 and 6 hours upon knock-down of *Klf2*. (B) Analysis of 6-hour open wound areas in percentage in MCMEC upon knock-down of *Klf2* or *Klf4* ($n = 4$). Scale bars equal 1 mm.

3.4.9. Inter-regulation of KLFs

The redundancy between KLFs has been previously reported [154]. In order to test whether redundancy and/or inter-regulation exists between KLF2 and KLF4 I analyzed gene expression of either one upon knock-down of the other in MCMEC. Interestingly, knock-down of *Klf2* led to significant downregulation of *Klf4* mRNA, while *Klf2* mRNA levels were not affected by knockdown of *Klf4* (Figure 37), suggesting a role of KLF2 in regulation of *Klf4* gene expression in MCMEC.

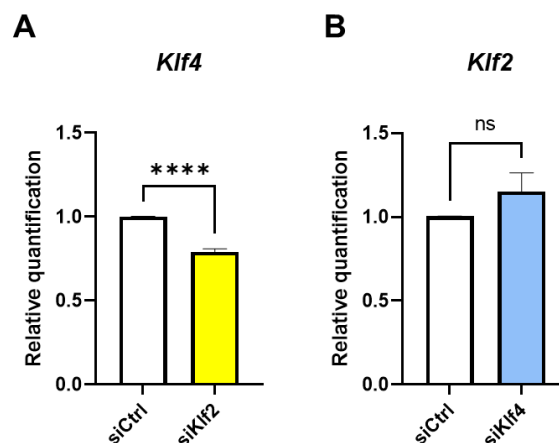


Figure 37. Inter-regulation of *Klf2* and *Klf4* in MCMEC. Quantitative PCR analysis of (A) *Klf4* gene expression upon knock-down of *Klf2* in MCMEC and (B) *Klf2* gene expression upon knock-down of *Klf4* in MCMEC, each compared to respective controls ($n = 4$).

3.4.10. Downstream inflammatory mediators of KLFs

Studies have highlighted the role of KLFs in regulating downstream inflammatory molecules in EC [143, 309-310]. These include, but are not limited to, vascular cell adhesion molecule 1 (VCAM1) and intercellular adhesion molecule 1 (ICAM1) [143, 309-311]. To find out whether upregulation of these inflammatory adhesion proteins can explain the observed phenotype in diabetic HCMEC, where KLFs are dysregulated, we analyzed VCAM1 and ICAM1 relative protein levels in lysates from non-diabetic or diabetic HCMEC. Indeed, VCAM1 was significantly upregulated in diabetic HCMEC, which conforms with their significantly reduced KLF2 expression, whereas the obvious trend in ICAM1 relative increase did not meet statistical significance (Figure 38). Accordingly, inhibition of miR-92a in diabetic HCMEC led to significant reduction in VCAM1 protein expression (Figure 38).

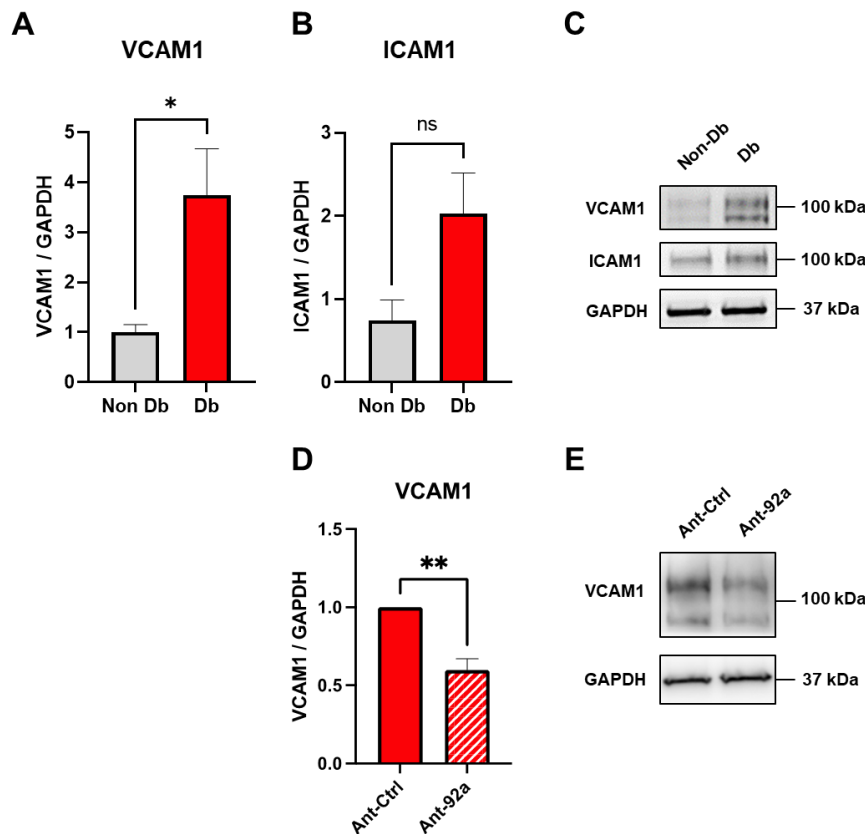


Figure 38. Expression of inflammatory adhesion molecules in diabetic HCMEC. (A, B) Analysis of relative protein expression of VCAM1 and ICAM1 in diabetic HCMEC relative to non-diabetic controls ($n = 4$). (C) Representative blot. (D) Analysis of relative protein expression of VCAM1 in diabetic HCMEC upon inhibition of miR-92a (Ant-92a) relative to control (Ant-Ctrl). (E) Representative blot. GAPDH is considered as housekeeping protein ($n = 3$).

3.4.11. Myocyte enhancer factors 2 (MEF2): novel targets in diabetic hearts

Several reports have highlighted the crucial role of MEF2 family in cardiovascular homeostasis [167, 169]. *In silico* analysis shows that the mRNA for human *MEF2D*, as well as its mouse orthologue, harbor a highly conserved target site for miR-92a's seed sequence in their 3'-UTR, i.e. 5'-GUGCAAUA-3' (Table 2). Interestingly, the human *MEF2D* 3'-UTR harbors a second miR-92a target site downstream, which is not present in the mouse's (Table 2) (Figure 39). Both sites are 8-mer target sites. Moreover, analysis of the predicted mRNA sequence of porcine *MEF2D* using the Nucleotide data base of the National Library of Medicine revealed conservation of the two 8-mer target sites found in the human orthologue (Figure 39).

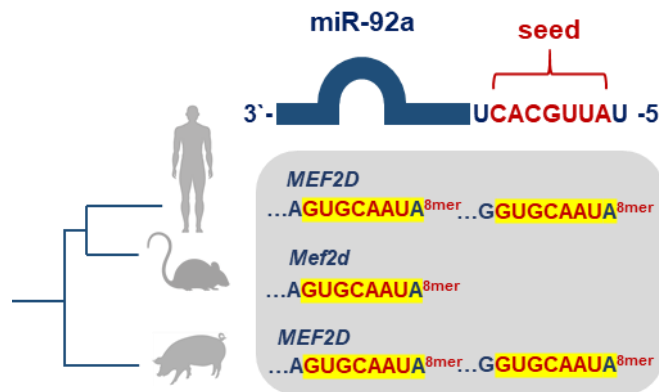


Figure 39. Evolutionary conservation of MEF2D miR-92a seed match in human, mouse and pig

Herein, dual-luciferase assays with human *MEF2D* 3'-UTR target clones revealed direct regulation by miR-92a, as evident from significant reduction in reporter luciferase activity upon miR-92a overexpression in HEK293 cells (Figure 40). Moreover, overexpression of miR-92a in non-diabetic HCMEC showed a slight, yet significant, downregulation of *MEF2D* mRNA by qPCR analysis (Figure 40).

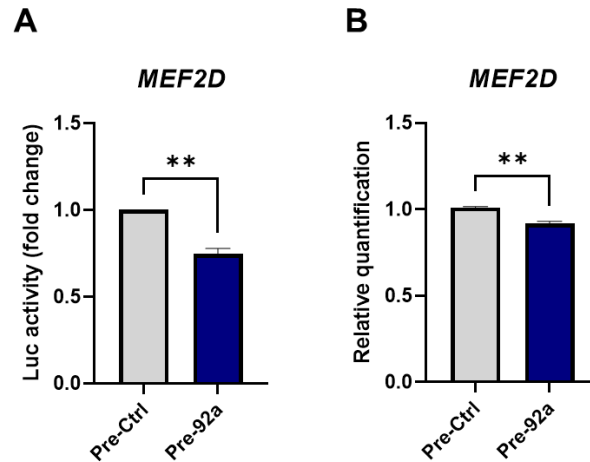


Figure 40. Direct targeting of *MEF2D* by *miR-92a*. (A) Dual luciferase reporter assay analysis of fold change in activity (Firefly / Renilla Luc) in mammalian expression vector of human *MEF2D*-3'-UTR downstream of firefly luciferase upon overexpression of *miR-92a* (pre-92a) in HEK293 cells compared to control (pre-Ctrl) ($n = 3$). (B) Quantitative PCR analysis of *MEF2D* in non-diabetic HCMEC upon pre-miR-mediated overexpression of *miR-92a* (pre-92a) vs control (pre-Ctrl) ($n = 3$).

Interestingly, analysis of *MEF2D* gene expression in diabetic HCMEC by qPCR shows significant downregulation of its mRNA levels relative to non-diabetic controls (Figure 41). Moreover, this applied to ventricular tissue from diabetic pigs where *MEF2D* mRNA was significantly ablated in extracts, as quantified by PCR (Figure 41). Indeed, inhibition of *miR-92a* restored *MEF2D* expression levels in diabetic HCMEC. Quantitative PCR analysis showed significant increase in *MEF2D* mRNA levels in 92a-anatgomiR transfected diabetic HCMEC (Ant-92a) relative to controls (Ant-Ctrl) (Figure 41).

Results

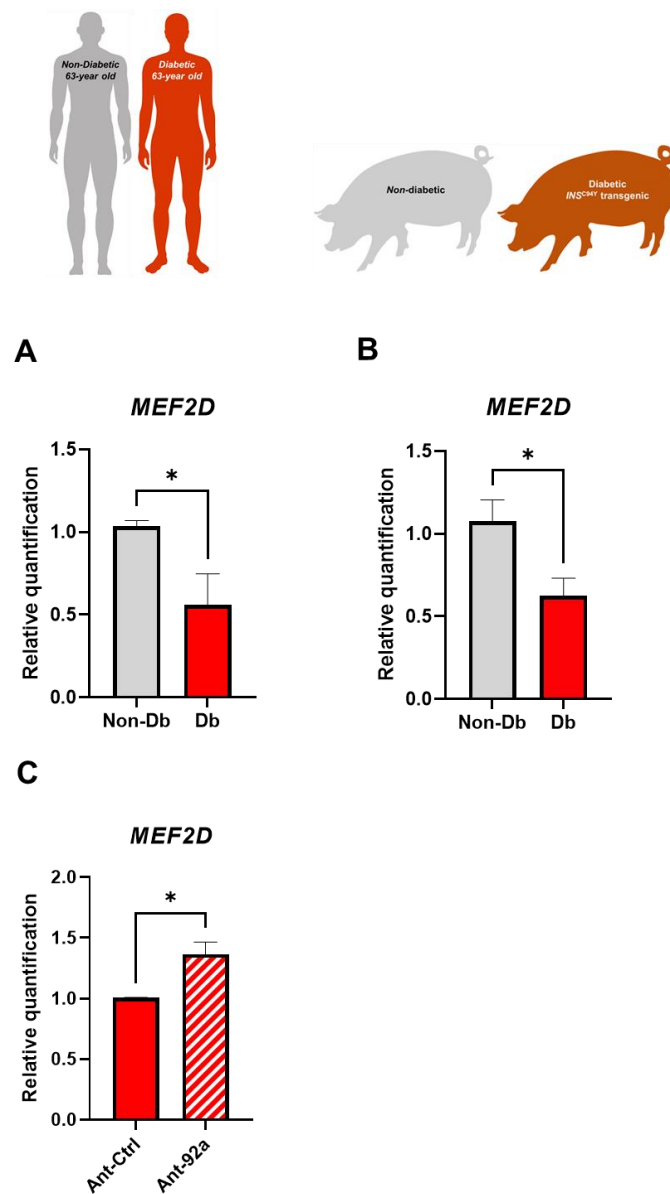


Figure 41. Expression of MEF2D in diabetes. Quantitative PCR analysis of MEF2D mRNA levels in (A) male diabetic HMEC relative to matched non-diabetic controls and (B) the left ventricle of *INS^{C94Y}* transgenic diabetic (Db) pig tissue vs non-diabetic wild-type littermates ($n = 4$). (C) qPCR analysis of MEF2D mRNA levels in male diabetic HMEC upon miR-92a inhibition (Ant-92a) relative to controls (Ant-Ctrl.) ($n = 3$).

Results

Earlier reports have demonstrated the close regulation of the glucose transporter 4, GLUT4, by MEF2 members A and D, where MEF2D was shown to compete with MEF2A over *GLUT4* promotor and, in turn, relatively reduce *GLUT4* (*SLC2A4*) gene expression [312-313]. Downregulation of MEF2D as a result of diabetes or via direct interaction with miR-92a might therefore be expected to influence *GLUT4* (*SLC2A4*) gene expression. I verified this by testing *SLC2A4* gene expression in diabetic HCMEC and upon miR-92a overexpression. Indeed, pre-92a transfection in non-diabetic HCMEC correlated with significant increase in quantified *SLC2A4* mRNA by qPCR relative to control transfected cells (pre-Ctrl). This was functionally asserted by glucose uptake assays, where I report significant increase in glucose uptake in miR-92a overexpressing non-diabetic HCMEC relative to controls (Figure 42). Therein, overexpression of miR-92a led to $\approx 65\%$ increase in glucose uptake relative to controls. In diabetic HCMEC however, basal glucose uptake was significantly diminished; there it was $\approx 34\%$ less compared to non-diabetic (Figure 42). Interestingly, there was no significant difference in *GLUT4* relative gene expression in diabetic HCMEC compared to non-diabetic controls (Figure 42). To find out whether the observed finding is due to other EC glucose transporter, I analyzed relative gene expression of *GLUT1* (*SLC2A1*). However, no significant difference was calculated either (Figure 42).

In accordance with these findings, no significant differences were observed in *MEF2A* mRNA levels in diabetic HCMEC relative to their non-diabetic controls, or in miR-92a-overexpressing non-diabetic HCMEC when relatively quantified to their control transfected counterparts (Figure 43).

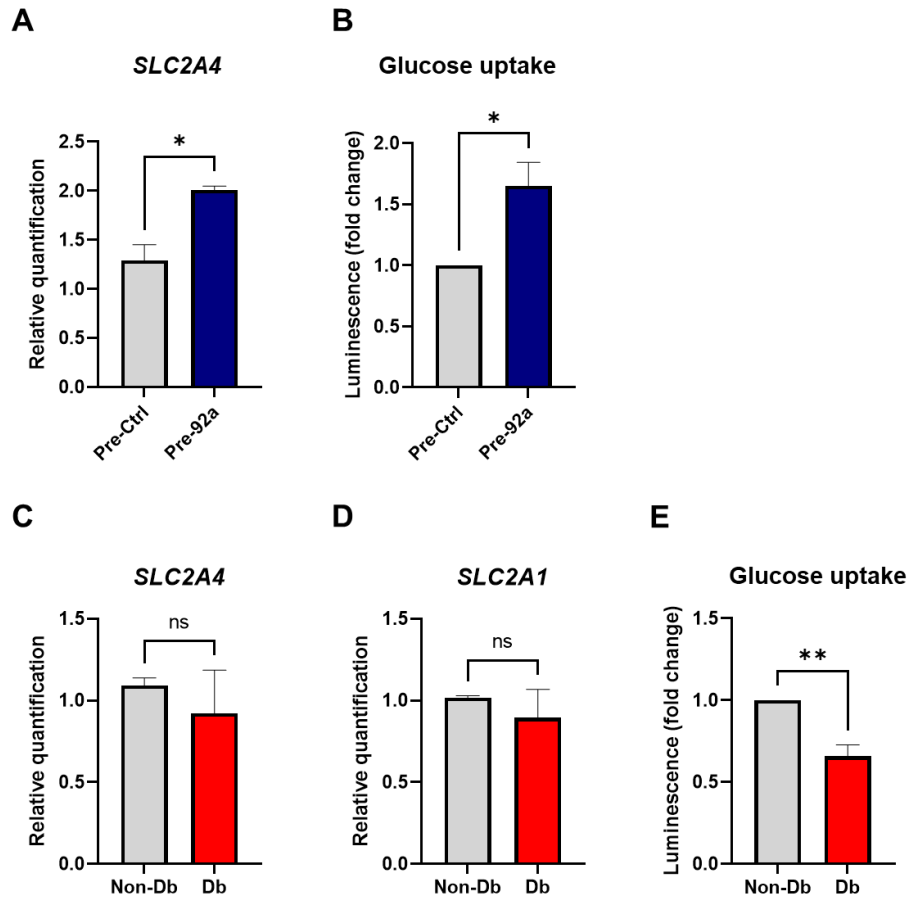


Figure 42. Expression of GLUT4 (SLC2A4) and glucose uptake in relation to miR-92a. (A) Quantitative PCR of GLUT4 (SLC2A4) in non-diabetic HCMEC upon miR-92a overexpression (pre-92a) relative to control (pre-Ctrl) ($n = 3$). (B) Analysis of glucose uptake luminescence assay (fold change) in non-diabetic HCMEC upon miR-92a overexpression (pre-92a) relative to controls (pre-Ctrl) ($n = 3$). (C, D) Quantitative PCR analysis of GLUT4 (SLC2A4), and GLUT1 (SLC2A1) in male diabetic HCMEC relative to non-diabetic counterparts ($n = 3$). (E) Glucose uptake luminescence assay analysis (fold change) in diabetic HCMEC relative to non-diabetic controls ($n = 3$).

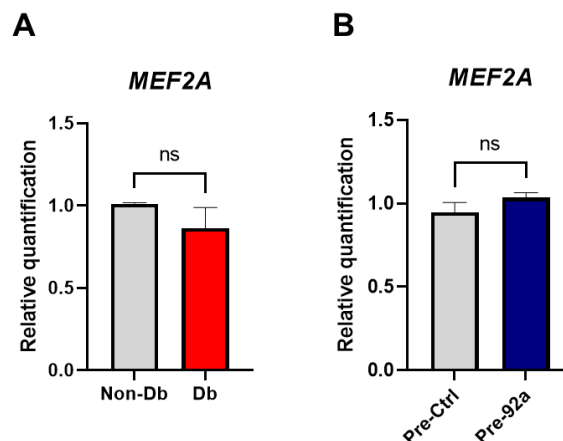


Figure 43. Expression of MEF2A in diabetic HCMEC and in relation to miR-92a. (A) qPCR analysis of relative MEF2A mRNA levels in non-diabetic vs diabetic HCMEC ($n = 6$). (B) qPCR analysis of MEF2A mRNA levels in non-diabetic HCMEC upon miR-92a overexpression (pre-92a) relative to control (pre-Ctrl) ($n = 3$).

3.4.12. Regulation of KLFs by MEF2

MEF2 transcription factors have been reported to be the master regulators of *KLF2* and *KLF4* expression in endothelial cells downstream of hemodynamic flow [314-315]. To find out whether this applies to our CMEC, and whether the observed dysregulation of KLF expression in diabetes are linked to the observed *MEF2D* dysregulation in our diabetic models, I knocked-down *MEF2A* or *MEF2D* in non-diabetic HCMEC and analyzed *KLF2* and *KLF4* gene expression. Indeed, knockdown of *MEF2D*, but not *MEF2A*, led to significant downregulation in *KLF2*, but not *KLF4*, gene expression (Figure 44). Interestingly, knockdown of *MEF2A* led to significant downregulation of *KLF4* and not *KLF2* (Figure 44). Neither did knockdown of *MEF2D* or *MEF2A* affect the expression level of each other (Figure 44).

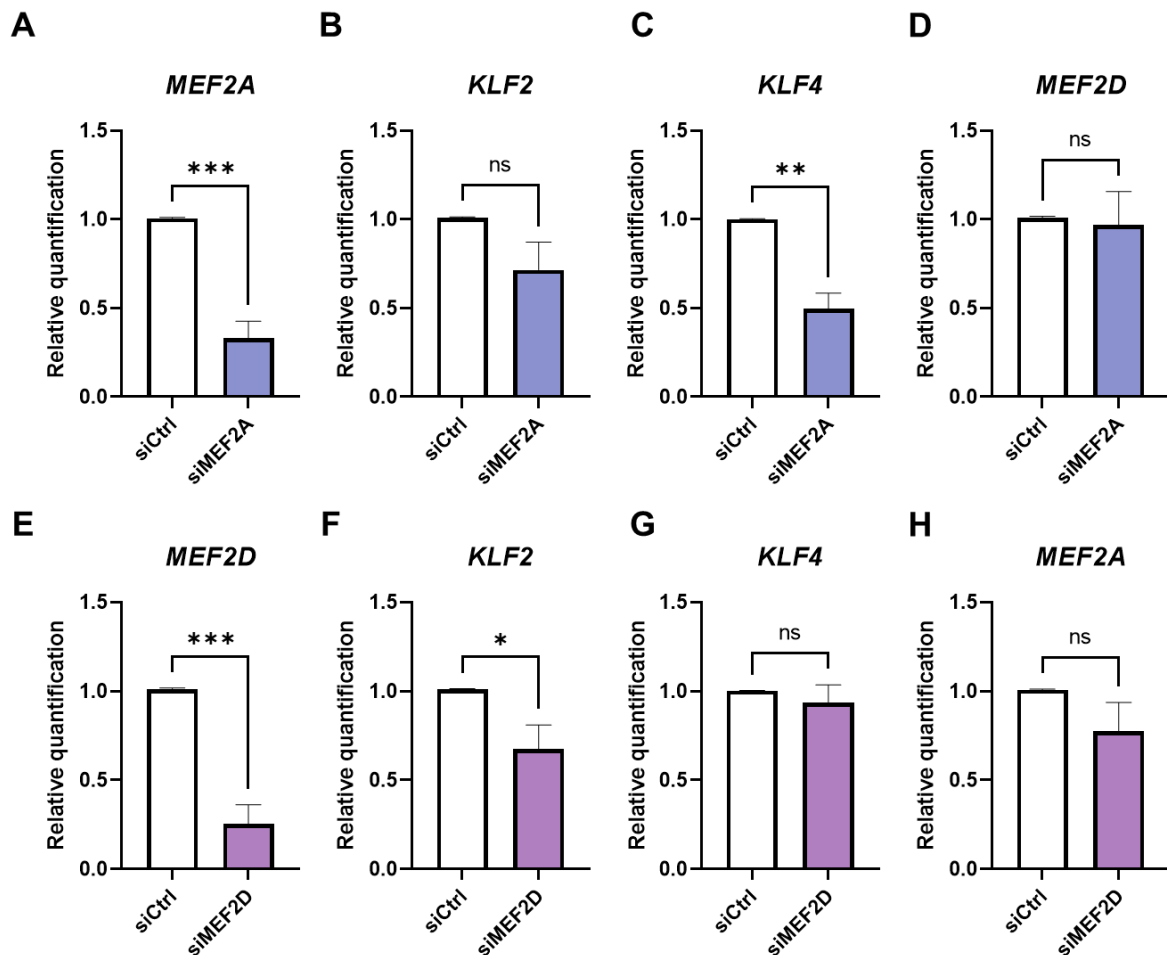


Figure 44. Regulation of *KLF2* and *KLF4* by *MEF2A* or *MEF2D*. Quantitative PCR analyses. (A, E) Evidence of knockdown of *MEF2A* or *MEF2D* by respective siRNAs (siMEF2A or siMEF2D). (B, C, F, G) Relative quantification of *KLF2* and *KLF4* upon knockdown of *MEF2A* or *MEF2D*, respectively, compared to controls (siCtrl) (D, H) Relative quantification of *MEF2D* or *MEF2A* upon knockdown of *MEF2D* or *MEF2A*, respectively, compared to control (siCtrl) ($n = 4$).

3.5. Human umbilical vein endothelial cells (HUVEC)

3.5.1. High glucose culture on HUVEC function and miR-92a levels

To understand the effect of high glucose culture, HUVEC were cultured and passaged in normal (5.5 mM) or high (30 mM) glucose before they were subjected to endothelial function assays. In tube formation assays, there was no significant difference in total tube length, tube count or branching point count between normal and high glucose (Figure 45). In wound healing assays, there was a significant difference in the wound area analyzed after 8 hours in normal (5.5 mM) and high (30 mM) glucose (Figure 45). High glucose wounds were $\geq 25\%$ larger than normal glucose ones.

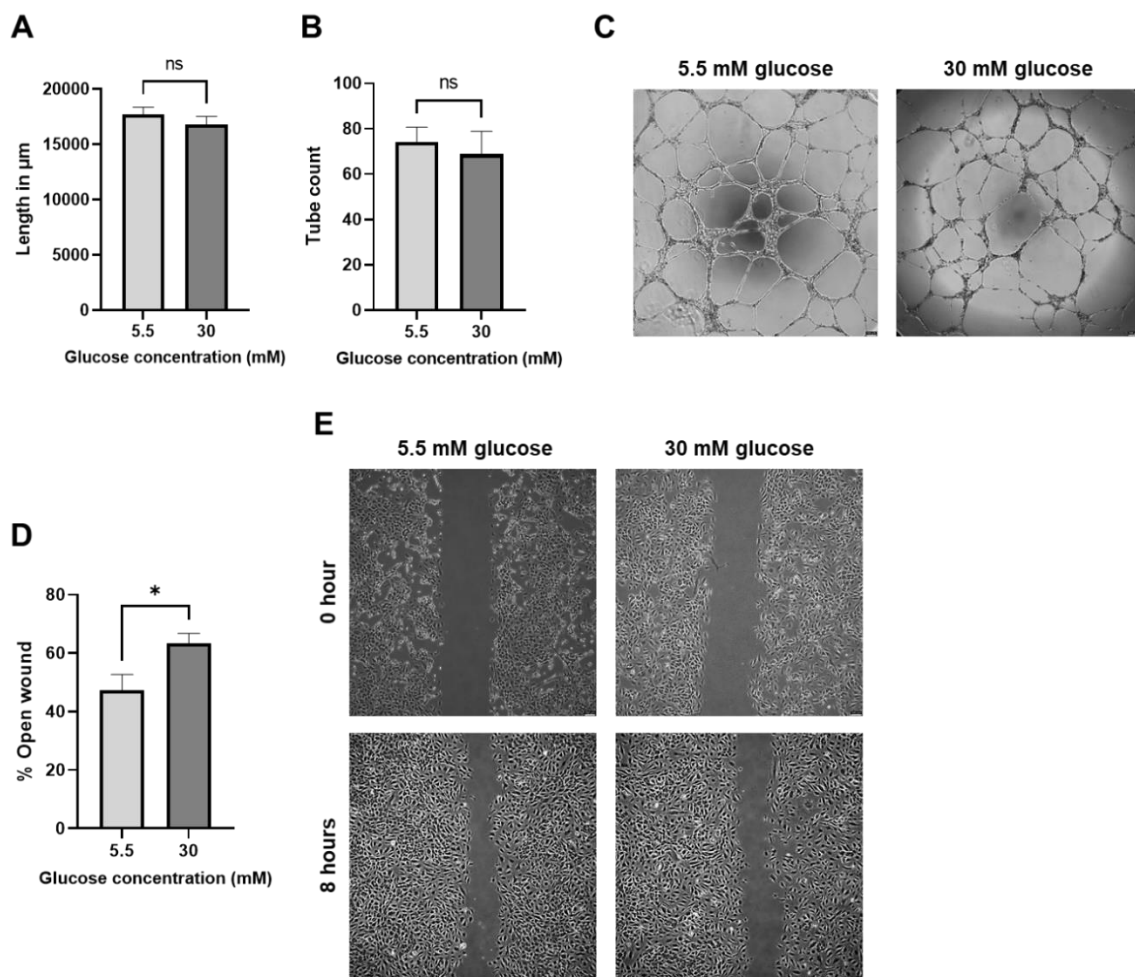


Figure 45. Effects of high glucose culture on HUVEC tube formation and migration. (A, B) Analysis of total tube length in μm and tube count in HUVEC under 5.5 or 30 mM glucose, respectively ($n = 5$). (C) Representative phase contrast images of tube formation. (D) Analysis of relative open wound area in percentage over 8 hours of migration in HUVEC under 5.5 or 30 mM glucose ($n = 5$). (E) Representative phase contrast images. Scale bars equal 100 μm .

Results

In flow chamber assays, no significant difference was observed in the adherent THP-1 cell count to HUVEC monolayers when they were cultured, and assayed, in normal (5.5 mM) or high (30 mM) glucose (Figure 46).

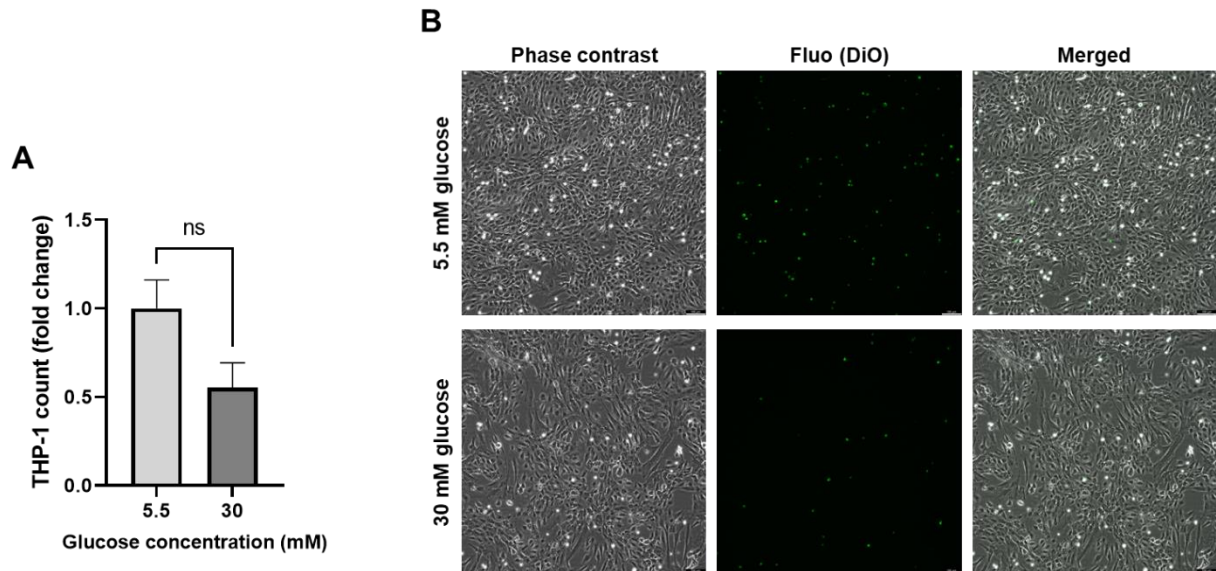


Figure 46. Effect of high glucose culture on HUVEC inflammatory state. (A) Analysis of fold change in adherent THP-1 count to HUVEC monolayers cultured in 5.5 or 30 mM glucose upon flow chamber assay ($n = 3$). (B) Representative phase contrast, fluorescence and merged images of HUVEC monolayers cultured in 5.5 or 30 mM glucose, and DiO-labeled THP-1 monocytes (green) after flow chamber assay. Scale bars equal 100 μm .

Interestingly, and unlike HCMEC, qPCR analysis of miR-92a levels in HUVEC revealed significant downregulation ($\approx 44.5\%$) in high glucose, compared to normal glucose cultures (Figure 47).

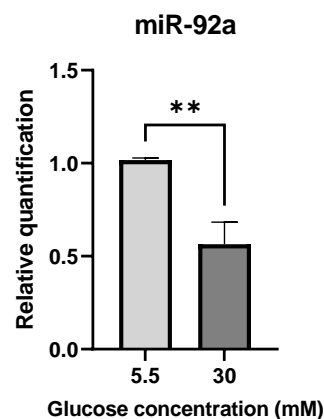


Figure 47. Effect of high glucose culture on miR-92a expression in HUVEC. Quantitative PCR analysis of miR-92a relative expression levels in HUVEC cultured 5.5 or 30 mM glucose ($n = 4$).

3.5.2. Overexpression of miR-92a in HUVEC

Earlier reports described an anti-angiogenic role of miR-92a in HUVEC [296]. I attempted to reproduce the published data. Therefore, I overexpressed miR-92a in HUVEC by pre-miR transfection, and subject the cells to tube formation and wound healing assays to investigate possible effects of miR-92a on HUVEC's angiogenic, and migratory potentials. Figure 48 shows proof of overexpression of miR-92a in HUVEC by pre-92a transfection, compared to control (pre-Ctrl). Transfection with pre-92a in HUVEC leads to significant, 20-fold increase in its levels compared to controls.

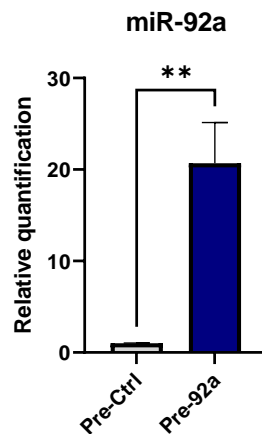


Figure 48. Overexpression of miR-92a in HUVEC. Quantitative PCR analysis of miR-92a in HUVEC upon pre-miR transfection (pre-92a) relative to control (pre-Ctrl) ($n = 5$).

In angiogenesis assays, no significant differences were observed in either total tube length or tube count in HUVEC cultured in normal (5.5 mM) or high (30 mM) glucose upon overexpression of miR-92a (pre-92a) compared to controls (pre-Ctrl) (Figure 49). Likewise, in wound healing assays, no differences were observed in the analyzed wound areas at 8 hours in HUVEC in either glucose concentration upon overexpression of miR-92a (pre-92a) compared to controls (pre-Ctrl) (Figure 49).

Results

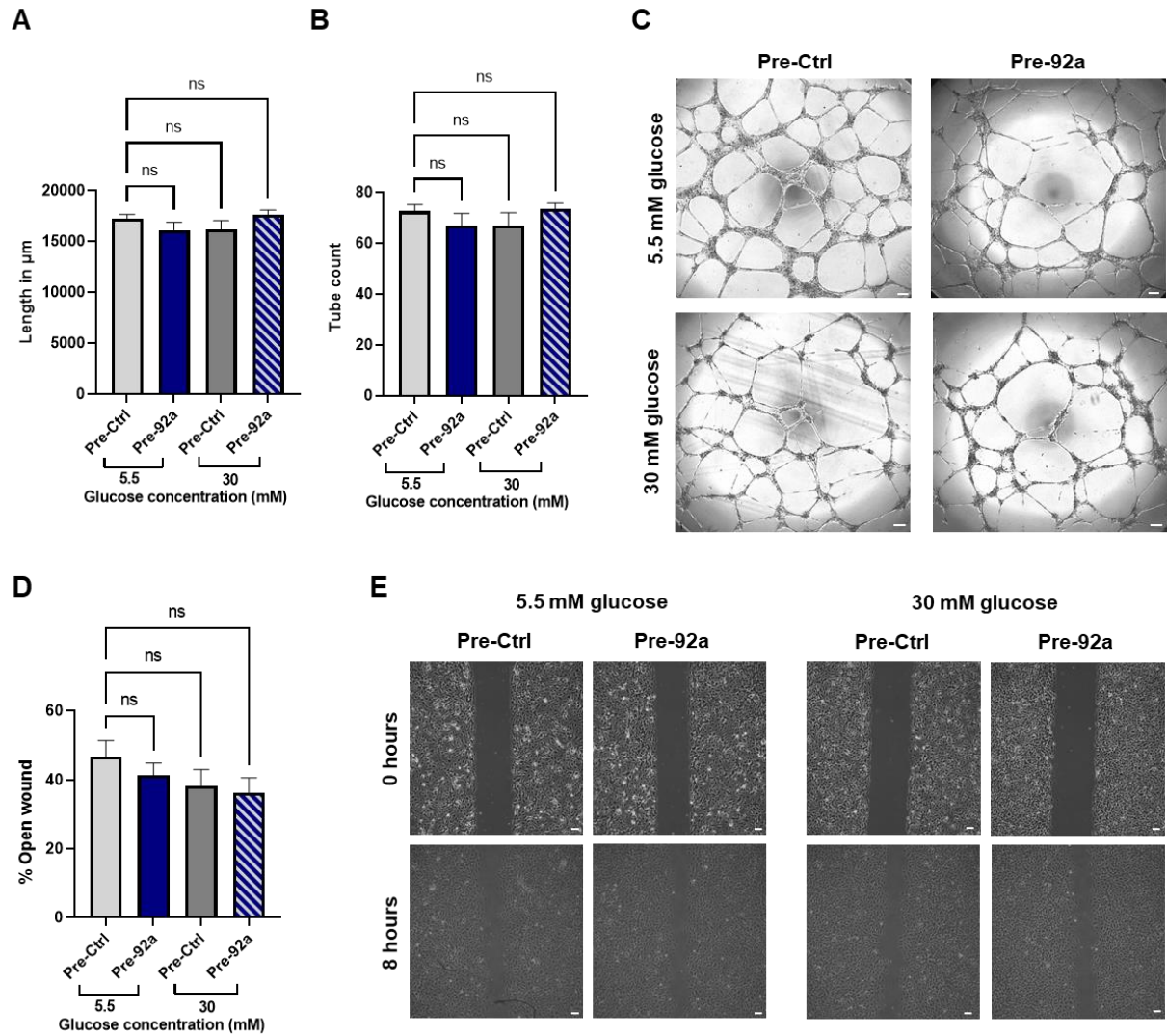


Figure 49. Overexpression of miR-92a upon high glucose culture on HUVEC tube formation and migration. (A, B) Analysis total tube length and tube count in HUVEC under 5.5 or 30 mM glucose upon overexpression of miR-92a by pre-miR transfection (pre-92a) or controls (pre-Ctrl). ($n = 7$). (C) Representative phase contrast images of HUVEC tube formation. (D) Analysis of relative open wound area in percentage in HUVEC cultured in 5.5 or 30 mM glucose upon overexpression of mir-92a by pre-miR transfection (pre-92a) or controls (pre-Ctrl) over 8 hours of migration ($n = 4$). (E) Representative phase contrast images. Scale bars equal 100 μm .

3.5.3. Downstream targets of miR-92a in HUVEC

The aforementioned observed disparity in HUVEC compared to HCMEC prompted further investigation of the miR-92a targets of interest. We performed quantitative PCR analysis of miR-92a target genes in HUVEC upon overexpression of miR-92a by pre-miR transfection. Interestingly, overexpression of miR-92a did not influence *ADAM10* mRNA levels in HUVEC, as no significant difference was observed between pre-92a-transfected cells compared to controls (pre-Ctrl) (Figure 50).

Results

Unlike HCMEC, overexpression of miR-92a (pre-92a) led to significant decrease in *KLF2* mRNA levels compared to controls (pre-Ctrl) (Figure 50). Like HCMEC, *KLF4* mRNA levels were significantly downregulated in HUVEC upon overexpression of miR-92a by pre-miR transfection (pre-92a) compared to controls (pre-Ctrl) (Figure 50).

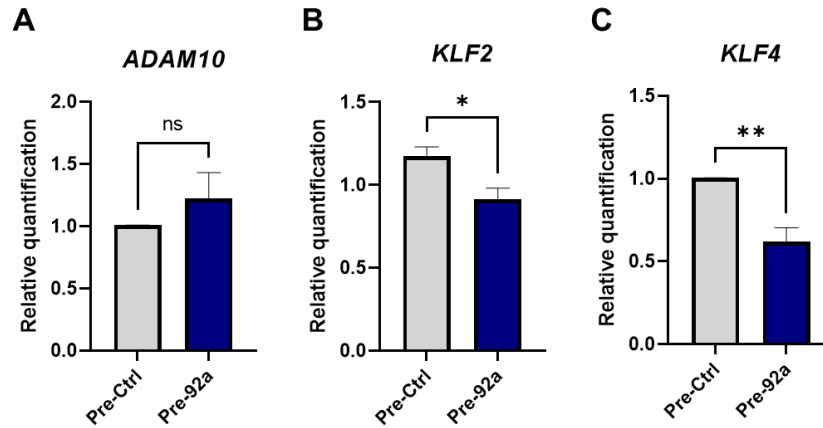


Figure 50. Analysis of gene expression of miR-92a targets in HUVEC upon its overexpression. Quantitative PCR analysis of (A) *ADAM10*, (B) *KLF2* and (C) *KLF4* in HUVEC upon overexpression of miR-92a by pre-miR transfection (pre-92a) or controls (pre-Ctrl) (n = 4).

Finally, I compared basal levels of expression of miR-92a targets in HCMEC and HUVEC by qPCR. Indeed, *ADAM10* gene expression analysis revealed significant increase in HCMEC than in HUVEC. Relative quantification revealed $\approx 50\%$ increase in *ADAM10* mRNA levels in non-diabetic HCMEC compared to HUVEC (Figure 51). On the other hand, gene expression analysis of *KLF2* and *KLF4* by qPCR revealed no significant differences between HUVEC and non-diabetic HCMEC (Figure 51).

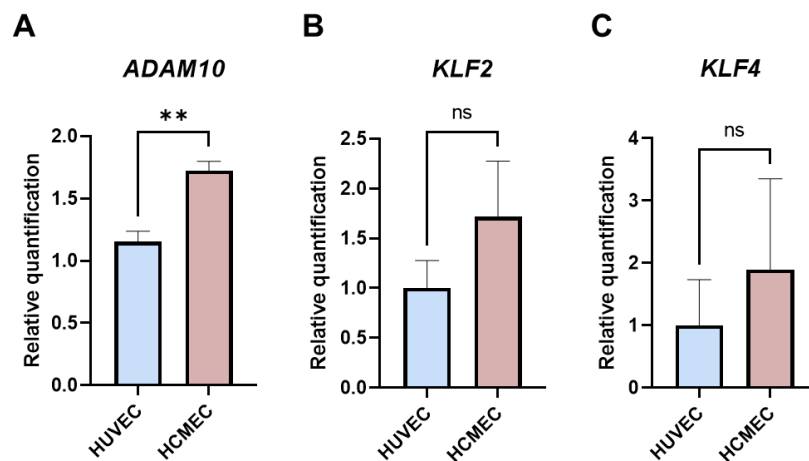


Figure 51. Gene expression analysis of miR-92a targets in HUVEC vs HCMEC. Quantitative PCR analysis of (A) *ADAM19*, (B) *KLF2* or (C) *KLF4* in HUVEC vs HCMEC (n = 3).

4. Discussion

Diabetes is a plight to modern human societies, particularly in developed and/or western countries. In the EU alone, 9% of the total health care budgets of Member States were spent on diabetes management in 2019, and figures are on the rise [316]. This is certainly a high price to pay, inasmuch as the abundance of other current challenges. Being the number one risk factor for cardiovascular disease and multiple organ failure, diabetes is no short of a health calamity. The rising numbers speak volumes about the inadequacy of our current disease management protocols, and call for novel therapeutic interventions. Timely, advents in molecular medical research over the past decades have opened doors to a better understanding of disease pathophysiology, and paved the way for the development of innovative therapeutic tools, e.g. small RNA / nucleic acid therapy. Therefore, in the present doctoral study I availed myself to the wealth of scientific knowledge to build an epistemological approach to diabetes-associated cardiovascular complications, and potential therapeutic targets. To this end, I designed research methodologies and applied several laboratory and analytical methods to investigate molecular determinants of diabetic vascular dysfunction, as well as promising therapeutic targets thereof. Herein, the previous work of Hinkel et al. on micro-RNAs, particularly miR-92a, was set as a foundation to this research project [66, 298].

4.4. Optimized *in vitro* models and the 3R principle

As introduced, the work presented here prioritizes cardiac microvascular complications in diabetes. To study this, I optimized relevant *in vitro* research models and utilized them throughout the course of this project. Optimized *in vitro* models are a corner stone of the so called “3R” principle, standing for “replace”, “reduce” and “refine” [317]. Since its introduction in the late fifties, the 3R principle aims at limiting animal experimentation, and any avoidable suffering it entails [318]. This emanates from an ethical standpoint of living sentient beings. The 3R principle advocates replacement of animal experiments wherever possible, reduction of the number of animals in scientific experiments, and refinement of experimental procedures on living animals, thus minimizing stress and suffering to indispensable levels [317]. The Laboratory Animal Science department at the German Primate Center is committed to the 3R principle in its research conduct. Hence, the work presented here does not include any live animal experiments, and no extra animals had to be sacrificed for its sake.

4.5. Endothelial cell models & endothelial heterogeneity

To study the diabetic vascular pathology, the *in vitro* research models utilized here are primarily endothelial cells (EC) of different origins. In order of presentation in the Results' section, HCMEC come first, followed by MCMEC and lastly, HUVEC. Chronologically, however, as I started with protocol generation and optimization, I used HUVEC due to their ease of obtainment and culture [319]. Moreover, there is an ample literature available on modeling diabetic vasculopathy, as well as the role of our miRNA of interest, i.e. miR-92a, where HUVEC is used as the main *in vitro* research model [320-323]. In fact, one of the leading studies addressing the role of miR-92a as a repressor of the EC angiogenic program reported their *in vitro* results in HUVEC [296]. In my hands, however, characterization of HUVEC under the set experimental conditions did not reflect the pathological alterations in the diabetic cardiac microvessels, much less with regard to miR-92a. The controversy on the role of miR-92a in HUVEC has already been reported by studies and is discussed in further detail later in this chapter [324]. However, upon incorporation of cardiac microvascular EC (CMEC), the findings were in stark difference compared to HUVEC. The gained experience, therefor, brings about a brief discussion of endothelial heterogeneity that shall aid in understanding of the findings presented here.

While general basic research questions can still be addressed in EC regardless of their origin, the vascular endothelium is far from homogenous. This trails its origins to the developing embryo. During embryogenesis, EC arise *de novo* from mesodermal progenitors to form primitive vascular plexi [325]. In the embryo proper, the nascent vascular network undergoes arteriovenous specification as a product of shear stress, which elicits differential gene expression programs in EC that govern their commitment to either arteries or veins, and later to lymphatic EC [326]. Specification to either arterial or venous EC is orchestrated by a set of well-studied signaling molecules, namely the Notch/VEGF or COUP transcription factor 2 (COUP-TFII), respectively [326]. On a macrovascular level, artery and vein EC display distinct transcriptomic and phenotypic profiles, which get even more heterogeneous on a microvascular level [327-328]. This is because as the endothelium expands during morphogenesis, it develops in an organ-specific manner, where the intimate interaction between EC and tissue-resident parenchymal and stem cells shapes the endothelial identity within each vascular bed, a phenomenon that persists through adulthood [329]. Recent studies employing single cell RNA sequencing (scRNA-Seq) have clearly demonstrated this by dissecting organ-specific transcriptomes of EC, which attributes overall tissue homeostasis [325, 330].

Discussion

In light of this knowledge on EC, the discrepancy of results between HUVEC and HCMEC can be understood, especially when cellular response to nutrients, such as glucose, or mRNA activities are under investigation. Whereas HUVEC are embryo-driven **macro**-vascular venous endothelial cells, HCMEC are highly-specialized adult **micro**-vascular coronary EC. Every identical aspect of these cells entails a degree of differentiation. Commercial availability of HCMEC, especially from diabetic donors, bestowed this project with a great advantage by enabling a more accurate modelling of the cardiac microvascular pathology in DM *in vitro*.

I present results of HCMEC from 4 different adult donors of Caucasian background; three non-diabetics and one type 2 diabetic. One non-diabetic donor was a female, and the other three were males, two of which were age-matched, i.e. 63-year olds non-diabetic and diabetic, while one was almost a decade younger. I used the cells over short term passages, i.e. until passage 8, to maintain cellular identity and avoid trans-differentiation. The cells retained their morphological characteristics and angiogenic ability throughout these passages. When primary HCMEC were cultured and passaged they typified endothelial morphology and proliferated, however at slightly different rates. Herein, female cells stretched over slightly larger areas, and proliferated at a relatively slower rate. Moreover, as seen from the results, the angiogenic phenotype displayed notable differences at normal culture conditions, judging from the two main outcomes I used to quantify tube formation, i.e. total tube length and tube count. Indeed, tubes formed by male HCMEC were almost 4 times higher in their cumulative length and over 7 times the count of the female HCMEC. Herein, the genomic sex of EC adds another layer of heterogeneity that gets more pronounced upon disease modeling, and therefore merits further discussion.

The vasculature of males and females have been deemed heterogeneous. Pioneered by Huxley et al., studies have shown remarkable distinctions in morphology as well as gene and protein expression between male and female macro- and microvascular EC [331-332]. Some prominent examples include, but are not limited to, cell area, proliferation rate, lactate production and expression of sex hormone receptor mRNA and protein. Interestingly, male microvascular EC significantly upregulated androgen receptor (AR), estrogen receptor- α (ER α) and VCAM1 levels, whereas female cells dominated in ICAM1, PECAM1 and integrins α_v and β_3 expression [331]. This well explains the prominent angiogenic phenotype seen here in male cells, considering the proangiogenic signaling of ER α [331]. In female cells, on the other hand, the morphology reflects the role of integrins in dictating how cells spread and line capillaries. Moreover, the cellular response to inflammatory stimuli, e.g. lipopolysaccharide

(LPS), was also shown to be sex specific, wherein male cells were more conspicuous in their inflammatory phenotype than female cells [332]. Certainly, there are important clinical implications of these findings. For instance, presentation of coronary heart disease is often microvascular in females, whereas in males, the macrovascular pathology is more dominant [333-334]. Importantly, with regard to diabetes, studies have shown that diabetic women had earlier occurrences and higher mortality from myocardial infarction, as well as lower revascularization rates than diabetic men [335-336]. In congruence with these clinical findings, the following discussion of my results shall also reflect aspects of sexual dimorphism in cardiac microvascular endothelial dysfunction upon *in vitro* modeling of DM. However, it is important to state that inter-individual genetic differences irrelevant of genomic sex were not addressed in the current study, hence their contribution to the observed phenotype cannot be excluded.

4.6. High glucose culture to model DM

Culturing in high glucose medium (30 mM) was one straight forward way to model diabetic hyperglycemia *in vitro*. Certainly, the diabetic pathogenic milieu is more complex, however, studies have shown that the mere exposure of EC in culture to high glucose elicits considerable alterations [320-321, 337-339]. The results presented here show an impact of high glucose on HCMEC angiogenesis, where female cells suffered greater deterioration of tube network than their male counterparts. Once more, this calls for further research into sex-driven heterogeneity of CMEC in response to hyperglycemic injury. The molecular effects of high glucose on endothelial tip and stalk cell behavior, crucial for angiogenesis, remains to be fully elucidated. However, it has been shown that tip and stalk EC differ in their glycolytic activity downstream of Notch/VEGF signaling, as well as key glycolytic enzyme, PFKFB3, both crucial for angiogenesis [340-341]. Despite the unsettled debate in the literature on which is more or less glycolytic, glycolytic differences are crucial to the sprouting and proliferation by tip and stalk EC, respectively, which culminate in a stable angiogenic network [340, 342-343]. Despite the lack of phenotype in HUVEC, in HCMEC, however, it is safe to assume that high glucose might disrupt the energetic balance necessary to establish the tip-stalk phenotype. In fact, this has been shown in human coronary artery EC (HCAEC), where high glucose culture induced alterations in cellular energetics, i.e. Warburg effect, via hypoxia-inducible factor 1 α (HIF-1 α) [344]. This can be understood given the tight regulation of both PFKFB3 and VEGF by HIF-1 α upon tip-stalk cell specification [343]. It would be of interest to examine this pathway in our model of glucose-induced disruption of angiogenesis in HCMEC, especially since most of the available literature on the matter are derived from HUVEC or retinal EC.

Discussion

While no significant effects of high glucose were reported in wound healing assays, there was an obvious trend of decreased migration and proliferation in female HCMEC in high glucose culture ($P = 0.08$). In inflammatory assays, male HCMEC displayed a prominent inflammatory phenotype upon high glucose culture. Indeed, previous studies have also pointed to the inflammation-triggering effect of glucose in microvascular EC by activation of NF- κ B-dependent signaling, and consequent elevation of IL1, IL6, TNF- α , VCAM1, ICAM1 expression [345]. In HUVEC, however, high glucose culture did not show any increase in inflammation. This comes in contrast to previously reported findings in HUVEC showing significant increases in the inflammatory surface markers, ICAM1, VCAM1 and endothelial-leukocyte adhesion molecular 1 (ELAM1) upon exposure to higher glucose concentrations, peaking at 16.5 mM [346-347]. Interestingly, in the study by Altannavch et al., neither 11 nor 22 mM of glucose cause significant increase in ICAM1 expression. Moreover, in the study by Takami et al., the increased ICAM1 expression was significant after 3 hours of exposure to 16.7 mM glucose, and correlated with increased THP-1 monocyte adhesion to HUVEC monolayers [346].

From a clinical perspective, the observed dysfunction of CMEC upon high glucose culture is alarming given the multiple under-the-radar bouts of acute hyperglycemia in undiagnosed or poorly managed diabetic patients, pre-diabetics, or even non-diabetics e.g. the Dawn Phenomenon, Somogyi effect and stress-hyperglycemia [348-350]. Such findings might be helpful in stratifying the diagnostic criteria for diabetes and pre-diabetes, e.g. revise cutoff values for glycosylated hemoglobin (GHb) [351]. Herein, a meta-analysis from 2012 found that for every 1% increase in GHb, there was a 25% increase in mortality from cardiovascular disease, and 17% increase in fatality from coronary heart disease [352]. This can be understood in light of the results presented here depicting the impact of acute hyperglycemia on CMEC.

One prominent finding here is the upregulation of miR-92a expression in both male and female HCMEC in response to high glucose culture. This is congruent with the previously reported findings from Hinkel et al., where miR-92a was among 3 micro-RNAs significantly upregulated in ventricular tissue from *INS*^{C94Y} diabetic porcine hearts [66]. The results discussed here represent the first report from human primary EC. Moreover, they provide an argument for the direct contribution of coronary microvascular EC to the reported overall cardiac tissue upregulation of miR-92a in diabetes. And finally, they show that the mere exposure to high glucose, though acute, can trigger miR-92a upregulation.

Interestingly, high glucose culture in HUVEC showed the opposite response with regard to miR-92a expression, highlighting the extent of heterogeneity in EC models. As introduced, miR-92a has been previously shown to be a vasoactive miRNA, with direct influence on EC angiogenesis and inflammatory response. In the following sections, I discuss a new model of subcellular signaling in which miR-92a plays a pivotal role in the phenotype of HCMEC under high glucose and, importantly, in HCMEC from diabetic patients.

4.7. Cardiac microvascular dysfunction in DM: the phenotype and the rescue

The availability of primary HCMEC from a type 2 diabetic patient enabled a direct comparison to those from non-diabetic donors. Herein, the diabetic patient matched in sex, age and ethnicity to our 63-year old male non-diabetic HCMEC. Therefore, we ran most of the molecular and functional characterization experiments comparing two 63-year old Caucasian male HCMECs from a non-diabetic or type 2 diabetic donors. One advantage provided by HCMEC from a diabetic patient is that they reflect the chronic nature of the disease, where biochemical, hemodynamic and epigenetic alterations accumulate over years – if not decades – *in situ*. As expected, characterization of the diabetic HCMEC showed significant shortcomings in all aspects of EC functions, also when compared to non-diabetic HCMEC in high glucose. Importantly, type 2 diabetic HCMEC also significantly upregulated miR-92a. This concurs with the clinical evidence from analysis of miR-92a in sera of type 2 diabetic patients with coronary artery disease [353]. In the referenced study by Wang et al., serum miR-92a levels showed a positive correlation with coronary artery disease in diabetic patients, as well as a number of inflammatory cytokines downstream of activated NF- κ B pathway. In congruence with this, I could show that diabetic HCMEC monolayers do display a heightened inflammatory phenotype, as well as elevated expression of the known NF- κ B-downstream adhesion molecule VCAM1. It would be of interest to investigate the activity of NF- κ B, e.g. nuclear p65 or phosphorylated-I κ B α , as well as, other downstream targets of this pathway, e.g. MCP1, in diabetic HCMEC. Interestingly, in the aforementioned study, miR-92a levels also correlated with blood HbA1c, establishing the link between glycemic control and the level of this miRNA. My results complement these clinical findings in patients' sera by arguing for direct contribution of cardiac micro-circulatory EC to blood miR-92a levels. In fact, it has been shown that miR-92a produced by EC can be liberated in circulating micro-particles and detected at higher levels in plasma from patients suffering acute myocardial infarction, as well

as those with stable coronary artery disease [354]. Herein, miR-92a-laden endothelial micro-particle levels were shown to be significantly higher in patients with acute myocardial infarction compared to those with stable coronary disease or healthy controls. Not only does this reflect the direct relation between EC activation and blood miR-92a levels, but also demonstrates a diagnostic value of circulating miR-92a in discriminating these two patient groups.

In light of the aforementioned findings, targeting miR-92a with anti-sense inhibitor was the next logical step to verify the contribution of miR-92a to the observed diabetic phenotype. As introduced, inhibition of miR-92a has already been proven to be of a therapeutic value in porcine models of myocardial ischemia; delivery of locked-nucleic antisense (LNA) to miR-92a enhanced collateralization and prevented capillary rarefaction in these models [298]. Here, I provide the first report on the utility of such approach in diabetic human CMEC. Antagomir-mediated inhibition of miR-92a led to a significant enhancement of tube formation (angiogenesis) in diabetic HCMEC, as well as an amelioration of their inflammatory status. Perhaps this is the most prominent result of the current study with particular translational relevance.

Inhibition of miR-92a, however, did not enhance diabetic HCMEC 2-dimensional migration or proliferation in wound healing or EdU-incorporation assays, respectively. This implies that the observed effect of miR-92a antagomir on angiogenesis is confined to regulation of tip and stalk cell-related molecular pathways induced when cells are cultured on extracellular matrix-like substance, i.e. Matrigel. Here, the increased transfection sensitivity of female HCMEC – where the effect of high glucose was greater – precluded an investigation of the effects of miR-92a inhibition on angiogenesis. This is one limitation of our study.

4.8. Why miR-92a is upregulated in DM: glucose-uptake hypothesis

Before exploring the molecular mechanism of miR-92a and/or its inhibition on regulation of angiogenesis and inflammation in diabetic HCMEC, the observation that high glucose and/or diabetes upregulates miR-92a level begs the question: why do CMEC upregulate miR-92 in response to a glycemic challenge? If this can be viewed as an adaptation selected for in EC, then it is safe to speculate that miR-92a upregulation might serve as a coping mechanism. Indeed, studies have previously highlighted the integral role of the miR-17~92 cluster in metabolic reprogramming in cancer cells by regulation of the mammalian target of rapamycin

complex 1 (mTORC1) signaling pathway [355]. Herein, miR-17 and 20, both sharing the same seed sequence, were reported to actively participate in such regulation by targeting the tumor suppressor *LKB1*. Interestingly, the cited study by Izreig et al. reported miR-17, miR-20 and miR-92a as the three most abundantly processed mature miRNAs from the miR-17~92 cluster in the Eμ-Myc lymphoma cells [355]. Nevertheless, they excluded a role for miR-92a in their described mechanisms. Whether miR-92a is just a processing byproduct or plays an actual role, and whether the same applies to CMEC upon diabetes or glycemic stress remains to be elucidated. I attempted to challenge the hypothesis by testing whether miR-92a increases HCMEC glucose uptake. Indeed, I could prove this by glucose uptake assays in non-diabetic cells overexpressing miR-92a. Moreover, qPCR analysis showing an increase in the glucose transporter *GLUT4* relative gene expression in non-diabetic HCMEC overexpressing miR-92a justifies this hypothesis. Interestingly, however, type 2 diabetic HCMEC displayed decreased glucose uptake despite insignificant changes in gene expression of the two EC glucose transporters, *GLUT1* and *GLUT4*, and overregulated miR-92a. One possibility is that diabetic HCMEC have impaired trafficking of GLUTs. In the coming sections, I discuss the possible mechanism by which miR-92a might serve by increasing EC *GLUT4* gene expression, and how this is dysregulated in diabetes despite miR-92a overexpression. However, one might argue that in their healthy state, HCMEC upregulation of miR-92a is coupled to their enhanced glucose uptake upon initial glycemic challenges, and that such ability is lost later over the chronic setting of diabetes.

4.9. How miR-92a is upregulated in DM

The previous section might explain why miR-92a is upregulated in HCMEC in response to high glucose, however, the mechanism by which miR-92a is upregulated remains elusive. As introduced, miR-26a and miR-133a were also reported by Hinkel et al. as upregulated in diabetic porcine hearts [66]. And in the previous section I discussed the reported abundance of miR-92a from its host cluster. One might ask: what are the molecular mechanisms, by which miR-92a, or even other micro-RNAs are overexpressed in diabetes? To answer this question, I first resort to epitranscriptomics as one way to explain the differential regulation of miRNAs in diabetes, among others [356-357]. While several layers of miRNA regulation have been described, post-transcriptional modification of miRNA has been reported as early as two decades ago [358]. Of the multiple post-transcriptional modifications on miRNAs that have later been identified to affect their maturation and activity, methylation on nitrogen-6 position of adenosines (m⁶A [N6-methyladenosine]) is one that has been recently reported in abundance

in multiple CVD, as well as cancers [356, 359-361]. The process of m⁶A RNA methylation is brought about by methyltransferase complexes composed of the so called “writer” enzymes in association with their cofactors [362-363]. Of the writer enzymes, methyltransferase-like 3 (METTL3) is of particular importance, as it harbors the catalytic domain capable of methylation of pri-miRNAs, which facilitates their further processing and maturation to miRNAs [364]. Interestingly, dysregulation of METTL3 has been reported in diabetes, and even under high glucose culture of different EC types [357]. A recent study reported an important role of METTL3 in the processing and maturation of the proangiogenic miRNA let-7e-5p and, importantly, the miR-17~92a cluster [365]. Therefore, it would be of great interest to interrogate the epitranscriptomic alterations in our diabetic models. This might as well clarify the discrepancy seen between HUVEC and HCMEC in this regard.

One important mechanism highlighted by studies explaining the regulation of relative expression of the miR-17~92 cluster members relies on the tertiary structure of its pri-miRNA. Chaulk et al. investigated this, and showed that the pri-miRNA transcript of the polycistronic cluster is folded in a globular tertiary structure over the 3'-terminal, i.e. towards both miR-19b and miR-92a, hence burying those two pri-miRNA members in the 3'-core of such globule [366-367]. This, in turn, leads to protection of these core pri-miRNAs from the Microprocessor's Drosha, resulting in generally decreased processing and expression levels of the mature forms of miR-19b and miR-92a, relative to other members of the cluster [366-367]. Moreover, it has been shown that Drosha processing on the pri-miRNA hairpin structure is accompanied by subsequent nuclear exosome-mediated degradation of the remaining cleavage product [368-369]. Therefore, in their model, processing of 'outer' pri-miRNAs one by one increases the likelihood of exonucleolytic degradation of the 'core' miRNAs. Indeed, they have shown that inhibition of one relevant nuclear exosome protein (PMscl100) led to ~2-fold increase in miR-92a levels and function [366]. If this model holds validity, it would be safe to speculate that the Drosha-coupled nuclear exosomal processing capacity is diminished in diabetic EC causing increased miR-92a expression levels. Importantly, this would also mean that one should expect elevated levels of the other miR-17~92 'core' member, miR-19b; yet another inhibitor of arteriogenesis (see 1.3.3.). These might be worthy of exploration to understand how miRNA dysregulation ensues upon cellular exposure to the diabetic milieu.

4.10. Fishing for targets: rationale of target selection

To understand the molecular mechanisms underlying the effects of miR-92a in EC, I sought after downstream targets with particular relevance to the observed phenotypes identified by functional characterization, i.e. angiogenesis, migration and EC bed inflammation. I confined the follow-up experiments to four downstream targets of miR-92a, i.e. *ADAM10*, *KLF2*, *KLF4* and *MEF2D*. ADAM10 is a metalloproteinase imperative for activation of endothelial Notch and its downstream signaling, which is indispensable for tip-stalk cell specification and development of organ-specific vascular beds, especially the coronaries [118]. Both Krüppel-like factors 2 and 4 are thoroughly studied in the context of endothelial inflammation [310]. MEF2D belongs to a family of transcription factors crucial for cardiovascular development and homeostasis; MEF2 are also known upstream regulators of both KLFs [169, 370]. As *in silico*-predicted miR-92a targets, to my knowledge, none of these has been previously described in the context of cardiac microvascular dysfunction in diabetes. Indeed, there are over a 1000 other miR-92a downstream targets that are predicted by TargetScan, many of which are worthy of further investigation in this context. However, there are factors that steered our selection decision beside literature knowledge, namely the level of conservation of seed sequence match in different species, as well as the context score. The former is strikingly apparent in our selected targets, especially *ADAM10*. The latter is helpful to predict the effective binding and regulation by miRNA; the lower the context++ score, the higher the predicted targeting effectiveness by the miRNA [221]. This could also be seen in *ADAM10* in both human and mouse context++ scores. TargetScan also offers data on canonical miRNA-mRNA targeting in zebrafish. Interestingly, the two seed sequence matches seen in the mammalian species presented here are conserved in the zebrafish *adam10a* ortholog, i.e. 7mer-A1 (position 977-983) and 7mer-m8 (position 2750-2756), reflecting the high degree of conservation in this particular interaction. Further, both human and pig share two 8mer target sites in their *MEF2D* orthologs; according to TargetScan, these two are also conserved among major orders of Eutheria. In rodents, however, both mouse and rat – but not squirrel – lack the second downstream 8mer site, indicating its loss in the muridae common ancestor. On the other hand, both human and mouse share two target sites of 7mer-A1 and 8mer in their *KLF4* orthologs, while pig shows only one, i.e. 8mer. The high level of conservation of these two sites in amniotes, and the conservation of the downstream 8mer site in amphibians, all indicate a recent loss of the upstream site in the domestic pig.

Importantly, neither do *mef2d* nor their downstream *klf2* or *klf4*, be it in their two fish paralogs, are predicted miR-92a targets in zebrafish despite the overall gene conservation. The two families of transcription factors, Mef2 and Klf2 were indeed shown to be highly conserved in vertebrates, and in zebrafish, were demonstrated to be crucial for cardiogenesis and vascular homeostasis, respectively – despite controversial reports on the role of zebrafish Klf2 in its vascular system [371-374]. However, the strong presence of miR-92a seed sequence matches in their orthologs in tetrapods adds a layer of regulation of those genes that reflects the evolution of cardiovascular complexity and associated regulatory networks upon the transition to land dwelling vertebrates, and later to endothermic homeothermy [375-376]. This is corroborated by studies showing the particularly imperative roles for the miR-17~92 cluster in mammalian heart development (see 1.3.3) [282, 377]. Moreover, this argues for the expression-buffering and evolution under canalization hypotheses postulated for the role of miRNAs in animal evolution (see 1.3.1) [233-235]. Importantly, the aforementioned findings exclude the zebrafish as a model to study these particular signaling molecules in relevance to miR-92a.

4.11. ADAM10: a novel player in diabetic microcirculatory dysfunction

In this study I describe the dysregulation of the miR-92a target *ADAM10* in the micro- and macrocirculation of the diabetic myocardium, with congruent evidence from both human and porcine models. Upon characterization, I show that ADAM10 ablation impacts all aspects of CMEC angiogenesis and migration. This can be easily understood in light of the available knowledge on ADAM10 regulation of tip-stalk cell specification via Notch [378]. In HCMEC, and MCMEC, I show an inverse relationship between miR-92a and ADAM10 expression. Indeed, I confirm the direct targeting of *ADAM10* by miR-92a, and the restoration of its expression by Antagomir treatment. In HUVEC, however, this could not be reproduced; miR-92a overexpression did not bring down *ADAM10* levels. Interestingly, this finding is reminiscent of a similar one reported in the literature, where miR-92a overexpression did not bring about significant downregulation of its target, *SIRT1* in HUVEC, but did significantly bring it down in coronary EC [300]. One way I interpret this is possibly as a product of alternative cleavage and polyadenylation (APA) affecting the length of 3'-UTR, and the *cis*-acting elements within [379-380]. This might apply to HUVEC considering their embryonic nature. Indeed, studies have shown that the process of 3'-UTR lengthening is associated with embryonic development and morphogenesis; highly differentiated cells display longer 3'-UTR

reflecting a higher level of posttranscriptional control [381]. However, it remains speculative whether HUVEC's *ADAM10* (or even *SIRT1*) mRNA bear shorter 3'-UTR than its HCMEC counterpart due to APA, thus possibly losing the miR-92a seed sequence matches. Moreover, qPCR shows that non-diabetic HCMEC display a significantly higher basal level of *ADAM10*. Altogether, this aids in understanding of why overexpression of miR-92a in our HUVEC did not impact angiogenesis.

ADAM10 is a critical regulator of angiogenesis and coronary vascular bed development [118-119], Diminished levels of *ADAM10* in diabetic HCMEC, as well as porcine ventricular tissue, can not only explain the observed phenotype, but also its rescue upon miR-92a inhibition in HCMEC. However, due to the minimal effects observed in non-diabetic HCMEC upon *ADAM10* knockdown, it is very likely that other molecular pathways might as well contribute to the diabetic angiogenic deficiency. The pro-angiogenic effects of miR-92a-antagomir in HCMEC can therefore involve other molecular pathways (discussed below). Further, I show that *ADAM10* was also downregulated in the macrocirculation of diabetic porcine ventricular tissue. However, on gene expression level, its downregulation in diabetic pig ventricles was confined to the apical side; this might reflect the relative dependence of the apical tissue on microcirculation and where fibrosis is also known to be more prominent [382]. At the time of writing this dissertation, and to my knowledge, the work presented here is the first report on *ADAM10* in the pathogenesis of diabetic cardiovascular dysfunction; we published this in 2021 [383].

4.12. KLFs dysregulation model to explain the diabetic vascular inflammation

Diabetic vascular inflammation is clinically indisputable. The cardiac microvasculature is particularly vulnerable to the heightened state of systemic inflammation in diabetes [81, 384]. Herein, the diabetic coronary microvasculature displays elevated oxidative stress and impaired eNOS bioavailability leading to endothelial dysfunction [384]. Here, characterization of *in vitro* models of diabetes revealed an exaggerated phenotype of endothelial bed inflammation manifested in increased retention of flowing THP-1 monocytes. Be it under high glucose culture in non-diabetic HCMEC or in their type 2 diabetic counterparts, the phenotype reflects increased endothelial adhesive properties. Mechanistically, this occurs as a result of increased expression of EC surface adhesion molecules, which mediate the process of tethering and rolling [104]. Since all my presented flow chamber experiments were performed with

unstimulated monocytes, the phenotype is attributed to the endothelial side. The endothelium-enriched KLF2 and KLF4, have been thoroughly studied as vascular protective transcription factors, regulating multiple anti-oxidant, anti-inflammatory, anti-thrombotic and anti-adhesive targets [310]. Here, I report dysregulation of both *KLF2* and *KLF4* in diabetic HCMEC, and in diabetic porcine left ventricles, implying a common pathway to the observed cardiovascular phenotypes in different diabetic models. While no previous reports have described these two factors in the context of diabetic microvascular dysfunction, earlier studies in HUVEC have demonstrated the impact of high glucose on KLF2 expression [163]. Others have shown that KLF2 activation prevented the high glucose-induced inflammatory phenotype in HUVEC by reducing monocyte adhesion [165]. One way KLF2 exerts such anti-inflammatory roles in the endothelium is by transactivation of the transcription factor EB (TFEB), which in turn thwarts the NF- κ B-downstream expression of adhesion molecules, such as VCAM1 and E-selectin [164]. In congruence with our findings, a study by Song et al. showed that TFEB activity was downregulated in diabetic mice [164]. Moreover, I verified the aforementioned findings by showing that downregulation of *KLF2* in non-diabetic HCMEC was enough to elicit the same inflammatory phenotype seen in their diabetic counterparts. As introduced, the anti-inflammatory role of KLF2 is not confined to EC. From the myeloid side, it has long been shown that KLF2 abrogates inflammatory activation of monocytes, macrophages and neutrophils [147, 385-386]. It would therefore be of interest to examine the expression level of KLF2 in the diabetic myeloid component. On the other hand, KLF4 was not significantly downregulated in diabetic HCMEC. This can be justified given the reported partial redundancy of the two KLFs, as well as the reported lethality of postnatal combined endothelial-specific knock-out in animal models [154, 158]. Therefore, maintenance of some activity of one KLF in the absence of the other can be understood as an essential adaptation. This is supported by the study of Sangwung et al., demonstrating the necessity of at least a single allele of either *Klf2* or *Klf4* for life in mice [154]. We have also alluded to this by gene expression analysis of MCMEC *Klf2* and *Klf4* upon knock-down of either one, revealing significant downregulation of *Klf4* upon knock-down of *Klf2*, but not the other way around. KLF2 might therefore be superior to KLF4 in regulating inflammation in the CMEC. Notwithstanding, KLF4 dysregulation has been reported to influence macrophage polarization [159]. In fact, studies have shown that in atheroprone microenvironment, EC liberate miR-92a-laden extracellular vesicle that signal and promote pro-inflammatory macrophage phenotypic polarization by downregulating macrophage KLF4 [387]. Interestingly, in the cited study by Chang et al., EC

inhibition of miR-92a thwarted this phenomenon. It is therefore worthy to extrapolate these findings to the situation in diabetes in future experiments.

Our dual luciferase reporter assays confirm that both *Klfs* are indeed direct miR-92a targets. This comes in concordance with our results, as well as previously published reports in HUVEC, wherein miR-92a downregulates both factors [388]. In a study by Wu et al., miR-92a downregulated *KLF2* in a flow-dependent manner in HUVEC, bovine aortic EC (BAEC) and in mouse carotid artery *ex-vivo* [297]. In their study, oscillatory (atherogenic flow) upregulated miR-92a leading to reduced levels of *KLF2* and its downstream targets eNOS and thrombomodulin (TM). Not only did inhibition of miR-92a in diabetic HCMEC restore *KLF2* levels, but probably also its function as a well-established inhibitor of the EC pro-inflammatory cell surface proteins, such as VCAM1 [143, 309-310]. Indeed, miR-92a Antagomir treatment of diabetic HCMEC led to significant reduction in protein expression of VCAM1, which also explains the anti-adhesive effect of miR-92a Antagomir in diabetic HCMEC in the flow-chamber assay. Interestingly, while miR-92a inhibition restored *KLF2* levels in diabetic HCMEC, overexpression of thereof did not alter *KLF2* mRNA levels in non-diabetic HCMEC. This implies that the increase of miR-92a in diabetes alone is not sufficient to explain the dysregulation of *KLF2*. This is not surprising since *KLF2* is one of the most evolutionary protected genes in recent species. This has been clearly demonstrated in a bioinformatics study by Sweet et al. showing substantial guanine/cytosine (GC) enrichment in mammalian and bird *KLF2* compared to their reptilian and non-amniotic orthologs, however without altering the protein's basic makeup [136]. Additionally, they showed that *KLF2* had accumulated more guanine or cytosine in the third position of its codons (GC3), allowing for mutational resistance by codon degeneracy, mRNA stability and translational efficiency. Herein, the human *KLF2* shows exceptionally higher GC content (74%) towards the 5' end of its coding sequence (CDS), corresponding to its activation and repression domains. Interestingly, they also reported significantly increased occurrence of KLF-binding motifs in recent species, with extraordinary enrichment in primates, and humans on top of this trajectory. This, along with empirical evidence of embryonic lethality from knock-out models, highlight the unequivocal importance of *KLF2* and the grave consequences of its dysregulation in diabetic cardiovascular system [141, 389]. Herein, restoration of *KLF2*, e.g. by miR-92a inhibitors, can therefore be of great therapeutic value in a clinically realizable setting.

4.13. MEF2D as a novel player in diabetic microvascular dysfunction

The aberrantly regulated KLFs in diabetic hearts is an alarming finding, begging an explanation. As expression of both KLF2 and KLF4 is associated with hemodynamic flow, disturbances thereof, e.g. as a result of diabetes-associated atherosclerosis, can inculcate their dysregulation. One way to explain this on the molecular level, is by examining their flow-dependent master regulators, i.e. myocyte enhance factor 2 (MEF2) group of transcription factors [155, 370]. MEF2 operate directly downstream of flow-induced activation of extracellular signal-regulated kinase 5 (ERK5), which in turn phosphorylates MEF2 to activate *KLF2* and *KLF4* expression by binding to their promotor and distal enhancer regions, respectively [314-315]. Of the four MEF2 members A, B, C and D, MEF2A and MEF2D were selected for further investigation in our study as the predominant isoforms in the adult heart [170]. Interestingly, as predicted by *in silico* analysis, *MEF2D* was verified by our reporter assays as a direct miR-92a target, and our gene expression analysis revealed its significant downregulation in our diabetic models. This is yet another novel finding of my project, describing a role for MEF2D in the cardiac microcirculation and its diabetes-induced pathology. I confirm these findings upon knock-down of *MEF2D*, showing a concomitant significant reduction in *KLF2* expression. Like KLF2 and KLF4, MEF2 behave in a partially redundant fashion; this has been demonstrated by studies on knock-out models [169, 390]. Expectedly, *MEF2A* expression was not significantly altered in diabetes. While the impact of miR-92a overexpression was of minimal effect in non-diabetic HCMEC, its inhibition was capable of restoring *MEF2D* expression level in their diabetic counterparts; again promising a therapeutic potential. Importantly, as the MEF2 family of transcription factors have been shown to be crucial for angiogenesis by regulation of the Notch gene family, their dysregulation in diabetic HCMEC as well as in diabetic porcine ventricles supports the explanation of the observed angiogenic defects thereof [169, 390]. After all, like ADAM10, the proangiogenic effects of miR-92a-antagomir can involve derepression of MEF2D. It would be of interest to follow up on our experiments by investigating the loss or knockdown of either MEF2, e.g. by siRNA knock-down, in the context of HCMEC angiogenesis.

Importantly, both MEF2A and MEF2D have been reported in regulation of expression of the glucose transporter *GLUT4*, where MEF2A is the more potent transactivator and MEF2D competes with it over the same promotor [312]. MEF2D, therefore acts as a partial agonist

controlling *GLUT4* expression in the presence of MEF2A. Herein, I postulate a hypothesis, wherein the overexpression of miR-92a is one way, by which highly glycolytic EC cope with the glyceic stress by downregulating MEF2D downstream of miR-92a, hence increasing MEF2A occupancy of *GLUT4* promotor, leading to its upregulated expression and increased glucose uptake. Indeed, I show a correlation between miR-92a overexpression and both *GLUT4* and glucose uptake in non-diabetic HCMEC, and probably explaining the initial response of HCMEC to glyceic challenge by overexpressing miR-92a. It would be of interest to test this further.

Finally, the downregulated *MEF2D* in diabetic HCMEC and porcine ventricular tissue can be understood in light of the epigenetic changes that ensue as a result of hyperglycemia, as well as hemodynamic disturbances. This is justified by the strict regulation of MEF2 by class IIa histone deacetylases (HDACs). Herein, HDAC5, a member of class IIa HDACs, forms a repressive complex with MEF2 that is released upon laminar flow (LF)-induced phosphorylation of HDAC5 by ERK5 and derepression of MEF2 [391]. This has been demonstrated to be the main mechanism by which MEF2 activate *KLF2* expression [391]. Indeed, HDACs have been thoroughly studied in the context of diabetes, where they have been ascribed the dysregulation in multiple gene expression programs [392]. For example, HDAC5 inhibitors have been shown to induce *GLUT4* expression and enhance insulin sensitivity in skeletal muscles [393]. Consistently, in diabetic HCMEC, glucose uptake was significantly reduced despite no significant differences in expression of either *GLUT1* or *GLUT4* in my hands. It would therefore be of interest to investigate the HDAC5 phosphorylation status, and the possible utility of HDAC5 inhibitors to restore MEF2D and/or *KLF2* levels in our diabetic models. Whereas miR-92a upregulation was postulated as an initial mechanism to increase glucose uptake in CMEC by fine tuning the MEF2D-MEF2A activity, later accumulation of epigenetic changes over the chronic diabetic setting might render this ineffective by severely downregulating *MEF2D* and disrupting the balanced regulation of *GLUT4* expression.

Figure 52 summarizes the molecular findings of the current study.

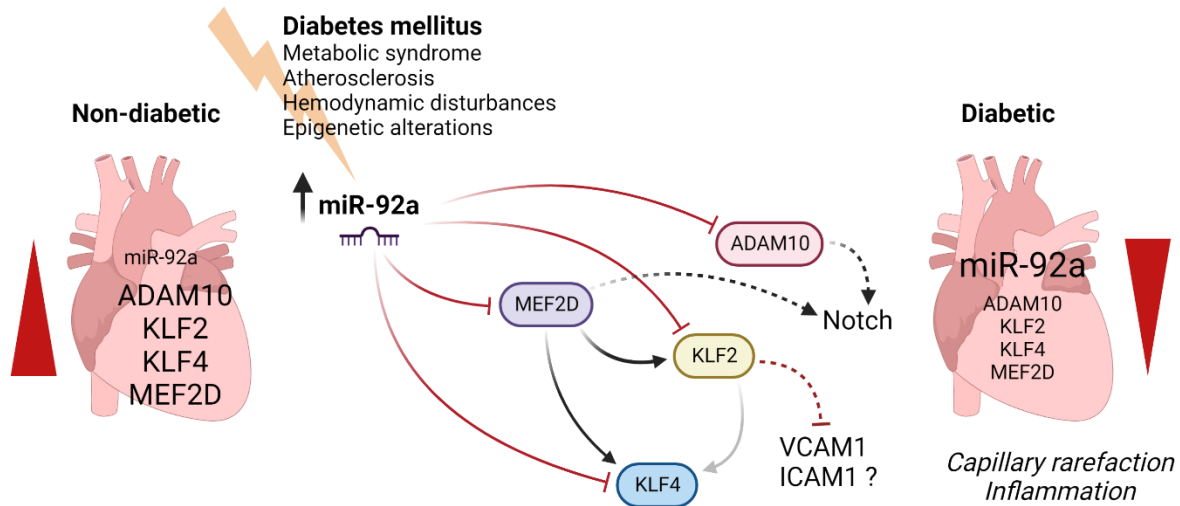


Figure 52. Molecular alterations of DM and the role of miR-92a in its cardiovascular phenotype.
(Created with BioRender.com)

4.14. Translational prospects

At the time of writing this dissertation, humanity is jubilating their triumph over the devastating pandemic of corona virus disease 2019 (COVID-19). By virtue of novel mRNA vaccines, the severe acute respiratory syndrome coronavirus 2 (SARS-CoV-2) is no longer a menace to the world population [394]. Such unprecedented success highlighted the eminence of RNA therapeutics as the horsepower of contemporary medicine [395-396]. However, long before the COVID-19 vaccines, RNA therapeutics have been heavily investigated in the context of CVD [397]. As of miRNAs, the aforementioned powerful findings from *in vitro* and pre-clinical research are awaiting their translational fruition. Indeed, some have already made it. The work of Thomas Thum at Hannover Medical School has recently demonstrated encouraging results in phase 1b clinical trials with CDR132L, a novel antisense oligonucleotide to cardiac miR-132-3p [398]. On such trail, miR-92a is not far behind. Born with great translational potential, miR-92a has been brought forward by elegant studies of Dimmeler and Hinkel et alia. Now, MRG-110 has become the first anti-miR-92a-3p to undergo a clinical trial for safety and efficiency in healthy adults – yet so far only via systemic infusion [399]. Notwithstanding, investigation of volunteers' peripheral blood compartment showed significant downregulation of miR-92a, as well as derepression of its target *ITGA5*. As demonstrated by Hinkel and colleagues in porcine animal models, therapeutic benefits were achieved only upon local myocardial delivery [298]. The challenge is up for future studies to develop and test effective delivery modes and validate the clinical efficacy of such novel miRNA inhibitors in patients.

5. Conclusion

The present doctoral study is an endeavor of empirical science to understand the molecular determinants of diabetic cardiovascular complications. It emphasizes pivotal aspects of microvascular dysfunction in the diabetic myocardium utilizing human *in vitro* primary endothelial models, combined with those of other mammalian species. Building on previously reported findings on micro-RNAs in diabetic cardio-vasculopathy, miR-92a was especially qualified for further investigation. Herein, I could demonstrate the pathogenic role of miR-92a dysregulation in the diabetic coronary microcirculation. Moreover, I described novel molecular targets and/or interactions in the diabetic myocardium, with particular relevance to miR-92a, namely ADAM10, KLF and MEF2, inter alia. The presented experiments and findings prove their unequivocal involvement in the microvascular phenotype of capillary rarefaction and inflammation, as well as direct interaction with miR-92a. Importantly, these findings strongly qualify miR-92a as a therapeutic target for this pathological condition and justify further clinical studies with miR-92a inhibitors. The study at hand seeks filling of knowledge gaps in the pathogenesis of diabetic cardiovascular complications, but more so opens new avenues of research into molecular understanding of cardiovascular disease and promising miRNA-based therapeutics for such a global health concern.

6. Study publications

- 1- Samak, M.; Kues, A.; Kaltenborn, D.; Klösener, L.; Mietsch, M.; Germena, G.; Hinkel, R., Dysregulation of Krüppel-like factor 2 and myocyte enhancer factor 2D drive cardiac microvascular inflammation in diabetes. *Int J Mol Sci* **2023**, 24 (3).
- 2- Samak, M.; Kaltenborn, D.; Kues, A.; Le Noble, F.; Hinkel, R.; Germena, G., Micro-RNA 92a as a Therapeutic Target for Cardiac Microvascular Dysfunction in Diabetes. *Biomedicines* **2021**, 10 (1).

7. Literature

1. Karamanou, M.; Protogerou, A.; Tsoucalas, G.; Androutsos, G.; Poulakou-Rebelakou, E., Milestones in the history of diabetes mellitus: The main contributors. *World J Diabetes* **2016**, *7* (1), 1-7.
2. WHO Diabetes. https://www.who.int/europe/health-topics/diabetes#tab=tab_2.
3. Saeedi, P.; Petersohn, I.; Salpea, P.; Malanda, B.; Karuranga, S.; Unwin, N.; Colagiuri, S.; Guariguata, L.; Motala, A. A.; Ogurtsova, K.; Shaw, J. E.; Bright, D.; Williams, R., Global and regional diabetes prevalence estimates for 2019 and projections for 2030 and 2045: Results from the International Diabetes Federation Diabetes Atlas, 9(th) edition. *Diabetes Res Clin Pract* **2019**, *157*, 107843.
4. International Diabetes Federation. IDF Diabetes Atlas, 10th edn. Brussels, Belgium. 2021; p <https://www.diabetesatlas.org>.
5. WHO Knowledgeable patients – are we ready for them? World Diabetes Day 2022. <https://www.who.int/europe/news/item/11-11-2022-knowledgeable-patients---are-we-ready-for-them-world-diabetes-day-2022>.
6. Heidemann, C.; Scheidt-Nave, C., Prevalence, incidence and mortality of diabetes mellitus in adults in Germany – A review in the framework of the Diabetes Surveillanc. Robert Koch-Institut, Epidemiologie und Gesundheitsberichterstattung: 2017; Vol. 2.
7. CDC Diabetes Fast Facts. <https://www.cdc.gov/diabetes/basics/quick-facts.html>.
8. Lam, A. A.; Lepe, A.; Wild, S. H.; Jackson, C., Diabetes comorbidities in low- and middle-income countries: An umbrella review. *J Glob Health* **2021**, *11*, 04040.
9. Federation, I., IDF Diabetes Atlas, 9th edn. 2019.
10. DiMeglio, L. A.; Evans-Molina, C.; Oram, R. A., Type 1 diabetes. *Lancet (London, England)* **2018**, *391* (10138), 2449-2462.
11. Belle, T. L. V.; Coppieters, K. T.; Herrath, M. G. V., Type 1 Diabetes: Etiology, Immunology, and Therapeutic Strategies. *Physiological reviews* **2011**, *91* (1), 79-118.
12. Thomas, N. J.; Jones, S. E.; Weedon, M. N.; Shields, B. M.; Oram, R. A.; Hattersley, A. T., Frequency and phenotype of type 1 diabetes in the first six decades of life: a cross-sectional, genetically stratified survival analysis from UK Biobank. *Lancet Diabetes Endocrinol* **2018**, *6* (2), 122-129.
13. Hope, S. V.; Wienand-Barnett, S.; Shepherd, M.; King, S. M.; Fox, C.; Khunti, K.; Oram, R. A.; Knight, B. A.; Hattersley, A. T.; Jones, A. G.; Shields, B. M., Practical Classification Guidelines for Diabetes in patients treated with insulin: a cross-sectional study of the accuracy of diabetes diagnosis. *Br J Gen Pract* **2016**, *66* (646), e315-22.
14. Redondo, M. J.; Fain, P. R.; Eisenbarth, G. S., Genetics of type 1A diabetes. *Recent Prog Horm Res* **2001**, *56*, 69-89.

Literature

15. Chobot, A.; Polanska, J.; Brandt, A.; Deja, G.; Glowinska-Olszewska, B.; Pilecki, O.; Szadkowska, A.; Mysliwiec, M.; Jarosz-Chobot, P., Updated 24-year trend of Type 1 diabetes incidence in children in Poland reveals a sinusoidal pattern and sustained increase. *Diabet Med* **2017**, *34* (9), 1252-1258.
16. Jacobson, A. M.; Musen, G.; Ryan, C. M.; Silvers, N.; Cleary, P.; Waberski, B.; Burwood, A.; Weinger, K.; Bayless, M.; Dahms, W.; Harth, J., Long-term effect of diabetes and its treatment on cognitive function. *The New England journal of medicine* **2007**, *356* (18), 1842-52.
17. Tonoli, C.; Heyman, E.; Roelands, B.; Pattyn, N.; Buyse, L.; Piacentini, M. F.; Berthoin, S.; Meeusen, R., Type 1 diabetes-associated cognitive decline: a meta-analysis and update of the current literature. *Journal of diabetes* **2014**, *6* (6), 499-513.
18. Seaquist, E. R., The Impact of Diabetes on Cerebral Structure and Function. *Psychosom Med* **2015**, *77* (6), 616-21.
19. Olsen, B. S.; Sjølie, A. K.; Hougaard, P.; Johannesen, J.; Marinelli, K.; Jacobsen, B. B.; Mortensen, H. B., The significance of the prepubertal diabetes duration for the development of retinopathy and nephropathy in patients with type 1 diabetes. *Journal of diabetes and its complications* **2004**, *18* (3), 160-4.
20. Groop, P. H.; Thomas, M. C.; Moran, J. L.; Wadèn, J.; Thorn, L. M.; Mäkinen, V. P.; Rosengård-Bärlund, M.; Saraheimo, M.; Hietala, K.; Heikkilä, O.; Forsblom, C., The presence and severity of chronic kidney disease predicts all-cause mortality in type 1 diabetes. *Diabetes* **2009**, *58* (7), 1651-8.
21. Sempere-Bigorra, M.; Julián-Rochina, I.; Cauli, O., Differences and Similarities in Neuropathy in Type 1 and 2 Diabetes: A Systematic Review. *J Pers Med* **2021**, *11* (3).
22. Laing, S. P.; Swerdlow, A. J.; Slater, S. D.; Burden, A. C.; Morris, A.; Waugh, N. R.; Gatling, W.; Bingley, P. J.; Patterson, C. C., Mortality from heart disease in a cohort of 23,000 patients with insulin-treated diabetes. *Diabetologia* **2003**, *46* (6), 760-5.
23. Miller, R. G.; Mahajan, H. D.; Costacou, T.; Sekikawa, A.; Anderson, S. J.; Orchard, T. J., A Contemporary Estimate of Total Mortality and Cardiovascular Disease Risk in Young Adults With Type 1 Diabetes: The Pittsburgh Epidemiology of Diabetes Complications Study. *Diabetes Care* **2016**, *39* (12), 2296-2303.
24. Bhupathiraju, S. N.; Tobias, D. K.; Malik, V. S.; Pan, A.; Hruby, A.; Manson, J. E.; Willett, W. C.; Hu, F. B., Glycemic index, glycemic load, and risk of type 2 diabetes: results from 3 large US cohorts and an updated meta-analysis. *Am J Clin Nutr* **2014**, *100* (1), 218-32.
25. Vlachos, D.; Malisova, S.; Lindberg, F. A.; Karaniki, G., Glycemic Index (GI) or Glycemic Load (GL) and Dietary Interventions for Optimizing Postprandial Hyperglycemia in Patients with T2 Diabetes: A Review. *Nutrients* **2020**, *12* (6).

26. DeFronzo, R. A.; Ferrannini, E.; Groop, L.; Henry, R. R.; Herman, W. H.; Holst, J. J.; Hu, F. B.; Kahn, C. R.; Raz, I.; Shulman, G. I.; Simonson, D. C.; Testa, M. A.; Weiss, R., Type 2 diabetes mellitus. *Nature Reviews Disease Primers* **2015**, *1* (1), 15019.
27. Thompson, A. K.; Minihane, A. M.; Williams, C. M., Trans fatty acids, insulin resistance and diabetes. *Eur J Clin Nutr* **2011**, *65* (5), 553-64.
28. Lima, J.; Moreira, N. C. S.; Sakamoto-Hojo, E. T., Mechanisms underlying the pathophysiology of type 2 diabetes: From risk factors to oxidative stress, metabolic dysfunction, and hyperglycemia. *Mutat Res Genet Toxicol Environ Mutagen* **2022**, 874-875, 503437.
29. Kim, J. A.; Montagnani, M.; Koh, K. K.; Quon, M. J., Reciprocal relationships between insulin resistance and endothelial dysfunction: molecular and pathophysiological mechanisms. *Circulation* **2006**, *113* (15), 1888-904.
30. Mahajan, A.; Taliun, D.; Thurner, M.; Robertson, N. R.; Torres, J. M.; Rayner, N. W.; Payne, A. J.; Steinthorsdottir, V.; Scott, R. A.; Grarup, N.; Cook, J. P.; Schmidt, E. M.; Wuttke, M.; Sarnowski, C.; Mägi, R.; Nano, J.; Gieger, C.; Trompet, S.; Lecoeur, C.; Preuss, M. H.; Prins, B. P.; Guo, X.; Bielak, L. F.; Below, J. E.; Bowden, D. W.; Chambers, J. C.; Kim, Y. J.; Ng, M. C. Y.; Petty, L. E.; Sim, X.; Zhang, W.; Bennett, A. J.; Bork-Jensen, J.; Brummett, C. M.; Canouil, M.; Ec Kardt, K. U.; Fischer, K.; Kardia, S. L. R.; Kronenberg, F.; Läll, K.; Liu, C. T.; Locke, A. E.; Luan, J.; Ntalla, I.; Nylander, V.; Schönherr, S.; Schurmann, C.; Yengo, L.; Bottinger, E. P.; Brandslund, I.; Christensen, C.; Dedoussis, G.; Florez, J. C.; Ford, I.; Franco, O. H.; Frayling, T. M.; Giedraitis, V.; Hackinger, S.; Hattersley, A. T.; Herder, C.; Ikram, M. A.; Ingelsson, M.; Jørgensen, M. E.; Jørgensen, T.; Kriebel, J.; Kuusisto, J.; Ligthart, S.; Lindgren, C. M.; Linneberg, A.; Lyssenko, V.; Mamakou, V.; Meitinger, T.; Mohlke, K. L.; Morris, A. D.; Nadkarni, G.; Pankow, J. S.; Peters, A.; Sattar, N.; Stančáková, A.; Strauch, K.; Taylor, K. D.; Thorand, B.; Thorleifsson, G.; Thorsteinsdottir, U.; Tuomilehto, J.; Witte, D. R.; Dupuis, J.; Peyser, P. A.; Zeggini, E.; Loos, R. J. F.; Froguel, P.; Ingelsson, E.; Lind, L.; Groop, L.; Laakso, M.; Collins, F. S.; Jukema, J. W.; Palmer, C. N. A.; Grallert, H.; Metspalu, A.; Dehghan, A.; Köttgen, A.; Abecasis, G. R.; Meigs, J. B.; Rotter, J. I.; Marchini, J.; Pedersen, O.; Hansen, T.; Langenberg, C.; Wareham, N. J.; Stefansson, K.; Gloyn, A. L.; Morris, A. P.; Boehnke, M.; McCarthy, M. I., Fine-mapping type 2 diabetes loci to single-variant resolution using high-density imputation and islet-specific epigenome maps. *Nature genetics* **2018**, *50* (11), 1505-1513.
31. Xue, A.; Wu, Y.; Zhu, Z.; Zhang, F.; Kemper, K. E.; Zheng, Z.; Yengo, L.; Lloyd-Jones, L. R.; Sidorenko, J.; Wu, Y.; Agbessi, M.; Ahsan, H.; Alves, I.; Andiappan, A.; Awadalla, P.; Battle, A.; Beutner, F.; Bonder, Marc J.; Boomsma, D.; Christiansen, M.; Claringbould, A.; Deelen, P.; Esko, T.; Favé, M.-J.; Franke, L.; Frayling, T.; Gharib, S.; Gibson, G.; Hemani, G.; Jansen, R.; Kähönen, M.; Kalnainen, A.; Kasela, S.; Kettunen, J.; Kim, Y.; Kirsten, H.; Kovacs, P.; Krohn, K.; Kronberg-Guzman, J.; Kukushkina, V.; Kutalik, Z.; Lee, B.; Lehtimäki, T.; Loeffler, M.; Marigorta, U. M.; Metspalu, A.; Milani, L.; Müller-Nurasyid, M.; Nauck, M.; Nivard, M.; Penninx, B.; Perola, M.; Pervjakova, N.; Pierce, B.; Powell, J.; Prokisch, H.; Psaty, B.; Raitakari, O.; Ring, S.; Ripatti, S.;

Literature

Rotzschke, O.; Rüeger, S.; Saha, A.; Scholz, M.; Schramm, K.; Seppälä, I.; Stumvoll, M.; Sullivan, P.; Teumer, A.; Thiery, J.; Tong, L.; Tönjes, A.; van Dongen, J.; van Meurs, J.; Verlouw, J.; Völker, U.; Vösa, U.; Yaghootkar, H.; Zeng, B.; McRae, A. F.; Visscher, P. M.; Zeng, J.; Yang, J.; e, Q. C., Genome-wide association analyses identify 143 risk variants and putative regulatory mechanisms for type 2 diabetes. *Nature communications* **2018**, *9* (1), 2941.

32. Vujkovic, M.; Keaton, J. M.; Lynch, J. A.; Miller, D. R.; Zhou, J.; Tcheandjie, C.; Huffman, J. E.; Assimes, T. L.; Lorenz, K.; Zhu, X.; Hilliard, A. T.; Judy, R. L.; Huang, J.; Lee, K. M.; Klarin, D.; Pyarajan, S.; Danesh, J.; Melander, O.; Rasheed, A.; Mallick, N. H.; Hameed, S.; Qureshi, I. H.; Afzal, M. N.; Malik, U.; Jalal, A.; Abbas, S.; Sheng, X.; Gao, L.; Kaestner, K. H.; Susztak, K.; Sun, Y. V.; DuVall, S. L.; Cho, K.; Lee, J. S.; Gaziano, J. M.; Phillips, L. S.; Meigs, J. B.; Reaven, P. D.; Wilson, P. W.; Edwards, T. L.; Rader, D. J.; Damrauer, S. M.; O'Donnell, C. J.; Tsao, P. S.; Atkinson, M. A.; Powers, A. C.; Naji, A.; Kaestner, K. H.; Abecasis, G. R.; Baras, A.; Cantor, M. N.; Coppola, G.; Economides, A. N.; Lotta, L. A.; Overton, J. D.; Reid, J. G.; Shuldiner, A. R.; Beechert, C.; Forsythe, C.; Fuller, E. D.; Gu, Z.; Lattari, M.; Lopez, A. E.; Schleicher, T. D.; Padilla, M. S.; Toledo, K.; Widom, L.; Wolf, S. E.; Pradhan, M.; Manoochehri, K.; Ulloa, R. H.; Bai, X.; Balasubramanian, S.; Barnard, L.; Blumenfeld, A. L.; Eom, G.; Habegger, L.; Hawes, A.; Khalid, S.; Maxwell, E. K.; Salerno, W. J.; Staples, J. C.; Yadav, A.; Jones, M. B.; Mitnau, L. J.; Aguayo, S. M.; Ahuja, S. K.; Ballas, Z. K.; Bhushan, S.; Boyko, E. J.; Cohen, D. M.; Concato, J.; Constans, J. I.; Dellitalia, L. J.; Fayad, J. M.; Fernando, R. S.; Florez, H. J.; Gaddy, M. A.; Gappy, S. S.; Gibson, G.; Godschalk, M.; Greco, J. A.; Gupta, S.; Gutierrez, S.; Hammer, K. D.; Hamner, M. B.; Harley, J. B.; Hung, A. M.; Huq, M.; Hurley, R. A.; Iruvanti, P. R.; Ivins, D. J.; Jacono, F. J.; Jhala, D. N.; Kaminsky, L. S.; Kinlay, S.; Klein, J. B.; Liangpunsakul, S.; Lichy, J. H.; Mastorides, S. M.; Mathew, R. O.; Mattocks, K. M.; McArdle, R.; Meyer, P. N.; Meyer, L. J.; Moorman, J. P.; Morgan, T. R.; Murdoch, M.; Nguyen, X.-M. T.; Okusaga, O. O.; Oursler, K.-A. K.; Ratcliffe, N. R.; Rauchman, M. I.; Robey, R. B.; Ross, G. W.; Servatius, R. J.; Sharma, S. C.; Sherman, S. E.; Sonel, E.; Sriram, P.; Stapley, T.; Striker, R. T.; Tandon, N.; Villareal, G.; Wallbom, A. S.; Wells, J. M.; Whittle, J. C.; Whooley, M. A.; Xu, J.; Yeh, S.-S.; Aslan, M.; Brewer, J. V.; Brophy, M. T.; Connor, T.; Argyres, D. P.; Do, N. V.; Hauser, E. R.; Humphries, D. E.; Selva, L. E.; Shayan, S.; Stephens, B.; Whitbourne, S. B.; Zhao, H.; Moser, J.; Beckham, J. C.; Breeling, J. L.; Romero, J. P. C.; Huang, G. D.; Ramoni, R. B.; Pyarajan, S.; Sun, Y. V.; Cho, K.; Wilson, P. W.; O'Donnell, C. J.; Tsao, P. S.; Chang, K.-M.; Gaziano, J. M.; Muralidhar, S.; Chang, K.-M.; Voight, B. F.; Saleheen, D.; The, H. C.; Regeneron Genetics, C.; Program, V. A. M. V., Discovery of 318 new risk loci for type 2 diabetes and related vascular outcomes among 1.4 million participants in a multi-ancestry meta-analysis. *Nature genetics* **2020**, *52* (7), 680-691.

33. Bellary, S.; Kyrou, I.; Brown, J. E.; Bailey, C. J., Type 2 diabetes mellitus in older adults: clinical considerations and management. *Nature Reviews Endocrinology* **2021**, *17* (9), 534-548.

Literature

34. Tönnies, T.; Röckl, S.; Hoyer, A.; Heidemann, C.; Baumert, J.; Du, Y.; Scheidt-Nave, C.; Brinks, R., Projected number of people with diagnosed Type 2 diabetes in Germany in 2040. *Diabet Med* **2019**, *36* (10), 1217-1225.
35. Khan, M. A. B.; Hashim, M. J.; King, J. K.; Govender, R. D.; Mustafa, H.; Al Kaabi, J., Epidemiology of Type 2 Diabetes - Global Burden of Disease and Forecasted Trends. *J Epidemiol Glob Health* **2020**, *10* (1), 107-111.
36. Type 2 diabetes mellitus. *Nature Reviews Disease Primers* **2015**, *1* (1), 15039.
37. Kraft, J. R., Detection of Diabetes Mellitus In Situ (Occult Diabetes). *Laboratory Medicine* **1975**, *6* (2), 10-22.
38. Sarwar, N.; Gao, P.; Seshasai, S. R.; Gobin, R.; Kaptoge, S.; Di Angelantonio, E.; Ingelsson, E.; Lawlor, D. A.; Selvin, E.; Stampfer, M.; Stehouwer, C. D.; Lewington, S.; Pennells, L.; Thompson, A.; Sattar, N.; White, I. R.; Ray, K. K.; Danesh, J., Diabetes mellitus, fasting blood glucose concentration, and risk of vascular disease: a collaborative meta-analysis of 102 prospective studies. *Lancet (London, England)* **2010**, *375* (9733), 2215-22.
39. Anand, S. S.; Dagenais, G. R.; Mohan, V.; Diaz, R.; Probstfield, J.; Freeman, R.; Shaw, J.; Lanas, F.; Avezum, A.; Budaj, A.; Jung, H.; Desai, D.; Bosch, J.; Yusuf, S.; Gerstein, H. C., Glucose levels are associated with cardiovascular disease and death in an international cohort of normal glycaemic and dysglycaemic men and women: the EpiDREAM cohort study. *Eur J Prev Cardiol* **2012**, *19* (4), 755-64.
40. Corrigendum to: 2019 ESC Guidelines on diabetes, pre-diabetes, and cardiovascular diseases developed in collaboration with the EASD. *European heart journal* **2020**, *41* (45), 4317.
41. Moss, S. E.; Klein, R.; Klein, B. E., Cause-specific mortality in a population-based study of diabetes. *Am J Public Health* **1991**, *81* (9), 1158-62.
42. Laakso, M., Hyperglycemia and cardiovascular disease in type 2 diabetes. *Diabetes* **1999**, *48* (5), 937-42.
43. Dal Canto, E.; Ceriello, A.; Rydén, L.; Ferrini, M.; Hansen, T. B.; Schnell, O.; Standl, E.; Beulens, J. W., Diabetes as a cardiovascular risk factor: An overview of global trends of macro and micro vascular complications. *Eur J Prev Cardiol* **2019**, *26* (2_suppl), 25-32.
44. Du, Y.; Heidemann, C.; Gößwald, A.; Schmich, P.; Scheidt-Nave, C., Prevalence and comorbidity of diabetes mellitus among non-institutionalized older adults in Germany - results of the national telephone health interview survey 'German Health Update (GEDA)' 2009. *BMC Public Health* **2013**, *13*, 166.
45. Booth, G. L.; Kapral, M. K.; Fung, K.; Tu, J. V., Relation between age and cardiovascular disease in men and women with diabetes compared with non-diabetic people: a population-based retrospective cohort study. *Lancet (London, England)* **2006**, *368* (9529), 29-36.
46. WHO The top 10 causes of death. <https://www.who.int/news-room/fact-sheets/detail/the-top-10-causes-of-death>.

Literature

47. Stirban, A.; Gawlowski, T.; Roden, M., Vascular effects of advanced glycation endproducts: Clinical effects and molecular mechanisms. *Mol Metab* **2014**, *3* (2), 94-108.
48. Brownlee, M., The Pathobiology of Diabetic Complications: A Unifying Mechanism. *Diabetes* **2005**, *54* (6), 1615-1625.
49. Lazo, M.; Halushka, M. K.; Shen, L.; Maruthur, N.; Rebholz, C. M.; Rawlings, A. M.; Hoogeveen, R. C.; Brinkley, T. E.; Ballantyne, C. M.; Astor, B. C.; Selvin, E., Soluble receptor for advanced glycation end products and the risk for incident heart failure: The Atherosclerosis Risk in Communities Study. *American heart journal* **2015**, *170* (5), 961-7.
50. Jia, G.; Whaley-Connell, A.; Sowers, J. R., Diabetic cardiomyopathy: a hyperglycaemia- and insulin-resistance-induced heart disease. *Diabetologia* **2018**, *61* (1), 21-28.
51. Marciniak, S. J.; Ron, D., Endoplasmic reticulum stress signaling in disease. *Physiological reviews* **2006**, *86* (4), 1133-49.
52. Jia, G.; DeMarco, V. G.; Sowers, J. R., Insulin resistance and hyperinsulinaemia in diabetic cardiomyopathy. *Nat Rev Endocrinol* **2016**, *12* (3), 144-53.
53. Tan, Y.; Zhang, Z.; Zheng, C.; Wintergerst, K. A.; Keller, B. B.; Cai, L., Mechanisms of diabetic cardiomyopathy and potential therapeutic strategies: preclinical and clinical evidence. *Nature reviews. Cardiology* **2020**, *17* (9), 585-607.
54. Rubler, S.; Dlugash, J.; Yuceoglu, Y. Z.; Kumral, T.; Branwood, A. W.; Grishman, A., New type of cardiomyopathy associated with diabetic glomerulosclerosis. *The American journal of cardiology* **1972**, *30* (6), 595-602.
55. Graves, L. E.; Donaghue, K. C., Vascular Complication in Adolescents With Diabetes Mellitus. *Frontiers in endocrinology* **2020**, *11*, 370.
56. Fowler, M. J., Microvascular and Macrovascular Complications of Diabetes. *Clinical Diabetes* **2008**, *26* (2), 77-82.
57. Sharma, A.; Green, J. B.; Dunning, A.; Lokhnygina, Y.; Al-Khatib, S. M.; Lopes, R. D.; Buse, J. B.; Lachin, J. M.; Van de Werf, F.; Armstrong, P. W.; Kaufman, K. D.; Standl, E.; Chan, J. C. N.; Distiller, L. A.; Scott, R.; Peterson, E. D.; Holman, R. R., Causes of Death in a Contemporary Cohort of Patients With Type 2 Diabetes and Atherosclerotic Cardiovascular Disease: Insights From the TECOS Trial. *Diabetes Care* **2017**, *40* (12), 1763-1770.
58. Schmitt, V. H.; Hobohm, L.; Münzel, T.; Wenzel, P.; Gori, T.; Keller, K., Impact of diabetes mellitus on mortality rates and outcomes in myocardial infarction. *Diabetes Metab* **2021**, *47* (4), 101211.
59. Peters, S. A.; Huxley, R. R.; Woodward, M., Diabetes as a risk factor for stroke in women compared with men: a systematic review and meta-analysis of 64 cohorts, including 775,385 individuals and 12,539 strokes. *Lancet (London, England)* **2014**, *383* (9933), 1973-80.

Literature

60. Sugiyama, T.; Yamamoto, E.; Bryniarski, K.; Xing, L.; Fracassi, F.; Lee, H.; Jang, I. K., Coronary Plaque Characteristics in Patients With Diabetes Mellitus Who Presented With Acute Coronary Syndromes. *Journal of the American Heart Association* **2018**, *7* (14).
61. Lynge, T. H.; Svane, J.; Pedersen-Bjergaard, U.; Gislason, G.; Torp-Pedersen, C.; Banner, J.; Risgaard, B.; Winkel, B. G.; Tfelt-Hansen, J., Sudden cardiac death among persons with diabetes aged 1-49 years: a 10-year nationwide study of 14 294 deaths in Denmark. *European heart journal* **2020**, *41* (28), 2699-2706.
62. Yuan, S. Y.; Rigor, R. R., Integrated Systems Physiology: From Molecule to Function to Disease. In *Regulation of Endothelial Barrier Function*, Morgan & Claypool Life Sciences
- Copyright © 2011 by Morgan & Claypool Life Sciences.: San Rafael (CA), 2010.
63. Tirziu, D.; Giordano, F. J.; Simons, M., Cell communications in the heart. *Circulation* **2010**, *122* (9), 928-37.
64. Brutsaert, D. L., Cardiac endothelial-myocardial signaling: its role in cardiac growth, contractile performance, and rhythmicity. *Physiological reviews* **2003**, *83* (1), 59-115.
65. Vancheri, F.; Longo, G.; Vancheri, S.; Henein, M., Coronary Microvascular Dysfunction. *Journal of clinical medicine* **2020**, *9* (9), 2880.
66. Hinkel, R.; Howe, A.; Renner, S.; Ng, J.; Lee, S.; Klett, K.; Kaczmarek, V.; Moretti, A.; Laugwitz, K. L.; Skrobilin, P.; Mayr, M.; Milting, H.; Dendorfer, A.; Reichart, B.; Wolf, E.; Kupatt, C., Diabetes Mellitus-Induced Microvascular Destabilization in the Myocardium. *Journal of the American College of Cardiology* **2017**, *69* (2), 131-143.
67. Sezer, M.; Kocaaga, M.; Aslanger, E.; Atici, A.; Demirkiran, A.; Bugra, Z.; Umman, S.; Umman, B., Bimodal Pattern of Coronary Microvascular Involvement in Diabetes Mellitus. *Journal of the American Heart Association* **2016**, *5* (11).
68. Padro, T.; Manfrini, O.; Bugiardini, R.; Canty, J.; Cenko, E.; De Luca, G.; Duncker, D. J.; Eringa, E. C.; Koller, A.; Tousoulis, D.; Trifunovic, D.; Vavlukis, M.; de Wit, C.; Badimon, L., ESC Working Group on Coronary Pathophysiology and Microcirculation position paper on 'coronary microvascular dysfunction in cardiovascular disease'. *Cardiovascular research* **2020**, *116* (4), 741-755.
69. Katz, P. S.; Trask, A. J.; Souza-Smith, F. M.; Hutchinson, K. R.; Galantowicz, M. L.; Lord, K. C.; Stewart, J. A., Jr.; Cismowski, M. J.; Varner, K. J.; Lucchesi, P. A., Coronary arterioles in type 2 diabetic (db/db) mice undergo a distinct pattern of remodeling associated with decreased vessel stiffness. *Basic research in cardiology* **2011**, *106* (6), 1123-34.
70. Assar, M. E.; Angulo, J.; Rodríguez-Mañas, L., Diabetes and ageing-induced vascular inflammation. *The Journal of physiology* **2016**, *594* (8), 2125-46.
71. Pechlivani, N.; Ajjan, R. A., Thrombosis and Vascular Inflammation in Diabetes: Mechanisms and Potential Therapeutic Targets. *Frontiers in cardiovascular medicine* **2018**, *5*, 1.

72. Jaffe, R.; Charron, T.; Puley, G.; Dick, A.; Strauss, B. H., Microvascular obstruction and the no-reflow phenomenon after percutaneous coronary intervention. *Circulation* **2008**, *117* (24), 3152-6.
73. Tromp, J.; Lim, S. L.; Tay, W. T.; Teng, T. K.; Chandramouli, C.; Ouwerkerk, W.; Wander, G. S.; Sawhney, J. P. S.; Yap, J.; MacDonald, M. R.; Ling, L. H.; Sattar, N.; McMurray, J. J. V.; Richards, A. M.; Anand, I.; Lam, C. S. P., Microvascular Disease in Patients With Diabetes With Heart Failure and Reduced Ejection Versus Preserved Ejection Fraction. *Diabetes Care* **2019**, *42* (9), 1792-1799.
74. Jouven, X.; Lemaître, R. N.; Rea, T. D.; Sotoodehnia, N.; Empana, J. P.; Siscovick, D. S., Diabetes, glucose level, and risk of sudden cardiac death. *European heart journal* **2005**, *26* (20), 2142-7.
75. Kobayashi, S.; Nagao, M.; Asai, A.; Fukuda, I.; Oikawa, S.; Sugihara, H., Severity and multiplicity of microvascular complications are associated with QT interval prolongation in patients with type 2 diabetes. *J Diabetes Investig* **2018**, *9* (4), 946-951.
76. Subbalakshmi, N. K.; Adhikari, P. M.; Sathyanarayana Rao, K. N.; Jeganathan, P. S., Influencing factors of QTc among the clinical characteristics in type 2 diabetes mellitus. *Diabetes Res Clin Pract* **2010**, *88* (3), 265-72.
77. Li, X.; Ren, H.; Xu, Z. R.; Liu, Y. J.; Yang, X. P.; Liu, J. Q., Prevalence and risk factors of prolonged QTc interval among Chinese patients with type 2 diabetes. *Experimental diabetes research* **2012**, *2012*, 234084.
78. Falkenberg, K. D.; Rohlenova, K.; Luo, Y.; Carmeliet, P., The metabolic engine of endothelial cells. *Nat Metab* **2019**, *1* (10), 937-946.
79. Kaiser, N.; Sasson, S.; Feener, E. P.; Boukobza-Vardi, N.; Higashi, S.; Moller, D. E.; Davidheiser, S.; Przybylski, R. J.; King, G. L., Differential regulation of glucose transport and transporters by glucose in vascular endothelial and smooth muscle cells. *Diabetes* **1993**, *42* (1), 80-9.
80. Stapor, P.; Wang, X.; Goveia, J.; Moens, S.; Carmeliet, P., Angiogenesis revisited - role and therapeutic potential of targeting endothelial metabolism. *J Cell Sci* **2014**, *127* (Pt 20), 4331-41.
81. Tabit, C. E.; Chung, W. B.; Hamburg, N. M.; Vita, J. A., Endothelial dysfunction in diabetes mellitus: molecular mechanisms and clinical implications. *Rev Endocr Metab Disord* **2010**, *11* (1), 61-74.
82. Knapp, M.; Tu, X.; Wu, R., Vascular endothelial dysfunction, a major mediator in diabetic cardiomyopathy. *Acta pharmacologica Sinica* **2019**, *40* (1), 1-8.
83. Du, X. L.; Edelstein, D.; Dimmeler, S.; Ju, Q.; Sui, C.; Brownlee, M., Hyperglycemia inhibits endothelial nitric oxide synthase activity by posttranslational modification at the Akt site. *The Journal of clinical investigation* **2001**, *108* (9), 1341-8.
84. Luo, B.; Soesanto, Y.; McClain, D. A., Protein modification by O-linked GlcNAc reduces angiogenesis by inhibiting Akt activity in endothelial cells. *Arteriosclerosis, thrombosis, and vascular biology* **2008**, *28* (4), 651-7.

Literature

85. Wautier, J. L.; Zoukourian, C.; Chappey, O.; Wautier, M. P.; Guillausseau, P. J.; Cao, R.; Hori, O.; Stern, D.; Schmidt, A. M., Receptor-mediated endothelial cell dysfunction in diabetic vasculopathy. Soluble receptor for advanced glycation end products blocks hyperpermeability in diabetic rats. *The Journal of clinical investigation* **1996**, *97* (1), 238-43.
86. Soro-Paavonen, A.; Zhang, W. Z.; Venardos, K.; Coughlan, M. T.; Harris, E.; Tong, D. C.; Brasacchio, D.; Paavonen, K.; Chin-Dusting, J.; Cooper, M. E.; Kaye, D.; Thomas, M. C.; Forbes, J. M., Advanced glycation end-products induce vascular dysfunction via resistance to nitric oxide and suppression of endothelial nitric oxide synthase. *J Hypertens* **2010**, *28* (4), 780-8.
87. Bierhaus, A.; Chevion, S.; Chevion, M.; Hofmann, M.; Quehenberger, P.; Illmer, T.; Luther, T.; Berentshtein, E.; Tritschler, H.; Müller, M.; Wahl, P.; Ziegler, R.; Nawroth, P. P., Advanced glycation end product-induced activation of NF-kappaB is suppressed by alpha-lipoic acid in cultured endothelial cells. *Diabetes* **1997**, *46* (9), 1481-90.
88. Cepas, V.; Collino, M.; Mayo, J. C.; Sainz, R. M., Redox Signaling and Advanced Glycation Endproducts (AGEs) in Diet-Related Diseases. *Antioxidants (Basel)* **2020**, *9* (2).
89. Basta, G.; Schmidt, A. M.; De Caterina, R., Advanced glycation end products and vascular inflammation: implications for accelerated atherosclerosis in diabetes. *Cardiovascular research* **2004**, *63* (4), 582-92.
90. Tan, K. C.; Chow, W. S.; Ai, V. H.; Metz, C.; Bucala, R.; Lam, K. S., Advanced glycation end products and endothelial dysfunction in type 2 diabetes. *Diabetes Care* **2002**, *25* (6), 1055-9.
91. Nigro, C.; Leone, A.; Raciti, G. A.; Longo, M.; Mirra, P.; Formisano, P.; Beguinot, F.; Miele, C., Methylglyoxal-Glyoxalase 1 Balance: The Root of Vascular Damage. *International journal of molecular sciences* **2017**, *18* (1).
92. Meza, C. A.; La Favor, J. D.; Kim, D. H.; Hickner, R. C., Endothelial Dysfunction: Is There a Hyperglycemia-Induced Imbalance of NOX and NOS? *International journal of molecular sciences* **2019**, *20* (15).
93. Matsumoto, S.; Shimabukuro, M.; Fukuda, D.; Soeki, T.; Yamakawa, K.; Masuzaki, H.; Sata, M., Azilsartan, an angiotensin II type 1 receptor blocker, restores endothelial function by reducing vascular inflammation and by increasing the phosphorylation ratio Ser(1177)/Thr(497) of endothelial nitric oxide synthase in diabetic mice. *Cardiovascular diabetology* **2014**, *13*, 30.
94. Zou, M. H.; Shi, C.; Cohen, R. A., Oxidation of the zinc-thiolate complex and uncoupling of endothelial nitric oxide synthase by peroxynitrite. *The Journal of clinical investigation* **2002**, *109* (6), 817-26.
95. Vásquez-Vivar, J.; Kalyanaraman, B.; Martásek, P.; Hogg, N.; Masters, B. S.; Karoui, H.; Tordo, P.; Pritchard, K. A., Jr., Superoxide generation by endothelial nitric oxide synthase: the influence of cofactors. *Proceedings of the National Academy of Sciences of the United States of America* **1998**, *95* (16), 9220-5.

Literature

96. Alp, N. J.; Mussa, S.; Khoo, J.; Cai, S.; Guzik, T.; Jefferson, A.; Goh, N.; Rockett, K. A.; Channon, K. M., Tetrahydrobiopterin-dependent preservation of nitric oxide-mediated endothelial function in diabetes by targeted transgenic GTP-cyclohydrolase I overexpression. *The Journal of clinical investigation* **2003**, *112* (5), 725-35.
97. Heitzer, T.; Krohn, K.; Albers, S.; Meinertz, T., Tetrahydrobiopterin improves endothelium-dependent vasodilation by increasing nitric oxide activity in patients with Type II diabetes mellitus. *Diabetologia* **2000**, *43* (11), 1435-8.
98. Muniyappa, R.; Montagnani, M.; Koh, K. K.; Quon, M. J., Cardiovascular actions of insulin. *Endocrine reviews* **2007**, *28* (5), 463-91.
99. Montagnani, M.; Chen, H.; Barr, V. A.; Quon, M. J., Insulin-stimulated activation of eNOS is independent of Ca²⁺ but requires phosphorylation by Akt at Ser(1179). *The Journal of biological chemistry* **2001**, *276* (32), 30392-8.
100. Zeng, G.; Nystrom, F. H.; Ravichandran, L. V.; Cong, L. N.; Kirby, M.; Mostowski, H.; Quon, M. J., Roles for insulin receptor, PI3-kinase, and Akt in insulin-signaling pathways related to production of nitric oxide in human vascular endothelial cells. *Circulation* **2000**, *101* (13), 1539-45.
101. Dimmeler, S.; Fleming, I.; Fisslthaler, B.; Hermann, C.; Busse, R.; Zeiher, A. M., Activation of nitric oxide synthase in endothelial cells by Akt-dependent phosphorylation. *Nature* **1999**, *399* (6736), 601-605.
102. Montagnani, M.; Golovchenko, I.; Kim, I.; Koh, G. Y.; Goalstone, M. L.; Mundhekar, A. N.; Johansen, M.; Kucik, D. F.; Quon, M. J.; Draznin, B., Inhibition of phosphatidylinositol 3-kinase enhances mitogenic actions of insulin in endothelial cells. *The Journal of biological chemistry* **2002**, *277* (3), 1794-9.
103. Marasciulo, F. L.; Montagnani, M.; Potenza, M. A., Endothelin-1: the yin and yang on vascular function. *Current medicinal chemistry* **2006**, *13* (14), 1655-65.
104. van Gils, J. M.; Zwaginga, J. J.; Hordijk, P. L., Molecular and functional interactions among monocytes, platelets, and endothelial cells and their relevance for cardiovascular diseases. *Journal of leukocyte biology* **2009**, *85* (2), 195-204.
105. Chisalita, S. I.; Nitert, M. D.; Arnqvist, H. J., Characterisation of receptors for IGF-I and insulin; evidence for hybrid insulin/IGF-I receptor in human coronary artery endothelial cells. *Growth Horm IGF Res* **2006**, *16* (4), 258-66.
106. Li, G.; Barrett, E. J.; Wang, H.; Chai, W.; Liu, Z., Insulin at physiological concentrations selectively activates insulin but not insulin-like growth factor I (IGF-I) or insulin/IGF-I hybrid receptors in endothelial cells. *Endocrinology* **2005**, *146* (11), 4690-6.
107. Imrie, H.; Viswambharan, H.; Sukumar, P.; Abbas, A.; Cubbon, R. M.; Yuldasheva, N.; Gage, M.; Smith, J.; Galloway, S.; Skromna, A.; Rashid, S. T.; Futers, T. S.; Xuan, S.; Gatenby, V. K.; Grant, P. J.; Channon, K. M.; Beech, D. J.; Wheatcroft, S. B.; Kearney, M. T., Novel role of the IGF-1 receptor

Literature

in endothelial function and repair: studies in endothelium-targeted IGF-1 receptor transgenic mice. *Diabetes* **2012**, *61* (9), 2359-68.

108. Harhaj, N. S.; Felinski, E. A.; Wolpert, E. B.; Sundstrom, J. M.; Gardner, T. W.; Antonetti, D. A., VEGF activation of protein kinase C stimulates occludin phosphorylation and contributes to endothelial permeability. *Invest Ophthalmol Vis Sci* **2006**, *47* (11), 5106-15.

109. Yuan, S. Y.; Ustinova, E. E.; Wu, M. H.; Tinsley, J. H.; Xu, W.; Korompai, F. L.; Taulman, A. C., Protein kinase C activation contributes to microvascular barrier dysfunction in the heart at early stages of diabetes. *Circulation research* **2000**, *87* (5), 412-7.

110. Haidari, M.; Zhang, W.; Willerson, J. T.; Dixon, R. A., Disruption of endothelial adherens junctions by high glucose is mediated by protein kinase C- β -dependent vascular endothelial cadherin tyrosine phosphorylation. *Cardiovascular diabetology* **2014**, *13*, 105.

111. Potente, M.; Gerhardt, H.; Carmeliet, P., Basic and therapeutic aspects of angiogenesis. *Cell* **2011**, *146* (6), 873-87.

112. Chen, W.; Xia, P.; Wang, H.; Tu, J.; Liang, X.; Zhang, X.; Li, L., The endothelial tip-stalk cell selection and shuffling during angiogenesis. *Journal of cell communication and signaling* **2019**, *13* (3), 291-301.

113. Akil, A.; Gutiérrez-García, A. K.; Guenter, R.; Rose, J. B.; Beck, A. W.; Chen, H.; Ren, B., Notch Signaling in Vascular Endothelial Cells, Angiogenesis, and Tumor Progression: An Update and Prospective. *Frontiers in cell and developmental biology* **2021**, *9*, 642352.

114. Kopan, R.; Ilagan, M. X., The canonical Notch signaling pathway: unfolding the activation mechanism. *Cell* **2009**, *137* (2), 216-33.

115. Suchting, S.; Freitas, C.; le Noble, F.; Benedito, R.; Bréant, C.; Duarte, A.; Eichmann, A., The Notch ligand Delta-like 4 negatively regulates endothelial tip cell formation and vessel branching. *Proceedings of the National Academy of Sciences of the United States of America* **2007**, *104* (9), 3225-30.

116. van Tetering, G.; van Diest, P.; Verlaan, I.; van der Wall, E.; Kopan, R.; Vooijs, M., Metalloprotease ADAM10 is required for Notch1 site 2 cleavage. *The Journal of biological chemistry* **2009**, *284* (45), 31018-27.

117. Bozkulak, E. C.; Weinmaster, G., Selective use of ADAM10 and ADAM17 in activation of Notch1 signaling. *Mol Cell Biol* **2009**, *29* (21), 5679-95.

118. Alabi, R. O.; Farber, G.; Blobel, C. P., Intriguing Roles for Endothelial ADAM10/Notch Signaling in the Development of Organ-Specific Vascular Beds. *Physiological reviews* **2018**, *98* (4), 2025-2061.

119. Farber, G.; Parks, M. M.; Lustgarten Guahmich, N.; Zhang, Y.; Monette, S.; Blanchard, S. C.; Di Lorenzo, A.; Blobel, C. P., ADAM10 controls the differentiation of the coronary arterial endothelium. *Angiogenesis* **2019**, *22* (2), 237-250.

120. Aquila, G.; Kostina, A.; Viecei Dalla Sega, F.; Shlyakhto, E.; Kostareva, A.; Marracino, L.; Ferrari, R.; Rizzo, P.; Malaschicheva, A., The Notch pathway: a novel therapeutic target for cardiovascular diseases? *Expert opinion on therapeutic targets* **2019**, *23* (8), 695-710.
121. Marracino, L.; Fortini, F.; Bouhamida, E.; Camponogara, F.; Severi, P.; Mazzoni, E.; Patergnani, S.; D'Aniello, E.; Campana, R.; Pinton, P.; Martini, F.; Tognon, M.; Campo, G.; Ferrari, R.; Viecei Dalla Sega, F.; Rizzo, P., Adding a "Notch" to Cardiovascular Disease Therapeutics: A MicroRNA-Based Approach. *Frontiers in cell and developmental biology* **2021**, *9*, 695114.
122. Kayama, Y.; Raaz, U.; Jagger, A.; Adam, M.; Schellinger, I. N.; Sakamoto, M.; Suzuki, H.; Toyama, K.; Spin, J. M.; Tsao, P. S., Diabetic Cardiovascular Disease Induced by Oxidative Stress. *International journal of molecular sciences* **2015**, *16* (10), 25234-63.
123. Pradhan, A. D.; Manson, J. E.; Rifai, N.; Buring, J. E.; Ridker, P. M., C-reactive protein, interleukin 6, and risk of developing type 2 diabetes mellitus. *Jama* **2001**, *286* (3), 327-34.
124. Schulze, M. B.; Rimm, E. B.; Li, T.; Rifai, N.; Stampfer, M. J.; Hu, F. B., C-reactive protein and incident cardiovascular events among men with diabetes. *Diabetes Care* **2004**, *27* (4), 889-94.
125. Vozarova, B.; Weyer, C.; Hanson, K.; Tataranni, P. A.; Bogardus, C.; Pratley, R. E., Circulating interleukin-6 in relation to adiposity, insulin action, and insulin secretion. *Obes Res* **2001**, *9* (7), 414-7.
126. Collins, T.; Cybulsky, M. I., NF-kappaB: pivotal mediator or innocent bystander in atherogenesis? *The Journal of clinical investigation* **2001**, *107* (3), 255-64.
127. de Winther, M. P.; Kanters, E.; Kraal, G.; Hofker, M. H., Nuclear factor kappaB signaling in atherogenesis. *Arteriosclerosis, thrombosis, and vascular biology* **2005**, *25* (5), 904-14.
128. Sen, R.; Baltimore, D., Inducibility of kappa immunoglobulin enhancer-binding protein Nf-kappa B by a posttranslational mechanism. *Cell* **1986**, *47* (6), 921-8.
129. Zhang, Q.; Lenardo, M. J.; Baltimore, D., 30 Years of NF-κB: A Blossoming of Relevance to Human Pathobiology. *Cell* **2017**, *168* (1-2), 37-57.
130. De Martin, R.; Hoeth, M.; Hofer-Warbinek, R.; Schmid, J. A., The transcription factor NF-kappa B and the regulation of vascular cell function. *Arteriosclerosis, thrombosis, and vascular biology* **2000**, *20* (11), E83-8.
131. Lorenzo, O.; Picatoste, B.; Ares-Carrasco, S.; Ramírez, E.; Egido, J.; Tuñón, J., Potential role of nuclear factor κB in diabetic cardiomyopathy. *Mediators of inflammation* **2011**, *2011*, 652097.
132. Brach, M. A.; Henschler, R.; Mertelsmann, R. H.; Herrmann, F., Regulation of M-CSF Expression by M-CSF: Role of Protein Kinase C and Transcription Factor NFκB. *Pathobiology* **1991**, *59* (4), 284-288.
133. Smith, J. D.; Trogan, E.; Ginsberg, M.; Grigaux, C.; Tian, J.; Miyata, M., Decreased atherosclerosis in mice deficient in both macrophage colony-stimulating factor (op) and apolipoprotein E. *Proceedings of the National Academy of Sciences* **1995**, *92* (18), 8264-8268.

Literature

134. Bond, M.; Fabunmi, R. P.; Baker, A. H.; Newby, A. C., Synergistic upregulation of metalloproteinase-9 by growth factors and inflammatory cytokines: an absolute requirement for transcription factor NF-kappa B. *FEBS letters* **1998**, *435* (1), 29-34.
135. Monahan-Earley, R.; Dvorak, A. M.; Aird, W. C., Evolutionary origins of the blood vascular system and endothelium. *Journal of thrombosis and haemostasis : JTH* **2013**, *11 Suppl 1* (Suppl 1), 46-66.
136. Sweet, D. R.; Lam, C.; Jain, M. K., Evolutionary Protection of Krüppel-Like Factors 2 and 4 in the Development of the Mature Hemovascular System. *Frontiers in cardiovascular medicine* **2021**, *8*, 645719.
137. Fan, Y.; Lu, H.; Liang, W.; Hu, W.; Zhang, J.; Chen, Y. E., Krüppel-like factors and vascular wall homeostasis. *J Mol Cell Biol* **2017**, *9* (5), 352-363.
138. Turner, J.; Crossley, M., Mammalian Krüppel-like transcription factors: more than just a pretty finger. *Trends Biochem Sci* **1999**, *24* (6), 236-40.
139. Botella, L. M.; Sánchez-Elsner, T.; Sanz-Rodriguez, F.; Kojima, S.; Shimada, J.; Guerrero-Esteo, M.; Cooreman, M. P.; Ratzliff, V.; Langa, C.; Vary, C. P.; Ramirez, J. R.; Friedman, S.; Bernabéu, C., Transcriptional activation of endoglin and transforming growth factor-beta signaling components by cooperative interaction between Sp1 and KLF6: their potential role in the response to vascular injury. *Blood* **2002**, *100* (12), 4001-10.
140. Suzuki, T.; Aizawa, K.; Matsumura, T.; Nagai, R., Vascular implications of the Krüppel-like family of transcription factors. *Arteriosclerosis, thrombosis, and vascular biology* **2005**, *25* (6), 1135-41.
141. Kuo, C. T.; Veselits, M. L.; Barton, K. P.; Lu, M. M.; Clendenin, C.; Leiden, J. M., The LKLF transcription factor is required for normal tunica media formation and blood vessel stabilization during murine embryogenesis. *Genes & development* **1997**, *11* (22), 2996-3006.
142. Methe, H.; Balcells, M.; Alegret Mdel, C.; Santacana, M.; Molins, B.; Hamik, A.; Jain, M. K.; Edelman, E. R., Vascular bed origin dictates flow pattern regulation of endothelial adhesion molecule expression. *American journal of physiology. Heart and circulatory physiology* **2007**, *292* (5), H2167-75.
143. SenBanerjee, S.; Lin, Z.; Atkins, G. B.; Greif, D. M.; Rao, R. M.; Kumar, A.; Feinberg, M. W.; Chen, Z.; Simon, D. I.; Luscinskas, F. W.; Michel, T. M.; Gimbrone, M. A., Jr.; García-Cardena, G.; Jain, M. K., KLF2 Is a novel transcriptional regulator of endothelial proinflammatory activation. *J Exp Med* **2004**, *199* (10), 1305-15.
144. Dekker, R. J.; van Soest, S.; Fontijn, R. D.; Salamanca, S.; de Groot, P. G.; VanBavel, E.; Pannekoek, H.; Horrevoets, A. J., Prolonged fluid shear stress induces a distinct set of endothelial cell genes, most specifically lung Krüppel-like factor (KLF2). *Blood* **2002**, *100* (5), 1689-98.
145. van Thienen, J. V.; Fledderus, J. O.; Dekker, R. J.; Rohlena, J.; van Ijzendoorn, G. A.; Kootstra, N. A.; Pannekoek, H.; Horrevoets, A. J., Shear stress sustains atheroprotective endothelial KLF2

Literature

expression more potently than statins through mRNA stabilization. *Cardiovascular research* **2006**, 72 (2), 231-40.

146. Jha, P.; Das, H., KLF2 in Regulation of NF- κ B-Mediated Immune Cell Function and Inflammation. *International journal of molecular sciences* **2017**, 18 (11).

147. Das, H.; Kumar, A.; Lin, Z.; Patino, W. D.; Hwang, P. M.; Feinberg, M. W.; Majumder, P. K.; Jain, M. K., Kruppel-like factor 2 (KLF2) regulates proinflammatory activation of monocytes. *Proceedings of the National Academy of Sciences of the United States of America* **2006**, 103 (17), 6653-8.

148. Wu, C.; Huang, R. T.; Kuo, C. H.; Kumar, S.; Kim, C. W.; Lin, Y. C.; Chen, Y. J.; Birukova, A.; Birukov, K. G.; Dulin, N. O.; Civelek, M.; Lysis, A. J.; Loyer, X.; Tedgui, A.; Dai, G.; Jo, H.; Fang, Y., Mechanosensitive PPAP2B Regulates Endothelial Responses to Atherorelevant Hemodynamic Forces. *Circulation research* **2015**, 117 (4), e41-e53.

149. Lin, Z.; Kumar, A.; SenBanerjee, S.; Staniszewski, K.; Parmar, K.; Vaughan, D. E.; Gimbrone, M. A., Jr.; Balasubramanian, V.; García-Cardena, G.; Jain, M. K., Kruppel-like factor 2 (KLF2) regulates endothelial thrombotic function. *Circulation research* **2005**, 96 (5), e48-57.

150. Lin, Z.; Natesan, V.; Shi, H.; Dong, F.; Kawanami, D.; Mahabeleshwar, G. H.; Atkins, G. B.; Nayak, L.; Cui, Y.; Finigan, J. H.; Jain, M. K., Kruppel-like factor 2 regulates endothelial barrier function. *Arteriosclerosis, thrombosis, and vascular biology* **2010**, 30 (10), 1952-9.

151. Dekker, R. J.; van Thienen, J. V.; Rohlena, J.; de Jager, S. C.; Elderkamp, Y. W.; Seppen, J.; de Vries, C. J.; Biessen, E. A.; van Berkel, T. J.; Pannekoek, H.; Horrevoets, A. J., Endothelial KLF2 links local arterial shear stress levels to the expression of vascular tone-regulating genes. *The American journal of pathology* **2005**, 167 (2), 609-18.

152. Wu, W.; Geng, P.; Zhu, J.; Li, J.; Zhang, L.; Chen, W.; Zhang, D.; Lu, Y.; Xu, X., KLF2 regulates eNOS uncoupling via Nrf2/HO-1 in endothelial cells under hypoxia and reoxygenation. *Chem Biol Interact* **2019**, 305, 105-111.

153. Doddaballapur, A.; Michalik, K. M.; Manavski, Y.; Lucas, T.; Houtkooper, R. H.; You, X.; Chen, W.; Zeiher, A. M.; Potente, M.; Dimmeler, S.; Boon, R. A., Laminar shear stress inhibits endothelial cell metabolism via KLF2-mediated repression of PFKFB3. *Arteriosclerosis, thrombosis, and vascular biology* **2015**, 35 (1), 137-45.

154. Sangwung, P.; Zhou, G.; Nayak, L.; Chan, E. R.; Kumar, S.; Kang, D. W.; Zhang, R.; Liao, X.; Lu, Y.; Sugi, K.; Fujioka, H.; Shi, H.; Lapping, S. D.; Ghosh, C. C.; Higgins, S. J.; Parikh, S. M.; Jo, H.; Jain, M. K., KLF2 and KLF4 control endothelial identity and vascular integrity. *JCI Insight* **2017**, 2 (4), e91700.

155. Villarreal, G., Jr.; Zhang, Y.; Larman, H. B.; Gracia-Sancho, J.; Koo, A.; García-Cardena, G., Defining the regulation of KLF4 expression and its downstream transcriptional targets in vascular endothelial cells. *Biochemical and biophysical research communications* **2010**, 391 (1), 984-9.

Literature

156. Zhang, X.; Wang, L.; Han, Z.; Dong, J.; Pang, D.; Fu, Y.; Li, L., KLF4 alleviates cerebral vascular injury by ameliorating vascular endothelial inflammation and regulating tight junction protein expression following ischemic stroke. *Journal of Neuroinflammation* **2020**, *17* (1).
157. Zhou, G.; Hamik, A.; Nayak, L.; Tian, H.; Shi, H.; Lu, Y.; Sharma, N.; Liao, X.; Hale, A.; Boerboom, L.; Feaver, R. E.; Gao, H.; Desai, A.; Schmaier, A.; Gerson, S. L.; Wang, Y.; Atkins, G. B.; Blackman, B. R.; Simon, D. I.; Jain, M. K., Endothelial Kruppel-like factor 4 protects against atherothrombosis in mice. *The Journal of clinical investigation* **2012**, *122* (12), 4727-31.
158. Chiplunkar, A. R.; Curtis, B. C.; Eades, G. L.; Kane, M. S.; Fox, S. J.; Haar, J. L.; Lloyd, J. A., The Krüppel-like factor 2 and Krüppel-like factor 4 genes interact to maintain endothelial integrity in mouse embryonic vasculogenesis. *BMC developmental biology* **2013**, *13*, 40.
159. Liao, X.; Sharma, N.; Kapadia, F.; Zhou, G.; Lu, Y.; Hong, H.; Paruchuri, K.; Mahabeleshwar, G. H.; Dalmas, E.; Venteclef, N.; Flask, C. A.; Kim, J.; Doreian, B. W.; Lu, K. Q.; Kaestner, K. H.; Hamik, A.; Clément, K.; Jain, M. K., Krüppel-like factor 4 regulates macrophage polarization. *The Journal of clinical investigation* **2011**, *121* (7), 2736-49.
160. Cherepanova, O. A.; Pidkovka, N. A.; Sarmiento, O. F.; Yoshida, T.; Gan, Q.; Adiguzel, E.; Bendeck, M. P.; Berliner, J.; Leitinger, N.; Owens, G. K., Oxidized phospholipids induce type VIII collagen expression and vascular smooth muscle cell migration. *Circulation research* **2009**, *104* (5), 609-18.
161. Shankman, L. S.; Gomez, D.; Cherepanova, O. A.; Salmon, M.; Alencar, G. F.; Haskins, R. M.; Swiatlowska, P.; Newman, A. A.; Greene, E. S.; Straub, A. C.; Isakson, B.; Randolph, G. J.; Owens, G. K., KLF4-dependent phenotypic modulation of smooth muscle cells has a key role in atherosclerotic plaque pathogenesis. *Nature medicine* **2015**, *21* (6), 628-37.
162. Hien, T. T.; Garcia-Vaz, E.; Stenkula, K. G.; Sjögren, J.; Nilsson, J.; Gomez, M. F.; Albinsson, S., MicroRNA-dependent regulation of KLF4 by glucose in vascular smooth muscle. *Journal of cellular physiology* **2018**, *233* (9), 7195-7205.
163. Lee, H. Y.; Youn, S. W.; Oh, B. H.; Kim, H. S., Krüppel-like factor 2 suppression by high glucose as a possible mechanism of diabetic vasculopathy. *Korean circulation journal* **2012**, *42* (4), 239-45.
164. Song, W.; Zhang, C. L.; Gou, L.; He, L.; Gong, Y. Y.; Qu, D.; Zhao, L.; Jin, N.; Chan, T. F.; Wang, L.; Tian, X. Y.; Luo, J. Y.; Huang, Y., Endothelial TFEB (Transcription Factor EB) Restrains IKK (IκB Kinase)-p65 Pathway to Attenuate Vascular Inflammation in Diabetic db/db Mice. *Arteriosclerosis, thrombosis, and vascular biology* **2019**, *39* (4), 719-730.
165. Wang, X.; Wu, Z.; He, Y.; Zhang, H.; Tian, L.; Zheng, C.; Shang, T.; Zhu, Q.; Li, D.; He, Y., Humanin prevents high glucose-induced monocyte adhesion to endothelial cells by targeting KLF2. *Mol Immunol* **2018**, *101*, 245-250.
166. Pon, J. R.; Marra, M. A., MEF2 transcription factors: developmental regulators and emerging cancer genes. *Oncotarget* **2016**, *7* (3), 2297-312.

Literature

167. Chen, X.; Gao, B.; Ponnusamy, M.; Lin, Z.; Liu, J., MEF2 signaling and human diseases. *Oncotarget* **2017**, *8* (67), 112152-112165.
168. Kumar, A.; Lin, Z.; SenBanerjee, S.; Jain, M. K., Tumor necrosis factor alpha-mediated reduction of KLF2 is due to inhibition of MEF2 by NF-kappaB and histone deacetylases. *Mol Cell Biol* **2005**, *25* (14), 5893-903.
169. Lu, Y. W.; Martino, N.; Gerlach, B. D.; Lamar, J. M.; Vincent, P. A.; Adam, A. P.; Schwarz, J. J., MEF2 (Myocyte Enhancer Factor 2) Is Essential for Endothelial Homeostasis and the Atheroprotective Gene Expression Program. *Arteriosclerosis, thrombosis, and vascular biology* **2021**, *41* (3), 1105-1123.
170. Cornwell, J. D.; McDermott, J. C., MEF2 in cardiac hypertrophy in response to hypertension. *Trends in cardiovascular medicine* **2022**.
171. Csipo, T.; Fulop, G. A.; Lipecz, A.; Tarantini, S.; Kiss, T.; Balasubramanian, P.; Csiszar, A.; Ungvari, Z.; Yabluchanskiy, A., Short-term weight loss reverses obesity-induced microvascular endothelial dysfunction. *Geroscience* **2018**, *40* (3), 337-46.
172. Janež, A.; Guja, C.; Mitrakou, A.; Lalic, N.; Tankova, T.; Czupryniak, L.; Tabák, A. G.; Prazny, M.; Martinka, E.; Smircic-Duvnjak, L., Insulin Therapy in Adults with Type 1 Diabetes Mellitus: a Narrative Review. *Diabetes Ther* **2020**, *11* (2), 387-409.
173. Oral Pharmacologic Treatment of Type 2 Diabetes Mellitus: A Clinical Practice Guideline Update From the American College of Physicians. *Annals of internal medicine* **2017**, *166* (4), 279-290.
174. Taqueti, V. R.; Di Carli, M. F., Coronary Microvascular Disease Pathogenic Mechanisms and Therapeutic Options: JACC State-of-the-Art Review. *Journal of the American College of Cardiology* **2018**, *72* (21), 2625-2641.
175. Salvatore, T.; Galiero, R.; Caturano, A.; Vetrano, E.; Loffredo, G.; Rinaldi, L.; Catalini, C.; Gjeloši, K.; Albanese, G.; Di Martino, A.; Docimo, G.; Sardu, C.; Marfella, R.; Sasso, F. C., Coronary Microvascular Dysfunction in Diabetes Mellitus: Pathogenetic Mechanisms and Potential Therapeutic Options. *Biomedicines* **2022**, *10* (9).
176. Solberg, O. G.; Stavem, K.; Ragnarsson, A.; Beitnes, J. O.; Skårdal, R.; Seljeflot, I.; Ueland, T.; Aukrust, P.; Gullestad, L.; Aaberge, L., Index of microvascular resistance to assess the effect of rosuvastatin on microvascular function in women with chest pain and no obstructive coronary artery disease: A double-blind randomized study. *Catheterization and cardiovascular interventions : official journal of the Society for Cardiac Angiography & Interventions* **2019**, *94* (5), 660-668.
177. Baan, J., Jr.; Chang, P. C.; Vermeij, P.; Pfaffendorf, M.; van Zwieten, P. A., Effects of losartan on vasoconstrictor responses to angiotensin II in the forearm vascular bed of healthy volunteers. *Cardiovascular research* **1996**, *32* (5), 973-979.
178. de Waha, S.; Patel, M. R.; Granger, C. B.; Ohman, E. M.; Maehara, A.; Eitel, I.; Ben-Yehuda, O.; Jenkins, P.; Thiele, H.; Stone, G. W., Relationship between microvascular obstruction and adverse events following primary percutaneous coronary intervention for ST-segment elevation myocardial

infarction: an individual patient data pooled analysis from seven randomized trials. *European heart journal* **2017**, 38 (47), 3502-3510.

179. Marso, S. P.; Bain, S. C.; Consoli, A.; Eliaschewitz, F. G.; Jódar, E.; Leiter, L. A.; Lingvay, I.; Rosenstock, J.; Seufert, J.; Warren, M. L.; Woo, V.; Hansen, O.; Holst, A. G.; Pettersson, J.; Vilsbøll, T., Semaglutide and Cardiovascular Outcomes in Patients with Type 2 Diabetes. *The New England journal of medicine* **2016**, 375 (19), 1834-1844.

180. Marso, S. P.; Daniels, G. H.; Brown-Frandsen, K.; Kristensen, P.; Mann, J. F. E.; Nauck, M. A.; Nissen, S. E.; Pocock, S.; Poulter, N. R.; Ravn, L. S.; Steinberg, W. M.; Stockner, M.; Zinman, B.; Bergenstal, R. M.; Buse, J. B., Liraglutide and Cardiovascular Outcomes in Type 2 Diabetes. *New England Journal of Medicine* **2016**, 375 (4), 311-322.

181. Hernandez, A. F.; Green, J. B.; Janmohamed, S.; D'Agostino, R. B., Sr.; Granger, C. B.; Jones, N. P.; Leiter, L. A.; Rosenberg, A. E.; Sigmon, K. N.; Somerville, M. C.; Thorpe, K. M.; McMurray, J. J. V.; Del Prato, S., Albiglutide and cardiovascular outcomes in patients with type 2 diabetes and cardiovascular disease (Harmony Outcomes): a double-blind, randomised placebo-controlled trial. *Lancet (London, England)* **2018**, 392 (10157), 1519-1529.

182. Kristensen, S. L.; Rørth, R.; Jhund, P. S.; Docherty, K. F.; Sattar, N.; Preiss, D.; Køber, L.; Petrie, M. C.; McMurray, J. J. V., Cardiovascular, mortality, and kidney outcomes with GLP-1 receptor agonists in patients with type 2 diabetes: a systematic review and meta-analysis of cardiovascular outcome trials. *Lancet Diabetes Endocrinol* **2019**, 7 (10), 776-785.

183. Boyle, J. G.; Livingstone, R.; Petrie, J. R., Cardiovascular benefits of GLP-1 agonists in type 2 diabetes: a comparative review. *Clinical science (London, England : 1979)* **2018**, 132 (15), 1699-1709.

184. Lee, R. C.; Feinbaum, R. L.; Ambros, V., The *C. elegans* heterochronic gene *lin-4* encodes small RNAs with antisense complementarity to *lin-14*. *Cell* **1993**, 75 (5), 843-54.

185. Reinhart, B. J.; Slack, F. J.; Basson, M.; Pasquinelli, A. E.; Bettinger, J. C.; Rougvie, A. E.; Horvitz, H. R.; Ruvkun, G., The 21-nucleotide *let-7* RNA regulates developmental timing in *Caenorhabditis elegans*. *Nature* **2000**, 403 (6772), 901-6.

186. Slack, F. J.; Basson, M.; Liu, Z.; Ambros, V.; Horvitz, H. R.; Ruvkun, G., The *lin-41* RBCC gene acts in the *C. elegans* heterochronic pathway between the *let-7* regulatory RNA and the LIN-29 transcription factor. *Molecular cell* **2000**, 5 (4), 659-69.

187. Pasquinelli, A. E.; Reinhart, B. J.; Slack, F.; Martindale, M. Q.; Kuroda, M. I.; Maller, B.; Hayward, D. C.; Ball, E. E.; Degnan, B.; Müller, P.; Spring, J.; Srinivasan, A.; Fishman, M.; Finnerty, J.; Corbo, J.; Levine, M.; Leahy, P.; Davidson, E.; Ruvkun, G., Conservation of the sequence and temporal expression of *let-7* heterochronic regulatory RNA. *Nature* **2000**, 408 (6808), 86-9.

188. Roush, S.; Slack, F. J., The *let-7* family of microRNAs. *Trends in cell biology* **2008**, 18 (10), 505-16.

189. Grosshans, H.; Slack, F. J., Micro-RNAs: small is plentiful. *J Cell Biol* **2002**, 156 (1), 17-21.

Literature

190. Lagos-Quintana, M.; Rauhut, R.; Lendeckel, W.; Tuschl, T., Identification of novel genes coding for small expressed RNAs. *Science (New York, N.Y.)* **2001**, *294* (5543), 853-8.
191. Griffiths-Jones, S.; Saini, H. K.; van Dongen, S.; Enright, A. J., miRBase: tools for microRNA genomics. *Nucleic Acids Res* **2008**, *36* (Database issue), D154-8.
192. Plotnikova, O.; Baranova, A.; Skoblov, M., Comprehensive Analysis of Human microRNA-mRNA Interactome. *Frontiers in genetics* **2019**, *10*, 933.
193. Moran, Y.; Agron, M.; Praher, D.; Technau, U., The evolutionary origin of plant and animal microRNAs. *Nat Ecol Evol* **2017**, *1* (3), 27.
194. Grundhoff, A.; Sullivan, C. S., Virus-encoded microRNAs. *Virology* **2011**, *411* (2), 325-43.
195. Olena, A. F.; Patton, J. G., Genomic organization of microRNAs. *Journal of cellular physiology* **2010**, *222* (3), 540-5.
196. Kim, V. N.; Nam, J. W., Genomics of microRNA. *Trends Genet* **2006**, *22* (3), 165-73.
197. Truscott, M.; Islam, A. B.; Frolov, M. V., Novel regulation and functional interaction of polycistronic miRNAs. *Rna* **2016**, *22* (1), 129-38.
198. Kim, V. N.; Han, J.; Siomi, M. C., Biogenesis of small RNAs in animals. *Nat Rev Mol Cell Biol* **2009**, *10* (2), 126-39.
199. Morlando, M.; Ballarino, M.; Gromak, N.; Pagano, F.; Bozzoni, I.; Proudfoot, N. J., Primary microRNA transcripts are processed co-transcriptionally. *Nat Struct Mol Biol* **2008**, *15* (9), 902-9.
200. Kim, Y. K.; Kim, V. N., Processing of intronic microRNAs. *The EMBO journal* **2007**, *26* (3), 775-83.
201. Ruby, J. G.; Jan, C. H.; Bartel, D. P., Intronic microRNA precursors that bypass Drosha processing. *Nature* **2007**, *448* (7149), 83-6.
202. Berezikov, E.; Chung, W. J.; Willis, J.; Cuppen, E.; Lai, E. C., Mammalian mirtron genes. *Molecular cell* **2007**, *28* (2), 328-36.
203. Lund, E.; Güttinger, S.; Calado, A.; Dahlberg, J. E.; Kutay, U., Nuclear export of microRNA precursors. *Science (New York, N.Y.)* **2004**, *303* (5654), 95-8.
204. Zhang, H.; Kolb, F. A.; Jaskiewicz, L.; Westhof, E.; Filipowicz, W., Single processing center models for human Dicer and bacterial RNase III. *Cell* **2004**, *118* (1), 57-68.
205. Kawamata, T.; Tomari, Y., Making RISC. *Trends Biochem Sci* **2010**, *35* (7), 368-76.
206. Siomi, H.; Siomi, M. C., On the road to reading the RNA-interference code. *Nature* **2009**, *457* (7228), 396-404.
207. Diederichs, S.; Haber, D. A., Dual role for argonautes in microRNA processing and posttranscriptional regulation of microRNA expression. *Cell* **2007**, *131* (6), 1097-108.
208. Matranga, C.; Tomari, Y.; Shin, C.; Bartel, D. P.; Zamore, P. D., Passenger-strand cleavage facilitates assembly of siRNA into Ago2-containing RNAi enzyme complexes. *Cell* **2005**, *123* (4), 607-20.

Literature

209. Guo, L.; Lu, Z., The fate of miRNA* strand through evolutionary analysis: implication for degradation as merely carrier strand or potential regulatory molecule? *PloS one* **2010**, *5* (6), e11387.
210. Treiber, T.; Treiber, N.; Meister, G., Regulation of microRNA biogenesis and its crosstalk with other cellular pathways. *Nature Reviews Molecular Cell Biology* **2019**, *20* (1), 5-20.
211. He, L.; Hannon, G. J., MicroRNAs: small RNAs with a big role in gene regulation. *Nature reviews. Genetics* **2004**, *5* (7), 522-31.
212. Bhaskaran, M.; Mohan, M., MicroRNAs: history, biogenesis, and their evolving role in animal development and disease. *Vet Pathol* **2014**, *51* (4), 759-74.
213. Perron, M. P.; Provost, P., Protein interactions and complexes in human microRNA biogenesis and function. *Frontiers in bioscience : a journal and virtual library* **2008**, *13*, 2537-47.
214. Yekta, S.; Shih, I. H.; Bartel, D. P., MicroRNA-directed cleavage of HOXB8 mRNA. *Science (New York, N.Y.)* **2004**, *304* (5670), 594-6.
215. Rivas, F. V.; Tolia, N. H.; Song, J. J.; Aragon, J. P.; Liu, J.; Hannon, G. J.; Joshua-Tor, L., Purified Argonaute2 and an siRNA form recombinant human RISC. *Nat Struct Mol Biol* **2005**, *12* (4), 340-9.
216. Bartel, D. P., MicroRNAs: target recognition and regulatory functions. *Cell* **2009**, *136* (2), 215-33.
217. Brennecke, J.; Stark, A.; Russell, R. B.; Cohen, S. M., Principles of microRNA-target recognition. *PLoS Biol* **2005**, *3* (3), e85.
218. Lai, E. C., Micro RNAs are complementary to 3' UTR sequence motifs that mediate negative post-transcriptional regulation. *Nature genetics* **2002**, *30* (4), 363-4.
219. Vella, M. C.; Choi, E. Y.; Lin, S. Y.; Reinert, K.; Slack, F. J., The C. elegans microRNA let-7 binds to imperfect let-7 complementary sites from the lin-41 3'UTR. *Genes & development* **2004**, *18* (2), 132-7.
220. Vella, M. C.; Reinert, K.; Slack, F. J., Architecture of a validated microRNA::target interaction. *Chem Biol* **2004**, *11* (12), 1619-23.
221. Agarwal, V.; Bell, G. W.; Nam, J. W.; Bartel, D. P., Predicting effective microRNA target sites in mammalian mRNAs. *Elife* **2015**, *4*.
222. Guo, H.; Ingolia, N. T.; Weissman, J. S.; Bartel, D. P., Mammalian microRNAs predominantly act to decrease target mRNA levels. *Nature* **2010**, *466* (7308), 835-40.
223. Lewis, B. P.; Burge, C. B.; Bartel, D. P., Conserved seed pairing, often flanked by adenosines, indicates that thousands of human genes are microRNA targets. *Cell* **2005**, *120* (1), 15-20.
224. Grimson, A.; Farh, K. K.; Johnston, W. K.; Garrett-Engle, P.; Lim, L. P.; Bartel, D. P., MicroRNA targeting specificity in mammals: determinants beyond seed pairing. *Molecular cell* **2007**, *27* (1), 91-105.
225. Clark, P. M.; Loher, P.; Quann, K.; Brody, J.; Londin, E. R.; Rigoutsos, I., Argonaute CLIP-Seq reveals miRNA targetome diversity across tissue types. *Scientific reports* **2014**, *4* (1), 5947.

Literature

226. Stroynowska-Czerwinska, A.; Fiszer, A.; Krzyzosiak, W. J., The panorama of miRNA-mediated mechanisms in mammalian cells. *Cellular and molecular life sciences : CMLS* **2014**, *71* (12), 2253-70.
227. Petersen, C. P.; Bordeleau, M. E.; Pelletier, J.; Sharp, P. A., Short RNAs repress translation after initiation in mammalian cells. *Molecular cell* **2006**, *21* (4), 533-42.
228. Kiriakidou, M.; Tan, G. S.; Lamprinak, S.; De Planell-Saguer, M.; Nelson, P. T.; Mourelatos, Z., An mRNA m7G cap binding-like motif within human Ago2 represses translation. *Cell* **2007**, *129* (6), 1141-51.
229. Baek, D.; Villén, J.; Shin, C.; Camargo, F. D.; Gygi, S. P.; Bartel, D. P., The impact of microRNAs on protein output. *Nature* **2008**, *455* (7209), 64-71.
230. Wang, X., Composition of seed sequence is a major determinant of microRNA targeting patterns. *Bioinformatics* **2014**, *30* (10), 1377-83.
231. Friedman, R. C.; Farh, K. K.; Burge, C. B.; Bartel, D. P., Most mammalian mRNAs are conserved targets of microRNAs. *Genome Res* **2009**, *19* (1), 92-105.
232. Eulalio, A.; Huntzinger, E.; Izaurralde, E., Getting to the root of miRNA-mediated gene silencing. *Cell* **2008**, *132* (1), 9-14.
233. Kittelmann, S.; McGregor, A. P., Modulation and Evolution of Animal Development through microRNA Regulation of Gene Expression. *Genes* **2019**, *10* (4).
234. Wu, C. I.; Shen, Y.; Tang, T., Evolution under canalization and the dual roles of microRNAs: a hypothesis. *Genome Res* **2009**, *19* (5), 734-43.
235. Grimson, A.; Srivastava, M.; Fahey, B.; Woodcroft, B. J.; Chiang, H. R.; King, N.; Degan, B. M.; Rokhsar, D. S.; Bartel, D. P., Early origins and evolution of microRNAs and Piwi-interacting RNAs in animals. *Nature* **2008**, *455* (7217), 1193-7.
236. Peterson, K. J.; Dietrich, M. R.; McPeck, M. A., MicroRNAs and metazoan macroevolution: insights into canalization, complexity, and the Cambrian explosion. *BioEssays : news and reviews in molecular, cellular and developmental biology* **2009**, *31* (7), 736-47.
237. Macfarlane, L. A.; Murphy, P. R., MicroRNA: Biogenesis, Function and Role in Cancer. *Curr Genomics* **2010**, *11* (7), 537-61.
238. Li, S.; Lei, Z.; Sun, T., The role of microRNAs in neurodegenerative diseases: a review. *Cell Biol Toxicol* **2022**, 1-31.
239. Rawal, S.; Manning, P.; Katare, R., Cardiovascular microRNAs: as modulators and diagnostic biomarkers of diabetic heart disease. *Cardiovascular diabetology* **2014**, *13*, 44.
240. Poy, M. N.; Eliasson, L.; Krutzfeldt, J.; Kuwajima, S.; Ma, X.; Macdonald, P. E.; Pfeffer, S.; Tuschl, T.; Rajewsky, N.; Rorsman, P.; Stoffel, M., A pancreatic islet-specific microRNA regulates insulin secretion. *Nature* **2004**, *432* (7014), 226-30.

Literature

241. Li, Y.; Xu, X.; Liang, Y.; Liu, S.; Xiao, H.; Li, F.; Cheng, H.; Fu, Z., miR-375 enhances palmitate-induced lipoapoptosis in insulin-secreting NIT-1 cells by repressing myotrophin (V1) protein expression. *Int J Clin Exp Pathol* **2010**, *3* (3), 254-64.
242. Poy, M. N.; Hausser, J.; Trajkovski, M.; Braun, M.; Collins, S.; Rorsman, P.; Zavolan, M.; Stoffel, M., miR-375 maintains normal pancreatic alpha- and beta-cell mass. *Proceedings of the National Academy of Sciences of the United States of America* **2009**, *106* (14), 5813-8.
243. El Ouaamari, A.; Baroukh, N.; Martens, G. A.; Lebrun, P.; Pipeleers, D.; van Obberghen, E., miR-375 targets 3'-phosphoinositide-dependent protein kinase-1 and regulates glucose-induced biological responses in pancreatic beta-cells. *Diabetes* **2008**, *57* (10), 2708-17.
244. Zhao, H.; Guan, J.; Lee, H. M.; Sui, Y.; He, L.; Siu, J. J.; Tse, P. P.; Tong, P. C.; Lai, F. M.; Chan, J. C., Up-regulated pancreatic tissue microRNA-375 associates with human type 2 diabetes through beta-cell deficit and islet amyloid deposition. *Pancreas* **2010**, *39* (6), 843-6.
245. Lovis, P.; Gattesco, S.; Regazzi, R., Regulation of the expression of components of the exocytotic machinery of insulin-secreting cells by microRNAs. *Biological chemistry* **2008**, *389* (3), 305-12.
246. Plaisance, V.; Abderrahmani, A.; Perret-Menoud, V.; Jacquemin, P.; Lemaigre, F.; Regazzi, R., MicroRNA-9 controls the expression of Granuphilin/Slp4 and the secretory response of insulin-producing cells. *The Journal of biological chemistry* **2006**, *281* (37), 26932-42.
247. Salunkhe, V. A.; Ofori, J. K.; Gandasi, N. R.; Salö, S. A.; Hansson, S.; Andersson, M. E.; Wendt, A.; Barg, S.; Esguerra, J. L. S.; Eliasson, L., MiR-335 overexpression impairs insulin secretion through defective priming of insulin vesicles. *Physiol Rep* **2017**, *5* (21).
248. Lovis, P.; Roggli, E.; Laybutt, D. R.; Gattesco, S.; Yang, J. Y.; Widmann, C.; Abderrahmani, A.; Regazzi, R., Alterations in microRNA expression contribute to fatty acid-induced pancreatic beta-cell dysfunction. *Diabetes* **2008**, *57* (10), 2728-36.
249. Roggli, E.; Britan, A.; Gattesco, S.; Lin-Marq, N.; Abderrahmani, A.; Meda, P.; Regazzi, R., Involvement of microRNAs in the cytotoxic effects exerted by proinflammatory cytokines on pancreatic beta-cells. *Diabetes* **2010**, *59* (4), 978-86.
250. Dávalos, A.; Goedeke, L.; Smibert, P.; Ramírez, C. M.; Warriar, N. P.; Andreo, U.; Cirera-Salinas, D.; Rayner, K.; Suresh, U.; Pastor-Pareja, J. C.; Esplugues, E.; Fisher, E. A.; Penalva, L. O.; Moore, K. J.; Suárez, Y.; Lai, E. C.; Fernández-Hernando, C., miR-33a/b contribute to the regulation of fatty acid metabolism and insulin signaling. *Proceedings of the National Academy of Sciences of the United States of America* **2011**, *108* (22), 9232-7.
251. Yang, W. M.; Min, K. H.; Lee, W., MiR-1271 upregulated by saturated fatty acid palmitate provokes impaired insulin signaling by repressing INSR and IRS-1 expression in HepG2 cells. *Biochemical and biophysical research communications* **2016**, *478* (4), 1786-91.
252. Wang, X.; Wang, M.; Li, H.; Lan, X.; Liu, L.; Li, J.; Li, Y.; Li, J.; Yi, J.; Du, X.; Yan, J.; Han, Y.; Zhang, F.; Liu, M.; Lu, S.; Li, D., Upregulation of miR-497 induces hepatic insulin resistance in E3

Literature

rats with HFD-MetS by targeting insulin receptor. *Molecular and cellular endocrinology* **2015**, *416*, 57-69.

253. Min, K. H.; Yang, W. M.; Lee, W., Saturated fatty acids-induced miR-424-5p aggravates insulin resistance via targeting insulin receptor in hepatocytes. *Biochemical and biophysical research communications* **2018**, *503* (3), 1587-1593.

254. Yang, W. M.; Jeong, H. J.; Park, S. W.; Lee, W., Obesity-induced miR-15b is linked causally to the development of insulin resistance through the repression of the insulin receptor in hepatocytes. *Mol Nutr Food Res* **2015**, *59* (11), 2303-14.

255. Yang, W. M.; Min, K. H.; Lee, W., Induction of miR-96 by Dietary Saturated Fatty Acids Exacerbates Hepatic Insulin Resistance through the Suppression of INSR and IRS-1. *PloS one* **2016**, *11* (12), e0169039.

256. Yang, W. M.; Jeong, H. J.; Park, S. Y.; Lee, W., Saturated fatty acid-induced miR-195 impairs insulin signaling and glycogen metabolism in HepG2 cells. *FEBS letters* **2014**, *588* (21), 3939-46.

257. He, A.; Zhu, L.; Gupta, N.; Chang, Y.; Fang, F., Overexpression of micro ribonucleic acid 29, highly up-regulated in diabetic rats, leads to insulin resistance in 3T3-L1 adipocytes. *Molecular endocrinology (Baltimore, Md.)* **2007**, *21* (11), 2785-94.

258. Ling, H. Y.; Ou, H. S.; Feng, S. D.; Zhang, X. Y.; Tuo, Q. H.; Chen, L. X.; Zhu, B. Y.; Gao, Z. P.; Tang, C. K.; Yin, W. D.; Zhang, L.; Liao, D. F., CHANGES IN microRNA (miR) profile and effects of miR-320 in insulin-resistant 3T3-L1 adipocytes. *Clinical and experimental pharmacology & physiology* **2009**, *36* (9), e32-9.

259. Huang, B.; Qin, W.; Zhao, B.; Shi, Y.; Yao, C.; Li, J.; Xiao, H.; Jin, Y., MicroRNA expression profiling in diabetic GK rat model. *Acta biochimica et biophysica Sinica* **2009**, *41* (6), 472-7.

260. Jiang, Y. H.; Man, Y. Y.; Liu, Y.; Yin, C. J.; Li, J. L.; Shi, H. C.; Zhao, H.; Zhao, S. G., Loss of miR-23b/27b/24-1 Cluster Impairs Glucose Tolerance via Glycolysis Pathway in Mice. *International journal of molecular sciences* **2021**, *22* (2).

261. Garavelli, S.; Bruzzaniti, S.; Tagliabue, E.; Di Silvestre, D.; Prattichizzo, F.; Mozzillo, E.; Fattorusso, V.; La Sala, L.; Ceriello, A.; Puca, A. A.; Mauri, P.; Strollo, R.; Marigliano, M.; Maffei, C.; Petrelli, A.; Bosi, E.; Franzese, A.; Galgani, M.; Matarese, G.; de Candia, P., Plasma circulating miR-23~27~24 clusters correlate with the immunometabolic derangement and predict C-peptide loss in children with type 1 diabetes. *Diabetologia* **2020**, *63* (12), 2699-2712.

262. Yang, W. M.; Jeong, H. J.; Park, S. Y.; Lee, W., Induction of miR-29a by saturated fatty acids impairs insulin signaling and glucose uptake through translational repression of IRS-1 in myocytes. *FEBS letters* **2014**, *588* (13), 2170-6.

263. Massart, J.; Sjögren, R. J. O.; Lundell, L. S.; Mudry, J. M.; Franck, N.; O'Gorman, D. J.; Egan, B.; Zierath, J. R.; Krook, A., Altered miR-29 Expression in Type 2 Diabetes Influences Glucose and Lipid Metabolism in Skeletal Muscle. *Diabetes* **2017**, *66* (7), 1807-1818.

Literature

264. Feng, B.; Chen, S.; George, B.; Feng, Q.; Chakrabarti, S., miR133a regulates cardiomyocyte hypertrophy in diabetes. *Diabetes Metab Res Rev* **2010**, *26* (1), 40-9.
265. Xiao, J.; Luo, X.; Lin, H.; Zhang, Y.; Lu, Y.; Wang, N.; Zhang, Y.; Yang, B.; Wang, Z., MicroRNA miR-133 represses HERG K⁺ channel expression contributing to QT prolongation in diabetic hearts. *The Journal of biological chemistry* **2011**, *286* (32), 28656.
266. Yu, X. Y.; Song, Y. H.; Geng, Y. J.; Lin, Q. X.; Shan, Z. X.; Lin, S. G.; Li, Y., Glucose induces apoptosis of cardiomyocytes via microRNA-1 and IGF-1. *Biochemical and biophysical research communications* **2008**, *376* (3), 548-52.
267. Ni, T.; Lin, N.; Lu, W.; Sun, Z.; Lin, H.; Chi, J.; Guo, H., Dihydromyricetin Prevents Diabetic Cardiomyopathy via miR-34a Suppression by Activating Autophagy. *Cardiovascular drugs and therapy* **2020**, *34* (3), 291-301.
268. Li, H.; Fan, J.; Yin, Z.; Wang, F.; Chen, C.; Wang, D. W., Identification of cardiac-related circulating microRNA profile in human chronic heart failure. *Oncotarget* **2016**, *7* (1), 33-45.
269. Li, H.; Fan, J.; Zhao, Y.; Zhang, X.; Dai, B.; Zhan, J.; Yin, Z.; Nie, X.; Fu, X. D.; Chen, C.; Wang, D. W., Nuclear miR-320 Mediates Diabetes-Induced Cardiac Dysfunction by Activating Transcription of Fatty Acid Metabolic Genes to Cause Lipotoxicity in the Heart. *Circulation research* **2019**, *125* (12), 1106-1120.
270. Dai, B.; Li, H.; Fan, J.; Zhao, Y.; Yin, Z.; Nie, X.; Wang, D. W.; Chen, C., MiR-21 protected against diabetic cardiomyopathy induced diastolic dysfunction by targeting gelsolin. *Cardiovascular diabetology* **2018**, *17* (1), 123.
271. Wang, X. H.; Qian, R. Z.; Zhang, W.; Chen, S. F.; Jin, H. M.; Hu, R. M., MicroRNA-320 expression in myocardial microvascular endothelial cells and its relationship with insulin-like growth factor-1 in type 2 diabetic rats. *Clinical and experimental pharmacology & physiology* **2009**, *36* (2), 181-8.
272. Caporali, A.; Meloni, M.; Völlenkle, C.; Bonci, D.; Sala-Newby, G. B.; Addis, R.; Spinetti, G.; Losa, S.; Masson, R.; Baker, A. H.; Agami, R.; le Sage, C.; Condorelli, G.; Madeddu, P.; Martelli, F.; Emanuelli, C., Deregulation of microRNA-503 contributes to diabetes mellitus-induced impairment of endothelial function and reparative angiogenesis after limb ischemia. *Circulation* **2011**, *123* (3), 282-91.
273. Raman, R.; Ramasamy, K.; Shah, U., A Paradigm Shift in the Management Approaches of Proliferative Diabetic Retinopathy: Role of Anti-VEGF Therapy. *Clin Ophthalmol* **2022**, *16*, 3005-3017.
274. McArthur, K.; Feng, B.; Wu, Y.; Chen, S.; Chakrabarti, S., MicroRNA-200b regulates vascular endothelial growth factor-mediated alterations in diabetic retinopathy. *Diabetes* **2011**, *60* (4), 1314-23.
275. Sun, X.; Icli, B.; Wara, A. K.; Belkin, N.; He, S.; Kobzik, L.; Hunninghake, G. M.; Vera, M. P.; Blackwell, T. S.; Baron, R. M.; Feinberg, M. W., MicroRNA-181b regulates NF- κ B-mediated vascular inflammation. *The Journal of clinical investigation* **2012**, *122* (6), 1973-90.

Literature

276. Sun, X.; He, S.; Wara, A. K. M.; Icli, B.; Shvartz, E.; Tesmenitsky, Y.; Belkin, N.; Li, D.; Blackwell, T. S.; Sukhova, G. K.; Croce, K.; Feinberg, M. W., Systemic delivery of microRNA-181b inhibits nuclear factor- κ B activation, vascular inflammation, and atherosclerosis in apolipoprotein E-deficient mice. *Circulation research* **2014**, *114* (1), 32-40.
277. Tian, F. J.; An, L. N.; Wang, G. K.; Zhu, J. Q.; Li, Q.; Zhang, Y. Y.; Zeng, A.; Zou, J.; Zhu, R. F.; Han, X. S.; Shen, N.; Yang, H. T.; Zhao, X. X.; Huang, S.; Qin, Y. W.; Jing, Q., Elevated microRNA-155 promotes foam cell formation by targeting HBP1 in atherogenesis. *Cardiovascular research* **2014**, *103* (1), 100-10.
278. Villeneuve, L. M.; Kato, M.; Reddy, M. A.; Wang, M.; Lanting, L.; Natarajan, R., Enhanced levels of microRNA-125b in vascular smooth muscle cells of diabetic db/db mice lead to increased inflammatory gene expression by targeting the histone methyltransferase Suv39h1. *Diabetes* **2010**, *59* (11), 2904-15.
279. Ota, A.; Tagawa, H.; Karnan, S.; Tsuzuki, S.; Karpas, A.; Kira, S.; Yoshida, Y.; Seto, M., Identification and characterization of a novel gene, C13orf25, as a target for 13q31-q32 amplification in malignant lymphoma. *Cancer Res* **2004**, *64* (9), 3087-95.
280. He, L.; Thomson, J. M.; Hemann, M. T.; Hernando-Monge, E.; Mu, D.; Goodson, S.; Powers, S.; Cordon-Cardo, C.; Lowe, S. W.; Hannon, G. J.; Hammond, S. M., A microRNA polycistron as a potential human oncogene. *Nature* **2005**, *435* (7043), 828-33.
281. O'Donnell, K. A.; Wentzel, E. A.; Zeller, K. I.; Dang, C. V.; Mendell, J. T., c-Myc-regulated microRNAs modulate E2F1 expression. *Nature* **2005**, *435* (7043), 839-43.
282. Ventura, A.; Young, A. G.; Winslow, M. M.; Lintault, L.; Meissner, A.; Erkeland, S. J.; Newman, J.; Bronson, R. T.; Crowley, D.; Stone, J. R.; Jaenisch, R.; Sharp, P. A.; Jacks, T., Targeted deletion reveals essential and overlapping functions of the miR-17 through 92 family of miRNA clusters. *Cell* **2008**, *132* (5), 875-86.
283. Mogilyansky, E.; Rigoutsos, I., The miR-17/92 cluster: a comprehensive update on its genomics, genetics, functions and increasingly important and numerous roles in health and disease. *Cell Death & Differentiation* **2013**, *20* (12), 1603-1614.
284. Bonauer, A.; Dimmeler, S., The microRNA-17-92 cluster: still a miRacle? *Cell cycle (Georgetown, Tex.)* **2009**, *8* (23), 3866-73.
285. Khorshidi, A.; Dhaliwal, P.; Yang, B. B., Anti-tumor activity of miR-17 in melanoma. *Cell cycle (Georgetown, Tex.)* **2015**, *14* (16), 2549-50.
286. Li, H.; Gupta, S.; Du, W. W.; Yang, B. B., MicroRNA-17 inhibits tumor growth by stimulating T-cell mediated host immune response. *Oncoscience* **2014**, *1* (7), 531-9.
287. Concepcion, C. P.; Bonetti, C.; Ventura, A., The microRNA-17-92 family of microRNA clusters in development and disease. *Cancer J* **2012**, *18* (3), 262-7.

Literature

288. Wang, J.; Greene, S. B.; Bonilla-Claudio, M.; Tao, Y.; Zhang, J.; Bai, Y.; Huang, Z.; Black, B. L.; Wang, F.; Martin, J. F., Bmp signaling regulates myocardial differentiation from cardiac progenitors through a MicroRNA-mediated mechanism. *Dev Cell* **2010**, *19* (6), 903-12.
289. Danielson, L. S.; Park, D. S.; Rotllan, N.; Chamorro-Jorganes, A.; Guijarro, M. V.; Fernandez-Hernando, C.; Fishman, G. I.; Phoon, C. K.; Hernando, E., Cardiovascular dysregulation of miR-17-92 causes a lethal hypertrophic cardiomyopathy and arrhythmogenesis. *FASEB journal : official publication of the Federation of American Societies for Experimental Biology* **2013**, *27* (4), 1460-7.
290. Qin, D. N.; Qian, L.; Hu, D. L.; Yu, Z. B.; Han, S. P.; Zhu, C.; Wang, X.; Hu, X., Effects of miR-19b overexpression on proliferation, differentiation, apoptosis and Wnt/ β -catenin signaling pathway in P19 cell model of cardiac differentiation in vitro. *Cell biochemistry and biophysics* **2013**, *66* (3), 709-22.
291. Suárez, Y.; Fernández-Hernando, C.; Yu, J.; Gerber, S. A.; Harrison, K. D.; Pober, J. S.; Iruela-Arispe, M. L.; Merckenschlager, M.; Sessa, W. C., Dicer-dependent endothelial microRNAs are necessary for postnatal angiogenesis. *Proceedings of the National Academy of Sciences of the United States of America* **2008**, *105* (37), 14082-7.
292. Yang, W. J.; Yang, D. D.; Na, S.; Sandusky, G. E.; Zhang, Q.; Zhao, G., Dicer is required for embryonic angiogenesis during mouse development. *The Journal of biological chemistry* **2005**, *280* (10), 9330-5.
293. Suárez, Y.; Fernández-Hernando, C.; Pober, J. S.; Sessa, W. C., Dicer dependent microRNAs regulate gene expression and functions in human endothelial cells. *Circulation research* **2007**, *100* (8), 1164-73.
294. Chamorro-Jorganes, A.; Lee, M. Y.; Araldi, E.; Landskroner-Eiger, S.; Fernández-Fuertes, M.; Sahraei, M.; Quiles Del Rey, M.; van Solingen, C.; Yu, J.; Fernández-Hernando, C.; Sessa, W. C.; Suárez, Y., VEGF-Induced Expression of miR-17-92 Cluster in Endothelial Cells Is Mediated by ERK/ELK1 Activation and Regulates Angiogenesis. *Circulation research* **2016**, *118* (1), 38-47.
295. Landskroner-Eiger, S.; Qiu, C.; Perrotta, P.; Siragusa, M.; Lee, M. Y.; Ulrich, V.; Luciano, A. K.; Zhuang, Z. W.; Corti, F.; Simons, M.; Montgomery, R. L.; Wu, D.; Yu, J.; Sessa, W. C., Endothelial miR-17~92 cluster negatively regulates arteriogenesis via miRNA-19 repression of WNT signaling. *Proceedings of the National Academy of Sciences of the United States of America* **2015**, *112* (41), 12812-7.
296. Bonauer, A.; Carmona, G.; Iwasaki, M.; Mione, M.; Koyanagi, M.; Fischer, A.; Burchfield, J.; Fox, H.; Doebele, C.; Ohtani, K.; Chavakis, E.; Potente, M.; Tjwa, M.; Urbich, C.; Zeiher, A. M.; Dimmeler, S., MicroRNA-92a controls angiogenesis and functional recovery of ischemic tissues in mice. *Science (New York, N.Y.)* **2009**, *324* (5935), 1710-3.
297. Wu, W.; Xiao, H.; Laguna-Fernandez, A.; Villarreal, G., Jr.; Wang, K. C.; Geary, G. G.; Zhang, Y.; Wang, W. C.; Huang, H. D.; Zhou, J.; Li, Y. S.; Chien, S.; Garcia-Cardena, G.; Shyy, J. Y., Flow-

Dependent Regulation of Kruppel-Like Factor 2 Is Mediated by MicroRNA-92a. *Circulation* **2011**, *124* (5), 633-41.

298. Hinkel, R.; Penzkofer, D.; Zuhlke, S.; Fischer, A.; Husada, W.; Xu, Q. F.; Baloch, E.; van Rooij, E.; Zeiher, A. M.; Kupatt, C.; Dimmeler, S., Inhibition of microRNA-92a protects against ischemia/reperfusion injury in a large-animal model. *Circulation* **2013**, *128* (10), 1066-75.

299. Loyer, X.; Potteaux, S.; Vion, A. C.; Guérin, C. L.; Boulkroun, S.; Rautou, P. E.; Ramkhalawon, B.; Esposito, B.; Dalloz, M.; Paul, J. L.; Julia, P.; Maccario, J.; Boulanger, C. M.; Mallat, Z.; Tedgui, A., Inhibition of microRNA-92a prevents endothelial dysfunction and atherosclerosis in mice. *Circulation research* **2014**, *114* (3), 434-43.

300. Daniel, J. M.; Penzkofer, D.; Teske, R.; Dutzmann, J.; Koch, A.; Bielenberg, W.; Bonauer, A.; Boon, R. A.; Fischer, A.; Bauersachs, J.; van Rooij, E.; Dimmeler, S.; Sedding, D. G., Inhibition of miR-92a improves re-endothelialization and prevents neointima formation following vascular injury. *Cardiovascular research* **2014**, *103* (4), 564-72.

301. Danaei, G.; Finucane, M. M.; Lu, Y.; Singh, G. M.; Cowan, M. J.; Paciorek, C. J.; Lin, J. K.; Farzadfar, F.; Khang, Y. H.; Stevens, G. A.; Rao, M.; Ali, M. K.; Riley, L. M.; Robinson, C. A.; Ezzati, M., National, regional, and global trends in fasting plasma glucose and diabetes prevalence since 1980: systematic analysis of health examination surveys and epidemiological studies with 370 country-years and 2·7 million participants. *Lancet (London, England)* **2011**, *378* (9785), 31-40.

302. Stachel, G.; Trenkwalder, T.; Gotz, F.; El Aouni, C.; Muenchmeier, N.; Pfosser, A.; Nussbaum, C.; Sperandio, M.; Hatzopoulos, A. K.; Hinkel, R.; Nelson, P. J.; Kupatt, C., SDF-1 fused to a fractalkine stalk and a GPI anchor enables functional neovascularization. *Stem cells (Dayton, Ohio)* **2013**, *31* (9), 1795-805.

303. Tetzlaff, F.; Fischer, A., Human Endothelial Cell Spheroid-based Sprouting Angiogenesis Assay in Collagen. *Bio Protoc* **2018**, *8* (17), e2995.

304. Laemmli, U. K., Cleavage of structural proteins during the assembly of the head of bacteriophage T4. *Nature* **1970**, *227* (5259), 680-5.

305. Garfin, D. E., One-dimensional gel electrophoresis. *Methods Enzymol* **1990**, *182*, 425-41.

306. Garfin, D. E., One-dimensional gel electrophoresis. *Methods Enzymol* **2009**, *463*, 497-513.

307. Dunn, M. J.; Bradd, S. J., Separation and analysis of membrane proteins by SDS-polyacrylamide gel electrophoresis. *Methods in molecular biology (Clifton, N.J.)* **1993**, *19*, 203-10.

308. Renner, S.; Braun-Reichhart, C.; Blutke, A.; Herbach, N.; Emrich, D.; Streckel, E.; Wünsch, A.; Kessler, B.; Kurome, M.; Bähr, A.; Klymiuk, N.; Krebs, S.; Puk, O.; Nagashima, H.; Graw, J.; Blum, H.; Wanke, R.; Wolf, E., Permanent neonatal diabetes in INS(C94Y) transgenic pigs. *Diabetes* **2013**, *62* (5), 1505-11.

309. Atkins, G. B.; Jain, M. K., Role of Krüppel-like transcription factors in endothelial biology. *Circulation research* **2007**, *100* (12), 1686-95.

Literature

310. Sweet, D. R.; Fan, L.; Hsieh, P. N.; Jain, M. K., Krüppel-Like Factors in Vascular Inflammation: Mechanistic Insights and Therapeutic Potential. *Frontiers in cardiovascular medicine* **2018**, *5*, 6.
311. Yoshida, T.; Yamashita, M.; Iwai, M.; Hayashi, M., Endothelial Krüppel-Like Factor 4 Mediates the Protective Effect of Statins against Ischemic AKI. *Journal of the American Society of Nephrology : JASN* **2016**, *27* (5), 1379-88.
312. Knight, J. B.; Eyster, C. A.; Griesel, B. A.; Olson, A. L., Regulation of the human GLUT4 gene promoter: interaction between a transcriptional activator and myocyte enhancer factor 2A. *Proceedings of the National Academy of Sciences of the United States of America* **2003**, *100* (25), 14725-30.
313. Thai, M. V.; Guruswamy, S.; Cao, K. T.; Pessin, J. E.; Olson, A. L., Myocyte enhancer factor 2 (MEF2)-binding site is required for GLUT4 gene expression in transgenic mice. Regulation of MEF2 DNA binding activity in insulin-deficient diabetes. *The Journal of biological chemistry* **1998**, *273* (23), 14285-92.
314. Sen-Banerjee, S.; Mir, S.; Lin, Z.; Hamik, A.; Atkins, G. B.; Das, H.; Banerjee, P.; Kumar, A.; Jain, M. K., Kruppel-like factor 2 as a novel mediator of statin effects in endothelial cells. *Circulation* **2005**, *112* (5), 720-6.
315. Maejima, T.; Inoue, T.; Kanki, Y.; Kohro, T.; Li, G.; Ohta, Y.; Kimura, H.; Kobayashi, M.; Taguchi, A.; Tsutsumi, S.; Iwanari, H.; Yamamoto, S.; Aruga, H.; Dong, S.; Stevens, J. F.; Poh, H. M.; Yamamoto, K.; Kawamura, T.; Mimura, I.; Suehiro, J.; Sugiyama, A.; Kaneki, K.; Shibata, H.; Yoshinaka, Y.; Doi, T.; Asanuma, A.; Tanabe, S.; Tanaka, T.; Minami, T.; Hamakubo, T.; Sakai, J.; Nozaki, N.; Aburatani, H.; Nangaku, M.; Ruan, X.; Tanabe, H.; Ruan, Y.; Ihara, S.; Endo, A.; Kodama, T.; Wada, Y., Direct evidence for pitavastatin induced chromatin structure change in the KLF4 gene in endothelial cells. *PloS one* **2014**, *9* (5), e96005.
316. Diabetes care in the EU. https://www.europarl.europa.eu/doceo/document/E-9-2020-006356_EN.html.
317. Kirk, R. G. W., Recovering The Principles of Humane Experimental Technique: The 3Rs and the Human Essence of Animal Research. *Sci Technol Human Values* **2018**, *43* (4), 622-648.
318. Russell, W. M. S. B., R.L., *The Principles of Humane Experimental Technique*. Methuen & Co. Limited: London, 1959.
319. Jacobo-Albavera, D. J. M.-L. M. D.-P. I. M. M. T. V.-M. L., Use of Human Umbilical Vein Endothelial Cells (HUVEC) as a Model to Study Cardiovascular Disease: A Review. *Applied Sciences* **2020**, *10* (3).
320. Zhao, X. Y.; Wang, X. F.; Li, L.; Zhang, L.; Shen, D. L.; Li, D. H.; Jin, Q. S.; Zhang, J. Y., Effects of high glucose on human umbilical vein endothelial cell permeability and myosin light chain phosphorylation. *Diabetol Metab Syndr* **2015**, *7*, 98.

321. Lin, F.; Yang, Y.; Wei, S.; Huang, X.; Peng, Z.; Ke, X.; Zeng, Z.; Song, Y., Hydrogen Sulfide Protects Against High Glucose-Induced Human Umbilical Vein Endothelial Cell Injury Through Activating PI3K/Akt/eNOS Pathway. *Drug design, development and therapy* **2020**, *14*, 621-633.
322. Gou, L.; Zhao, L.; Song, W.; Wang, L.; Liu, J.; Zhang, H.; Huang, Y.; Lau, C. W.; Yao, X.; Tian, X. Y.; Wong, W. T.; Luo, J. Y.; Huang, Y., Inhibition of miR-92a Suppresses Oxidative Stress and Improves Endothelial Function by Upregulating Heme Oxygenase-1 in db/db Mice. *Antioxidants & redox signaling* **2018**, *28* (5), 358-370.
323. Chen, Z.; Wen, L.; Martin, M.; Hsu, C. Y.; Fang, L.; Lin, F. M.; Lin, T. Y.; Geary, M. J.; Geary, G. G.; Zhao, Y.; Johnson, D. A.; Chen, J. W.; Lin, S. J.; Chien, S.; Huang, H. D.; Miller, Y. I.; Huang, P. H.; Shyy, J. Y., Oxidative stress activates endothelial innate immunity via sterol regulatory element binding protein 2 (SREBP2) transactivation of microRNA-92a. *Circulation* **2015**, *131* (9), 805-14.
324. Zhang, L.; Zhou, M.; Qin, G.; Weintraub, N. L.; Tang, Y., MiR-92a regulates viability and angiogenesis of endothelial cells under oxidative stress. *Biochemical and biophysical research communications* **2014**, *446* (4), 952-8.
325. Hou, S.; Li, Z.; Dong, J.; Gao, Y.; Chang, Z.; Ding, X.; Li, S.; Li, Y.; Zeng, Y.; Xin, Q.; Wang, B.; Ni, Y.; Ning, X.; Hu, Y.; Fan, X.; Hou, Y.; Li, X.; Wen, L.; Zhou, B.; Liu, B.; Tang, F.; Lan, Y., Heterogeneity in endothelial cells and widespread venous arterialization during early vascular development in mammals. *Cell research* **2022**, *32* (4), 333-348.
326. Trimm, E.; Red-Horse, K., Vascular endothelial cell development and diversity. *Nature reviews. Cardiology* **2022**, 1-14.
327. Minami, T.; Muramatsu, M.; Kume, T., Organ/Tissue-Specific Vascular Endothelial Cell Heterogeneity in Health and Disease. *Biol Pharm Bull* **2019**, *42* (10), 1609-1619.
328. Nolan, D. J.; Ginsberg, M.; Israely, E.; Palikuqi, B.; Poulos, M. G.; James, D.; Ding, B. S.; Schachterle, W.; Liu, Y.; Rosenwaks, Z.; Butler, J. M.; Xiang, J.; Rafii, A.; Shido, K.; Rabbany, S. Y.; Elemento, O.; Rafii, S., Molecular signatures of tissue-specific microvascular endothelial cell heterogeneity in organ maintenance and regeneration. *Dev Cell* **2013**, *26* (2), 204-19.
329. Augustin, H. G.; Koh, G. Y., Organotypic vasculature: From descriptive heterogeneity to functional pathophysiology. *Science (New York, N.Y.)* **2017**, *357* (6353).
330. Kalucka, J.; de Rooij, L.; Goveia, J.; Rohlenova, K.; Dumas, S. J.; Meta, E.; Conchinha, N. V.; Taverna, F.; Teuwen, L. A.; Veys, K.; García-Caballero, M.; Khan, S.; Geldhof, V.; Sokol, L.; Chen, R.; Treps, L.; Borri, M.; de Zeeuw, P.; Dubois, C.; Karakach, T. K.; Falkenberg, K. D.; Parys, M.; Yin, X.; Vinckier, S.; Du, Y.; Fenton, R. A.; Schoonjans, L.; Dewerchin, M.; Eelen, G.; Thienpont, B.; Lin, L.; Bolund, L.; Li, X.; Luo, Y.; Carmeliet, P., Single-Cell Transcriptome Atlas of Murine Endothelial Cells. *Cell* **2020**, *180* (4), 764-779.e20.
331. Huxley, V. H.; Kemp, S. S.; Schramm, C.; Sieveking, S.; Bingaman, S.; Yu, Y.; Zaniletti, I.; Stockard, K.; Wang, J., Sex differences influencing micro- and macrovascular endothelial phenotype in vitro. *The Journal of physiology* **2018**, *596* (17), 3929-3949.

Literature

332. Huxley, V. H.; Kemp, S. S., Sex-Specific Characteristics of the Microcirculation. *Advances in experimental medicine and biology* **2018**, *1065*, 307-328.
333. Patel, H.; Rosengren, A.; Ekman, I., Symptoms in acute coronary syndromes: does sex make a difference? *American heart journal* **2004**, *148* (1), 27-33.
334. Wei, K.; Kaul, S., The coronary microcirculation in health and disease. *Cardiology clinics* **2004**, *22* (2), 221-31.
335. Juutilainen, A.; Kortelainen, S.; Lehto, S.; Rönnekaa, T.; Pyörälä, K.; Laakso, M., Gender difference in the impact of type 2 diabetes on coronary heart disease risk. *Diabetes Care* **2004**, *27* (12), 2898-904.
336. Garcia, M.; Mulvagh, S. L.; Merz, C. N.; Buring, J. E.; Manson, J. E., Cardiovascular Disease in Women: Clinical Perspectives. *Circulation research* **2016**, *118* (8), 1273-93.
337. Lin, J.; Li, X.; Lin, Y.; Huang, Z.; Wu, W., Exogenous sodium hydrosulfide protects against high glucose-induced injury and inflammation in human umbilical vein endothelial cells by inhibiting necroptosis via the p38 MAPK signaling pathway. *Molecular medicine reports* **2021**, *23* (1).
338. Wang, X.; Gao, L.; Xiao, L.; Yang, L.; Li, W.; Liu, G.; Chen, L.; Zhang, J., 12(S)-hydroxyeicosatetraenoic acid impairs vascular endothelial permeability by altering adherens junction phosphorylation levels and affecting the binding and dissociation of its components in high glucose-induced vascular injury. *J Diabetes Investig* **2019**, *10* (3), 639-649.
339. Grismaldo Rodríguez, A.; Zamudio Rodríguez, J. A.; Mendieta, C. V.; Quijano Gómez, S.; Sanabria Barrera, S.; Morales Álvarez, L., Effect of Platelet-Derived Growth Factor C on Mitochondrial Oxidative Stress Induced by High d-Glucose in Human Aortic Endothelial Cells. *Pharmaceuticals (Basel)* **2022**, *15* (5).
340. Yetkin-Arik, B.; Vogels, I. M. C.; Neyazi, N.; van Duinen, V.; Houtkooper, R. H.; van Noorden, C. J. F.; Klaassen, I.; Schlingemann, R. O., Endothelial tip cells in vitro are less glycolytic and have a more flexible response to metabolic stress than non-tip cells. *Scientific reports* **2019**, *9* (1), 10414.
341. Xu, Y.; An, X.; Guo, X.; Habetsion, T. G.; Wang, Y.; Xu, X.; Kandala, S.; Li, Q.; Li, H.; Zhang, C.; Caldwell, R. B.; Fulton, D. J.; Su, Y.; Hoda, M. N.; Zhou, G.; Wu, C.; Huo, Y., Endothelial PFKFB3 plays a critical role in angiogenesis. *Arteriosclerosis, thrombosis, and vascular biology* **2014**, *34* (6), 1231-9.
342. De Bock, K.; Georgiadou, M.; Schoors, S.; Kuchnio, A.; Wong, B. W.; Cantelmo, A. R.; Quaegebeur, A.; Ghesquière, B.; Cauwenberghs, S.; Eelen, G.; Phng, L. K.; Betz, I.; Tembuyser, B.; Brepoels, K.; Welti, J.; Geudens, I.; Segura, I.; Cruys, B.; Bifari, F.; Decimo, I.; Blanco, R.; Wyns, S.; Vangindertael, J.; Rocha, S.; Collins, R. T.; Munck, S.; Daelemans, D.; Imamura, H.; Devlieger, R.; Rider, M.; Van Veldhoven, P. P.; Schuit, F.; Bartrons, R.; Hofkens, J.; Fraisl, P.; Telang, S.; Deberardinis, R. J.; Schoonjans, L.; Vinckier, S.; Chesney, J.; Gerhardt, H.; Dewerchin, M.; Carmeliet, P., Role of PFKFB3-driven glycolysis in vessel sprouting. *Cell* **2013**, *154* (3), 651-63.

Literature

343. Min, J.; Zeng, T.; Roux, M.; Lazar, D.; Chen, L.; Tudzarova, S., The Role of HIF1 α -PFKFB3 Pathway in Diabetic Retinopathy. *J Clin Endocrinol Metab* **2021**, *106* (9), 2505-2519.
344. Iacobini, C.; Vitale, M.; Pugliese, G.; Menini, S., Normalizing HIF-1 α Signaling Improves Cellular Glucose Metabolism and Blocks the Pathological Pathways of Hyperglycemic Damage. *Biomedicines* **2021**, *9* (9).
345. Sweet, I. R.; Gilbert, M.; Maloney, E.; Hockenbery, D. M.; Schwartz, M. W.; Kim, F., Endothelial inflammation induced by excess glucose is associated with cytosolic glucose 6-phosphate but not increased mitochondrial respiration. *Diabetologia* **2009**, *52* (5), 921-31.
346. Takami, S.; Yamashita, S.; Kihara, S.; Kameda-Takemura, K.; Matsuzawa, Y., High concentration of glucose induces the expression of intercellular adhesion molecule-1 in human umbilical vein endothelial cells. *Atherosclerosis* **1998**, *138* (1), 35-41.
347. Altannavch, T. S.; Roubalová, K.; Kucera, P.; Andel, M., Effect of high glucose concentrations on expression of ELAM-1, VCAM-1 and ICAM-1 in HUVEC with and without cytokine activation. *Physiol Res* **2004**, *53* (1), 77-82.
348. Porcellati, F.; Lucidi, P.; Bolli, G. B.; Fanelli, C. G., Thirty years of research on the dawn phenomenon: lessons to optimize blood glucose control in diabetes. *Diabetes Care* **2013**, *36* (12), 3860-2.
349. Rybicka, M.; Krysiak, R.; Okopień, B., The dawn phenomenon and the Somogyi effect - two phenomena of morning hyperglycaemia. *Endokrynol Pol* **2011**, *62* (3), 276-84.
350. Dungan, K. M.; Braithwaite, S. S.; Preiser, J. C., Stress hyperglycaemia. *Lancet (London, England)* **2009**, *373* (9677), 1798-807.
351. Kumar, R.; Nandhini, L. P.; Kamalanathan, S.; Sahoo, J.; Vivekanadan, M., Evidence for current diagnostic criteria of diabetes mellitus. *World J Diabetes* **2016**, *7* (17), 396-405.
352. Zhang, Y.; Hu, G.; Yuan, Z.; Chen, L., Glycosylated hemoglobin in relationship to cardiovascular outcomes and death in patients with type 2 diabetes: a systematic review and meta-analysis. *PloS one* **2012**, *7* (8), e42551.
353. Wang, W. Y.; Zheng, Y. S.; Li, Z. G.; Cui, Y. M.; Jiang, J. C., MiR-92a contributes to the cardiovascular disease development in diabetes mellitus through NF- κ B and downstream inflammatory pathways. *European review for medical and pharmacological sciences* **2019**, *23* (7), 3070-3079.
354. Zhang, Y.; Cheng, J.; Chen, F.; Wu, C.; Zhang, J.; Ren, X.; Pan, Y.; Nie, B.; Li, Q.; Li, Y., Circulating endothelial microparticles and miR-92a in acute myocardial infarction. *Biosci Rep* **2017**, *37* (2).
355. Izreig, S.; Samborska, B.; Johnson, R. M.; Sergushichev, A.; Ma, E. H.; Lussier, C.; Loginicheva, E.; Donayo, A. O.; Poffenberger, M. C.; Sagan, S. M.; Vincent, E. E.; Artyomov, M. N.; Duchaine, T. F.; Jones, R. G., The miR-17~92 microRNA Cluster Is a Global Regulator of Tumor Metabolism. *Cell Rep* **2016**, *16* (7), 1915-28.

Literature

356. De Paolis, V.; Lorefice, E.; Orecchini, E.; Carissimi, C.; Laudadio, I.; Fulci, V., Epitranscriptomics: A New Layer of microRNA Regulation in Cancer. *Cancers (Basel)* **2021**, *13* (13).
357. Geng, X.; Li, Z.; Yang, Y., Emerging Role of Epitranscriptomics in Diabetes Mellitus and Its Complications. *Frontiers in endocrinology* **2022**, *13*, 907060.
358. Luciano, D. J.; Mirsky, H.; Vendetti, N. J.; Maas, S., RNA editing of a miRNA precursor. *Rna* **2004**, *10* (8), 1174-7.
359. Wu, S.; Zhang, S.; Wu, X.; Zhou, X., m(6)A RNA Methylation in Cardiovascular Diseases. *Molecular therapy : the journal of the American Society of Gene Therapy* **2020**, *28* (10), 2111-2119.
360. Qin, Y.; Li, L.; Luo, E.; Hou, J.; Yan, G.; Wang, D.; Qiao, Y.; Tang, C., Role of m6A RNA methylation in cardiovascular disease (Review). *International journal of molecular medicine* **2020**, *46* (6), 1958-1972.
361. Huang, H.; Weng, H.; Chen, J., m(6)A Modification in Coding and Non-coding RNAs: Roles and Therapeutic Implications in Cancer. *Cancer Cell* **2020**, *37* (3), 270-288.
362. Fu, Y.; Dominissini, D.; Rechavi, G.; He, C., Gene expression regulation mediated through reversible m⁶A RNA methylation. *Nature reviews. Genetics* **2014**, *15* (5), 293-306.
363. Liu, N.; Pan, T., N6-methyladenosine–encoded epitranscriptomics. *Nat Struct Mol Biol* **2016**, *23* (2), 98-102.
364. Alarcón, C. R.; Lee, H.; Goodarzi, H.; Halberg, N.; Tavazoie, S. F., N6-methyladenosine marks primary microRNAs for processing. *Nature* **2015**, *519* (7544), 482-5.
365. Chamorro-Jorganes, A.; Sweaad, W. K.; Katare, R.; Besnier, M.; Anwar, M.; Beazley-Long, N.; Sala-Newby, G.; Ruiz-Polo, I.; Chandrasekera, D.; Ritchie, A. A.; Benest, A. V.; Emanuelli, C., METTL3 Regulates Angiogenesis by Modulating let-7e-5p and miRNA-18a-5p Expression in Endothelial Cells. *Arteriosclerosis, thrombosis, and vascular biology* **2021**, *41* (6), e325-e337.
366. Chaulk, S. G.; Thede, G. L.; Kent, O. A.; Xu, Z.; Gesner, E. M.; Veldhoen, R. A.; Khanna, S. K.; Goping, I. S.; MacMillan, A. M.; Mendell, J. T.; Young, H. S.; Fahlman, R. P.; Glover, J. N., Role of pri-miRNA tertiary structure in miR-17~92 miRNA biogenesis. *RNA Biol* **2011**, *8* (6), 1105-14.
367. Chaulk, S. G.; Xu, Z.; Glover, M. J.; Fahlman, R. P., MicroRNA miR-92a-1 biogenesis and mRNA targeting is modulated by a tertiary contact within the miR-17~92 microRNA cluster. *Nucleic Acids Res* **2014**, *42* (8), 5234-44.
368. Ballarino, M.; Pagano, F.; Girardi, E.; Morlando, M.; Cacchiarelli, D.; Marchioni, M.; Proudfoot, N. J.; Bozzoni, I., Coupled RNA processing and transcription of intergenic primary microRNAs. *Mol Cell Biol* **2009**, *29* (20), 5632-8.
369. Morlando, M.; Ballarino, M.; Gromak, N.; Pagano, F.; Bozzoni, I.; Proudfoot, N. J., Primary microRNA transcripts are processed co-transcriptionally. *Nature Structural & Molecular Biology* **2008**, *15* (9), 902-909.
370. Parmar, K. M.; Larman, H. B.; Dai, G.; Zhang, Y.; Wang, E. T.; Moorthy, S. N.; Kratz, J. R.; Lin, Z.; Jain, M. K.; Gimbrone, M. A., Jr.; García-Cardena, G., Integration of flow-dependent

- endothelial phenotypes by Kruppel-like factor 2. *The Journal of clinical investigation* **2006**, *116* (1), 49-58.
371. Ticho, B. S.; Stainier, D. Y.; Fishman, M. C.; Breitbart, R. E., Three zebrafish MEF2 genes delineate somitic and cardiac muscle development in wild-type and mutant embryos. *Mech Dev* **1996**, *59* (2), 205-18.
372. Kemmler, C. L.; Riemsdijk, F. W.; Moran, H. R.; Mosimann, C., From Stripes to a Beating Heart: Early Cardiac Development in Zebrafish. *Journal of cardiovascular development and disease* **2021**, *8* (2).
373. Nayak, L.; Lin, Z.; Jain, M. K., "Go with the flow": how Krüppel-like factor 2 regulates the vasoprotective effects of shear stress. *Antioxidants & redox signaling* **2011**, *15* (5), 1449-61.
374. Novodvorsky, P.; Watson, O.; Gray, C.; Wilkinson, R. N.; Reeve, S.; Smythe, C.; Beniston, R.; Plant, K.; Maguire, R.; A, M. K. R.; Elworthy, S.; van Eeden, F. J.; Chico, T. J., klf2ash317 Mutant Zebrafish Do Not Recapitulate Morpholino-Induced Vascular and Haematopoietic Phenotypes. *PloS one* **2015**, *10* (10), e0141611.
375. Michel, J. B., Phylogenic Determinants of Cardiovascular Frailty, Focus on Hemodynamics and Arterial Smooth Muscle Cells. *Physiological reviews* **2020**, *100* (4), 1779-1837.
376. Nachtigall, P. G.; Bovolenta, L. A.; Patton, J. G.; Fromm, B.; Lemke, N.; Pinhal, D., A comparative analysis of heart microRNAs in vertebrates brings novel insights into the evolution of genetic regulatory networks. *BMC Genomics* **2021**, *22* (1), 153.
377. Han, Y. C.; Vidigal, J. A.; Mu, P.; Yao, E.; Singh, I.; González, A. J.; Concepcion, C. P.; Bonetti, C.; Ogradowski, P.; Carver, B.; Selleri, L.; Betel, D.; Leslie, C.; Ventura, A., An allelic series of miR-17 ~ 92-mutant mice uncovers functional specialization and cooperation among members of a microRNA polycistron. *Nature genetics* **2015**, *47* (7), 766-75.
378. Toonen, J. A.; Ronchetti, A.; Sidjanin, D. J., A Disintegrin and Metalloproteinase10 (ADAM10) Regulates NOTCH Signaling during Early Retinal Development. *PloS one* **2016**, *11* (5), e0156184.
379. Pereira-Castro, I.; Moreira, A., On the function and relevance of alternative 3'-UTRs in gene expression regulation. *Wiley Interdiscip Rev RNA* **2021**, *12* (5), e1653.
380. Neve, J.; Patel, R.; Wang, Z.; Louey, A.; Furger, A. M., Cleavage and polyadenylation: Ending the message expands gene regulation. *RNA Biol* **2017**, *14* (7), 865-890.
381. Ji, Z.; Lee, J. Y.; Pan, Z.; Jiang, B.; Tian, B., Progressive lengthening of 3' untranslated regions of mRNAs by alternative polyadenylation during mouse embryonic development. *Proceedings of the National Academy of Sciences of the United States of America* **2009**, *106* (17), 7028-33.
382. Galati, G.; Leone, O.; Pasquale, F.; Olivetto, I.; Biagini, E.; Grigioni, F.; Pilato, E.; Lorenzini, M.; Corti, B.; Foà, A.; Agostini, V.; Cecchi, F.; Rapezzi, C., Histological and Histometric Characterization of Myocardial Fibrosis in End-Stage Hypertrophic Cardiomyopathy: A Clinical-Pathological Study of 30 Explanted Hearts. *Circulation. Heart failure* **2016**, *9* (9).

Literature

383. Samak, M.; Kaltenborn, D.; Kues, A.; Le Noble, F.; Hinkel, R.; Germena, G., Micro-RNA 92a as a Therapeutic Target for Cardiac Microvascular Dysfunction in Diabetes. *Biomedicines* **2021**, *10* (1).
384. Sorop, O.; Heinonen, I.; van Kranenburg, M.; van de Wouw, J.; de Beer, V. J.; Nguyen, I. T. N.; Octavia, Y.; van Duin, R. W. B.; Stam, K.; van Geuns, R. J.; Wielopolski, P. A.; Krestin, G. P.; van den Meiracker, A. H.; Verjans, R.; van Bilsen, M.; Danser, A. H. J.; Paulus, W. J.; Cheng, C.; Linke, W. A.; Joles, J. A.; Verhaar, M. C.; van der Velden, J.; Merkus, D.; Duncker, D. J., Multiple common comorbidities produce left ventricular diastolic dysfunction associated with coronary microvascular dysfunction, oxidative stress, and myocardial stiffening. *Cardiovascular research* **2018**, *114* (7), 954-964.
385. Nayak, L.; Goduni, L.; Takami, Y.; Sharma, N.; Kapil, P.; Jain, M. K.; Mahabeleshwar, G. H., Kruppel-like factor 2 is a transcriptional regulator of chronic and acute inflammation. *The American journal of pathology* **2013**, *182* (5), 1696-704.
386. Mahabeleshwar, G. H.; Kawanami, D.; Sharma, N.; Takami, Y.; Zhou, G.; Shi, H.; Nayak, L.; Jeyaraj, D.; Greal, R.; White, M.; McManus, R.; Ryan, T.; Leahy, P.; Lin, Z.; Haldar, S. M.; Atkins, G. B.; Wong, H. R.; Lingrel, J. B.; Jain, M. K., The myeloid transcription factor KLF2 regulates the host response to polymicrobial infection and endotoxic shock. *Immunity* **2011**, *34* (5), 715-28.
387. Chang, Y. J.; Li, Y. S.; Wu, C. C.; Wang, K. C.; Huang, T. C.; Chen, Z.; Chien, S., Extracellular MicroRNA-92a Mediates Endothelial Cell-Macrophage Communication. *Arteriosclerosis, thrombosis, and vascular biology* **2019**, *39* (12), 2492-2504.
388. Fang, Y.; Davies, P. F., Site-specific microRNA-92a regulation of Kruppel-like factors 4 and 2 in atherosusceptible endothelium. *Arteriosclerosis, thrombosis, and vascular biology* **2012**, *32* (4), 979-87.
389. Wani, M. A.; Means, R. T., Jr.; Lingrel, J. B., Loss of LKLF function results in embryonic lethality in mice. *Transgenic Res* **1998**, *7* (4), 229-38.
390. Sacilotto, N.; Chouliaras, K. M.; Nikitenko, L. L.; Lu, Y. W.; Fritzsche, M.; Wallace, M. D.; Nornes, S.; García-Moreno, F.; Payne, S.; Bridges, E.; Liu, K.; Biggs, D.; Ratnayaka, I.; Herbert, S. P.; Molnár, Z.; Harris, A. L.; Davies, B.; Bond, G. L.; Bou-Gharios, G.; Schwarz, J. J.; De Val, S., MEF2 transcription factors are key regulators of sprouting angiogenesis. *Genes & development* **2016**, *30* (20), 2297-2309.
391. Wang, W.; Ha, C. H.; Jhun, B. S.; Wong, C.; Jain, M. K.; Jin, Z. G., Fluid shear stress stimulates phosphorylation-dependent nuclear export of HDAC5 and mediates expression of KLF2 and eNOS. *Blood* **2010**, *115* (14), 2971-9.
392. Dewanjee, S.; Vallamkondu, J.; Kalra, R. S.; Chakraborty, P.; Gangopadhyay, M.; Sahu, R.; Medala, V.; John, A.; Reddy, P. H.; De Feo, V.; Kandimalla, R., The Emerging Role of HDACs: Pathology and Therapeutic Targets in Diabetes Mellitus. *Cells* **2021**, *10* (6).

Literature

393. Raichur, S.; Teh, S. H.; Ohwaki, K.; Gaur, V.; Long, Y. C.; Hargreaves, M.; McGee, S. L.; Kusunoki, J., Histone deacetylase 5 regulates glucose uptake and insulin action in muscle cells. *J Mol Endocrinol* **2012**, *49* (3), 203-11.
394. Thorn, C. R.; Sharma, D.; Combs, R.; Bhujbal, S.; Romine, J.; Zheng, X.; Sunasara, K.; Badkar, A., The journey of a lifetime - development of Pfizer's COVID-19 vaccine. *Current opinion in biotechnology* **2022**, *78*, 102803.
395. Rohner, E.; Yang, R.; Foo, K. S.; Goedel, A.; Chien, K. R., Unlocking the promise of mRNA therapeutics. *Nature biotechnology* **2022**, *40* (11), 1586-1600.
396. Wang, F.; Zuroske, T.; Watts, J. K., RNA therapeutics on the rise. *Nature reviews. Drug discovery* **2020**, *19* (7), 441-442.
397. Boada, C.; Sukhovshin, R.; Pettigrew, R.; Cooke, J. P., RNA therapeutics for cardiovascular disease. *Current opinion in cardiology* **2021**, *36* (3), 256-263.
398. Täubel, J.; Hauke, W.; Rump, S.; Viereck, J.; Batkai, S.; Poetzsch, J.; Rode, L.; Weigt, H.; Genschel, C.; Lorch, U.; Theek, C.; Levin, A. A.; Bauersachs, J.; Solomon, S. D.; Thum, T., Novel antisense therapy targeting microRNA-132 in patients with heart failure: results of a first-in-human Phase 1b randomized, double-blind, placebo-controlled study. *European heart journal* **2021**, *42* (2), 178-188.
399. Abplanalp, W. T.; Fischer, A.; John, D.; Zeiher, A. M.; Gosgnach, W.; Darville, H.; Montgomery, R.; Pestano, L.; Allée, G.; Paty, I.; Fougereousse, F.; Dimmeler, S., Efficiency and Target Derepression of Anti-miR-92a: Results of a First in Human Study. *Nucleic Acid Ther* **2020**, *30* (6), 335-345.

Curriculum vitae

Mostafa Samak

Date and place of birth: July 9th 1988 – Cairo, Egypt | Nationality: Egyptian

Current address: Südring 2, 37079 Göttingen

Mobile: +4917637636301 | E-mail: samak.mostafa@gmail.com



Education

October 2018 – Feb. 2023: Doctoral student

Molecular Medicine Ph.D. program – Georg-August University of Göttingen

German Primate Center (GmbH) – Leibniz Association

Laboratory Animal Science Department – Prof. Dr. Rabea Hinkel

Project: “**Cardiac microvascular dysfunction in diabetes mellitus: elucidation of molecular determinants and therapeutic targets**”

October 2011 – June 2013: Master of Science in Molecular Medicine

Universitätsmedizin Göttingen (UMG) – Georg-August University of Göttingen

Grade: 1.93 – Good (German grading system)

Master thesis (Department of Neurodegeneration and Restorative Research – Prof. Dr. Tiago F. Outeiro):

“**Deciphering the role of Sirtuin 2 in Parkinson’s disease models**”

Sept. 2005 – May 2010:

Bachelor of Science in Pharmaceutical Sciences

Faculty of Pharmacy – Helwan University – Cairo

Grade: Very Good (Honors) – licensed pharmacist

Sept. 2002 – June 2005:

General Egyptian Secondary School Certificate

Major: natural sciences

Grade: 96.2 %

Work experience

January – Sept. 2018:

Lecturer of Molecular Medicine

Faculty of Biotechnology – Misr University for Science & Technology (MUST)

6th of October City – Egypt

Duties: lecturing – lab demonstration – student supervision

June 2014 – October 2015: Research Assistant

Department of Cardiothoracic Surgery – Cologne University Hospital

Laboratory of Cardiac Regeneration – Prof. Dr. med. Yeong-Hoon Choi

Project: “**Elucidating the role of inflammation in cardiac hypertrophy**”

Languages

Arabic: native

English: fluent in both oral and written (TOEFL IBT score: 109)

German: very good command of oral and written (Goethe B2)

Portuguese: good command of oral and written

Publications

1. Samak M, Kues A, Kaltenborn D, Klösener L, Mietsch M, Germena G, Hinkel R. Dysregulation of Krüppel-like factor 2 and myocyte enhancer factor 2D drive cardiac microvascular inflammation in diabetes. *Int J Mol Sci.* 2023; 24(3):2482.
2. Schoger E, Bleckwedel F, Germena G, Rocha C, Tucholla P, Sobitov I, Möbius W, Sitte M, Lenz C, Samak M, Hinkel R, Varga ZV, Giricz Z, Salinas G, Gross JC, Zelarayán LC. *Commun Biol.* 2023; 6(1):79.
3. Samak M, Kaltenborn D, Kues A, Le Noble F, Hinkel R, Germena G. Micro-RNA 92a as a Therapeutic Target for Cardiac Microvascular Dysfunction in Diabetes. *Biomedicines.* 2021;10(1):58.
4. Samak M, Hinkel R. Stem Cells in Cardiovascular Medicine: Historical Overview and Future Prospects. *Cells.* 2019; 8(12):1530.
5. Samak M, Fatullayev J, Sabashnikov A, Zeriouh M, Schmack B, Ruhparwar A, Karck M, Popov AF, Dohmen PM, Weymann A. Total Arterial Revascularization: Bypassing Antiquated Notions to Better Alternatives for Coronary Artery Disease. *Med Sci Monit Basic Res.* 2016; 22:107-114.
6. Samak M, Fatullayev J, Sabashnikov A, Zeriouh M, Schmack B, Farag M, Popov AF, Dohmen PM, Choi YH, Wahlers T, Weymann A. Cardiac Hypertrophy: An Introduction to Molecular and Cellular Basis. *Med Sci Monit Basic Res.* 2016; 22:75-9.
7. Samak M, Fatullayev J, Sabashnikov A, Zeriouh M, Rahmanian PB, Choi YH, Wippermann J, Wahlers T, Schmack B, Ruhparwar A, Dohmen PM, Karck M, Popov AF, Simon AR, Weymann A. Past and Present of Total Artificial Heart Therapy: A Success Story. *Med Sci Monit Basic Res.* 2015; 21:183-90.
8. Fatullayev J*, Samak M*, Sabashnikov A, Weymann A, Mohite PN, García-Sáez D, Patil NP, Dohmen PM. Non-Heart-Beating Donor Heart Transplantation: Breaking the Taboo. *Med Sci Monit Basic Res.* 2015; 21:153-6. *equal contribution
9. Fatullayev J, Samak M, Sabashnikov A, Zeriouh M, Rahmanian PB, Choi YH, Schmack B, Kallenbach K, Ruhparwar A, Eghbalzadeh K, Dohmen PM, Karck M, Wippermann J, Wahlers T, Popov AF, Simon AR, Weymann A. Continuous-Flow Left Ventricular Assist Device Thrombosis: A Danger Foreseen is a Danger Avoided. *Med Sci Monit Basic Res.* 2015; 21:141-4.